Solid Phase Microextraction as a Sample Preparation Tool for Targeted and Untargeted Analysis of Biological Matrices

by

Nathaly Reyes-Garcés

A thesis

presented to the University of Waterloo

in fulfillment of the

thesis requirement for the degree of

Doctor of Philosophy

in

Chemistry

Waterloo, Ontario, Canada, 2017

Examining Committee Membership

The following served on the Examining Committee for this thesis. The decision of the Examining Committee is by majority vote.

External Examiner   Prof. Oliver Fiehn
                                      Director West Coast Metabolomics Center
                                      UC Davis Genome Center - Metabolomics

Supervisor(s)   Prof. Janusz Pawliszyn
                                      University Professor and Canada Research Chair
                                      Department of Chemistry, University of Waterloo

Internal Member   Prof. Michael Chong
                                      Professor
                                      Department of Chemistry, University of Waterloo

Internal-external Member   Prof. Paul Craig
                                      Assistant Professor
                                      Department of Biology, University of Waterloo

Other Member(s)   Prof. Wojciech Gabryelski
                                      Associate Professor
                                      Department of Chemistry, University of Guelph

Author's Declaration

This thesis consists of material all of which I authored or co-authored: see Statement of Contributions included in the thesis. This is a true copy of the thesis, including any required final revisions, as accepted by my examiners.

I understand that my thesis may be made electronically available to the public. I understand that my thesis may be made electronically available to the public.

Statement of Contributions

Chapter 1 includes an excerpt (500 words) that is already published in the review article "A critical review of the state of the art of solid phase microextraction of complex matrices III. Bioanalytical and clinical applications" (*Trends Anal. Chem.* **2015**, *71*, 249-264) which was co-authored with E.A. Souza-Silva, N. Reyes-Garcés, G.A. Gómez-Ríos, E. Boyaci, and B. Bojko under the supervision J. Pawliszyn. The author of this thesis was the sole writer of the excerpt that is being included in this document.

Chapter 2 of the thesis is already published as an article under the title "High throughput quantification of prohibited substances in plasma using thin-film solid phase microextraction" (*J. Chromatogr. A* **2014**, *1374*, 40-49) which was co-authored with B. Bojko under the under the supervision J. Pawliszyn. In all cases, experimental planning and design, experimental work conducted in the laboratory, data analysis, interpretation, and writing were performed by the author of the thesis.

Chapter 3 of the thesis is already published as an article under the title "Solid phase microextraction devices prepared on plastic support as potential single-use samplers for bioanalytical applications" (*Anal. Chem.* **2015**, *87*, 9722–9730) which was co-authored with B. Bojko and D. Hein under the under the supervision J. Pawliszyn. In all cases, experimental planning and design, experimental work conducted in the laboratory, data analysis, interpretation, and writing were performed by the author of the thesis.

The results presented in Chapter 4 have not yet been published in any journal. In all cases, experimental planning and design, experimental work conducted in the laboratory, data analysis,

interpretation, and writing were performed by the author of the thesis. Md. N. Alam also participated in the data interpretation and discussion, and J. Pawliszyn supervised the work.

The results presented in Chapter 5 have yet to be published in any journal. In all cases, experimental planning and design, experimental work conducted in the laboratory, data analysis, interpretation, and writing were performed by the author of the thesis. E. Boyacı contributed to the experimental work, the data processing, and the discussion of the results herein presented. The chromatographic conditions employed for the analysis of lipids were provided by the research group led by D. Vuckovic from Concordia University and J. Pawliszyn supervised the work.

The results presented in Chapter 6 have not yet been published in any journal. *In vivo* sampling was carried out in the facilities of the Center for Addiction and Mental Health (CAMH) in Toronto. C. Hamani, B. Bojko, and J. Pawliszyn participated in the design of the experiment. C. Hamani surgically implanted the sampling cannulas and DBS electrodes into the brains of the animals. All animals used in this study were solely handled by M. Diwan. In all cases, experimental work conducted in the laboratory, data analysis, interpretation, and writing were performed by the author of the thesis. B. Bojko, E. Boyaci, G.A. Gómez-Ríos, and T. Vasilejvic also participated in the experimental work.

Abstract

Successful determination of small molecules in complex biological systems requires implementation of robust analytical methodologies able to provide reliable information in a cost-effective and efficient manner. Solid phase microextraction (SPME) is a versatile, non-exhaustive sample preparation tool that has been demonstrated to be well-suited for facile analysis of biological matrices such as plasma, blood, and tissue. In SPME, a small amount of extraction phase immobilized on a solid support is utilized for the extraction of analytes of interest, either from the sample headspace or by direct immersion of the fiber in the matrix of choice. For the analysis of non-volatile compounds in complex biological matrices, SPME coatings made of sorbents embedded in a biocompatible binder (*e.g.* polyacrylonitrile (PAN)) are directly immersed into the sample under study for a defined period of time so as to allow for sufficient and reproducible extraction of analytes. The main advantages of such coating materials rely on their ability to provide high selectivity for extraction of small molecules; their aptness for immobilization in different support geometries; their inertness and robustness, which even enables their reusability in complex biological matrices; and their suitability towards *in vivo* extractions. In view of these advantages, the body of this doctoral thesis presents novel applications and developments of SPME for both targeted and untargeted analysis of different biological matrices such as biofluids and brain tissue.

The first part of the research conducted for this thesis encompasses the application of SPME in thin-film format for high throughput determination of multiple prohibited substances in plasma. A biocompatible SPME extraction phase made of hydrophilic-lipophilic balance (HLB) particles immobilized with PAN was employed for extractions, demonstrating satisfactory extraction capabilities for 25 compounds of a wide range of polarities (logP from -2 to 6.8). By taking full

advantage of the 96 thin-film handling capability of the automated system, a preparation time of approximately 1.5 min per sample can be achieved. Rewarding results in terms of absolute matrix effects were found for the majority of the studied analytes, given that 24 out of 25 compounds exhibited values in the range 100 - 120%. The method was validated in terms of linearity ($R^2>$ 0.99), inter and intra-day accuracy (85 – 130%) and precision ($< 20\%$), and limits of quantitation (0.25 – 10 ng mL^{-1} for most compounds).

Based on the positive results obtained after employing the developed method for the analysis of doping compounds in plasma samples, and considering the need for cost-effective and single use devices, the possibility of employing alternative materials to manufacture SPME devices was explored. To that end, new thin-film SPME devices prepared on plastic as potential single-use samplers for bioanalysis were developed and tested. Polybutylene terephthalate (PBT) was selected as a support based on its chemical resistance, low cost, and suitability as a material for different medical grade components. The proposed devices were assessed in terms of robustness, chemical stability, and possible interferences upon exposure to different solvents and matrices. Satisfactory results were obtained upon utilization of the manufactured samplers for the quantitation of multiple drugs in biofluids such as urine, plasma, and whole blood. Interestingly, our results showed that more than 20 extractions in complex biofluids can be performed without incurring significant changes in coating performance. These findings evidenced the robustness of PAN-based coatings applied on polymeric substrates, and opened up opportunities for the introduction of new support materials for manufacture of SPME biocompatible devices aimed at a wide range of applications.

Taking into account that SPME is a non-exhaustive extraction technique where analytes are extracted via free concentration, assessing the effect of variable matrix composition on final SPME

recoveries is invaluable in avoiding biased results. With this in mind, part of this thesis also involved the investigation of the effect of hematocrit (Hct) levels on SPME extractions from whole blood. The obtained results demonstrated that the Hct effect in SPME is dependent on the analytes of interest, and that different outcomes can be attained by varying experimental conditions such as coating type, convection, and extraction time. Interestingly, the relative affinities of target compounds for matrix components and coating materials were demonstrated to be one of the main determining factors on the final effect that erythrocyte levels impart on SPME recoveries. Although Hct content was shown to affect the extraction of each analyte differently, and be dependent on experimental parameters, correction of matrix variability is enabled through the use of appropriate internal standards.

In view of the rewarding results obtained in the analysis of a broad range of target analytes, SPME in its fibre configuration was evaluated based on its performance for untargeted analysis of brain tissue. For that purpose, the metabolite coverage provided by C18, mixed mode (MM), and HLB 7 mm fibres following extraction from brain homogenate at static conditions was assessed. Our results demonstrated that for compounds of medium to high polarity, both HLB and MM coatings were able to offer similar coverage at the same desorption conditions. For extraction of lipids, C18 and HLB exhibited the best recoveries with the use of 1:1 methanol:isopropyl alcohol as desorption solvent. Interestingly, the use of different desorption solvents was found to greatly influence the final composition of the brain extract obtained via SPME. Other parameters such as extraction time, coating washing step, and inter-fibre reproducibility were also considered and discussed.

Lastly, the balanced metabolite coverage provided by SPME was successfully utilized for *in vivo* monitoring of metabolic changes occurring in the hippocampus of rat brain after electrical stimulation (DBS) of the ventromedial prefrontal cortex (vmPFC), which has been previously

shown to induce anti-depressant like effects in rodents. The use of *in vivo* SPME enabled the monitoring of significant variations, not only among small polar metabolites such as amino acids, but also in lipids belonging to different classes. Compounds such as citrulline, glutamate, taurine, uric acid, sphingomyelins, and phosphatidylethanolamines, among others, exhibited statistically significant changes after acute exposure of animals to electrical stimulation for 3 hours. Although additional studies are needed to establish the contribution of the biochemical changes observed in this study to the effect of DBS in the treatment of depression, our work provided new directions towards a better understanding of the mechanisms taking place in the brain upon application of electrical stimulation to the vmPFC.

Acknowledgements

First and foremost, I am highly grateful to God for granting me this wonderful opportunity of pursuing my graduate studies abroad.

I would like to express my deepest gratitude to my supervisor and mentor, Professor Janusz Pawliszyn, for giving me the opportunity to be part of his research group - first as a Masters student, and now as a PhD candidate. I am sincerely grateful for being given the opportunity to be involved in so many exciting projects, for having been allowed to attend important conferences and scientific meetings where I could present my results and learn from other researchers, and for the valuable learning opportunities provided by Prof. Pawliszyn's research group.

I would like to thank my committee members, Professor Wojciech Gabryelski, Professor Michael Chong, and Dr. David Bell, for the time and efforts they have spent reading my thesis, and for their guidance and advice. I would also like to thank my external examiner, Professor Oliver Fienh, and my internal examiner, Professor Paul Craig, for accepting the invitation to be part of the evaluation committee of my work, and for the time and patience they spent in examining my thesis. Thanks to the examining committee for nominating my thesis to the Pearson Medal award.

I would like to extend my gratitude to those colleagues that helped me in different ways during my doctoral studies. I would like to specially thank Dr. Barbara Bojko for her guidance and help at the beginning of my PhD.

I want to say a big thank you to my lovely friends Ezel Boyaci and Emanuela Gionfriddo for their constant support, great company, and genuine friendship throughout these years - I was very lucky to have you both around to discuss science, to chat about life, and to laugh at everything. I want to also thank my dearest friends Erica Silva, Erasmus Cudjoe, and Jiang Ruifen for being so

Dedication

This thesis is dedicated to God, who gave me the resilience I needed during my journey towards the completion of this program; to my wonderful husband - without his unconditional love and encouragement, none of this would be possible; and lastly, to my parents, Emilce and Henry, and my siblings, Henry Mauricio and Estefania, for always being there to support and inspire me.

Table of Contents

List of Tables

List of Figures

List of Abbreviations

20-HETE   20-hydroxyeicosatetraenoic acid

6-OHDA   6-hydroxydopamine

ACN   acetonitrile

ADSA   axisymmetric drop shape analysis

AGC   automatic gain control

AMPA   α-amino-3-hydroxy-5-methyl-4-isoxazole propionic acid

ANOVA   analysis of variance

BG   basal ganglia

BL   baseline

BSA   bovine serum albumin

CAMH   Center for Addiction and Mental Health

CE   capillary electrophoresis

cGMP   cyclic guanosine monophosphate

CNS   central nervous system

CSF   cerebrospinal fluid

CUMS   chronic unpredictable mild stress model

CV   coefficient of variation

CW/TPR   carbowax/templated resin

DBS   deep brain stimulation

DBSS   dried blood spots

DI   direct immersion

DMF	N,N-dimethyl formamide
DS	dilute-and-shoot
DVB	divinylbenzene
EDTA	ethylenediaminetetraacetic acid
GABA	gamma-aminobutyric acid
GalCer	galactosylceramide
GC	gas chromatography
GluCer	glucosylceramide
GPi	globus pallidus internus
Hct	hematocrit
H-ESI	heated electrospray ionization
HILIC	hydrophilic interaction chromatography
HLB	hydrophilic lipophilic balanced
HLB-D	hydrophilic lipophilic balanced coated devices
HPLC	high performance LC
HRMS	high resolution MS
HS	headspace
IsoPs	isoprostane
LC	liquid chromatography
LHb	lateral habenula
LLE	liquid-liquid extraction
log P	logarithmic octanol-water partition coefficients
LOQ	limit of quantitation

LysoPE	lysophosphatidylethanolamine
MALDI	matrix-assisted laser desorption ionization
MD	microdialysis
MEPS	microextraction by packed sorbent
MIP	molecularly imprinted polymers
MM	mixed mode, C18 or C8 with benzenesulfonic acid group
MM-F	mixed mode fibres
MRPL	minimum required performance levels
MS	mass spectrometry
MS/MS	tandem MS
MTBE	methyl tert-butyl ether
NCE	normalized collision energy
NMDA	N-methyl-D-aspartate
NMR	nuclear magnetic resonance
NO	nitric oxide
NOS	nitric oxide synthase
OPLS	orthogonal partial least squares
PA	polyacrylate
PAN	polyacrylonitrile
PBA	phenyl boronic acid
PBS	phosphate-buffered saline solution
PBT	polybutylene terephthalate
PC	phosphocholine

PCA	principal component analysis
PD	Parkinson's disease
PDMS	polydimethylsiloxane
PE	phosphatidylethanolamine
PET	positron emission tomography
PFP	pentafluorophenyl
PLS	partial least squares
PP	protein precipitation
ppb	parts per billion
ppm	part per million
PPY	polypyrrole-based polymers
PRM	parallel reaction monitoring
PS-DVB	polystyrene-divinylbenzene
QC	quality control
RAM	restricted access materials
RP	reversed phase
rpm	revolutions per minute
RSDs	relative standard deviations
SEM	scanning electron microscopy
SM	sphingomyelin
SNpr	substantia nigra pars reticulate
SPE	solid phase extraction
SPME	solid phase microextraction

SRM	selected reaction monitoring
STN	subthalmic nucleus
TA	tranexamic acid
THC	tetrahydrocannabinol
THCCOOH	($\pm$)11-nor-9-carboxy-Δ^9- tetrahydrocannabinol
TOF	time-of-flight
UV	ultraviolet detection
VAMS	volumetric absorptive microsampling
vmPFC	ventromedial prefrontal cortex
WADA	World Antidoping Agency
XOR	xanthine oxidoreductase
β-NAD	β-nicotinamide adenine dinucleotide

Chapter 1: Introduction

1.1. Preamble

Nathaly Reyes-Garcés was the sole writer of this chapter. An excerpt of this introduction (500 words) was already published in the paper "E.A. Souza-Silva, N. Reyes-Garcés, G.A. Gómez-Ríos, E. Boyaci, B. Bojko and J. Pawliszyn. A critical review of the state of the art of solid phase microextraction of complex matrices III. Bioanalytical and clinical applications. *Trends Anal. Chem.* **2015**, *71*, 249-264", and is being reprinted in this thesis with permission of Elsevier, and in compliance with Elsevier and University of Waterloo policies.

I, Erica Souza-Silva, authorize Nathaly Reyes-Garcés to use the material for her thesis.

I, German A. Gómez-Ríos, authorize Nathaly Reyes-Garcés to use the material for her thesis.

I, Ezel Boyaci, authorize Nathaly Reyes-Garcés to use the material for her thesis.

I, Barbara Bojko, authorize Nathaly Reyes-Garcés to use the material for her thesis.

1.2. Sample preparation in bioanalysis

Bioanalysis can be defined as the field that covers the measurement of analytes of interest in a given biological system. In this sub-discipline of analytical chemistry, exogenous and endogenous compounds in complex biological matrices, such as biofluids and tissue, for instance, are analysed by employment of multiple methodologies tailored according to the analyte(s) of interest. The general bioanalytical workflow involves a series of steps, namely sampling, sample storage, sample preparation, instrumental analysis, and data processing, all of which are critical in guaranteeing reliable measurements. Considering the complexity of certain biological matrices and, in some cases, the demand for the processing of large numbers of samples in short periods of

time, bioanalytical chemists are constantly seeking new strategies that allow for cheap, fast, and accurate results. Currently, procedures encompassing mass spectrometry (MS) coupled with separation techniques such as gas chromatography (GC) or liquid chromatography (LC) have been adopted as instrumental methodologies in various analytical laboratories. For that reason, new developments in sample preparation strategies are almost always oriented to be compatible with such type of instrumentation. Taking into account the high selectivity offered by MS, and more specifically tandem MS (MS/MS) and high resolution MS (HRMS), the time spent optimizing sample preparation in targeted analysis today has certainly been minimized as compared to that needed for previously used procedures such as the earlier technique of choice, high performance LC (HPLC) coupled with ultraviolet detection (UV).[1] In regards to untargeted analysis, while simple and non-selective sample preparation methodologies are highly preferred, special precautions in terms of sample manipulation must be taken into consideration so as to ensure analyte integrity. Irrespective of the type of analysis being carried out, non-selective sample preparation of highly complex biological matrices can lead to the co-extraction of interferences capable of inducing ion suppression/enhancement in electrospray ionization (ESI) and/or compromising the performance of the analytical instrumentation. In this context, the evaluation and introduction of alternative sample preparation methodologies able to fulfill the needs of the application of interest are invaluable in the progress towards more efficient analytical strategies. With this in mind, in the following sub-section, a summary centered on the advantages and disadvantages of typical sample preparation approaches used to handle biological matrices, such as dilute-and-shoot (DS), protein precipitation (PP), liquid-liquid extraction (LLE) and solid phase extraction (SPE), is presented. As the molecular composition of such complex matrices is quite diverse, for the purpose of the currently presented work, only analysis of small compounds and

2

metabolites with molecular weights below 1200 Da has been considered for discussion. Next, important aspects pertaining to sample preparation for *in vivo* and untargeted metabolomics studies are discussed. Lastly, solid phase microextraction (SPME) is introduced as an attractive alternative tool in sample preparation of biological matrices for both targeted and untargeted studies.

1.2.1. Traditional sample preparation methods for LC-MS-based bioanalytical studies

The most common sample preparation approaches for the analysis of biofluids are DS, PP, LLE, and SPE. Depending on the type of matrix being analyzed, as well as the compounds of interest, one or a combination of these approaches is typically employed. DS, for instance, has been broadly reported as an adequate technique for processing of urine samples prior to LC-MS. In DS, an aliquot of sample matrix is further diluted with water by a factor ranging from 1:1 to 1:10.[2] As urine is a nearly protein-free matrix, this approach seems quite convenient for multiresidue studies. However, the salt content and highly variable composition of urine render this methodology very prone to ion suppression effects, particularly for the analysis of early eluting compounds.[3]

For analysis of biofluids characterized by a high protein content, PP is perhaps the most widely used sample preparation method. In this approach, an aliquot of sample matrix is mixed with a miscible organic solvent such as methanol or acetonitrile in proportions that vary from 1 to 4 "parts" of solvent per each "part" of biofluid. Use of other precipitating agents, such as salts, strong acids, and even heat, has also been reported.[4] In addition, several authors have studied the efficiency of different precipitants in terms of the percentage of protein being removed from the matrix. For example, in terms of protein removal efficiency, acetonitrile, 10% trichloroacetic acid (w/v), and zinc sulfate have been observed to be more effective than other precipitants.[5] However, in terms of LC-MS compatibility and absolute matrix effects, acetonitrile and 10% trichloroacetic

acid (w/v) are indicated as the best options for protein removal.[4,5] Although PP is a very simple strategy that provides good coverage for both polar and non-polar compounds, the final extract may contain high concentrations of matrix interferences that can hinder mass spectrometry analysis of certain compounds.

LLE, in turn, involves the use of a non-water miscible organic solvent to extract analytes of interest. Organic solvents such as hexane, cyclohexane, ether, ethylacetate, and methyl tert-butyl ether (MTBE) have all been used in different applications.[4] LLE offers satisfactory performance in terms of salt and protein removal. As extraction of a given analyte is affected by its charge (pKa) in this approach, the pH of the solution as well as the physicochemical characteristics of the analyte of interest play an important role in determining the extraction efficacy of LLE applications. Similarly to PP, LLE is a simple technique that has been used for decades. Nonetheless, the significant disadvantages this method imparts in terms of poor recovery of polar analytes, the possibility of emulsion formation, and lack of selectivity when conducting targeted analysis should not be neglected. It is worth emphasizing that both LLE and PP have been semi and fully automated in a 96-well plate format for the high-throughput analysis of biological fluids.[6,7] As a means to account for ionization effects and for the poor selectivity of both PP and LLE, careful evaluation of these methodologies in different sample batches with the use of appropriate internal standards is highly recommended as part of the method validation.

SPE, as one of the most widely employed sample preparation methods, has also been extensively reported in the analysis of different biological matrices.[8] In SPE, the sample matrix is passed through a cartridge packed with a sorbent material that displays high affinity for the target analytes. Prior to elution of compounds of interest from the sorbent bed, different rinsing solutions can be used to remove interferences from the cartridge so as to allow for improved selectivity. The

availability of various types of sorbent chemistries that enable the isolation of a wide range of compounds is undoubtedly an important advantage of SPE. Indeed, the development of new sorptive materials has been closely related to the expansion and broad acceptance of this technique as a sample preparation strategy in different fields. In many cases, SPE overcomes the disadvantages of LLE and PP in regards to sample dilution, lack of selectivity, and ionization suppression effects.[4] However, SPE requires longer optimization and sample preparation times, the extraction cartridges are usually expensive and single-use, and, depending on the complexity of the sample under study, clogging of cartridges may occur. When aiming for concomitant exhaustive extraction of multiple compounds with SPE, careful attention should be paid so as to not exceed the breakthrough volume of the compounds with lesser affinity for the sorbent material. To date, SPE has been successfully automated for multiple sample analysis, and is available in a 96-well plate format, providing sufficient throughput in bioanalytical applications.[9,10] For analysis of small sample volumes (around 10 µL), a miniaturized version of SPE, or MEPS (microextraction by packed sorbent), has gained wide acceptability in the bioanalytical field. Unlike typical SPE applications, in MEPS, each cartridge can be used several times, and on-line coupling with GC and LC is enabled. Applications of MEPS in bioanalysis have been thoroughly reviewed.[11]

In a discussion of sample preparation workflows employed to analyse biofluids, the dried blood spots (DBSS) technique is also worth of mention. DBSS is an alternative to traditional blood sampling that has gained wide acceptance in clinical analysis due to its low sampling invasiveness.[12,13] In DBSS, a small volume of blood (less than 20 µL) from a finger prick is collected onto filter paper cards and allowed to dry; subsequent desorption of the spot is then performed into an LC compatible solvent. As samples are deposited onto a paper and stored at

room temperature, no special storage or handling conditions are required for this technique. The main limitations of DBSS are associated with the need for highly sensitive instrumentation due to the low sample volume loaded on the paper (particularly in cases where the analyte is present at very low concentration), the potential degradation of unstable analytes due to storage conditions, and considerable variability in blood spreading owing to the type of paper used (chromatographic effect) and hematocrit levels (blood viscosity depends on hematocrit).[14] A more in-depth discussion pertaining to DBSS considerations is provided in Chapter 4. Due to the increasing applicability of DBSS in bioanalysis, significant progress has been made on automated on-line desorption of DBSS coupled with LC-MS/MS.[12,15–17] Based on the simplicity and low invasiveness of DBSS, further implementation in tests of clinical interest is foreseen for this technique.

The analysis of tissue, as a complex yet indispensable matrix in bioanalytical studies, also plays a vital role in targeted and untargeted analysis. It is well-known that workflows for isolation of analytes of interest from such complex media are labour intensive and time consuming. When preparing such types of samples, a homogenization step prior to the extraction process is almost always required. Depending on the type of tissue matrix (*e.g.* soft tissue such as brain or liver, tough tissue such as muscle or heart, or hard tissue such as skeletal bone) as well as on the analytes of interest (stable compounds or fragile metabolites), different homogenization strategies, such as grinding, cryogenic pulverizing, bead beating, sonication, and enzymatic homogenization, among others, can be used prior to extraction.[18,19] Further, the addition of solvent during the homogenization step has been observed to greatly facilitate the homogenization process as well as the extraction of analytes.[20] After tissue homogenates are obtained, PP and/or LLE, followed in some cases by SPE to improve extraction selectivity, can be carried out to isolate the analytes of interest.

1.2.2. *In vivo* sample preparation for tissue analysis

The study of biological systems typically involves a sampling step, where an aliquot representative of the status of the system is taken for further analysis. However, continuous monitoring of the system under investigation at close to real-time conditions can elucidate important information regarding the system that is not always accessible via traditional sample preparation workflows. For tissue analysis, the attainment of representative samples with aims of monitoring an organism at different time points is unlikely to be achieved without significantly compromising the status of the studied system. In this context, strategies for *in vivo* sample preparation have been proposed and implemented in several study cases. Of the currently available techniques today, microdialysis (MD) is perhaps the most widely used and accepted, with its applicability for *in vivo* and continuous measurement of several metabolites in various types of human and animal tissue demonstrated in various studies. In MD, a small probe with a semi-permeable membrane (typical molecular cut-off 10-50 kDa) is employed to determine the extra-cellular concentration of the analyte of interest. As illustrated in Figure 1.1, a perfusate solution, generally a buffer selected to resembles the composition of the extra cellular fluid, is pumped through a catheter (0.5 – 10 µL/min) that has been previously placed in the sampling site. As the perfusate flows, diffusion of analytes from the sampling media into the membrane takes place due to a concentration gradient. Simultaneously to the permeation of analytes into the acceptor phase, molecules of perfusate can also diffuse towards the sampling media. The dialysate (perfusate containing analytes) is collected for a defined period of time for further instrumental analysis.[21] MD has been successfully used in conjunction with LC-MS for *in vivo* determinations of several hydrophilic and small metabolites such as neurotransmitters and peptides, and also in pharmacokinetic studies involving different
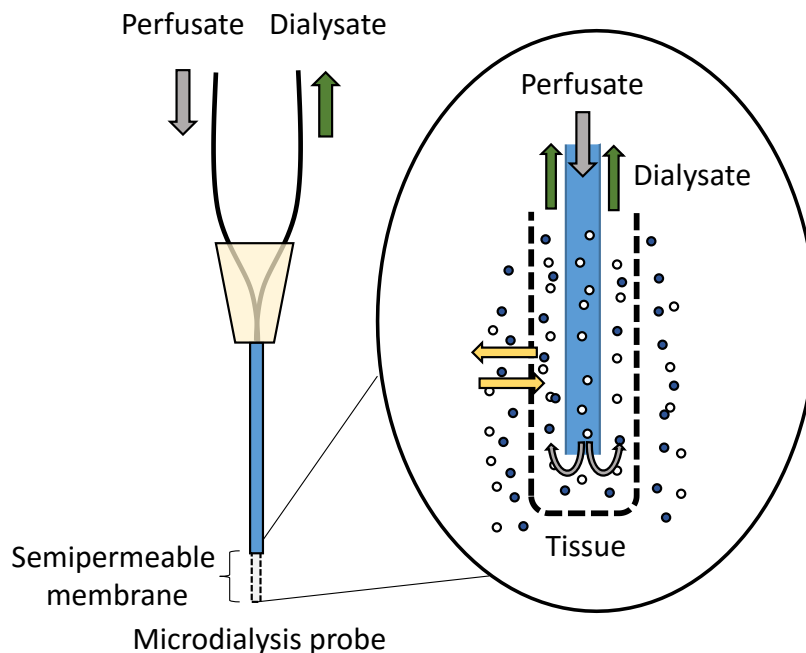
Figure 1.1. Microdialysis system. The perfusate inlet is connected to a slow flow pump. The dialysate is collected for further analysis.

drugs and drug metabolites.[22] Nonetheless, MD exhibits some limitations in the analysis of compounds prone to non-specific adsorption.[22,23] As a strategy to overcome this shortcoming, the incorporation of additives such as cyclodextrin and bovine serum albumin (BSA) in the perfusate solution has been proposed.[22,24] Although this approach has proven to be useful in the determination of several neuropeptides and endocannabinoids, decreases in the mass transfer process have been observed to occur in certain applications; further, the addition of BSA has been shown to restrict the attainment of a protein-free dialysate, thus requiring the addition of another step to the sample preparation workflow. Another disadvantage of MD relates to the not-so-compatible composition of the dialysate for MS analysis.[22] The high content of salts found in the perfusate solution, as well as the typical low concentrations that are attained in MD, both hinder the determination of several analytes of interest due to ion suppression effects and/or occasional

clogging of the MS inlet. To overcome this hindrance, a number of strategies aimed at avoiding the introduction of salts into the MS analyzer, including the use of divert valves, employment of an additional sample preparation step such as LLE or SPE (on-line or off-line), and column switching, have been reported by various authors in the literature.[25–27] Yet, despite the rewarding results obtained in the determination of several metabolites and exogenous compounds through the use of such approaches, the employment of MD in bioanalytical applications is limited due to its unsuitability for analysis of large hydrophobic compounds such as lipids, which are known biomarkers of significant biochemical interest. In this regard, SPME has been demonstrated to provide complementary information to MD. A more in-depth discussion regarding the application of SPME towards *in vivo* determinations of different compounds and metabolites can be found in Section 1.3.

Push-pull perfusion is yet another *in vivo* sampling approach that allows for the collection of tissue interstitial fluid. In this technique, artificial fluid is infused into tissue through one tube, while the collection of the infused fluid is performed with a second tube placed close to the infused area. Although push-pull perfusion is a relatively simple approach to access tissue information, this technique can induce significant tissue damage, as fluid is pumped into tissue using flows in the range of µL/min. With aims of overcoming this drawback and so as to improve spatial resolution, researchers introduced a modified version of this technique, namely low-flow push-pull perfusion, that employs significantly smaller flows and uses narrow bore capillaries.[28] The suitability of this methodology for *in vivo* tissue monitoring, particularly in neurochemical studies, has been demonstrated and also reviewed.[28–31] Although further evaluation of this technique is needed to assess its performance in the analysis of a broader range of compounds, it is anticipated that

similarly to MD, push-pull perfusion is not well-suited for the determination of hydrophobic analytes.

1.3. Sample preparation in MS-based metabolomics

Metabolomics can be defined as a field aimed at the systematic and comprehensive study of metabolite content (metabolome) present in biological systems. As metabolomics is the endpoint of the "omics cascade", the metabolome directly reflects the biochemical status of the system under study, and therefore, can be said to provide the closest representation of the individual phenotype of said system. However, due to the highly complex composition of the full metabolome, to date, no single platform is capable of accurately measuring all of its components.[32] In this context, several analytical workflows have been developed and evaluated in terms of metabolite coverage, limits of detection, and robustness.[2,33–36] Although nuclear magnetic resonance (NMR)-based platforms have shown rewarding results in multiple applications, their insufficient performance in the detection of metabolites occurring at low concentration levels have limited their applicability in certain metabolomics studies.[32,36] Conversely, MS-based approaches have been gaining increasing attention in metabolomics applications, owing to their capabilities for the analysis of compounds at pico and nanomolar concentrations.[36] Moreover, the suitability of MS for hyphenation with separation techniques such as GC, LC, and capillary electrophoresis (CE) has greatly facilitated the study of complex metabolite mixtures, while also aiding in the reduction of matrix effects.[36] While there are several different separation-MS combinations available to date, considering that LC-MS is the most widely used combination in bioanalytical applications, and also the approach of choice for the currently presented work, further discussion will be focused on LC-MS-based metabolomics workflows.

Two main strategies can be followed when performing metabolomics studies. The first, referred to as targeted metabolomics, applies to cases where a defined set of metabolites is measured owing to their involvement in a specific metabolic pathway, or because such metabolites belong to a particular class of compounds. The second strategy is called untargeted metabolomics, also known as global metabolomics, and relates to the determination of all detectable metabolites present in a given sample.[36] Whereas in the first strategy, experimental conditions can be tuned to enhance the recovery and detection of metabolites of interest, in the second approach, non-selective parameters must be selected with aims to gather unbiased information regarding the biological system under study. In regards to the advantages imparted by each approach, in the case of targeted metabolomics, fully quantitative information can be obtained, allowing for the validation of hypotheses regarding pathways being affected by different stimuli. On the other hand, in untargeted metabolomics, new information corresponding to unknown biological mechanisms can be unveiled, allowing for an enhanced understanding of biological systems.[36] Typical metabolomics methodologies, either for targeted or untargeted analysis, generally involve comparisons of at least two different groups of samples or individuals, where each group represents a defined biological status (*e.g.* control versus treatment group, or healthy versus diseased group). Comparisons can also be drawn out between samples taken from a single group of individuals before and after application of a given treatment. The employment of statistical tools allows for comparisons to be made between the metabolomes representative of each group, imparting valuable information regarding dysregulated compounds associated with different biochemical pathways affected by the treatment under investigation. Such studies have been successfully undertaken in different research areas with the use of cells, microorganisms, plants, animals, and

humans models.[37–40] As the scope of this thesis involves the analysis of biological matrices from animal and human origin, the oncoming discussion will be primarily focused on such matrices.

The success of any metabolomics experiment strongly relies on the appropriate execution of each of the steps of the analytical workflow (Figure 1.2). As can be seen in Figure 1.2, the first stage of a metabolomics study involves sample collection and storage, which must be controlled so as to avoid metabolome alterations. While different biological matrices can be used for metabolomics, with each demanding an optimized protocol for sample collection and analysis, biofluids are commonly selected as matrices of choice owing to their easy collection and biological significance. Urine, for instance, is a highly abundant matrix that contains representative information regarding all biochemical pathways occurring in a given organism. In addition, urine allows for non-invasive collection, which facilitates the sampling step.[41] To ensure proper preservation of the metabolites of interest, any bacterial activity should be avoided by filtering urine through a 0.22 µm filter after sample collection.[42] In addition, metabolome integrity should be guaranteed by keeping urine samples at - 80 °C, and by avoiding freeze-and-thaw cycles.[41] Other important biofluids in metabolomics studies are blood fractions. Blood fractions are the most widely used matrices in metabolomics, and unlike urine sample collection, collection of such matrices requires the involvement of professionally trained personnel. Although both serum and plasma have been successfully employed in multiple reports, the clotting procedure undertaken in the collection of serum samples has been previously shown to induce changes in metabolome composition.[43,44] As such, the use of plasma as a matrix of choice may enable a more accurate picture of the metabolic status of the investigated individual. When working with plasma and serum, certain factors must be taken into consideration. For instance, a suitable workflow for sample collection and storage
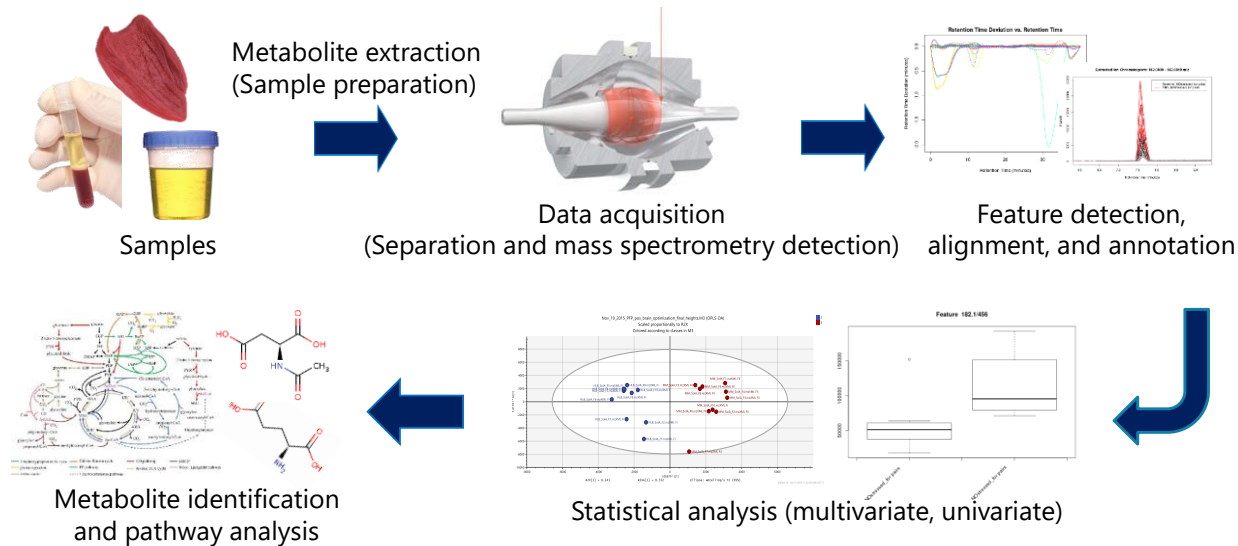
Figure 1.2. General MS-based metabolomics workflow.

should ensure that all samples are collected with the same type of anticoagulant (in the case of plasma),clotting conditions are controlled (in the case of serum), and that the method being employed is capable of avoiding hemolysis during the fractionation step. In addition, a storage protocol for blood fractions should include storage of samples preferably at - 80 °C, and be designed so as to prevent freeze-and-thaw cycles, which can greatly impact metabolome integrity. Other biofluids, such as cerebrospinal fluid (CSF), saliva, human breast milk, and bile, have been also utilized in metabolomics.[45] However, due their restricted availability, the number of publications reporting the analysis of such biofluids is significantly less extensive than that of urine and blood fractions. In addition to the use of biofluids, the analysis of tissue in metabolomics studies has gained a lot of attention, owing to the site-specific information that this matrix is capable of imparting. Nonetheless, collection of tissue is a very invasive procedure that requires highly trained medical personnel, while studies involving rodents usually involve their sacrifice during sampling. In sample manipulation of tissue, a rinsing step, either with water or buffer, is

recommended prior to storage of tissue specimens so as to avoid alterations of metabolome composition stemming from any remaining blood.[34,46] Liquid nitrogen is typically used for tissue metabolism quenching, with storage of samples also performed at -80 °C. As this matrix is solid and also heterogeneous, a homogenization step at very well-controlled conditions is required prior to extraction. Further information regarding considerations in tissue metabolomics is provided in Chapter 5.

After ensuring that the integrity of the metabolites of interest is maintained through application of proper controls to sample collection and storage, isolation of the metabolome from other matrix constituents can be undertaken. Given the complexity of any biological sample, the sample preparation method employed should be able to preserve the metabolome composition, while allowing for fast turnover times, reproducible results, and maximum metabolite coverage. Typical sample preparation approaches for metabolomics studies involve traditional methods such as DS, PP, and LLE, all which have already been described in Section 1.1.1. The advantages of these methods rely on their simplicity, affordability, and non-selectivity, which facilitate the processing of large volumes of samples. DS, for instance, has been demonstrated to be a suitable approach in untargeted urine metabolomics, with satisfactory results in terms of instrumental drifting, retention time stability, and repeatability for highly abundant compounds (coefficient of variation (CV) < 15%) reported when using reversed phase chromatography in combination with MS.[47] However, in the same study, low intensity signals were found to be characterized by high variability, which could be correlated to the absence of a clean-up step and possible matrix effects. For solvent-based extraction approaches, PP with the use of organic solvents is recognized as the most broadly used strategy in untargeted analysis of biofluids. Several studies directed at the identification of optimum PP conditions have shown that the use of methanol, either alone or with other solvents

such as ethanol and acetonitrile, offers optimal results in terms of detected metabolite features.[48,49] Moreover, aiming to reduce metabolome alterations, the use of cold solvents has been reported in several sample preparation workflows as part of the metabolism quenching step.[35,40,50] However, it should be highlighted that complete precipitation of proteins is not always easily attained when using solvents. For that reason, a careful assessment of LC column performance should always be considered in method development, as protein build up has been shown to decrease typical column lifetime.[2] As another well-known sample preparation technique, LLE is also widely applied in both targeted and untargeted metabolomics. Due to the selectivity of LLE for the extraction of hydrophobic compounds, this approach has been particularly useful for the analysis of multiple lipid classes. For this purpose, different solvents have been tested with aims to determine which solvents enable the best recoveries for various biological matrices. Among recent lipidomics studies, the most commonly employed solvent combinations are chloroform/methanol and MTBE/methanol.[51] Alternatively to using PP and LLE independently, a combination of both approaches has been proposed with aims of expanding the coverage of the metabolome extracted from a single sample.[52] In this interesting methodology, sample preparation of only 20 µL of plasma is performed in an HPLC vial by adding small aliquots of water, methanol, and 200 µL of MTBE. After mixing and centrifuging the vial contents, separation of the different solvent phases occurring in the same vial can be accomplished. Analysis in two different chromatographic methods, one for metabolites and one for lipids, is conducted by injecting from the same vial at two different needle positions. Besides facilitating the recovery of a broad range of metabolites from plasma, this approach has been demonstrated to be highly reproducible in comparison to methods that require evaporation and reconstitution. Based on the positive results provided by this methodology, an evaluation of its performance in analysis of brain tissue homogenate was also

conducted.[53] Rewarding results were obtained, with approximately 4000 metabolite features detected from 3 mg of tissue. Further assessments of this in-vial dual approach towards the analysis of more tissue types should enable better insights regarding its applicability. Another sample preparation technique that has been evaluated in metabolomics studies is SPE. Although it may seem that the selectivity offered by SPE sorbents is not ideal for global metabolomics applications, results worthy of discussion have been obtained. For instance, Michopholus et al. compared PP with acetonitrile and methanol versus SPE using C18 cartridges in terms of metabolite features extracted from human plasma. Their results demonstrated that SPE allowed for significant improvement in method repeatability compared to other methodologies.[54] In more recent work, a thorough comparison of seven methods, including different conditions for PP, LLE, and SPE, was conducted using plasma as a model matrix.[55] Results showed that although SPE provided an additional 600 features not detected by other methods, the use of multiple extraction approaches for analysis of individual samples did not translate into significant improvements in metabolome coverage. In addition, the same study confirmed that the best coverages were observed for methods using PP with methanol; however, PP approaches were also evidenced to be highly prone to matrix effects, which hinder the analysis of low intensity features and can also lead to biased results. As can be inferred from the discussion presented until now, there is no sample preparation approach available today that is capable of providing a complete, unbiased snapshot of the entire metabolome of a given system. In view of the short-comings of the available methodologies, various strategies have been implemented to facilitate the gathering of high quality data in metabolomics, such as including quality control samples to ensure analytical precision (technical replicates) and instrumental stability (instrumental replicates), addition of internal standards to account for variations in sample preparation and instrumental drift, randomization of samples

injections to avoid any systematic bias, analysis of blank samples to account for background artefacts, and the incorporation of sufficient biological replicates, among others. Alternative to more conservative methodologies where sample preparation is performed *in vitro*, the use of *in vivo* sampling/sample preparation for metabolomics presents an interesting opportunity for investigations of biological systems from a different perspective. As extractions are carried out directly from the living organism, improved recovery of unstable compounds and reduced risks of metabolome alterations are facilitated.[2,56,57] Moreover, as *in vivo* applications enable the monitoring of the same system or organism at different time points, such applications facilitate the detection of small changes that could shed light on different biological processes. MD, for instance, has been extensively employed for the concurrent targeted analysis of selected neurotransmitters.[29] Pertaining to applications covering a broader range of metabolites, only few reports analysing MD dialysates via LC-MS have been published to date, likely due to the complex composition of the perfusion solution. In one of those studies, analysis of dialysates obtained *in vivo* from a crustacean hemolymph was undertaken with the use of CE and matrix-assisted laser desorption ionization (MALDI) coupled to ion mobility MS, and also through employment of LC-MS. By employing this multifaceted platform, the authors were able to identify 208 metabolites, from which 39 were found to be neurotransmitters.[58] Similarly, in recent work, MD was employed for the *in vivo* monitoring of wound fluids released from bone and soft tissue healing.[59] Results showed that the use of proteomics and metabolomics workflows enabled the determination of important biological differences between the two wound scenaRíos. Despite the limited number of metabolomics works reported in the *in vivo* sampling/sample preparation field, this approach imparts great promise in the metabolomics field, as it can provide complementary information to what is already known

from typical *in vitro* workflows. The role of SPME is this modality will be further discussed in Section 1.3.4.

In regard to the use of LC-MS for instrumental analysis of global metabolomics extracts, a plethora of methodologies employing multiple LC columns and various MS analyzers have been described and recently reviewed.[36,60–62] In terms of separation conditions, distinct chromatographic methods using stationary phases such as C18 for reversed phase analysis and hydrophilic interaction chromatography (HILIC) are normally applied in the same study. This strategy allows for an expansion in metabolome coverage by facilitating the retention of compounds with different polarities. Regarding MS analyzers, high resolution instruments such as time-of-flight (TOF) and Orbitrap, either with or without quadrupoles, are typically used.[36] As the body of this work is mostly focused on the sample preparation aspects of metabolomics applications, an in-depth discussion of different LC-MS conditions is not presented.

The last part of the metabolomics workflow involves data processing, statistical analysis, and interpretation. As this topic is significantly broad and detailed protocols providing guidance in metabolomics data processing and statistical analysis have been published by several authors, only a brief overview of the different steps that are normally followed are herein provided.[63–67]

In metabolomics data processing and analysis, various software and algorithms can be employed to enable extraction of information regarding the detected metabolite features in the entire sample set. Each feature is characterized by its m/z, retention time, and intensity. As each metabolite can be defined by different adducts, isotopes, and, in some cases, in-source fragments, the annotation of features via packages such as CAMERA can aid in the identification of various features related to a given analyte.[68] Once this information is obtained, statistical analysis can then be carried out.

For this purpose, univariate and/or multivariate data analyses are conducted with aims to determine which metabolites are being dysregulated due to the condition or treatment under study. Univariate analysis is undertaken with aims to estimate statistical changes of individual features or compounds across different groups; depending on whether the data is normally distributed and on the analytical variance, different parametric (*e.g.* t-test, Welch's test and ANOVA) and non-parametric tests (*e.g.* Mann Whitney U and Kruskal-Wallis) can be performed. On the other hand, in multivariate analysis, all variables (metabolite features) are simultaneously analysed through employment of unsupervised (principal component analysis (PCA) and/or supervised methods (partial least squares (PLS), and orthogonal partial least squares (OPLS)). Once statistically significant discriminating features or metabolites are detected, their identity is confirmed by searching their accurate masses in available databases, by interpreting their fragmentation patterns, and when available, by running certified standards. Lastly, biochemical interpretation of the data can be performed in view of the specific condition and/or treatment being studied. Although this step must often be accompanied by in-depth literature revision, several tools to aid in the interpretation and correlation of affected metabolic pathways are available and free of charge.

1.4. Solid phase microextraction (SPME)

1.4.1. The principle of SPME

SPME is a non-exhaustive sample preparation approach that integrates sampling and sample preparation in a single step. In this microextraction technique, a small amount of extraction phase immobilized in the outer part of a solid support is used to isolate analytes of interest from a given sample matrix. The microextraction process is undertaken by exposing the SPME probe to the sample of interest for a defined period of time at a constant set of experimental conditions. During extraction, an amount of analyte proportional to its concentration in the sample is collected

onto/into the SPME coating. Depending on the characteristics of the analyte of interest, the SPME device can be placed in the headspace (HS) of the sample matrix (only for volatile and semi-volatile compounds), or can be directly exposed to sampling media via direct immersion (DI). Instrumental analysis is carried out either by thermally desorbing the analytes extracted by the SPME probe in the injector of a gas chromatograph, or by exposing the SPME coating to a desorption solvent, and subsequently injecting the final extract into an LC-MS or any other suitable analytical instrument. A schematic illustrating the general SPME workflow is presented in Figure 1.3.
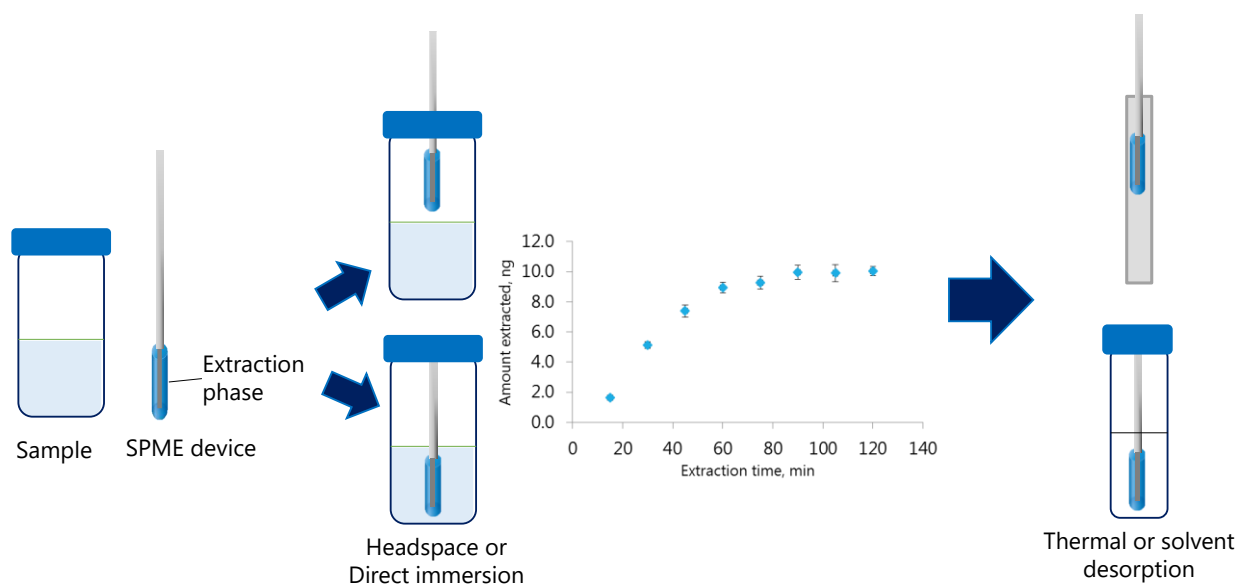
Figure 1.3. General schematic of the SPME process.

The successful implementation of SPME for any type of application is strongly dependent on a good understanding of the microextraction principles that govern extraction. As SPME is an equilibrium extraction technique, maximum analytical sensitivity is attained when the coating is exposed to the sample matrix for a time period that is long enough as to allow for equilibration. In other words, no further increases in the amount of analyte collected will be observed after

equilibration has been reached. At such conditions, the amount of analyte extracted is given by

Equation 1.1, where n is the amount of analyte extracted onto the coating, C_f^∞ is the concentration

of analyte in the fibre coating at equilibrium, V_f is the volume of extraction phase, C_0 is the

concentration of analyte in the sample matrix, K_{fs} is the distribution constant of analyte between

the extraction phase and the sample matrix, and V_s is the sample volume.

$$n = C_f^\infty V_f = C_0 \frac{K_{fs}V_sV_f}{K_{fs}V_f+V_s} \qquad\qquad 1.1$$

In cases where the volume of sample is much larger than the volume of the extraction

phase, $K_{fs}V_f \ll V_s$, Equation 1.1 can be simplified to Equation 1.2. Thus, quantification of

analytes of interest in systems with volumes considerably larger than that of the extraction phase

can be accomplished without knowledge of the volume of the sampling media (*e.g.* on-site

analysis).

$$n = K_{fs}V_fC_0 \qquad\qquad 1.2$$

From Equation 1.2, it is also clear that the amount of analyte extracted at equilibrium is

proportional to K_{fs}, namely the distribution constant. This parameter is directly correlated with

other factors such as the physicochemical properties of a given analyte, coating chemistry, and

sample matrix characteristics (including temperature, pH, and ionic strength, among others). In

view of this, satisfactory method sensitivity can be obtained by ensuring favorable K_{fs} values,

which can be accomplished by selecting appropriate coatings, and/or through modifications to the

sample matrix. It should be noted that Equation 1.1 only applies for coating materials such as

polydimethylsiloxane (PDMS) or polyacrylate (PA), which extract via absorption. For adsorptive

extraction phases, the surface active sites where analytes bind should be taken into consideration.

In such cases, the equilibrium amount of analyte can be estimated as follows:

$$n = C_f^\infty V_f = \frac{KC_0 V_s V_f (C_{f\,max} - C_f^\infty)}{KV_f(C_{f\,max} - C_f^\infty) + V_s} \qquad 1.3$$

where K is the analyte's adsorption equilibrium constant, $C_{f\,max}$ is the maximum concentration of active sites in the coating, and C_f^∞ is the equilibrium concentration of analyte in the fibre.

One of the most important parameters in any microextraction process is extraction time. As emphasized previously, maximum sensitivity is achieved at equilibrium conditions; however, as large K_{fs} provide long equilibration times, the use of SPME at pre-equilibrium, which can achieved by accurately controlling extraction time, is certainly preferred in many cases. At such conditions, the amount extracted is calculated by using Equation 1.4, where a is a time constant and t is extraction time.[69]

$$n = (1 - e^{-at}) \frac{C_0 K_{fs} V_s V_f}{K_{fs} V_f + V_s} \qquad 1.4$$

Other parameters that affect equilibration time are the convection conditions, the thickness of the coating $(b - a)$, and the analyte's diffusion coefficient in the sample (D_s). Considering that equilibrium is reached when 95% of the equilibrium amount is extracted, equilibrium time can be calculated by employing the following Equation:

$$t_e = t_{95\%} = 3 \frac{\delta K_{fs}(b-a)}{D_s} \qquad 1.4$$

The term δ in Equation 1.4 refers to the thickness of the boundary layer. The boundary layer comprises a region in between the bulk of the sample matrix and the extraction phase, where the flux of a given analyte is mostly controlled by diffusion. As the thickness of the boundary layer is determined by both the agitation conditions and the diffusion coefficient of a given analyte, distinct analytes in the same system will have different δ values.

At this point, several experimental variables that influence the microextraction process have been listed and discussed. As can be inferred from the above discussion, successful application of SPME toward any type of study certainly depends on the degree to which experimental parameters that affect extraction recoveries are controlled (*e.g.* convection, temperature, extraction time, etc). Another factor that needs to be taken into consideration when employing SPME or any other microextraction technique relates to the distribution of the analyte among the different phases present in the sampling system. For instance, if SPME is to be applied for the determination of hydrophobic compounds in water samples, the stability of the analytes under study should be carefully controlled so as to avoid altering their respective concentrations within the sample matrix. In such cases, the poor solubility of the analytes in water can lead to losses due to adsorption on vessel walls, or owing to their precipitation. As this is not likely to occur in sample preparation approaches such as LLE, where the sample container is rinsed with extraction solvent, the applicability of SPME can be underestimated by inexperienced users. On this note, it should be emphasized that the extraction process in SPME occurs via free concentration. Accordingly, in analyses of complex systems or matrices where multiple phases that could display affinity for analytes coexist (*e.g.* proteins, cells, organic matter, particles, et.), the amount of analyte extracted by SPME is not only proportional to its overall concentration in the sampling media, but also proportional to the its free concentration at the moment of the extraction. While SPME method sensitivity towards the analysis of compounds that exhibit high binding for matrix components can be hindered owing to the low availability of such analytes, modifications to the sample matrix may be considered to increase their free fractions (*e.g.* addition of organic solvent). Thus, in spite of the limitations it may impose on certain applications that involve the determination of highly bound analytes, SPME's ability to only extract via free concentrations is an attractive bonus in

analysis, as it enable determinations of free, total, and therefore bound concentrations of analytes in complex systems through the use of appropriate calibration strategies.

Several SPME calibration approaches have been developed to date, with the choice of calibration strategy being dependent on the goals of the research and parameters such as analyte and system under investigation.[70] Although some calibration methods are not conventional due to the non-exhaustive nature of SPME, various studies both demonstrating their applicability and reporting details regarding their principles and procedures have been published and reviewed in recent years.[71–73] In the currently presented thesis, matrix-matched calibration was employed as an SPME quantification strategy. In matrix matched calibration, total concentrations can be calculated by spiking known amounts of analyte in a blank matrix that can truly mimic the intrinsic conditions and characteristics of the sample under study. In application of this method, it is critically important that satisfactory simulation of the characteristics of the sample matrix be achieved, since changes in pH, ionic strength, and protein or organic matter content can significantly affect degree to which a given analyte is bound to the matrix; consequently, erroneous concentrations may be estimated in cases where such characteristics are not sufficiently accounted for. To compensate for possible variations in the extraction conditions and in the sample matrix, the use of an appropriate internal standard, ideally deuterated, is highly recommended. If information regarding the free and bound concentrations of the analyte is also required, a calibration curve for the analyte should also be prepared in a physiological buffer where the analyte is free of binding components (free concentration = total concentration). Other important factors should also be taken into account when performing quantification via SPME: first, the organic solvent volume used to spike analytes ideally should be kept below 1% so as to avoid alterations in the binding conditions in the sample matrix.[74] Second, once analytes and internal standards are spiked in the blank matrix for

24

determination of total analyte concentrations, enough incubation time should be allowed so as to ensure a complete binding. Third, the sample/solvent volume should be large enough so as to ensure that the whole SPME coating is immersed during extraction/desorption. Since sample and desorption solvent volumes are typically very similar, sufficient analyte pre-concentration might not be achieved through employment of SPME, especially if the analyte under study is present at a considerably low concentration level. In such cases, addition of steps such as solvent evaporation and reconstitution may be required in the workflow.

1.4.2. Thin-film microextraction: another geometry of SPME

The most well-known configuration for SPME devices is the fibre geometry, which consists of a wire that has a well-defined coated length. However, in accordance with SPME principles, extraction devices can adopt multiple geometries and shapes that are tuned based on the application of interest. As SPME is a non-exhaustive extraction technique, sensitivity issues can arise in cases of considerably low analyte concentrations (C_0) or low affinity of compounds of interest for the extraction phase (K_{fs}). Therefore, as a strategy to improve method sensitivity, the use of larger extraction phase volumes (V_f) can be considered as a suitable option (Equation 1.2). While increases to extraction phase thickness will lead to longer equilibration times (Equation 1.4), the use of larger extraction phase areas, on the other hand, allows for improved sensitivity without sacrificing method throughput.[75] Such devices, consisting of a large coated surface area and a thin coating thickness (large extraction phase surface area-to-volume ratio), are known as thin-film microextraction devices, and have been employed in several applications involving GC- and LC- amenable compounds.[76] In GC applications, PDMS self-supported membranes, as well as extraction devices made on a solid supports using PDMS and embedded sorbent particles, have

been used for the analysis of samples of environmental origin.[75,77,78] Thin-film microextraction devices prepared by immobilizing biocompatible extraction phases on stainless steel blades have also been employed in various studies involving determination of non-volatile compounds, including studies of bioanalytical interest.[79,80] Pertaining to the analysis of LC-amenable compounds, a fully automated workstation that allows for the high-throughput, simultaneous analysis of up to 96 samples is currently available.[81] Indeed, the second chapter of this thesis is fully dedicated to the application of this high throughput platform for the analysis of multiple doping substances in plasma samples. Considering that the use of thin-film microextraction may also allow for close to exhaustive recoveries in certain cases, the term open-bed SPE is also applicable to such devices in cases where significant amounts of analyte are extracted, or when remarkable depletion of analytes occurs after the extraction. Further details regarding the applications, advantages, and disadvantages of thin-film microextraction for the analysis of biological matrices are provided in the following sections.

1.4.3. Analysis of biofluids using SPME and LC-MS

Although SPME was initially introduced for the analysis of volatile compounds of environmental interest, the evolution of this sample preparation technique in terms of coating chemistries and manufacturing materials has enabled its application in the determination of non-volatile compounds in complex biological matrices. The first reports documenting the use of DI-SPME for the analysis of different biofluids involved employment of coatings such as PDMS, PA, PDMS/ divinylbenzene (DVB) and carbowax/templated resin (CW/TPR).[82] Other extraction phases employed for the extraction of different compounds from matrices such as blood fractions include restricted access materials (RAM), molecularly imprinted polymers (MIP), polypyrrole-based

26

polymers (PPY), sol-gels, as well as immunoaffinity sorbents, where antibodies are immobilized for highly selective extractions.[82] Although all of the above-mentioned coatings types were able to provide satisfactory results in several studies, their low affinity for certain compounds, in addition to their short life-times when immersed in complex samples, hindered their further implementation in the analysis of biological samples. In this context, the introduction of coatings made of a biocompatible binder, such as polyacrylonitrile (PAN), and diverse sorbents, such as SPE particles, has greatly facilitated the development and application of SPME as a sample preparation tool in bioanalytical applications.[83] Among the most important advantages of PAN-based SPME extraction phases, features such as outstanding robustness in direct exposure applications to complex, untreated biological matrices; high selectivity for small molecules; satisfactory biocompatibility; and manufacturing cost-effectiveness stand out to showcase the high suitability of this coating towards bioanalytical applications. Moreover, given that different types of SPE sorbent chemistries can be used in the preparation of PAN-based coatings, such coatings enable "tuning" of the most convenient SPME extraction phase according to the analytes of interest. Several studies published in the last years have demonstrated the suitability of such coatings, in both fibre and thin-film formats, for the determination of various analytes in matrices such as urine, plasma, serum, blood, and bile.[80,84–88] For instance, in 2012, Boyacı et al. demonstrated the suitability of thin-film microextraction devices prepared using C18 and PAN for the quantitation of a broad range of controlled substances in urine samples.[80] In such work, the authors were able to achieve satisfactory results in terms of absolute matrix effects with minimum sample pre-treatment, thus supporting the feasibility of employing SPME prior to LC-MS. Bojko et al. proved the potential of automated thin-film SPME in clinical analysis by monitoring tranexamic acid (TA) in plasma samples of patients undergoing cardiac bypass surgery.[89] The

27

high-throughput feature offered by this technology enabled prompt analysis of a large number of samples, as well as the determination of TA pharmacokinetic profiles for each patient (n=10). Good agreement was found between the proposed methodology and PP. Similarly, Gorynski et al. proposed a high-throughput SPME method for the concomitant analysis of both rocuronium bromide and TA in plasma.[90] Despite the considerable differences between the two target analytes, satisfactory results were obtained by employing a weak cation exchanger as an SPME extraction phase. In addition to drug analysis, high throughput SPME in thin-film format has been employed for the determination of polyunsaturated fatty acids in plasma samples. In that study, the use of a C18-PAN as extraction phase enabled the determination of changes in concentrations of fatty acids such as α-linolenic acid, arachidonic acid, and docosahexanoic acid in plasma samples of patients undergoing cardiac surgery.[91] The results obtained from this study certainly demonstrated the applicability of SPME towards the quantitative measurement of highly hydrophobic compounds that display significant affinity for plasma components. A variety of alternative coating materials, including aptamers, magnetic molecularly imprinted polymers, and polythiophene, among others, have also been reported as suitable for DI-SPME in biofluids.[92–94] In more recent work conducted by Gionfriddo et al., a type of fluoropolymer was introduced as a promising binder to immobilize hydrophilic lipophilic balanced (HLB) particles for SPME, with extraction followed by instrumental analysis with GC and LC platforms.[95] The coatings developed in this study demonstrated satisfactory performance in evaluations involving whole blood extractions. Given their simple manufacturing process, which does not require a thermal curing step, their further implementation in a broader range of applications is anticipated.

Other SPME formats successfully employed in biofluid analyses are in-tube and in-tip SPME. In-tube SPME, which uses a piece of capillary column as extraction medium, was the first fully

automated SPME approach designed specifically for compatibility with LC analysis. Although this technique is limited by the need for very clean samples (so as to avoid clogging of the capillary) and its comparative low throughput, in-tube SPME has been reported as the sample preparation technique of choice in quite a large number of biomedical analysis studies.[96,97] In-tip SPME, in turn, is an alternative high-throughput configuration of SPME introduced by Xie, Mullett, Miller-Stein & Pawliszyn in 2009.[98] In this SPME approach, commercial SPME fibers are in-housed in poly-propylene pipette tips through employment of polyethylene frits to secure and hold fibres in place. The most important advantage of this approach is its compatibility with automated liquid handling systems for 96-well plates (*e.g.*, Tomtec Quadra 96) typically used in the pharmaceutical industry. In this approach, the SPME sample preparation workflow consists of multiple aspiration/dispense cycles. To date, in-tip SPME has been employed for the analysis of drug candidates (MK-0533) and (MK-0974) in human plasma, and for the determination of vitamin D3 in human serum through chemical derivatization.[98–100]

1.4.4. DI-SPME and LC-MS for *in vivo* animal studies

One of the most attractive features of SPME is its suitability for *in vivo* analysis. Indeed, several studies reported to date have demonstrated the applicability of this technology towards monitoring of concentrations of different drugs and metabolites in several living biological systems.[73,101,102] As it pertains to the analysis of biofluids, SPME has been successfully used for pharmacokinetic monitoring of benzodiazepines, carbamazepine, and carbamazepine-10,11 epoxide (carbamazepine metabolite) in animal models, including models such as beagle dogs and rats.[103,104] The main advantage of such approach is the elimination of the blood withdrawal step from the analytical workflow, which serves to reduce the risk of changes in sample matrix

composition and in the free concentration of non-stable analytes. Furthermore, since *in vivo* SPME allows for multiple samplings of the same system over time, the study of ongoing dynamic processes, such as drug pharmacokinetics, is facilitated to a considerable extent. A detailed protocol regarding the experimental parameters that should be used to determine intravenous concentrations of drugs and metabolites by application of SPME is available in the literature.[105] With reference to tissue determinations, SPME has been applied for *in vivo* analysis of several matrices; a schematic of the general workflow is depicted in Figure 1.4.[102] Togunde et al., for instance, were able to quantify drugs such as fluoxetine, venlafaxine, sertraline, paroxetine, and carbamazepine in rainbow trout and fathead minnow by performing *in vivo* non-lethal sampling
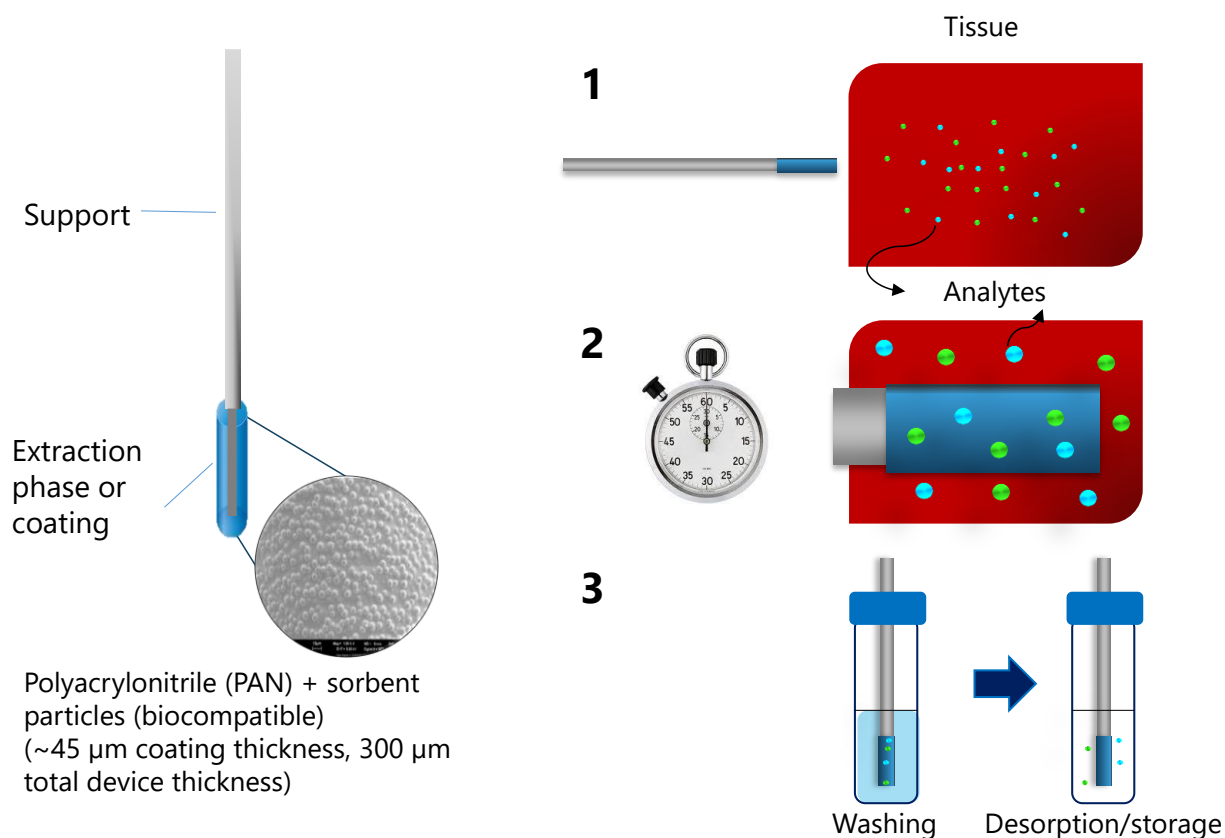
Figure 1.4. Schematic of SPME workflow for analysis of tissue samples.

using C18-PAN coatings.[106] The rewarding findings of that work indicated that SPME is a well-suited tool for environmental studies related to fish bioconcentration, as the technique allows for continuous monitoring of the same individual specimens over time. Polydopamine sheathed nanofibers have also been employed to monitor pharmaceuticals in fish tissue.[107] A comparison between concentrations of fluoxetine determined in fish tissue through application of LLE and SPME demonstrated that both techniques provide statistically equivalent results. In another study, SPME and MD were successfully used to measure dopamine, serotonin, gamma amino- butyric acid, and glutamic acid changes in rat brain at different time points following fluoxetine administration.[56] By using 4 mm fibres coated with C18 and benzene sulfonic acid functionality, the authors of that work were able to obtain comparable results with both sampling techniques, validating the applicability of SPME towards such studies. As evidenced in the literature, the biocompatibility of SPME together with its simple deployment has facilitated its evaluation in diverse *in vivo* scenarios. The advantages of this approach for metabolomics studies will be presented in the following section.

1.4.5. SPME and LC-MS in clinical metabolomics

The applicability of SPME for metabolomics studies was initially proposed for profiling of volatile metabolites. This particular approach has been satisfactorily implemented in field applications for analysis of different matrices, such as serum, urine, bacteria cultures, saliva, and feces, among others, via headspace extraction.[108–113] Conversely, application of DI-SPME has only been recently introduced and evaluated for metabolomics studies using LC-MS analysis. In initial work conducted to identify potential SPME coatings suitable for such purpose, Vuckovic et al. reported a complete assessment of several SPE-based extraction phase chemistries in terms of metabolite

coverage.[114] To this end, 42 types of SPE particles, including silica-based, polymer-based, and carbon based particles, were immobilized and used in the manufacture of SPME coatings for a broad set of metabolites, covering polarities from Log P -7.9 to 7.4. Results showed that mixed mode (MM) (C18 or C8 with benzenesulfonic acid group), phenyl boronic acid (PBA), and polystyrene-divinylbenzene (PS-DVB) coatings performed best in terms of hydrophilic and hydrophobic metabolite extractions. In this context, it is worth highlighting that the applicability of SPME for untargeted studies via DI relies on the fact that analytes are extracted via free concentration, as was already highlighted in Section 1.3.1. Hence that in biological samples such as plasma, where multiple matrix components such as proteins and metabolites occur, it is expected that hydrophilic analytes will be present at high free concentrations, as they normally do not display significant affinity for any matrix constituents. On the other hand, hydrophobic compounds will exhibit low free fractions, as such compounds are usually bound to different matrix components such as proteins. Considering that SPME typically provides better extraction efficiencies for compounds that display a certain degree of hydrophobicity, balanced metabolite coverage can be expected in cases where this technique is used for untargeted studies. Based on results obtained in a coating evaluation study, Millipore Sigma (previously Supelco) developed SPME devices coated with MM and C18 biocompatible extraction phases for both *in vitro* and *in vivo* applications.[87] In order to assess the performance of SPME versus other sample preparation techniques traditionally employed in untargeted metabolomics, a comparison, using human plasma as model matrix, was conducted in terms of metabolite features extracted with SPME MM coatings versus those detected with ultrafiltration and PP.[114] The results obtained in this study demonstrated that not only is SPME able to perform comparably in relation to the other two techniques studied as it pertains to the number of metabolite features detected, this micro sampling technique was also

shown to allow for better recoveries of non-polar metabolites (SPME vs ultrafiltration), as well as for a reduction in ionization effects (SPME vs PP). Similar results were observed when SPME and MD were used for *in vivo* sampling from rat brains.[56] The findings of this work evidenced that SPME was able to facilitate the extraction of hydrophobic metabolites such as lipids, which are usually poorly or non-detected in MD extracts, whereas MD allowed for the detection of hydrophilic dipeptides and aliphatic amino acids that were not observed with SPME. Thus, the obtained findings of this study support the applicability of SPME as a complementary tool to MD for *in vivo* metabolomics studies. As unstable compounds can be lost or degraded into different metabolites during traditional sampling and sample preparation steps, in this sense, the feasibility of capturing the entire *in vivo* metabolome of a given system enables the exploration and further understanding of biological systems. For instance, in an experiment that sought to compare results of *in vivo* blood sampling versus those obtained by *ex vivo* SPME, protein precipitation, and ultrafiltration, researchers found that unstable compounds such as β-nicotinamide adenine dinucleotide (β-NAD) were only present in extracts corresponding to *in vivo* SPME.[57] Although further studies are required in order to confirm the stability of different metabolite types extracted *in vivo* on SPME coatings, the results of the abovementioned study support the notion that SPME is capable of capturing an elusive portion of the metabolome by employment of *in vivo* sampling strategies. Other studies involving untargeted analysis via *in vivo* SPME sampling have been undertaken towards the monitoring of metabolic changes in lung and liver grafts during transplantation in a pig model.[115,116] In this application, researchers were able to observe differentiation among extracts obtained from SPME fibres exposed to organ grafts at various stages of organ preservation throughout the transplantation process. One of the main advantages of this approach includes its feasibility towards monitoring of organ quality with minimum invasiveness,

thus minimizing the risk of compromising the organ through its submission to multiple biopsies at various sampling points. However, a more in-depth study with a larger number of biological replicates is required in order to fully demonstrate the potential of SPME for this application.

In addition to metabolomics studies applying SPME for *in vivo* sampling, progress on the evaluation and application of SPME thin-film format for high throughput global metabolomics has also been observed. In recent work, Mousavi et al. evaluated different coating chemistries for extraction of metabolites from *Escherichia coli* bacteria culture, including PS-DVB, hydrophilic-lipophilic balance (HLB), PBA, silica-based ionic liquid, and silica-based reversed phase in thin-film format.[117] With aims to expand metabolome coverage, mixtures of different sorbents were also investigated. Interestingly, a mixture of HLB and PS-DVB particles in a proportion 1:1 provided the best results in terms of features detected and covered polarity range. Indeed, this approach saw extraction and determination of metabolites with logP values spanning from -7 to 15, including amino acids, peptides, nucleotides, carbohydrates, polycarboxylic acids, vitamins, phosphorylated compounds, and lipids. The developed methodology was then further applied for characterization of antibacterial action of cinnamaldehyde and clove oil in *E. coli* cultures, where several metabolic pathways and dysregulated metabolites were successfully identified.[118,119]

1.5. Research objective

The main scope of this doctoral dissertation encompasses the application, evaluation, and further development of SPME as an alternative technology for the investigation of complex biological systems. To this end, the body of this work presents novel progress in SPME coupled to LC-MS for both targeted and untargeted analyses of biological fluids and brain tissue.

In reference to targeted analysis, Chapter 2 provides a thorough evaluation of SPME in thin-film microextraction format for the automated and high throughput analysis of a broad range of doping substances (drugs and metabolites) in plasma samples. This work, which was financed by the World Antidoping Agency (WADA), demonstrates the capabilities of SPME to provide satisfactory sample clean-up prior to LC-MS and to facilitate the concomitant quantitation of multiple substances of variable physicochemical properties (logP from -2 to 6.8). With the purpose of expanding the range of applications of SPME, Chapter 3 describes the development of new thin-film SPME samplers consisted of plastic as an alternative support material. The robustness of such devices as well as their potential applicability in clinical studies is successfully proven through the determination of a broad range of compounds in several biofluids, including plasma, urine, and whole blood. In a more fundamental approach, Chapter 4 discloses the effect of variable red blood cell content, also known as hematocrit, on the determination of different drugs by application of SPME as a sample preparation technique. Parameters such as coating types, agitation conditions, extraction time, and the use of an internal standard are all considered throughout the investigation and in the development of possible hematocrit effect correction methods.

In reference to untargeted analysis, Chapter 5 includes an evaluation of SPME in fibre configuration as an analytical tool in metabolomics studies of brain tissue. As part of the assessment, different available extraction phases (C18, HLB and MM), desorption conditions, washing step strategies, and extraction times are discussed based on the metabolite features detected after extraction from cow brain homogenate. Lastly, the application of SPME for the *in vivo* monitoring of metabolic changes in rat brains after deep brain stimulation is presented in Chapter 6. Interesting results in terms of determination of dysregulated metabolites and lipids in groups of control and treated animals are shown, and a discussion about the biological relevance

of such findings is also presented. Chapter 7 summarizes the main contribution of this work and provides future directions to be considered in regards to the applicability of SPME towards the investigation of biological systems.

Chapter 2: High throughput targeted analysis in plasma using thin-film solid phase microextraction

2.1. Preamble and introduction

2.1.1. Preamble

This chapter of the thesis is already published as an article under the title "High throughput quantification of prohibited substances in plasma using thin-film solid phase microextraction" by Nathaly Reyes-Garcés, Barbara Bojko and Janusz Pawliszyn., *J. Chromatogr. A* **2014**, *1374*, 40-49. The content of the article is being reprinted in this thesis with permission of Elsevier, and in compliance with Elsevier and University of Waterloo policies.

I, Barbara Bojko, authorize Nathaly Reyes-Garcés to use the material for her thesis.

2.1.2. Introduction

One of the ultimate goals in doping control is the development of a simple, fast, reliable and comprehensive analytical methods for biological matrices such as blood and urine. Due to the complexity of such matrices, as well as the diversity of prohibited substances listed by the World Antidoping Agency (WADA), sample preparation is often a challenging task.[120] Currently, WADA has stipulated minimum required performance levels only for the detection and identification of prohibited substances in urine samples.[121] However, analytical determinations in blood (plasma/serum) as a means to obtain complementary information to urinalysis results have been garnering a wealth of interest.[122–126] Some advantages of blood analysis in doping control include finding intact unknown doping substances, determining temporal information regarding drugs prohibited in-competition only, and detecting if an athlete is participating in blood doping

37

practices.[122,125,126] Sample preparation procedures reported for analysis of prohibited substances in blood, serum, and plasma include protein precipitation, solid phase extraction (SPE) and more recently, dried blood spots (DBSS).[122,127–130] Several studies using these sample preparation methods for comprehensive screening of human and equine plasma/blood have been reported in recent years.[123,124,131–137] Despite these approaches being effective, they can be time-consuming, unsuitable in some cases for automation, and prone to ion suppression/enhancement effects. Regarding instrumentation, undoubtedly, liquid chromatography coupled to mass spectrometry (LC-MS) has become the preferred method in sports drug testing due to its flexibility compared to gas chromatography-mass spectrometry (GC-MS) and to immunological assays.[126,138–140] For these reasons, simple and effective sample preparation protocols suitable for automation and compatible with LC-MS based methods are highly desired. Recently, the introduction of thin-film solid phase microextraction (SPME) in an automated configuration has opened up a new alternative in sample preparation for bioanalysis. Biocompatible SPME coatings prepared by immobilizing various sorbents with polyacrylonitrile have demonstrated great performance in the extraction of drugs from complex matrices. By taking advantage of this technology, a comprehensive protocol for automated quantitative urinalysis of doping agents was recently introduced.[80] In that work, more than 100 compounds of different classes and polarities were simultaneously extracted from urine samples using a C18-polyacrylonitrile (PAN) extraction phase and the Concept 96 automated sample preparation station. By using the 96 SPME thin-films that the aforementioned system can handle, the optimized method was able to provide throughput of less than 2 min per sample. Furthermore, the proposed automated SPME method allowed satisfactory sample clean-up since negligible absolute matrix effects were observed for the majority of the compounds. Considering the good performance of the proposed method, and by taking advantage of the biocompatibility of

the SPME extraction phases, a new high throughput SPME-based protocol for plasma analysis is introduced herein. Twenty-five compounds of a wide range of polarities (logP from -2 to 6.8), including different prohibited drug classes and some metabolites such as benzoylecgonine, morphine-3β, and 6β glucuronide, were selected for this study. Given that SPME only extracts an amount of analyte proportional to its free concentration, the method was carefully optimized, taking into account the binding that some compounds might experience due to the high protein content of plasma. For this purpose, simultaneous SPME pre-conditioning and sample pre-incubation under a controlled temperature were enabled by modifying the software of the Concept-96 autosampler. With the aim of covering a broad range of compounds in a single extraction, a thin-film SPME coating made of hydrophilic-lipophilic balance (HLB) Oasis particles immobilized with polyacrylonitrile (PAN) was chosen. To the best of our knowledge, this is the first time that such SPME coating is used in a multi-residue bioanalytical application.

2.2. Experimental

2.2.1. Materials and supplies

Amphetamine, methamphetamine, 17-α-trenbolone, morphine, benzoylecgonine, codeine, codeine-d$_3$, oxycodone-d$_3$, cannabidiol-d$_3$, methadone-d$_3$, stanozolol, (±)11-nor-9-carboxy-Δ^9-tetrahydrocannabinol (THC) (THCCOOH), (±)11-nor-9-carboxy-Δ^9-THC-d$_3$ (THCCOOH-d$_3$), cortisol-d$_4$, morphine-3β-glucuronide, morphine-6β-glucuronide, morphine-3β-glucuronide-d$_3$, (±)11-nor-9-carboxy-Δ^9-THC glucuronide (THCCOOH-glu), and (±)11-nor-9-carboxy-Δ^9-THC glucuronide-d$_3$ (THCCOOH-glu-d$_3$) standards were purchased from Cerilliant Corporation (Round Rock, TX, USA). Nikethamide, propranolol, metoprolol, clenbuterol, exemestane, bisoprolol, budenoside, dexamethasone, furosemide, salbutamol, prednisolone, strychnine and testosterone-d$_3$ were purchased from Sigma-Aldrich (Oakville, ON, Canada). Salbutamol-d$_3$ was purchased

from CDN isotopes (Pointe-Claire, Quebec, Canada). Toremifene and GW501516 were purchased from Toronto Research Chemicals (Toronto, ON, Canada).

Sodium chloride, potassium chloride, potassium phosphate monobasic, sodium phosphate dibasic, formic acid, and polyacrylonitrile (PAN) were also purchased from Sigma-Aldrich (Oakville, ON, Canada). N,N-dimethyl formamide (DMF) was purchased from Caledon Labs (Georgetown, ON, Canada). Modified polystyrene divinylbenzene (PS-DVB) was obtained from Macherey-Nagel (Düren, Germany), Oasis hydrophilic-lipophilic balance 30 μm sorbent particles (HLB) were obtained from Waters (Milford, MA, USA), and Discovery silica-based C18 5 µm particles were obtained from Supelco (Bellefonte, PA, USA). Polypropylene Nunc U96 deep well plates were purchased from VWR international (Mississauga, ON, Canada) and bare stainless steel blades were obtained from Professional Analytical System (PAS) Technology (Magdala, Germany). LC-MS grade acetonitrile, methanol, and water were obtained from Fisher Scientific.

2.2.2. Working solutions

A stock methanolic solution (20 µg mL^{-1}) containing all analytes was prepared and further dilutions were done as required. A stock solution (8 µg mL^{-1}) containing multiple deuterated compounds as internal standards was prepared in methanol.

2.2.3. Plasma samples

Different lots of potassium (K$_2$) ethylenediaminetetraacetic acid (EDTA) pooled human plasma from healthy donors were purchased from Lampire Biological Laboratories (Pipersville, PA, USA). A phosphate-buffered saline solution (PBS) (pH 7.4) was prepared by adding 8.0 g of sodium chloride, 0.2 g of potassium chloride, 0.2 g of potassium phosphate monobasic, and 1.44 g of sodium phosphate dibasic to 1 L of nanopure water.

2.2.4. Thin-film SPME devices

Various coating chemistries in thin-film SPME format were prepared by immobilizing different SPE sorbents (C18, PS-DVB and HLB) with a PAN-DMF solution according to the procedure already reported by Mirnaghi et al.[88] The only exception to the original protocol was the curing temperature, which was decreased from 180 to 150 °C.

2.2.5. Sample preparation: automated Concept 96-blade SPME system

Automated SPME extractions were carried out using the Concept-96 system (Professional Analytical Systems (PAS) Technology, Magdala, Germany). This robotic sample preparation unit has been described in detail elsewhere.[81,141] A typical SPME protocol using this automated station involves preconditioning, extraction, washing and desorption steps. In this work, a simple modification of the controlling software allowed for the simultaneous pre-incubation of samples at a given temperature (extraction station) and pre-conditioning of SPME devices (preconditioning station).

The SPME method was developed and optimized in terms of coating selection, pH control, extraction time and temperature, type of desorption solvent used, and desorption duration. A recent work on doping control using SPME demonstrated the suitability of C18 coatings for the extraction of a wide range of doping substances from urine samples.[80] Due to the high protein content in plasma, and consequently the decrease of free concentrations of drugs that typically exhibit high protein binding, it was critical to evaluate the performance of different coating chemistries at such conditions. For optimization of the SPME method, both plasma and PBS standards were prepared by spiking analytes from stock solutions, keeping the organic solvent content constant at 1%. Spiked plasma aliquots were pre-incubated in the fridge overnight to allow complete binding

before extraction. Sample preparation involved mixing 1080 µL spiked plasma aliquots with 10 µL internal standard solution and 120 µL of 1 M phosphate buffer (pH = 7). Subsequently, samples were homogenized in the 96-well plate at constant agitation for 30 min before starting the SPME procedure. Optimum SPME conditions were set as follows: pre-conditioning of SPME devices in 1:1 methanol:water (1500 µL) for 30 min and simultaneous plasma samples pre-incubation at 30 °C, then 90 min extraction at 30 °C, 10 s washing step in deionized water (1500 µL), and 20 min desorption in 4:1 methanol:acetonitrile with 0.1% formic acid (1200 µL). Agitation rate was set at 1500 (revolutions per minute) rpm. It is worth emphasizing that the total incubation time of plasma aliquots after adding buffer and internal standard solution was 1 h.

2.2.6. LC-MS/MS conditions

Samples were run on a LC-MS system consisting of an Accela pump, an Accela autosampler and a triple quadrupole mass spectrometer TSQ vantage equipped with a heated electrospray (H-ESI) source (Thermo Scientific, San Jose, USA). Chromatographic separation was carried out using a Kinetex pentafluorophenyl core shell column (1.7 µm, 2.1 mm x 10 mm) connected to a PFP security guard ultracartridge (Phenomenex, Torrance, CA, USA). The mobile phases used were water with 0.1% formic acid (A), acetonitrile with 0.1% formic acid (B) and methanol with 0.1% formic acid (C). Mobile phase gradient conditions were as follows: hold at 90% A, 5% B, and 5% C for 0.5 min, linear increase of both solvents B and C to 50% in 9.5 min, linear increase of C to 62.5 % and decrease of B to 37.5% in 5 min. Lastly, the column was re-equilibrated for 2 min at the starting conditions. The overall run time was 17.3 min, the flow rate was 400 µL min^{-1} and the column temperature was maintained at 35 °C. The injection volume was 10 µL in full loop injection mode. MS conditions were set as follows: spray voltage = 1300 V, vaporizer temperature = 275 °C, sheath gas = 45 units, auxiliary gas = 30 and capillary temperature = 280 °C. Samples

were run in positive and negative selected reaction monitoring (SRM) mode. Optimum collision energy and S-lenses conditions were determined for each compound by using direct infusion of standards (please refer to Table 2.1 and Table 2.2). Due to the multiple transitions monitored in this particular method, MS data was collected by defining acquisition windows based on chromatographic retention time. Xcalibur software (2.0.7 SP1) was employed for data acquisition and processing.

Table 2.1. Optimum MS/MS parameters and chromatographic conditions for the selected target compounds (positive mode). Underlined compounds were tuned in positive and negative mode.

| Compound | Retention time | Parent ion (m/z) | Product ion (m/z) | Collision energy | Windows, min | | S-Lenses |
					Start time	End time	
Amphetamine	5.94	136.099	65.138	36	5.5	7	36
			91.114	17			
Methamphetamine	6.88	150.112	91.12	19	6	7.5	45
			119.139	9			
Nikethamide	3.76	179.1	80.127	29	3	4.5	76
			108.102	18			
Salbutamol	3.26	240.143	148.103	18	2.7	4	59
			166.116	12			
Salbutamol-d$_3$	3.26	243.16	151.123	18	2.7	4	64
			169.138	12			
Propranolol	12.08	260.123	116.138	17	11.5	13	89
			183.116	17			
Metoprolol	8.0	268.14	77.105	50	7.5	9	94
			116.146	18			
Trenbolone	6.80	271.133	165.106	56	5.5	7.5	97
			199.17	24			
Clenbuterol	8.62	277.068	132.1	30	8.2	9.5	70
			203.049	15			
Morphine	2.78	286.119	152.092	61	2.2	3.5	110
			165.101	40			
Benzoylecgonine	5.53	290.133	77.141	47	4.8	5.8	93
			168.164	18			
Testosterone-d$_3$	7.40	292.248	97.135	22	6.5	8.5	93
			109.137	25			
Exemestane	7.80	297.173	91.128	39	7.2	8.2	72

			121.118	19			
Codeine	4.87	300.105	152.092	64	4	6	104
			165.102	42			
Codeine-d$_3$	4.87	303.149	165.096	41	4	6	104
			215.138	25			
Methadone-d$_3$	16.0	313.214	105.091	29	13.8	17.3	87
			268.224	13			
Bisoprolol	9.45	326.16	74.126	27	8.5	10.5	102
			116.135	17			
Stanozolol	8.62	329.229	81.108	44	8	9.5	130
			95.115	38			
Strychnine	6.97	335.155	156.126	45	6	8	136
			184.129	36			
(±)11-nor-9-carboxy-Δ^9-THC	9.0	345.153	193.168	28	8	9.5	90
			299.265	18			
(±)11-nor-9-carboxy-Δ9-THC-d$_3$	9.0	348.162	196.204	27	8	9.5	95
			302.282	18			
Prednisolone	5.72	361.145	147.078	24	5	6.5	59
			325.243	6			
Cortisol-d$_4$	5.97	367.196	121.046	28	5	6.5	102
			331.254	14			
Dexamethasone	6.67	393.199	266.226	27	6	7.5	64
			373.226	5			
Toremifene	15.90	406.21	70.157	36	14.5	17.3	108
			72.167	24			
Budesonide	7.86	431.222	147.069	30	6.5	8.5	78
			323.215	13			
GW501516	9.76	454.091	188.079	46	9	10.3	108
			257.068	29			
Morphine-3β-glu	1.1	462.147	201.101	42	0.5	2.3	101
			286.149	29			
Morphine-6β-glu	1.49	462.147	201.101	42	0.5	2.3	101
			286.149	29			
(±)11-nor-9-carboxy-Δ9-THC glucuronide	8.20	521.173	327.182	23	7.5	9	89
			345.237	14			
(±)11-nor-9-carboxy-Δ9-THC glucuronide-d$_3$	8.20	524.178	330.214	22	7.5	9	90
			348.239	12			
Cannabidiol-d$_3$		318.146	123.041	33	8.3	10.3	82
			196.129	22			

Compound		Parent ion (m/z)	Product ion (m/z)	Collision energy			S-Lenses
Oxycodone-d$_3$		319.118	244.13	28	4.5	6.5	82
			259.155	25			
Morphine-3β-glucuronide-d$_3$	1.1	465.156	201.09	40	0.5	2.3	101
			289.168	29			

Table 2.2. Optimum MS/MS parameters and chromatographic conditions for the selected target compounds (negative mode).

Compound	Retention time	Parent ion (m/z)	Product ion (m/z)	Collision energy	S-Lenses
Furosemide	6.07	329.013	205.083	24	75
			285.152	18	
THCCOOH (±)11-nor-9-carboxy-Δ9-THC	9.0	343.167	245.29	30	83
			299.359	23	
(±)11-nor-9-carboxy-Δ9-THC-d$_3$	9.0	346.236	248.297	32	85
			302.374	24	
Prednisolone	5.72	405.2	280.239	38	72
			329.308	20	
Cortisol-d$_4$	5.97	411.226	286.24	41	74
			335.365	21	
Dexamethasone*	6.67	437.21	307.274	34	84
			361.354	21	
Budenoside*	7.86	475.183	339.296	24	76
			357.317	18	
(±)11-nor-9-carboxy-Δ9-THC glucuronide	8.2	519.192	299.349	37	114
			343.347	28	
(±)11-nor-9-carboxy-Δ9-THC glucuronide-d$_3$	8.2	522.194	193.142	21	115
			302.358	39	

*Formiate adducts

2.3.   Results and discussion

Target analytes were selected for plasma method development according to various xenobiotics reported in the literature as likely to occur in blood in case of positive doping.[123,124] With the aim of expanding the range of drug chemical properties, glucuronide forms of morphine and

THCCOOH were also included in the target compound list. Although 17-β-trenbolone might prevail in plasma in case of positive doping, 17-α-trenbolone was used as model compound based on availability of the standard. Overall, the studied compounds represented several drug classes such as narcotics, stimulants, steroids, hormones (including an aromatase inhibitor and a selective estrogen modulator), a metabolic modulator (GW501516), cannabinoids, beta-blockers, beta-agonists, other anabolics, diuretics and glucocorticosteroids, and offered a wide range of polarities, with logP values ranging from -2 to 6.8.

2.3.1. Coating selection and desorption conditions

The first part of the SPME method development involved coating selection. It is worth noting that the performance of SPME depends on the affinity of the analytes towards a given extraction phase at a defined set of experimental conditions. At equilibrium, the affinity of analytes towards the coating is represented by the fiber coating/sample matrix distribution constant. Based on these reasons, when selecting a SPME coating for a complex matrix such as plasma, both the affinity of the analytes towards the extraction phase, and the selectivity of the coating towards the target compounds versus possible matrix interferences should be considered.[142] In addition, multiple proteins occurring in plasma constitute a binding matrix that depletes the free concentration of compounds exhibiting significant protein-drug interactions. Since the amount of analyte extracted using SPME is proportional to the free analyte concentration in the matrix at the end of the extraction process, substances characterized by high protein binding are expected to exhibit higher limits of quantification. As such, and considering the broad range of polarities of the drugs selected for this study, the selection of an extraction phase able to provide sufficient coverage for all compounds was a crucial step in the present work. Previously, Boyacı *et al.* reported the evaluation of C18, mixed mode, phenyl boronic acid (PBA), and PS-DVB coatings for the extraction of more

than 100 doping substances from synthetic urine.[80] Although the PS-DVB coating exhibited better extraction efficiency for most of the compounds spiked in urine, the authors selected C18 as the extraction phase due to its lower carryover but still sufficient coverage. Considering the reusability of the SPME devices herein used, carryover is an important aspect that should be carefully addressed. Optimum SPME conditions should ensure not only satisfactory extraction recoveries, but also maximum desorption efficiency and no-cross contamination. For the purposes of the current work, the performance of C18, PS-DVB, and HLB coatings to extract the target compounds from plasma was investigated. Figure 2.1 shows the absolute recoveries obtained for the different extraction phases when a mixture of 2:2:1 acetonitrile:methanol:water with 0.1% formic acid was used as desorption solvent. As can be seen in Figure 2.1, for this particular set of analytes, HLB showed the best performance in terms of analyte coverage. Highly polar compounds such as morphine 3β and 6β glucuronide, as well as non-polar compounds such as toremifene and THCCOOH were successfully extracted. Because of its hydrophilic N-vinylpyrrolidone and lipophilic divinylbenzene functionalities, HLB displays balanced analyte coverage and shows recoveries comparable with those exhibited by C18 coating, even for less polar compounds. In addition, HLB did not exhibit significant carryover at the initial desorption conditions selected for the coating evaluation (data not shown). Indeed, the decreased free concentration of some compounds due to high protein binding reduces chances of carryover at moderate or high concentrations. Another advantage of selecting HLB as the SPME extraction phase is its characteristic wettability, which facilitates its interaction with aqueous matrices. Based on these reasons, the HLB coating was chosen as the SPME extraction phase for this method. The next step of the SPME method development involved selection of desorption solvent and optimization of desorption time. Various desorption solvents were evaluated, including the desorption solution

selected by Boyacı *et al.*, (2:2:1 acetonitrile:methanol:water with 0.1% formic acid), as well as other solutions comprised by different proportions of methanol, acetonitrile and water acidified with formic acid at 0.1%. Results in terms of carryover for each desorption solvent tested are presented in Table 2.3.
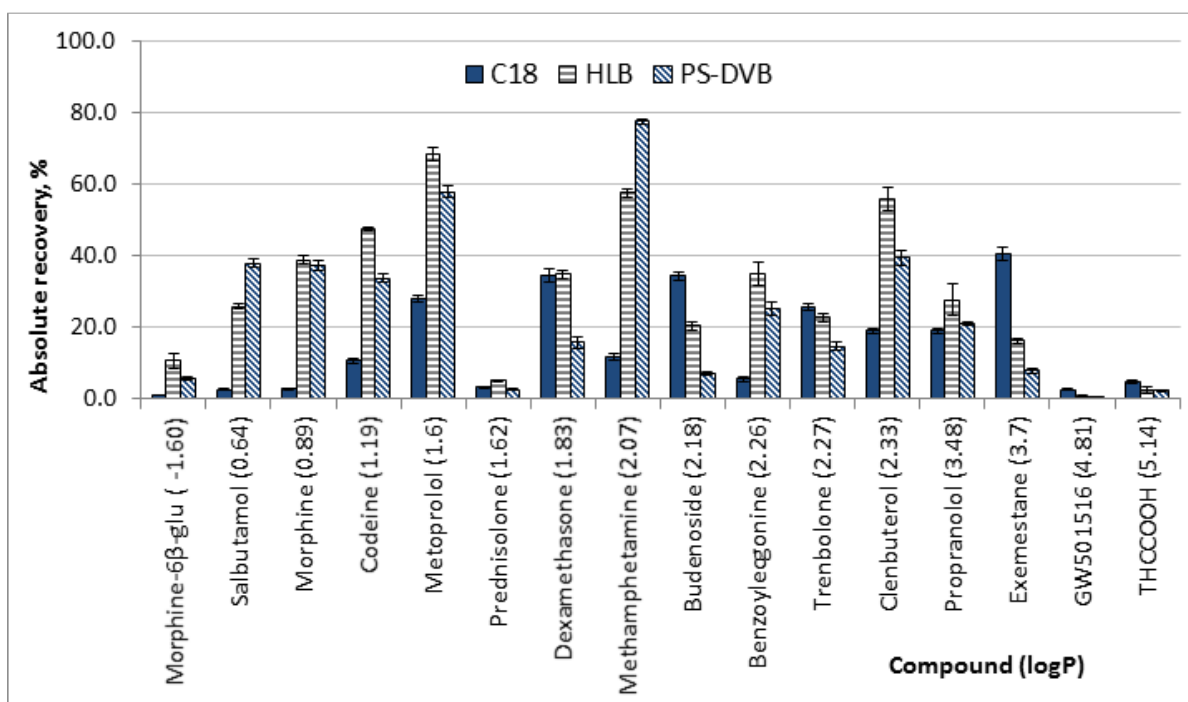
Figure 2.1. Comparison of C18, HLB and PS-DVB coatings performance in the extraction of various drugs from plasma spiked at 100 ng mL-1 (logP values in brackets). Extraction time was set at 75 min and the sample volume was 1200 μL (9:1 plasma:buffer).

Ideally, a desorption solution for SPME should offer minimum carryover, as already emphasized, and be compatible with the LC conditions, ensuring good chromatographic separation. As a matter of fact, general SPE protocols recommend methanol for elution of a wide range of analytes retained in HLB cartridges. However, in SPME configuration, and for this particular application, methanol showed a moderate carryover for some non-polar compounds such as GW501516 and THCCOOH. It was observed that by introducing some percentage of acetonitrile in the desorption solution,

Table 2.3. Carryover found for different solvent compositions (all desorption solvents tested were acidified with 0.1% formic acid). Results obtained from the second desorption after extracting from a PBS solutions spiked at 100 ng mL^{-1}. Desorption volume and time were 1200 µL and 60 min in all the cases.

Carryover, %	MeOH 40%, ACN 40%, water 20%	MeOH 100%	MeOH 80%, water 20%	45% ACN,45% MeOH, 10% water	50% ACN, 50% MeOH	80% ACN, 20% MeOH	80% MeOH, 20% ACN
Morphine-3β-glu	8.7	3.9	4.6	10.0	17.6	-	5.1
Morphine-6β-glu	3.0	3.0	3.7	3.1	3.9	7.6	3.4
Morphine	4.0	3.5	5.2	3.6	3.0	5.1	3.6
Salbutamol	3.4	3.1	3.5	3.0	3.0	5.3	3.0
Nikethamide	2.0	2.7	2.4	2.2	2.7	3.2	2.5
Codeine	4.4	3.7	5.8	4.0	3.1	4.8	3.5
Benzoylecgonine	2.3	1.9	3.4	2.2	2.1	2.7	1.9
Amphetamine	4.8	4.6	5.6	4.6	4.4	6.4	5.0
Prednisolone	2.4	3.5	4.8	2.6	2.6	3.3	3.1
Methamphetamine	4.5	3.9	5.5	3.9	3.3	4.7	3.7
Dexamethasone	3.2	3.0	5.2	2.1	2.2	2.4	2.3
Trenbolone	4.1	5.4	11.6	3.5	3.4	3.2	3.8
Strychnine	6.2	3.8	8.5	5.4	3.1	5.8	3.9
Testosterone	4.3	4.4	10.7	3.4	3.5	3.3	3.6
Formoterol	6.0	4.9	7.9	4.4	3.6	6.4	4.1
Metoprolol	4.3	3.8	5.9	3.4	3.0	3.8	3.3
Exemestane	4.8	5.8	13.6	3.4	3.5	2.7	3.8
Budenoside	4.8	5.3	12.3	3.1	3.0	2.8	3.6
Clenbuterol	6.1	4.7	7.5	4.3	3.5	4.9	3.8
THCCOOH-glu	5.6	5.3	11.9	3.7	3.7	6.5	3.3
Stanozolol	6.7	4.6	13.1	4.4	4.1	5.3	3.6
THCCOOH	14.3	8.8	26.0	6.7	4.9	6.8	5.1
Bisoprolol	4.5	3.9	6.2	3.5	3.3	3.9	3.3
Cocaine	6.1	4.9	8.1	5.5	4.3	5.0	4.5
GW501516	18.0	14.5	35.9	9.1	5.4	5.6	6.7
Propranolol	7.5	5.0	9.8	4.8	3.6	5.4	4.2
Toremifene	12.2	5.2	12.6	6.7	3.7	4.4	4.8

carryover of those compounds decreased. Conversely, by increasing water content in the desorption solvent, desorption efficiency of several non-polar compounds was worsened. For this

reason, and as a compromise between desorption efficiency and chromatographic resolution, 1200 μL of a mixture of 4:1 methanol:acetonitrile acidified with 0.1% formic acid was found as optimum. Following the selection of desorption solvent, it was necessary to determine the optimum desorption time. Considering the composition of the selected desorption solvent, which is 100% organic, fast equilibration between the target analytes extracted on the SPME coating and the selected desorption medium was expected due to the dramatic decrease in the coating/medium distribution constant. For this reason, 10, 20 and 45 min were tested as desorption times. As can be seen in Figure 2.2, no significant differences were observed between desorbed amounts at 20 and 45 min. In addition, the same carryover values found after 20 min desorption were observed at 45 min (data not shown). Conversely, 10 min showed smaller desorption amounts for some analytes, as well as a higher carryover level. Based on these findings, 20 min was selected as
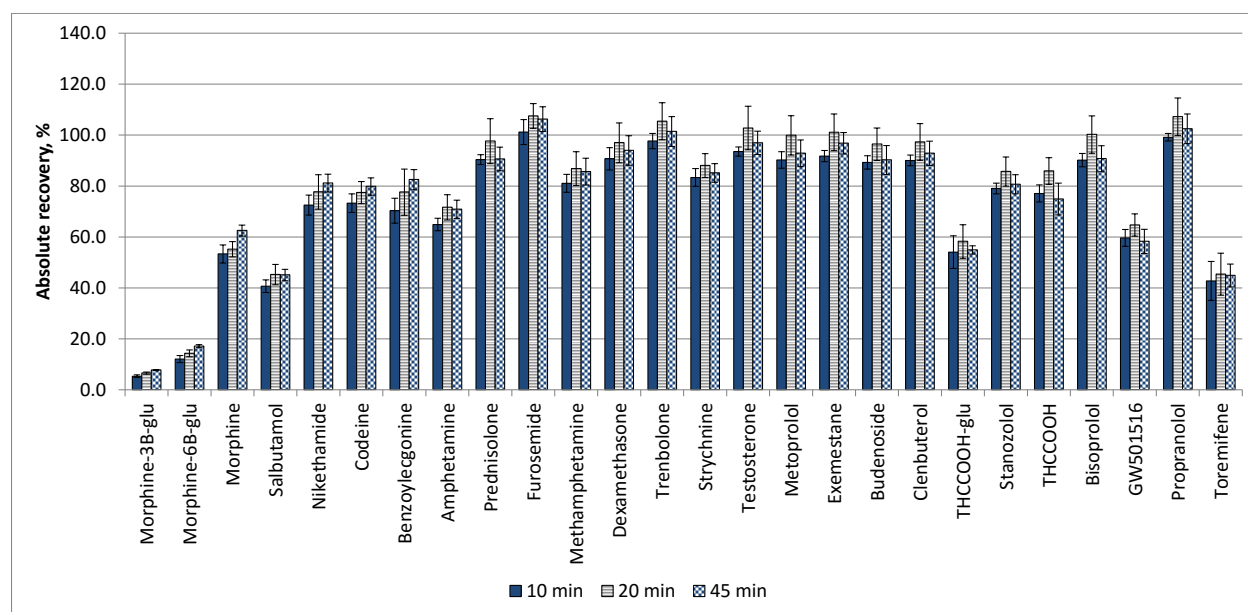
Figure 2.2. Comparison of desorption efficiency at 10, 20 and 45 min (n = 4 pins and 1200 μL of desorption solution (4:1 methanol:acetonitrile with 0.1% formic acid)). Extractions were performed from PBS spiked at 100 ng mL^{-1}.

desorption time, and an additional cleaning step was added to ensure no carryover. Cleaning of the blades was carried out by desorbing the blades in a 2:1:1 methanol:acetonitrile:isopropanol solution for 30 min. It is worth emphasizing that desorption and cleaning conditions herein optimized allowed for negligible carryover of the target compounds. However, confirming an adverse analytical finding in a real doping case with this methodology might require reporting that only new or disposable SPME samplers were used.

2.3.2. Extraction conditions: pH, temperature, time and selection of internal standards

Once the SPME coating was selected and desorption conditions were carefully optimized, other extraction parameters such as pH, extraction time and temperature were also considered. It is worth emphasizing that the main goal of the current work was to simplify the sample preparation required to extract a wide range of analytes present in complex matrices such as plasma. Bearing this is mind, minimum modifications to the sample matrix were considered. As already stated, SPME is able to extract an amount of analyte proportional to its free concentration. Since pH and temperature can influence the degree of binding of a given substance in plasma,[143,144] controlling these variables was necessary in the development of this SPME method. For instance, physiological pH in plasma varies from 7.35 to 7.45. However, upon storage or sample preparation, plasma pH shifts more than 1 unit towards alkaline values, affecting protein-binding measurements and even causing degradation of some pH-labile compounds.[145] As an effective means to stabilize plasma pH during sample preparation, Fura *et al.* reported the use of buffer concentrations above 0.5 M and plasma:buffer ratios greater than 10:1. In this study, 1 M phosphate buffer in 9:1 plasma:buffer proportion was used to control plasma pH during the sample preparation process. Temperature control was possible by taking advantage of the Concept-96 system extraction stage.

This unit consists of an orbital shaker equipped with a heating surface that ensures uniform temperature distribution along the 96-wells tray (see Figure 2.3).
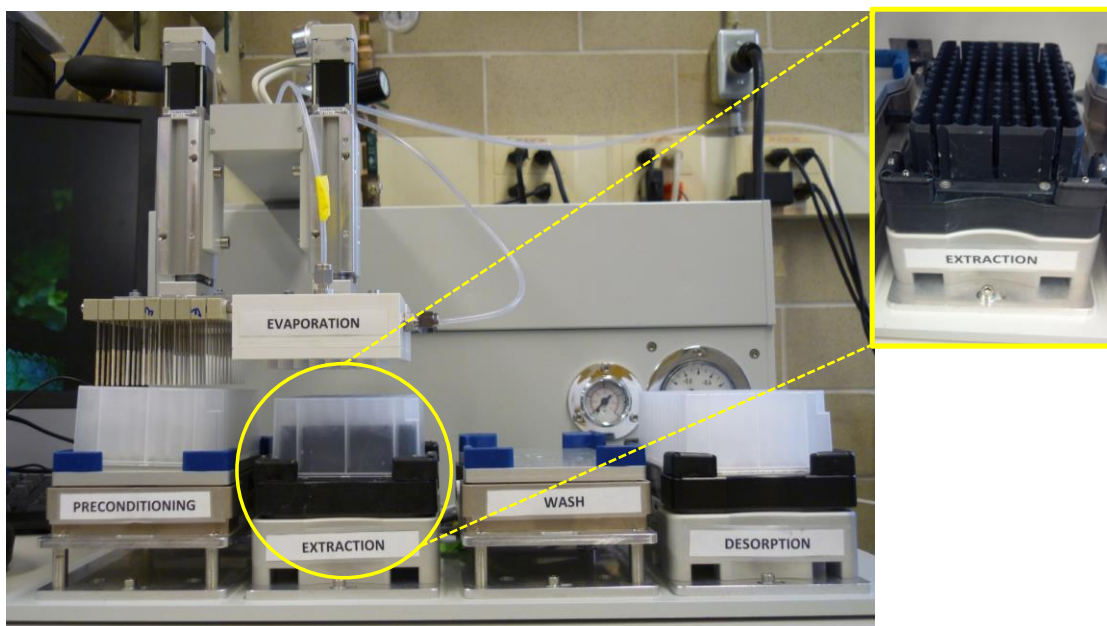
Figure 2.3. Concept 96 blade system with uniform temperature control on the extraction station.

The effect of temperature on the amount extracted was evaluated at 25, 30 and 37 °C in both PBS and plasma, while keeping the extraction time constant at 75 min. Table 2.4 shows results corresponding to the amounts extracted at different temperatures from both sample matrices. As can be seen in Table 2.4, no significant differences were observed in the amount extracted from PBS for most of the compounds at the investigated temperatures. In other words, these results showed that increasing the temperature from 25 to 37 °C did not affect the fiber/sample distribution coefficient, or the affinity of the HLB coating towards the majority of studied compounds. Only toremifene and GW501516, which are characterized for a high lipophilicity, exhibited a slight increase in the amount extracted as extraction temperature was increased. A possible explanation for this observation might be related to the temperature effect on the extraction kinetics, given that

Table 2.4. Evaluation of the effect of temperature on the amount extracted from PBS and plasma spiked at 100 ng mL-1 and mixed with 1 M buffer (9:1 plasma:buffer). Extraction time was fixed at 75 min (n=4 pins).

Compound	PBS						Plasma					
	25 ˚C		30˚C		37˚C		25˚C		30˚C		37˚C	
	ng	RSD, %	ng	RSD, %	ng	RSD, %	ng	RSD, %	ng	RSD, %	ng	RSD, %
Morphine-3β-glu	6.0	9	6.2	6	6.1	5	7.2	6	8.3	11	8.5	9
Morphine-6β-glu	15.3	11	16.0	8	16.0	5	11.8	29	15.8	14	15.3	12
Morphine	58.5	9	61.1	8	58.2	4	56.6	10	61.2	11	55.4	11
Salbutamol	41.9	10	43.0	9	42.6	4	40.5	9	43.0	9	38.9	9
Nikethamide	69.7	9	72.3	8	73.4	5	60.6	13	64.2	13	59.1	12
Codeine	75.9	8	80.2	7	79.0	2	69.6	8	75.9	9	68.9	9
Benzoylecgonine	66.8	12	69.7	9	72.2	6	54.4	12	58.2	14	54.8	13
Amphetamine	66.6	9	66.8	8	65.0	2	61.5	8	64.7	9	56.4	8
Prednisolone	67.6	6	67.0	7	69.3	8	7.9	10	12.9	7	22.1	4
Furosemide	67.0	4	66.4	4	64.9	10	3.4	11	3.9	11	3.9	16
Methamphetamine	75.7	6	77.4	8	77.4	2	72.7	8	77.9	10	71.6	8
Dexamethasone	81.4	6	86.0	7	90.4	2	38.1	7	45.1	9	45.4	6
Trenbolone	91.1	7	94.5	6	98.6	1	29.1	8	34.7	6	35.9	5
Strychnine	84.1	6	88.8	6	82.8	1	43.2	7	52.2	7	53.5	6
Metoprolol	85.7	7	90.4	6	93.4	1	77.4	7	85.4	9	80.8	6
Exemestane	86.6	9	90.7	6	96.9	1	23.2	12	29.0	3	30.5	4
Budenoside	82.1	7	87.8	6	92.1	2	25.3	8	29.5	12	30.6	8
Clenbuterol	88.4	7	92.4	6	94.5	0	53.6	5	60.9	7	60.0	5
THCCOOH-glu	32.4	24	35.7	31	38.3	26	6.6	6	8.2	14	8.3	9
Stanozolol	76.5	6	78.4	5	79.1	2	3.1	13	4.0	7	4.8	8
THCCOOH	71.3	7	79.2	6	80.6	5	2.2	2	2.6	19	2.6	10
Bisoprolol	83.5	6	89.3	7	92.5	2	63.0	6	69.6	7	66.9	6
GW501516	63.2	7	74.5	7	68.2	2	1.4	11	1.4	6	1.4	9
Propranolol	92.4	7	96.5	6	96.3	1	40.2	8	48.2	8	52.7	5
Toremifene	26.6	11	30.9	7	39.8	14	0.8	13	0.8	6	0.8	11

at 75 min and 25 °C these two compounds were not likely at equilibrium conditions. It is also worth noting that these compounds are prone to get attached on the plastic walls of the 96 well tray due to their high hydrophobicity. Hence, concentration of such analytes in PBS available for SPME extraction may be affected. A reduction in secondary interactions of those compounds with plastic and an improvement in their solubility in PBS is expected by increasing the extraction temperature. Conversely, results observed in plasma demonstrated that an increment of only five degrees in the extraction temperature produced a statistically significant increase in the amounts extracted for some of the studied drugs. Prednisolone, for instance, was greatly affected by temperature changes, with 8, 13 and 22 ng extracted by SPME at 25, 30 and 37 °C, respectively. As already documented by several authors, the binding affinity of multiple drugs towards plasma proteins is a function of temperature.[143,144,146] Indeed, in the literature, differences of up to 50% have been reported for unbound drug fractions determined at room temperature (25 °C) and at 37 °C.[143] To the best of our knowledge, studies of the effect of temperature on prednisolone protein binding have not been reported previously. However, it has been documented that raising the temperature from 37 to 41 °C produces an increase of 80% in serum-free cortisol, an endogenous steroid hormone that exhibits competitive protein binding towards prednisolone.[147–149] For these reasons, and to avoid jeopardizing method accuracy and reproducibility, 30 °C was selected as the extraction temperature. In cases where temperature control is not possible and SPME procedures for samples and matrix calibration points are not performed simultaneously, using an appropriate internal standard that closely mimics the binding behavior of the target analytes is highly recommended.

After choosing adequate temperature and pH conditions, the determination of an appropriate extraction time for the proposed method was undertaken. Due to the wide variety of target analytes

selected for this study, the extraction time was selected based on a compromise between sufficient sensitivity and satisfactory throughput. For this purpose, solutions of all target analytes were prepared in PBS and plasma at 100 ng mL^{-1} (final concentration after adding buffer was 90 ng mL^{-1}). Extractions were performed at 15, 30, 45, 60, 75, 90, 105 and 120 min. As shown in Figure 2.4, two general trends were observed: compounds with low binding, generally those more polar, exhibited similar extractions profiles in PBS and plasma at the same extraction conditions. On the other hand, compounds characterized by high binding towards plasma proteins, such as stanozolol, were able to reach an extraction amount plateau within 30 min in PBS, while in plasma an increasing trend in the amount extracted was observed even after 120 min extraction. This behavior occurs due to the complexity of the system (plasma), where multiple types of binding interactions take place; more in-depth studies required to fully understand this phenomenon are ongoing, and will be reported in the near future. As an acceptable balance between throughput and sensitivity, 90 min was selected as the extraction time. Although the selected extraction time involves pre-equilibrium SPME conditions for plasma analysis, satisfactory precision was ensured, as the Concept-96 system allows accurate and automated control of stirring, temperature and extraction time conditions.

Aiming to account for possible pin-to-pin variations, instrumental fluctuations, as well as for differences among plasma samples, deuterated drugs of different binding affinities,[150–153] polarities and moieties were introduced as internal standards (Table 2.5). Due to the high protein binding behavior that some of the studied substances might exhibit in plasma, the final concentration of internal standard in the samples was fixed at 100 ng mL^{-1}.[81]

A general schematic summarizing optimum SPME conditions for plasma analysis is presented in
Figure 2.5. Once internal standard solution and buffer were added to plasma samples,
homogenization of samples was conducted for 30 min prior to starting the SPME procedure.
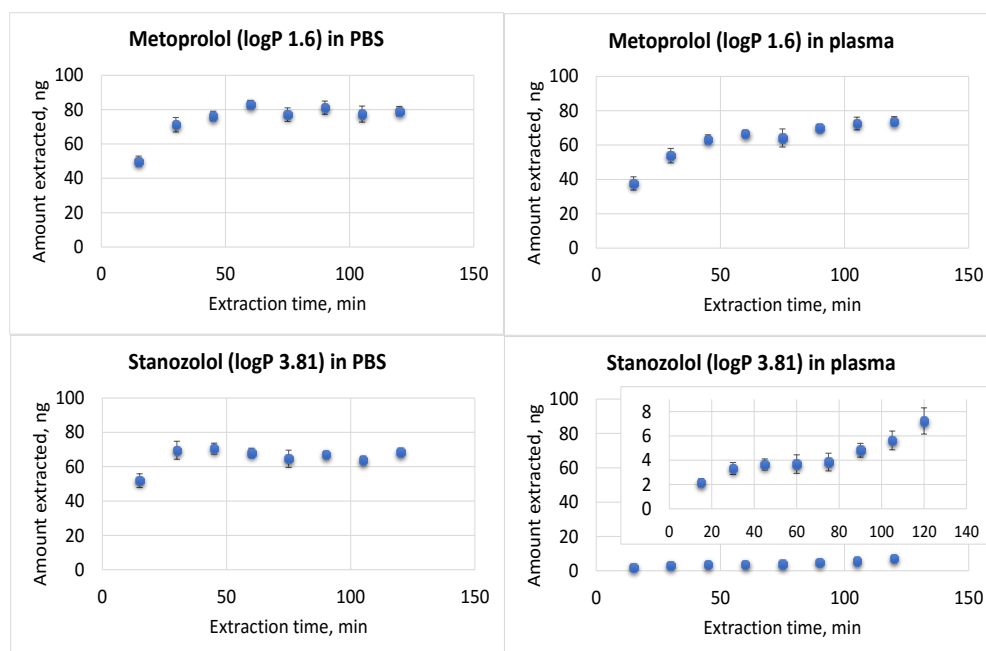
Figure 2.4. Extraction time profiles in PBS and plasma for metoprolol (logP 1.6) and stanozolol
(logP 3.81) (n=4).

Table 2.5. Internal standards used in the proposed SPME method.

Internal standard	logP[a]	Protein binding, %[b]
Morphine-3β-glucurunide-d$_3$	-2.02±0.78	10[c]
Codeine-d$_3$	1.19	7 - 25
Salbutamol-d$_3$	0.64	NA
Oxycodone-d$_3$	1.43	45
Testosterone-d$_3$	3.32	98
Cannabidiol-d$_3$	7.03	NA
Cortisol-d$_4$	1.43	95
THCCOOH-d$_3$	6.36	92.0 ± 8.7[d]
THCCOOH-glucuronide-d$_3$	NA	96.4 ± 3.0 [d]

NA (not available)
[a] Data taken from Chemspider [150]
[b] Data taken from Drugbank [151]
[c] [152]

[d] Serum protein binding reported in [153] determined in authentic samples.
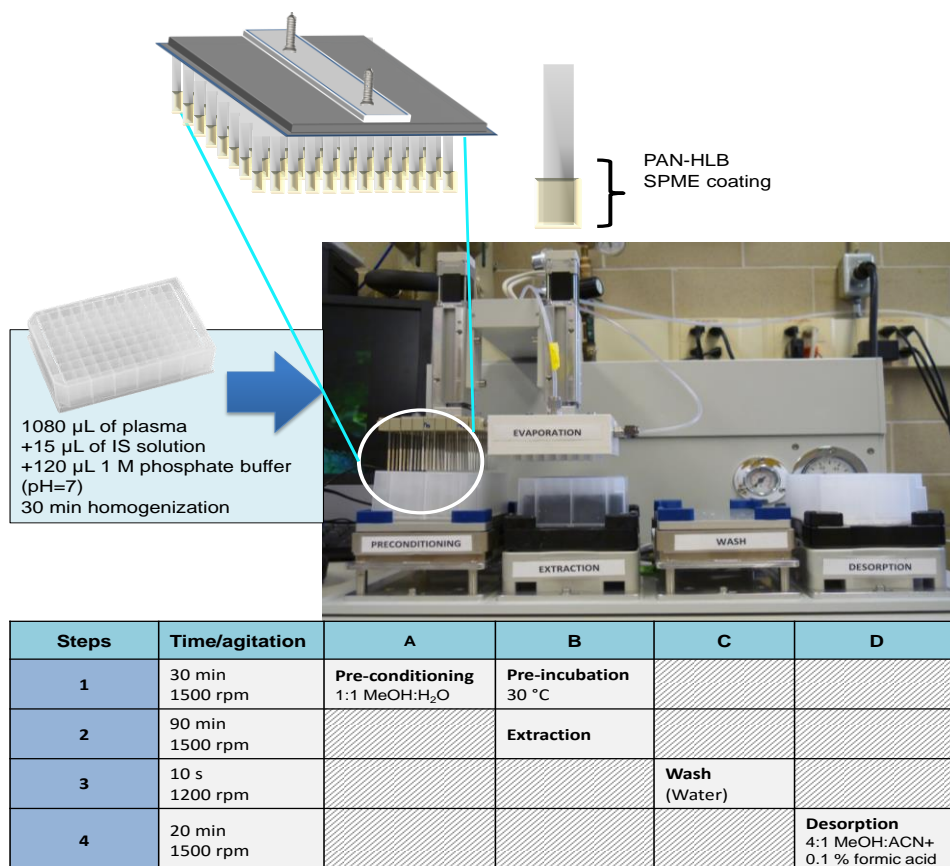
Figure 2.5. Summary of optimized SPME conditions for the analysis of prohibited substances in plasma.

2.3.3. Absolute and relative matrix effects

After determining optimum experimental parameters for SPME, it was important to evaluate the selectivity and reliability of the proposed protocol. The typical approach employed to determine drugs in plasma samples is protein precipitation, which is an exhaustive technique. However, the lack of selectivity of this sample preparation method may lead to undesired ion suppression or enhancement effects caused by interferences that can get dissolved in the extraction solvent. Absolute matrix effects for the studied compounds were estimated by comparing absolute peak areas of blank plasma extracts obtained at optimum SPME conditions (n=5) and neat desorption solvent, both spiked at the same concentration level (50 ng mL^{-1}).[154] As can be seen in Table 2.6,

Table 2.6. Absolute and relative matrix effects found for the proposed method.

Compound (Ionization mode)	logP	Internal Standard	Linear dynamic range, ng mL^{-1}	Relative matrix effects								Absolute matrix effects, %
				Slopes					Average	SD	RSD, %	
				Lot A	Lot B	Lot C	Lot D	Lot E				
Morphine-3β-glu (+)	-2.02±0.78	Morphine-3β-glu-d$_3$	5 -1000	0.0077	0.0077	0.0072	0.0072	0.0066	0.0072	0.0004	6.2	99
Morphine-6β-glu (+)	-1.60±0.77	Morphine-3β-glu-d$_3$	5 - 1000	0.019	0.017	0.017	0.016	0.017	0.017	0.0011	6.4	108
Morphine (+)	0.89	Codeine-d$_3$	1 - 250	0.0069	0.0070	0.0069	0.0067	0.0059	0.0067	0.0004	6.7	112
Salbutamol (+)	0.64	Salbutamol-d$_3$	0.25 - 1000	0.011	0.011	0.010	0.010	0.010	0.010	0.0006	6.3	110
Nikethamide (+)	0.33	Oxycodone-d$_3$	0.5 - 250	0.027	0.026	0.024	0.022	0.021	0.024	0.0023	9.8	110
Codeine (+)	1.19	Codeine-d$_3$	0.5 - 1000	0.013	0.013	0.012	0.012	0.011	0.012	0.0007	6.0	114
Benzoylecgonine (+)	2.26	Morphine-3β-glu-d$_3$	1 - 250	0.37	0.36	0.34	0.33	0.35	0.35	0.0164	4.7	110
Amphetamine (+)	1.76	Salbutamol-d$_3$	0.5 - 100	0.0090	0.0084	0.0086	0.0082	0.0078	0.0084	0.0004	5.2	111
Methamphetamine (+)	2.07	Salbutamol-d$_3$	0.5 - 100	0.032	0.028	0.031	0.027	0.026	0.029	0.0026	9.0	112
Strychnine (+)	1.93	Codeine-d$_3$	1 - 250	0.013	0.014	0.014	0.013	0.013	0.013	0.0008	5.8	118
Exemestane (+)	3.7	Testosterone-d$_3$	1 - 100	0.0079	0.0072	0.0080	0.0075	0.0071	0.0075	0.0004	5.4	110
Trenbolone (+)	2.27	Testosterone-d$_3$	1 - 100	0.0073	0.0072	0.0068	0.0065	0.0061	0.0068	0.0005	7.2	109
Metoprolol (+)	1.6	Oxycodone-d$_3$	0.25 - 500	0.012	0.012	0.012	0.011	0.011	0.012	0.0007	5.8	111
Stanozolol (+)	3.81	Testosterone-d$_3$	0.5 - 250	0.011	0.014	0.011	0.011	0.009	0.011	0.0016	14.4	103
Clenbuterol (+)	2.33	Oxycodone-d$_3$	0.5 - 500	0.043	0.043	0.043	0.041	0.039	0.042	0.0017	4.1	97
Bisoprolol (+)	1.89	Oxycodone-d$_3$	0.5 - 500	0.063	0.064	0.063	0.061	0.058	0.062	0.0023	3.7	104
GW501516 (+)	4.81	Cannabidiol-d$_3$	10 - 500	0.23	0.24	0.21	0.18	0.23	0.22	0.0243	11.0	103
Propranolol (+)	3.48	Oxycodone-d$_3$	1 - 500	0.050	0.049	0.045	0.045	0.044	0.047	0.0028	6.0	112
Toremifene (+)	6.8	Cannabidiol-d$_3$	25 - 1000	0.057	0.031	0.060	0.060	0.064	0.055	0.0133	24.4	109
Budenoside (-)	2.18	No internal standard	1 - 500	341.8	342.7	305.4	311.4	252.4	310.7	36.8	11.8	117
Dexamethasone (-)	1.83	No internal standard	0.5 - 500	7502.4	7574.5	7554.2	7206.7	6773.1	7322.2	340.9	4.7	110
Prednisolone (-)	1.62	Cortisol-d$_4$	5 - 250	0.015	0.015	0.015	0.013	0.013	0.014	0.0010	7.2	114
Furosemide (-)	2.03	THCCOOH-d$_3$	5 - 500	0.013	0.010	0.012	0.012	0.014	0.012	0.0016	13.6	110
THCCOOH-glu (-)	NA	THCCOOH-glu-d$_3$	10 - 500	0.015	0.014	0.015	0.016	0.014	0.015	0.0007	5.1	152
THCCOOH (-)	5.14	THCCOOH-d$_3$	1 - 500	0.013	0.012	0.011	0.012	0.010	0.011	0.0012	10.3	104

absolute matrix effects for all target compounds were within 99 and 120%. The only compound that exhibited a significant ion enhancement effect was THCCOOH-glucuronide (150%). As already discussed elsewhere, PAN-based biocompatible SPME coatings are able to provide sufficient selectivity towards small compounds, avoiding protein attachment or co-extraction of several interferences.[83] Results herein shown demonstrated that the HLB SPME coating provides efficient sample clean-up for a wide range of compounds when extracted from a complex matrix such as plasma. Certainly, the open bed geometry of SPME surpasses clogging issues typically encountered when using SPE for such type of samples. In addition, these findings demonstrated that the HLB extraction phase in SPME configuration might be a convenient sample preparation approach for screening and quantification purposes. This can be particularly useful when considering the potential occurrence of unknown prohibited substances and the need of retrospective analysis in some doping control cases. Relative matrix effects were also investigated according to the procedure proposed by Matuszewski *et al.*, 2003.[154] Table 2.6 presents the slopes of the calibration curves (area drug/area IS vs. nominal concentration) prepared in pooled plasma from different lots (n=5). Considering the principles of SPME, where the amount of analyte extracted is proportional to its unbound fraction at the end of the extraction process, biased quantitative results might be expected when dealing with significant variations in plasma protein levels among different samples. As seen in Table 2.6, the relative standard deviations of the slopes of the studied compounds were mostly below 7%. RSD values above 9% were mainly observed for compounds with a high logP such as toremifene, GW501516 and THCCOOH, which also display a high binding affinity towards plasma proteins. Other compounds characterized by high protein binding, such as budenoside and stanozolol, also showed higher RSD values. However, in general, RSDs for the slopes of all the model compounds were below 15%, and only toremifene

exhibited a relative standard deviation above 20%. An observed decrease in relative matrix effects might be expected by using deuterated analogues for each compound.

2.3.4. Method validation

The proposed method was evaluated according to the guidelines stipulated by the Food and Drug Administration (FDA).[155] Calibration points were prepared at 0.25, 0.5, 1, 5, 10, 25, 50, 75, 100, 250, 500 and 1000 ng mL^{-1} by spiking plasma aliquots with 1% of stock standards prepared in methanol. Weighted calibration curves were constructed using 1/x as a weighting factor. Although concentration levels in the order of hundreds of parts per billion (ppb) are not likely to occur for many of the studied drugs, it was important to investigate the linearity of the proposed method in a wide range of concentrations. Accuracy, as well as intra and inter-day precision were evaluated at five different concentrations levels: 1.6, 15, 35, 70, and 200 ng mL^{-1}. Limit of quantitation (LOQ) was defined as the lowest concentration at which the back-calculated value deviated less than 20% from the nominal value, the precision of the measurements at such concentration level was below 20%, and the signal-to-noise ratio was at least 10:1. Table 2.7 shows method validation results for all the target compounds at optimized SPME conditions. As can be seen, good linearity ($R^2 > 0.99$) for the broad set of studied compounds was achieved in a wide range of concentrations. LOQ values for all the analyzed substances were in the low ppb range, except for toremifene, GW501516, and THCCOOH-glu, which are characterized by high protein binding and lipophilicity. Improved LOQ values can be attained by decreasing the volume of desorption solvent, and even increasing the extraction time. In cases of limited sample availability, smaller plasma volumes or even diluted plasma can always be used. Intra and inter-day accuracy values were in the ranges of 85 to 124 and 87 to 130% for all the studied compounds, respectively. In terms of inter-day precision, only four compounds, which had previously shown LOQ values of

Table 2.7. Method validation for plasma analysis at optimized SPME conditions.

Compound	LOQ, ng mL⁻¹	R²	Intra-day accuracy (n=5), %					Intra-day precision (n=5), %					Inter-day accuracy (n=9), %					Inter-day precision (n=9), %				
			1.6 ng mL⁻¹	15 ng mL⁻¹	35 ng mL⁻¹	70 ng mL⁻¹	200 ng mL⁻¹	1.6 ng mL⁻¹	15 ng mL⁻¹	35 ng mL⁻¹	70 ng mL⁻¹	200 ng mL⁻¹	1.6 ng mL⁻¹	15 ng mL⁻¹	35 ng mL⁻¹	70 ng mL⁻¹	200 ng mL⁻¹	1.6 ng mL⁻¹	15 ng mL⁻¹	35 ng mL⁻¹	70 ng mL⁻¹	200 ng mL⁻¹
Morphine-3β-glu	5	0.9995	-	97	98	105	96	-	5.3	8.0	5.5	5.8	-	96	94	108	99	-	4.8	7.4	6.1	6.6
Morphine-6β-glu	5	0.9947	-	99	98	103	88	-	7.9	6.3	4.9	7.8	-	98	93	109	90	-	7.0	8.3	8.0	11.8
Morphine	1	0.9983	99	103	104	109	94	8.6	5.8	7.4	9.7	5.9	95	101	100	113	96	8.2	5.2	7.8	8.8	11.3
Salbutamol	0.25	0.9994	109	98	98	107	99	3.6	4.0	7.7	2.8	6.2	106	95	93	105	101	14.2	5.8	8.6	3.8	6.0
Nikethamide	0.5	0.9976	90	93	91	93	94	12.1	3.9	5.5	6.0	8.5	91	92	88	95	95	10.6	6.7	6.8	7.4	13.6
Codeine	0.5	0.9996	102	97	97	107	100	6.9	4.3	7.2	6.5	3.8	102	94	94	109	100	10.2	5.4	7.5	5.8	6.0
Benzoylecgonine	1	0.9953	91	100	96	98	98	19.1	5.3	9.0	7.3	8.7	98	93	91	100	95	17.8	8.3	10.0	5.9	8.5
Amphetamine	0.5	0.9988	101	97	100	112	-	3.4	8.8	10.0	14.5	-	94	95	99	120	100	7.8	7.1	8.1	13.6	-
Methamphetamine	0.5	0.9981	116	104	103	109	-	3.3	4.5	6.9	3.6	-	105	100	99	113	101	10.5	6.3	7.6	6.0	-
Strychnine	1	0.9973	113	116	118	123	102	4.6	3.5	8.7	8.7	7.4	95	112	114	130	105	18.7	8.6	10.3	9.9	9.0
Exemestane	1	0.9976	124	107	105	108	-	8.8	6.3	7.3	4.5	-	107	101	98	110	-	17.7	8.2	9.9	6.5	-
Trenbolone	1	0.9915	124	115	108	107	-	10.5	4.7	9.3	2.9	-	104	104	98	101	-	20.1	11.9	13.9	9.1	-
Metoprolol	0.25	0.9989	108	98	97	109	101	6.6	5.3	4.4	6.7	11.2	103	98	95	108	105	7.5	5.1	4.6	6.0	10.1
Stanozolol	0.5	0.9952	104	100	99	101	95	7.9	4.5	6.9	6.4	10.0	100	96	91	97	101	12.4	11.0	13.1	10.7	10.0
Clenbuterol	0.5	0.9987	98	93	93	104	95	6.4	4.0	5.0	6.6	7.8	97	98	95	109	101	5.8	7.1	4.8	8.0	10.9
Bisoprolol	0.5	0.9987	100	95	94	105	97	6.1	5.8	5.3	7.8	7.3	97	97	94	108	101	5.5	5.5	4.2	6.6	8.8
GW501516	10	0.9927	-	103	102	106	90	-	2.9	8.9	3.2	17.2	-	-	101	105	96	-	-	8.2	9.3	15.3
Propranolol	1	0.9995	109	103	103	112	97	5.5	3.6	8.2	4.0	8.1	99	102	100	116	102	11.0	4.4	7.8	5.7	9.9
Toremifene	25	0.9968	-	-	111	119	106	-	-	7.2	8.2	10.9	-	-	110	115	102	-	-	9.5	12.4	12.0
Budenoside	1	0.9937	87	93	90	93	85	6.8	14.2	15.5	11.8	19.9	93	93	88	90	87	19.0	14.9	14.9	12.6	18.4
Dexamethasone	0.5	0.9929	96	101	100	102	88	4.2	2.8	3.8	3.6	17.1	93	94	92	93	87	13.8	12.3	11.9	11.6	16.2
Prednisolone	5	0.9941	-	95	100	110	97	-	11.8	11.7	4.7	7.3	-	89	94	107	101	-	17.7	12.5	5.8	8.4
Furosemide	5	0.9940	-	106	105	110	101	-	13.2	15.3	14.5	6.8	-	101	98	106	101	-	11.1	14.4	11.8	5.5
THCCOOH-glu	10	0.9914	-	94	107	121	109	-	6.6	9.0	4.2	6.0	-	91	100	122	111	-	7.5	10.3	6.2	5.4
THCCOOH	1	0.9976	118	100	97	105	96	3.4	4.1	6.1	2.2	9.8	112	98	94	103	101	11.0	6.3	8.0	4.1	11.5

1 ng mL^{-1}, exhibited RSDs above 15% at 1.6 ng mL^{-1}. At 200 ng mL^{-1}, only budenoside and dexamethasone showed inter-day RSDs higher than 15%. Satisfactory figures of merit observed for the studied glucuronide compounds revealed that SPME is a suitable approach for the direct analysis of such metabolites without requiring an additional hydrolysis step. This might be of especial utility in cases where glucuronide standards are available, a poor yield after enzymatic hydrolysis is expected, or information about the concentrations of a given drug and its glucuronide form is required.

SPME is an equilibrium-based sample preparation technique where a small amount of extraction phase is exposed to the sample matrix. A common misconception among potential SPME users involves potential saturation of the coating in direct immersion mode due to the presence of multiple substances in the sample media. It is worth emphasizing that extraction in SPME depends on the extraction phase/sample matrix partition coefficient, and achieving an exhaustive recovery is not necessarily the ultimate goal of this microextraction technique. A recent work where SPME and SPE were thoroughly compared from their fundamental aspects has been recently published.[156] In this work, it was experimentally verified that for the same set of compounds, breakthrough volume affects SPE, whereas it does not have any effect on SPME quantitation. In this sense, using SPME for the determination of multiple substances of diverse chemistries and varying concentrations is highly convenient, provided that there is no limitation in terms of breakthrough, and that efficient sample clean-up can be easily attained.

2.4. Conclusions

The herein proposed methodology demonstrated its suitability for high-throughput determination of a wide range of compounds in complex matrices such as plasma with minimum sample

handling. Rewarding results in terms of matrix effects evidenced the satisfactory performance of this sample clean-up approach. The HLB extraction phase used for this study was demonstrated to be a versatile coating in cases where analysis of multiple compounds of varying physicochemical characteristics is required. LOQs were within 0.25 and 10 ng mL^{-1} for most of the studied compounds; however, further improvement might be attainable by introducing solvent evaporation and reconstitution steps in the automated sample preparation workflow. Satisfactory results for figures of merit such as inter and intra-day precision and accuracy were also found. Although the method herein presented was developed using LC-MS/MS analysis, comprehensive plasma screening might be feasible by combining the proposed sample preparation methodology and full scan high resolution MS. By incorporating a sample pre-incubation feature at controlled temperature conditions, it is possible to normalize bound concentrations, reduce chances of error due to temperature fluctuations, and facilitate automated drug-binding studies.

Overall, the most important advantages of the proposed method compared to typical approaches (*e.g.* SPE and protein precipitation) can be listed as follows: requirement of minimum sample pre-treatment, satisfactory selectivity of the SPME extraction phase towards small compounds, no concerns regarding sorbent breakthrough in multi-residue analysis and/or clogging of cartridges, and suitability of full automation and high throughput sample preparation. On the other hand, weak points of this protocol rely on the relative large volume of sample needed to completely cover the thin-film coating (>500 µL), the high limits of detection/quantitation expected for those compounds that exhibit high protein binding, and the lack of pre-concentration when the same sample and desorption volumes are used.

This SPME-based analytical workflow can be further expanded for the analysis of other biological samples in applications where sufficient coverage for a broad range of analytes is required. Even

though the reusability of biocompatible SPME coatings in thin-film format has been already demonstrated, future directions foresee the introduction of single use thin-film devices in order to absolutely avoid cross-contamination concerns in doping controls.

Chapter 3: Solid phase microextraction devices prepared on plastic support as potential single-use samplers for bioanalytical applications

3.1. Preamble and introduction

3.1.1. Preamble

This chapter of the thesis is already published as an article under the title "Solid phase microextraction devices prepared on plastic support as potential single-use samplers for bioanalytical applications" by Nathaly Reyes-Garcés, Barbara Bojko, Dietmar Hein and Janusz Pawliszyn., *Anal. Chem.* **2015**, *87*, 9722–9730. The content of the article is being reprinted in this thesis with permission of the American Chemical Society, and in compliance with the American Chemical Society and University of Waterloo policies.

I, Barbara Bojko, authorize Nathaly Reyes-Garcés to use the material for her thesis.

I, Dietmar Hein, authorize Nathaly Reyes-Garcés to use the material for her thesis.

3.1.2. Introduction

Solid phase microextraction (SPME) has demonstrated unquestionable advantages as an alternative sample preparation approach over traditional methods for several applications (*e.g.* liquid-liquid extraction and protein precipitation). Minimum solvent use, integration of sampling and sample preparation steps, simple operation, and suitability for on-site and *in vivo* determinations are just some of the important benefits of using SPME. Indeed, the introduction of biocompatible coatings suitable for direct extraction of diverse compounds from complex matrices has led to an expansion in SPME applications, especially in the field of bioanalysis.[73,74,102,157–159] These coatings, which consist of a biocompatible binder used to immobilize solid phase extraction

(SPE) particles and other sorbents, have demonstrated great selectivity towards small molecules, minimum or negligible protein fouling, and sufficient stability even for long-term reusability (140 extractions from plasma).[83,88]

Biocompatible SPME coatings are available in two main configurations: fibers and thin-films. The term "thin-film" is used to designate another geometry of SPME, in which devices consisting of a large coated surface area and a thin coating thickness (large extraction phase surface area-to-volume ratio) provide better sensitivity than traditional SPME fibers without sacrificing analysis time (short equilibration times).[75] Both, fiber and thin-film SPME devices, have been subjected to automation for high throughput analysis in the 96-well plate format; however, the enhanced sensitivity offered by thin-film geometry is preferred in several cases (*e.g. in vitro* biofluids analysis). Various studies reporting on the suitability of high-throughput thin-film SPME for analytical determinations in different matrices have been published recently.[84,160,161] In the area of bioanalysis, some recently reported applications of thin-film SPME include for instance the determination of tranexamic acid and rocuronium bromide in plasma, and the analysis of multiple doping substances in both urine and plasma samples.[80,90,162] Although, as already emphasized, the robustness of these biocompatible devices allows for reusability even in complex matrices, in some cases (*e.g.* doping analysis), it is certainly preferable, if not mandatory, to use disposable or single-use samplers. In this sense, exploring alternative materials for the construction of SPME devices, as well as simplifying the manufacturing process itself, are key factors to facilitate the widespread acceptance of this sample preparation method.

The introduction of novel materials in the fabrication of SPME samplers has been mainly directed towards finding alternative and cost-effective coating types.[87,163,164] However, broadening the current list of substrate materials used to immobilize different SPME extraction phases can also

provide unique opportunities. While self-supported SPME samplers (*e.g.* polydimethylsiloxane sheet pieces (PDMS)) are available for selected applications,[75,165] a solid substrate is typically required as base for application of the SPME coating, as well as to define the device geometry (*e.g.* wire or monofilament type of substrate for traditional SPME fibers, flat supports for thin-films and blade spray devices, and a metallic mesh for SPME-transmission mode).[79,166,167] Fused silica, StableFlex™, and metal non-ferrous alloys such as nitinol have been all used as fiber cores for gas chromatography (GC)-amenable SPME coatings (Table 3.1), while stainless steel and nitinol are currently employed as substrate materials of choice to immobilize biocompatible extraction phases.[87,163,164] Despite the satisfactory performance of biocompatible SPME samplers manufactured on such supports, certain applications will definitely benefit from the introduction of biocompatible substrates that are cheaper to manufacture, in addition to being more flexible, and easier to mold. For example, while the original *in vivo* SPME approach involves the use of traditional fibers by exposing them directly to the bloodstream or by inserting them in different types of tissue, [21,56,115,168] the development of devices for less invasive *in vivo* applications, such as saliva and mucosa analysis, might require alternative support materials.

Table 3.1. List of support materials commonly used to manufacture SPME devices.[82]

Material (geometry)	SPME coating application	Advantages	Disadvantages
Fused silica (fibers)	GC	Inertness, thermal stability, availability and low cost	It can easily break, especially at the point where the coating contacts the fibre plunger.
StableFlex (fused silica coated with a thermally stable polymer)	GC	It is more robust than bare fused silica. Provides more stable attachment for some adsorbent coatings.	Thermally stable at maximum 320 °C. Depending on extraction conditions, artefact peaks could appear.

(fibers)			
Non-ferrous alloy (nitinol) (fibers)	GC and LC	Flexibility, tensile strength, shape memory properties, thermal stability (450 °C) and inertness.	High cost
Stainless steel (thin-films)	LC	Accessibility and robustness.	Presence of iron can lead to a lower inertness compared to nitinol. Limited flexibility.

Various requirements should be fulfilled when looking for substitute materials to manufacture SPME devices for bioanalysis. First of all, the material should be biocompatible, suitable for sterilization, and able to handle temperatures normally employed to cure the polymeric binders used for SPME coatings. Once applied, the coating should be sufficiently stable on the substrate, and ideally, the coated material should not release any type of interferences, neither in the sample nor in the desorption medium. Substitute support materials for SPME should also offer good chemical resistance, low moisture absorption, affordability, and be easily accessible. Several materials, including metals and polymers, are used to manufacture various commercially available medical devices.[169,170] Among this list of medical grade materials, thermoplastics represent an important group of polymers that are widely used for the production of healthcare components.[169,170] Given that these plastics display many of the features required for the preparation of SPME samplers, in this work, polybutylene terephthalate (PBT) was tested as a potential support for application of SPME biocompatible extraction phases. For this purpose, coating preparation conditions were modified according to the new support material characteristics, and thin-film SPME devices were prepared using two different PBT geometries: rounded and flat. In this study, an SPME coating made of hydrophilic-lipophilic balanced particles

(HLB) and polyacrylonitrile (PAN) was selected due to its suitability to extract a wide range of compounds.[162] A thorough evaluation of the newly prepared samplers in terms of stability, reproducibility, and performance in the extraction of seventeen doping substances from various biological matrices (urine, plasma, and whole blood) is herein presented. The model compounds chosen for this work covered logarithmic octanol-water partition coefficients (log P) values ranging from 0.33 to 6.56, and included drugs bearing different structural moieties. Figures of merit corresponding to determinations of total concentrations of the selected analytes spiked in different biofluids are also reported. Lastly, this work presents a discussion regarding the impact of sorbent type on coating wettability; a comparison of water contact angles measured on HLB-PAN, C18-PAN, and only-PAN coatings provided remarkable evidence on the advantages of using HLB-PAN as SPME coating for the analysis of aqueous matrices.

3.2. Experimental section

3.2.1. Materials and supplies

A 250 mL flask-type sprayer, formic acid, PAN, potassium chloride, sodium chloride, potassium phosphate monobasic, and sodium phosphate dibasic were obtained from Sigma-Aldrich (Oakville, ON, Canada). Oasis hydrophilic-lipophilic balance 30 μm sorbent particles (HLB) were obtained from Waters (Milford, MA, USA). Discovery silica-based C18 5 μm particles were gently provided by Supelco Sigma-Aldrich (Bellefonte, PA, USA). N,N-dimethyl formamide (DMF) was purchased from Caledon Labs (Georgetown, ON, Canada). PBT rounded pieces (1.7 mm diameter) were obtained from Professional Analytical System (PAS) Technologies (Magdala, Germany), and PBT film (300 mm width, 2 m length, 0.5 mm thickness) was purchased from Goodfellow (London, UK). Polypropylene Nunc U96 deep well plates were obtained from VWR international

(Mississauga, ON, Canada) and LC-MS grade solvents (acetonitrile, methanol, and water) were purchased from Fisher Scientific.

The following compounds were selected as model analytes to evaluate the SPME-HLB-PBT devices: amphetamine, 17-α-trenbolone, benzoylecgonine, bisoprolol, clenbuterol, codeine, exemestane, GW501516, methamphetamine, metoprolol, morphine, nikethamide, propranolol, salbutamol, stanozolol, strychnine, and toremifene. Codeine-d_3, oxycodone-d_3, cannabidiol-d_3, methadone-d_3, (±)11-nor-9-carboxy-Δ^9-THC-d_3 (THCCOOH-d_3), testosterone-d_3 and salbutamol-d_3 were used as internal standards. Further details about compounds suppliers are provided in Chapter 2.

3.2.2. Preparing thin-film SPME devices on PBT support

Rounded PBT pieces were trimmed to 53 mm length. In the case of SPME-HLB-PBT devices on flat support, rectangular PBT pieces with a 0.5 mm thickness (10 x 8 cm) were cut using a conventional paper trimmer. Prior to the application of the coating, the area to be coated was uniformly sanded using commercial sandpaper (first using a sandpaper of a medium macro grit (P150) and then using one of ultra-fine micro grit (1500)). All PBT pieces were cleaned with methanol and acetonitrile (20 min in each solvent under sonication), and then left to dry at room temperature.

For the coating procedure, a slurry was prepared by mixing approximately 0.7 g of HLB particles, 3 mL of DMF, and 10 mL of 7% (w/w) PAN/DMF solution (prepared by mixing PAN with DMF, and heating the obtained solution at 90 ˚C for 1 h). A 2 cm length coating was applied by spraying uniform layers of slurry and curing each layer at 125 ˚C for 2.5 min (14 cycles in total) (Figures 3.1A, 3.1B and 3.1C). From the coated rectangular pieces, SPME-HLB-PBT samplers with a 2.3

mm width were cut using a paper trimmer as well. Six of these devices were over-coated with PAN by dipping them in 7% PAN solution, as reported in the literature.[171] Finally, twelve SPME-HLB-PBT devices on flat support (6 of them over-coated with PAN) were arranged to ensure compatibility with the Concept 96 system, as shown in Figure 3.1D. All the SPME devices were cleaned in a solution of 2:1:1 v/v methanol:acetonitrile:isopropanol for 120 min.

To characterize the prepared devices, scanning electron microscopy (SEM) images were taken using a LEO 1530 field emission (Carl Zeiss NTS GmbH, Germany), and microscope pictures were taken using an Olympus SZX10 stereomicroscope system equipped with a SC30 digital camera (Olympus, Japan).

The previously described coating procedure was also followed to apply HLB-PAN, C18-PAN and only-PAN (without sorbent particles) coatings on flat PBT pieces (2 x 10 cm). These coated PBT pieces were subsequently used to investigate the wettability of these extraction phases. The wettability of these three coatings was assessed by measuring the contact angle of 30 µL water drops according to the sessile drop method. Images were acquired every 2 s, and contact angle measurements were collected using Axisymmetric Drop Shape Analysis (ADSA).

3.2.3. Sample preparation for LC-MS/MS analysis

An initial assessment of PBT as a substrate for the manufacture of thin-film SPME devices was carried out with the rounded pieces (Figures 3.1A and 3.1B). For this purpose, phosphate buffer solution (PBS) and three different biological matrices (urine, plasma, and whole blood) were used to test the plastic devices. Aliquots (1080 µL) of each matrix were spiked with methanolic stock solutions containing the model compounds. The organic solvent content was kept below 1% in all cases. Once spiked, sample pre-incubation was allowed for 1 h under constant vortex agitation

71

conditions to ensure proper equilibration between the model compounds and the different tested matrices. Table 3.2 summarizes sample preparation parameters selected for urine, plasma, and blood analysis. These experimental conditions were chosen based on previous work done in our group.[80,162] As can be seen, the same parameters used for plasma analysis were employed for extraction from whole blood, except for an additional washing step that was introduced after pre-conditioning, and three 5 s wash steps conducted after each extraction. In addition, a higher concentration of internal standard was used for blood and plasma samples compared to urine samples with the aim of compensating for low recoveries due to matrix binding effects. Since the number of SPME-HLB-PBT samplers on rounded PBT support was limited, matrix matched calibration curves were constructed for each biological fluid using one device per calibration level (0.1, 0.25, 0.5, 1, 5, 10, 25, 50, 75, and 100 ng mL^{-1}). Accuracy and precision were evaluated at 1.6, 15, 35, and 70 ng mL^{-1}, using three devices per concentration level. Limits of quantification (LOQ) were determined as the lowest concentration points at which both deviations from nominal concentration values and relative standard deviations were below 20% for each individual compound. All steps of the SPME method were carried out at room temperature, and uniform stirring was conducted by placing the vials in a multi-tube vortex agitator. SPME-HLB-PBT devices on flat PBT support were employed to evaluate the robustness of the coating immobilized on the selected substrate. For this purpose, consecutive extractions from plasma and whole blood spiked with six of the model compounds were performed using a set of 12 films arranged in the Concept 96 system (Figure 3.1 D). For this part of the study, experimental conditions were kept as already described for whole blood analysis, except for extraction time and desorption volume, which were set at 60 min and 1200 µL, respectively. All extracts were analyzed using liquid chromatography-tandem mass spectrometry (LC-MS/MS).

3.2.4. LC-MS/MS conditions

All the extracts were run using an LC-MS/MS system comprised by an Accela autosampler, an Accela pump and a triple quadrupole mass spectrometer TSQ vantage with a heated electrospray ionization source operating in positive mode (Thermo Scientific, San Jose, USA). For chromatographic separation, a pentafluorophenyl core shell column (1.7 µm, 2.1 mm × 10 mm) with guard (PFP security guard ultracartridge) was employed (Phenomenex, Torrance, CA, USA). A ternary mobile phase system consisting of 0.1% formic acid (A), acetonitrile with 0.1% formic acid (B) and methanol with 0.1% formic acid (C) was used for LC separation. Gradient elution conditions were set as follows: A, B and C were held at 90, 5 and 5%, respectively, for 0.5 min, B and C were linearly increased to 50% in 6.5 min, then C was increased to 75% and B decreased to 25% in 5 min and held for 3.5 min. Finally, the column was kept at the initial gradient composition for 2 min. The column temperature was maintained at 35 ˚C, the total run time was 17.5 min, and the column flow was set at 0.3 mL/min. Samples were stored in the autosampler at 5 ˚C and the injection volume was 10 µL. MS analysis was carried out using selective reaction monitoring (SRM) mode (please refer to Table 2.1 in Chapter 2) and conditions were optimized by doing direct infusion of the standards. Other parameters were the following: spray voltage = 1300 V, vaporizer temperature = 275◦C, sheath gas = 45 units, auxiliary gas = 30 and capillary temperature = 280◦C.

Table 3.2. Summary of experimental conditions selected for SPME.

Parameter	Urine	Plasma	Whole blood
Sample volume	1080 µl		
Phosphate buffer (pH = 7)	120 µL (2 M buffer)	120 µL (1 M buffer)	

Parameter	Urine	Plasma	Whole blood
Internal standard	Spiked in buffer at 200 ng mL^{-1}	15 µL of 8 µg mL^{-1} solution	
Preconditioning	30 min in 1500 µL of 1:1 methanol:water	30 min in 1500 µL of 1:1 methanol:water + 10 s wash in nanopure water	
Extraction time	90 min		
Washing	10 s in 1500 µL of nanopure water (manually performed using vortex agitation)	3 times each in 1500 µL of nanopure water for 5 s	
Desorption	20 min in 600 µL of 4:1 methanol: acetonitrile acidified with 0.1% formic acid		

3.3. Results and discussion

3.3.1. Characterization of PAN-HLB coating prepared on plastic and evaluation of PBT as a support for SPME

The optimized procedure for preparing thin-film PAN-based SPME coatings on a stainless steel support has been already reported.[88] In that study, spraying over a previously etched surface and curing at 180 ˚C for 2 min were found to be optimum conditions. Due to the characteristics of the material selected as a new support for SPME devices, modifications to the already reported protocol were necessary. First of all, since etching with concentrated acid was not feasible, the plastic surface was only sanded with regular sandpaper (as indicated in section 3.2.2). This step was taken with the aim of improving the adherence of the biocompatible coating on PBT. Secondly, considering that the maximum temperature for long term use of PBT is 125 ˚C, the coating curing procedure was conducted at 125 ˚C for 2.5 min.
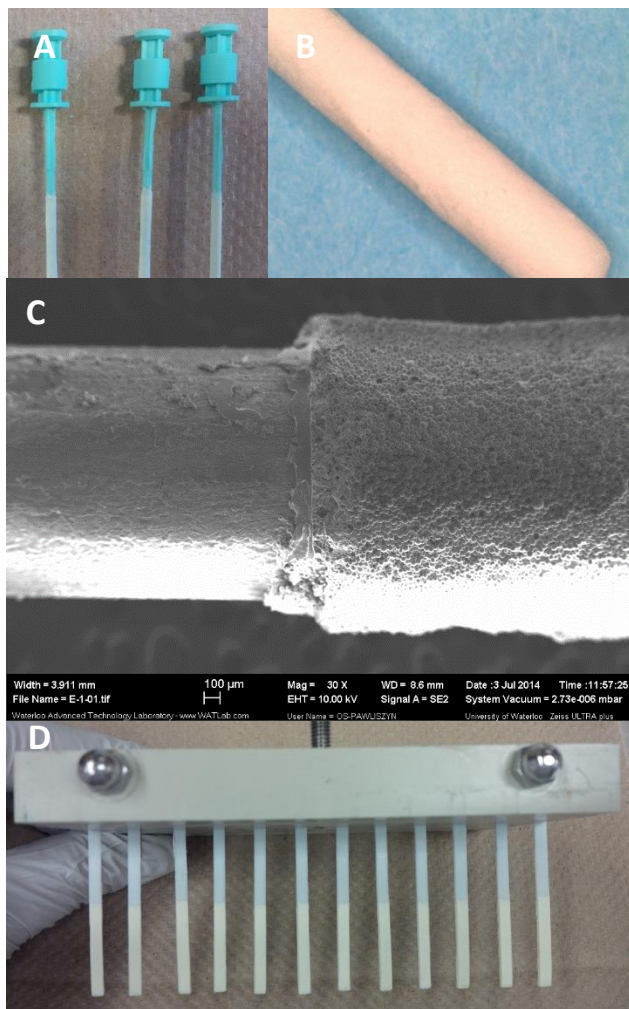
Figure 3.1. Rounded thin-film SPME devices prepared as described (A), microscope pictures of the HLB coating applied on the rounded plastic pieces (B), SEM image of the morphology of the coating on PBT support using 30x magnification (C) and SPME-HLB-PBT devices (on flat PBT support) in an arrangement compatible with the Concept 96 system (D).

As can be seen in both the microscope picture and SEM image presented in Figures 3.1B and 3.1C, a uniformly coated surface was obtained. The robustness of the coated plastic devices was tested by exposing them to water, methanol, and acetonitrile for a total period of 20 h under constant vortex agitation. No noticeable changes in the coating structure were observed, and no detachment of the coating from the plastic surface occurred. These findings demonstrated the stability of the HLB-PAN layer immobilized on the newly proposed substrate and validated the selected

conditions for the coating procedure. Provided that no etching with concentrated hydrochloric acid is required, a simplified and greener coating application approach can be established.

After verifying the stability of the SPME coating on PBT, inter-device reproducibility was also assessed. Satisfactory results were obtained for 20 rounded devices employed to extract from spiked PBS, showing RSD values below 13% for all the tested compounds (Figure 3.2). However, it is worth noting that the rounded shape of the plastic support may have hindered the uniform application of the SPME coating by spraying. Although 13% was an acceptable RSD value, better results were obtained when a flat support was used.
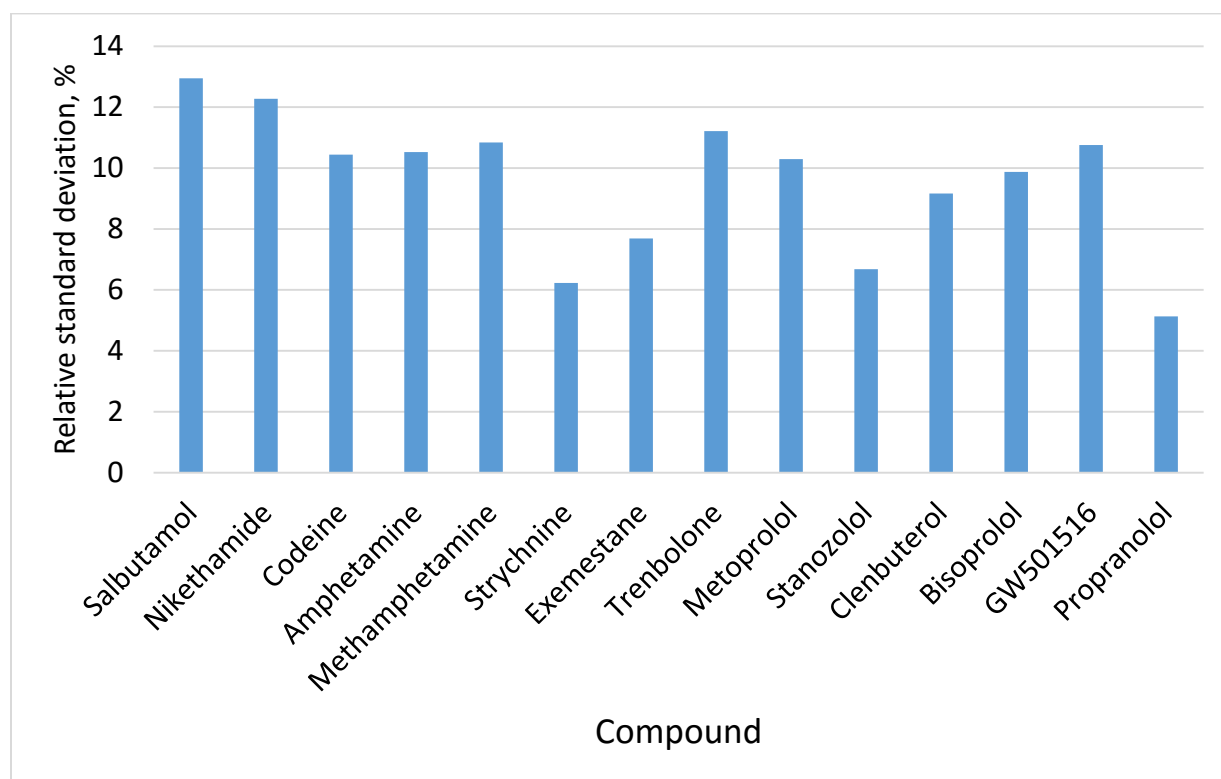
Figure 3.2. Inter-device relative standard deviation values (RSDs, %) obtained from coated rounded PBT pins (n=20) for various drugs. Extractions were performed from PBS spiked at 50 ng mL-1. The extraction time was 45 min.

Following the initial positive results obtained for the new coated material, an evaluation was conducted regarding possible interferences arising from the substrate that may be introduced into the sample or desorption media. For this purpose, an initial assessment of the background provided by the SPME coating prepared on the PBT support was carried out. Various new SPME-HLB-PBT devices were desorbed in 4:1 methanol:acetonitrile (v/v) acidified with 0.1% formic acid for 20 min. Prior to blank desorption, a cleaning step was performed by exposing the plastic devices to a mixture of organic solvents (2:1:1 v/v methanol:acetonitrile:isopropanol) under vortex agitation conditions for 120 min. Extracts were then run in full scan mode and compared with solvent blanks and extracts from the new HLB-PAN coatings prepared on a regular stainless steel. As can be seen in Figure 3.3, no significant differences were observed among the background signals obtained for all blanks. As a second means of verifying the absence of interferences coming from the proposed devices, absolute matrix effects were estimated according to the procedure proposed by Matuszewski et al.[154] Extracts obtained from the desorption of blank SPME-HLB-PBT samplers were spiked with the target compounds at 50 ng mL^{-1}, and their response (peak area) was compared with the one from standards prepared in neat solvent at the same concentration level. Likewise, extracts from urine and plasma blanks obtained with SPME-HLB-PBT devices (n = 6) were post-spiked and compared with neat standards as well. As shown in Table 3.3, no absolute matrix effects coming from the devices prepared on the PBT support were found for all the studied compounds. In addition, no significant matrix effects (80 – 112%) were observed for the compounds spiked in urine and plasma blank extracts. These results demonstrated the stability of the SPME coatings on the polymeric support, while proving the absence of possible interferences that might be released upon contact between the coated PBT and the sample medium or desorption solvent.
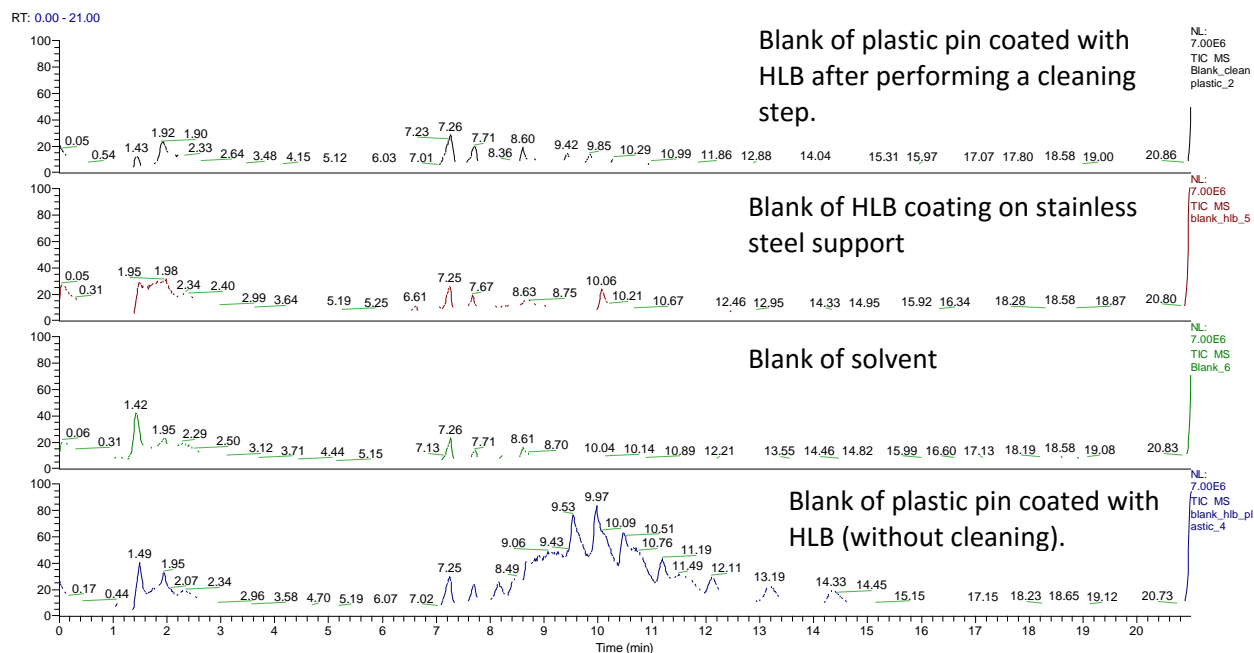
Figure 3.3. Blanks run in positive full scan mode (100 – 1000 m/z) using TSQ vantage. A cleaning step was performed by exposing the rounded coated PBT devices to a mixture of organic solvents (2:1:1 v/v methanol:acetonitrile:isopropanol) for 60 min under vortex agitation conditions.

Table 3.3. Evaluation of absolute matrix effects in blank solution coming from desorption of new plastic HLB devices, and in extracts of blank urine and plasma obtained with such plastic devices (n=6, extracts spiked at 50 ng mL^{-1} and analyzed in positive ionization mode).

Compound	Absolute matrix effects, %		
	Plastic devices blank extract	**Plasma blank extract**	**Urine blank extract**
Morphine	99	106	93
Salbutamol	100	107	112
Nikethamide	101	108	108
Codeine	99	107	88
Benzoylecgonine	96	110	107
Amphetamine	95	103	102
Methamphetamine	100	105	101
Trenbolone	97	103	81
Strychnine	94	94	88
Metoprolol	98	91	95
Exemestane	95	97	87
Clenbuterol	99	92	94
Stanozolol	94	92	93

Bisoprolol	99	89	79
GW501516	101	103	103
Propranolol	99	99	90
Toremifene	103	107	102

3.3.2. Using SPME devices on polymeric support for the analysis of doping substances in urine, plasma, and blood

3.3.2.1. Urine and plasma analysis

The proposed rounded PBT devices were used for the analysis of urine and plasma samples according to the experimental conditions provided in Table 3.2. As can be seen in Table 3.4, rewarding figures of merit were obtained when using SPME-HLB-PBT devices in both matrices. Satisfactory results were observed for most analyzed drugs, with good linearity ($R^2 > 0.99$), accuracy (80 – 120%), and precision (RSD < 7%) measures. As expected, less polar compounds such as toremifene (logP 6.56) and GW501516 (logP 6.46) exhibited higher LOQ values in plasma than in urine due to protein binding effects. On the other hand, polar compounds such as salbutamol (log P 0.64) and morphine (log P 0.89), which are not significantly affected by protein binding interactions, showed the same LOQ values in both matrices. Indeed, the LOQ value for a given analyte is directly correlated to the absolute SPME recovery, which, in turn, depends on several parameters, namely, the extraction time, the convection conditions, the coating volume, and the affinity of the compound for the matrix components and for the SPME coating. Although in SPME a small amount of analyte proportional to the analyte concentration in the sample is extracted, depending on the previously listed factors and on the proportion between coating and sample volumes, exhaustive, or almost exhaustive extraction can take place. For some of the model compounds, this can be reflected in the higher enrichment factors (EF, analyte concentration in the extract/analyte concentration in the sample) estimated in urine compared to those EFs calculated

Table 3.4. Figures of merit for urine and plasma analysis using rounded SPME-HLB-PBT devices.

Compound (logP)[a]	Urine						Plasma					
	LOQ, ng mL^{-1}	R^2	Accuracy %, (RSD, n=3)				LOQ, ng mL^{-1}	R^2	Accuracy %, (RSD, n=3)			
			1.6 ng mL^{-1}	15 ng mL^{-1}	35 ng mL^{-1}	70 ng mL^{-1}			1.6 ng mL^{-1}	15 ng mL^{-1}	35 ng mL^{-1}	70 ng mL^{-1}
Morphine (0.89)	0.1	0.9984	100 (0.1)	89 (1.0)	102 (1.4)	102 (0.4)	0.1	0.9958	116 (0.1)	107 (1.1)	92 (3.8)	110 (2.0)
Salbutamol (0.64)	0.1	0.9952	103 (0.1)	87 (0.7)	97 (0.9)	98 (1.7)	0.1	0.9936	109 (0.1)	104 (0.5)	103 (2.7)	108 (3.7)
Nikethamide (0.33)	0.5	0.9895	103 (0.1)	81 (1.5)	90 (1.7)	85 (1.7)	0.5	0.9986	100 (0.1)	102 (1.2)	100 (3.2)	104 (5.3)
Codeine (1.19)	0.1	0.9977	101 (0.1)	87 (0.5)	103 (1.1)	101 (1.0)	0.1	0.994	109 (0.1)	104 (0.4)	105 (2.7)	109 (3.9)
Benzoylecgonine (2.71)	0.5	0.9978	99 (0.1)	86 (1.8)	114 (0.8)	107 (3.0)	1	0.9993	87 (0.3)	110 (2.5)	107 (3.9)	113 (3.2)
Amphetamine (1.76)	0.25	0.9935	95 (0.1)	82 (1.4)	88 (1.6)	94 (3.8)	0.25	0.9919	105 (0.2)	104 (0.7)	112 (3.1)	99 (2.5)
Methamphetamine (2.07)	0.1	0.9928	94 (0.1)	84 (2.1)	89 (1.4)	94 (3.4)	0.25	0.9909	105 (0.2)	103 (0.9)	115 (2.5)	98 (4.2)
Strychnine (1.93)	0.5	0.9959	94 (0.1)	85 (1.9)	103 (1.6)	99 (4.6)	5	0.9935	-	121 (0.7)	94 (3.8)	116 (5.5)
Exemestane (3.11)	1	0.9975[b]	107 (0.1)	87 (0.8)	88 (1.1)	108 (3.2)	1	0.9922	118 (0.2)	106 (1.0)	112 (2.2)	111 (4.7)
Trenbolone (2.27)	1	0.9958[b]	104 (0.2)	74 (0.6)	81 (0.5)	98 (7.8)	1	0.9922	107 (0.1)	105 (1.0)	105 (4.4)	105 (4.8)
Metoprolol (1.88)	0.25	0.9940	102 (0.1)	84 (0.6)	102 (1.9)	88 (2.3)	0.25	0.9982	107 (0.1)	107 (0.4)	112 (3.1)	109 (4.6)
Stanozolol (4.42)	0.1	0.9997[b]	94 (0.1)	81 (0.5)	87 (1.0)	105 (2.7)	5	0.9843	-	95 (0.4)	102 (3.2)	93 (4.4)
Clenbuterol (2.61)	0.1	0.9906	102 (0.1)	86 (1.0)	106 (1.7)	95 (1.6)	1	0.9968	79 (1.3)	123 (1.5)	105 (2.9)	118 (5.7)
Bisoprolol (1.89)	0.1	0.9953	93 (0.1)	82 (1.1)	103 (2.2)	86 (3.5)	0.5	0.9951	79 (1.0)	116 (0.7)	118 (2.7)	112 (5.7)
GW501516 (6.46)	0.1	0.9963	96 (0.4)	80 (1.8)	80 (4.9)	96 (3.9)	5	0.9940	-	98 (0.5)	98 (3.2)	103 (1.7)
Propranolol (3.48)	0.1	0.9913	91 (0.1)	74 (2.0)	93 (1.7)	86 (3.1)	5	0.9952	-	110 (0.9)	101 (3.4)	112 (2.1)
Toremifene (6.56)	1	0.9959	105 (0.2)	75 (1.3)	72 (4.8)	96 (6.5)	5	0.9976	-	85 (2.0)	101 (3.4)	118 (5.3)

Regression coefficients were calculated using LOQ values and 100 ng mL^{-1} as the lowest and highest calibration points, respectively.

[a]log P values were taken from Chemspider[150]

[b]Highest calibration point was 75 ng mL^{-1}

Table 3.5. Enrichment factors calculated in the different matrices evaluated.

Compound	Enrichment factors (Cextract/Csample)		
	Urine (RSD, %)	Plasma (RSD, %)	Blood (RSD, %)
Morphine	0.56 (6)	0.52 (6)	0.62 (4)
Salbutamol	0.65 (2)	0.21 (6)	0.33 (1)
Nikethamide	1.03 (3)	0.80 (5)	0.90 (9)
Codeine	0.90 (7)	0.71 (7)	0.85 (3)
Benzoylecgonine	0.59 (7)	0.51 (6)	0.42 (7)
Amphetamine	0.89 (9)	0.39 (7)	0.61 (1)
Methamphetamine	1.10 (9)	0.60 (8)	0.73 (3)
Strychnine	1.10 (5)	0.28 (12)	0.53 (4)
Exemestane	1.41 (3)	0.22 (9)	0.27 (20)
Trenbolone	1.34 (4)	0.32 (10)	0.47 (11)
Metoprolol	1.20 (4)	0.69 (13)	0.96 (4)
Stanozolol	1.59 (6)	0.02 (12)	0.06 (12)
Clenbuterol	1.33 (8)	0.52 (10)	0.86 (5)
Bisoprolol	1.12 (7)	0.75 (11)	0.97 (6)
GW501516	1.44 (7)	0.01 (16)	0.02 (10)
Propranolol	1.42 (6)	0.29 (7)	0.20 (10)
Toremifene	1.22 (12)	0.01 (14)	0.04 (12)

in plasma or in whole blood (Table 3.5). In regards to urine results, it is also worth emphasizing that the LOQs determined complied with or were lower than the minimum required performance levels (MRPL) stipulated by WADA. For instance, the LOQ value determined for clenbuterol, the compound with the lowest MRPL (0.2 ng mL^{-1}), not only fulfills WADA requirements but also allows for a quantification that is two times lower than the drug MRPL. Indeed, the observed differences between the LOQ values presented in this work and those already reported by BoyacI et al.[80] and Reyes- Garcés et al.[162] can be attributed to a reduction in the desorption solvent volume (600 μL instead of 1200 μL), a distinct SPME coating volume (coated stainless steel blades vs. coated rounded devices) and, in the case of urine, the use of HLB particles instead of C18. Figure 3.4 shows representative chromatograms corresponding to extracts obtained from the different biofluids spiked at LOQ levels.
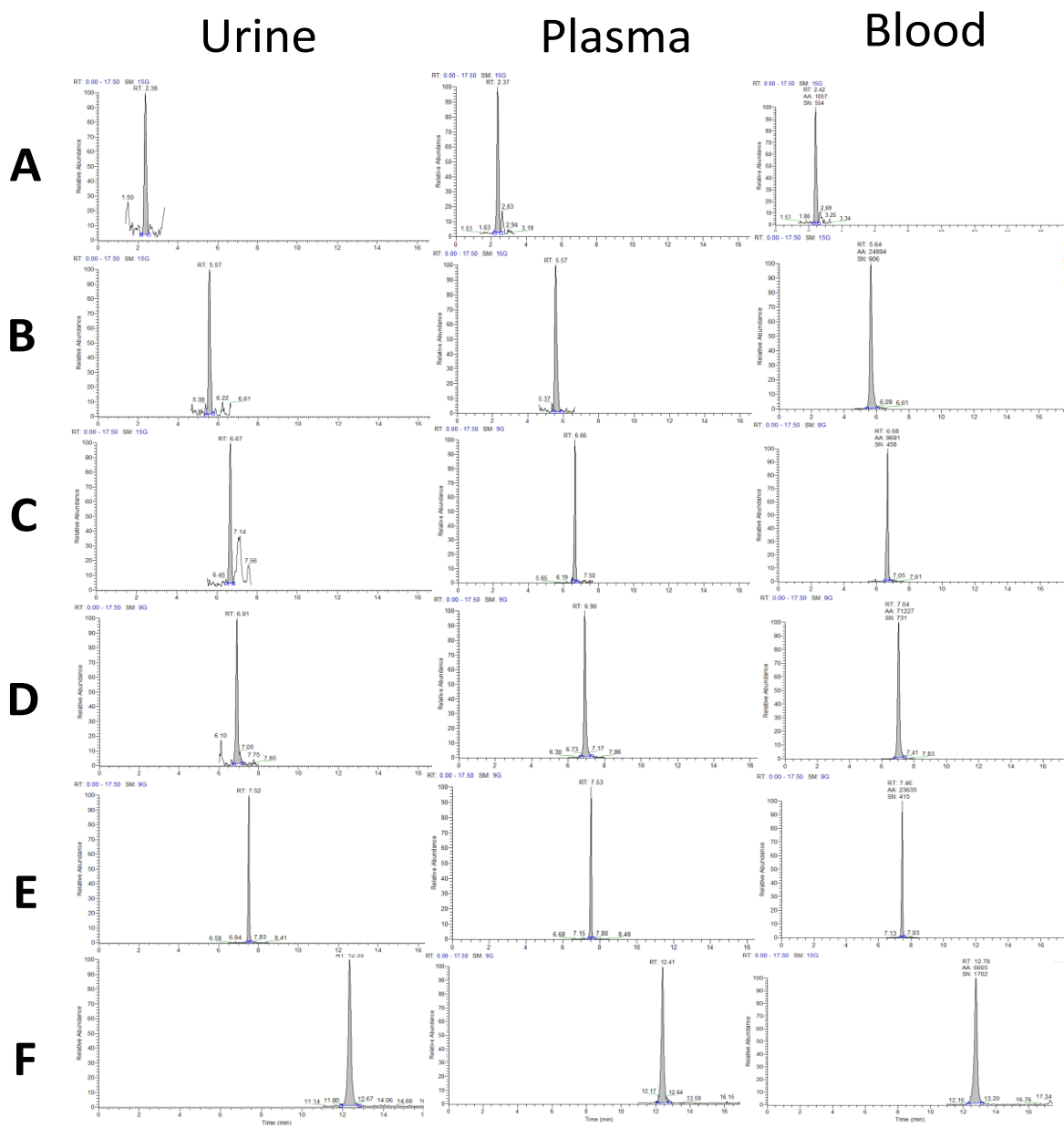
Figure 3.4. Representative SRM chromatograms corresponding to extracts obtained from urine, plasma and whole blood spiked at LOQ levels. Salbutamol (A), methamphethamine (B), stanozolol (C), clenbuterol (D), GW501516 (E), and toremifene (F).

3.3.2.2. Whole blood analysis

Due to the high content of proteins and the presence of red blood cells, using whole blood as a matrix is more challenging and subsequently less common than analyzing serum and plasma. Based on the already discussed results corresponding to urine and plasma, the suitability of SPME-HLB-PBT devices for whole blood analysis was also investigated.

A previous study published by Mirnaghi and Pawliszyn in 2012 reported irreversible attachment of red blood cells to C18-PAN thin-film SPME devices when they undergo direct immersion in whole blood using the Concept 96 workstation system.[171] As a feasible solution to this problem, and looking toward coating reusability in an automated fashion, a modified extraction phase consisting of an external layer of PAN over a C18-PAN coating was proposed.[171] This approach considerably improved the coating compatibility with blood and enabled its reusability for multiple extractions in such a complex matrix. However, it is worth emphasizing that the presence of the extra PAN layer leads to a decrease in extraction kinetics, and therefore affects method sensitivity, especially at pre-equilibrium conditions. Figure 3.5 shows a comparison of the absolute recoveries obtained for six of the model compounds, using SPME-HLB-PBT devices prepared on flat support with and without a PAN over-coating (applied by dipping). As can be seen, a decrease of more than 70% for some of the analytes was found due to the over-coating PAN layer. Given that in this case, potential application of the proposed devices as single use samplers is being considered, a different approach to test the rounded PBT coated pieces in whole blood analysis was taken.

The typical SPME workflow was modified by introducing three additional washing steps, as described in Table 3.2. A washing step was implemented after preconditioning in order to remove any excess organic solvent remaining on the coating. This prevented possible protein precipitation or cell disruption from occurring on the extraction phase when the wet SPME coating got in contact

with the whole blood matrix. Three wash steps of 5 s were also conducted after direct blood extraction (each wash step was performed in a new vial with clean water). It is worth highlighting that an evaluation of four different washing approaches (10 s static, 10 s with vortex agitation, two washing steps of 5 s with vortex agitation and three washing steps of 5 s with vortex agitation) showed that three consecutive washing steps did not cause any significant losses for any of the
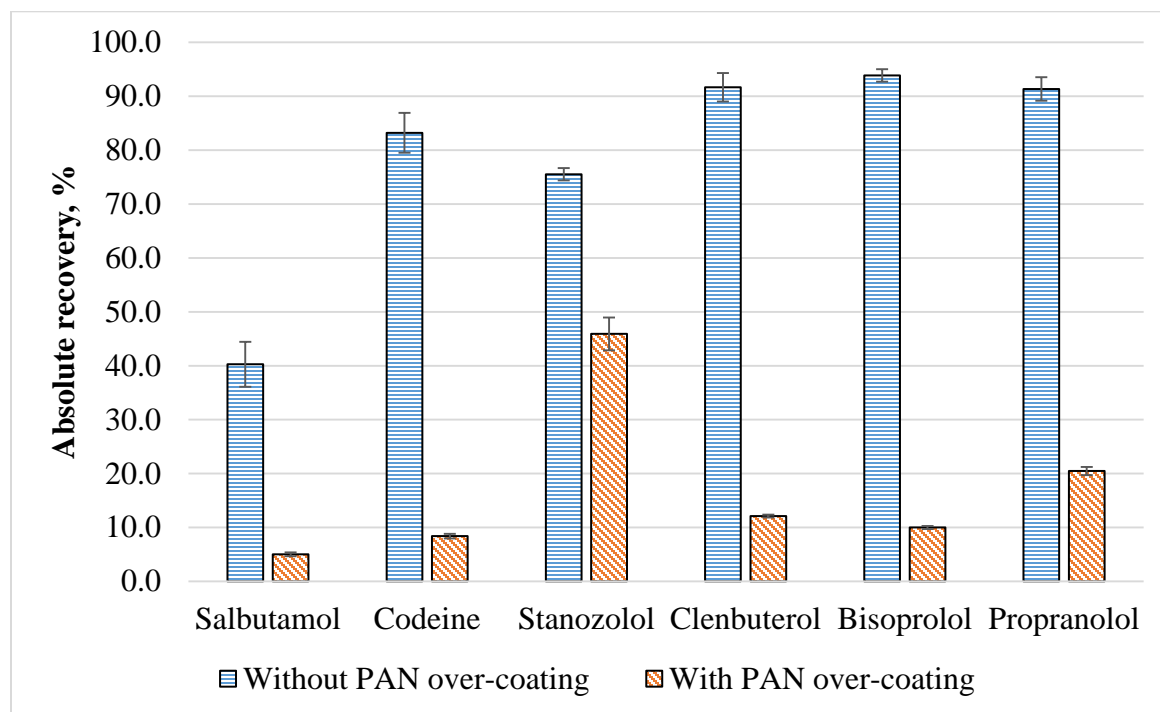
Figure 3.5. Comparison of absolute recoveries found using HLB thin-films with and without PAN over-coating applied by dipping. Extractions were performed from PBS spiked at 70 ng mL^{-1}. The extraction time was 60 min.

studied compounds for SPME devices coated with HLB particles (see Figure 3.6). Indeed, the washing step should be carefully optimized according to the SPME coating selected and the analytes of interest. For example, in the case of the HLB-PAN, it is expected to observe high affinity toward compounds bearing on their structures lone electron pairs and able to display π-π interactions with the divinylbenzene moiety.[172,173] The almost exhaustive recoveries provided by

84

HLB-PAN coating when used for the extraction of basic (*e.g.* clenbuterol, bisoprolol, and propranolol) and steroidal analytes (*e.g.* 17-α-trenbolone and stanozolol) from PBS are in agreement with other reports where the properties of HLB as SPE sorbent were investigated.[174,175] It is also worth to emphasize that, among the model compounds, salbutamol presented the lowest absolute recovery. Albeit for this compound a lower distribution coefficient is predictable due to its high hydrophilicity and degree of ionization, reproducible recoveries, even after several washing steps, were still attained.
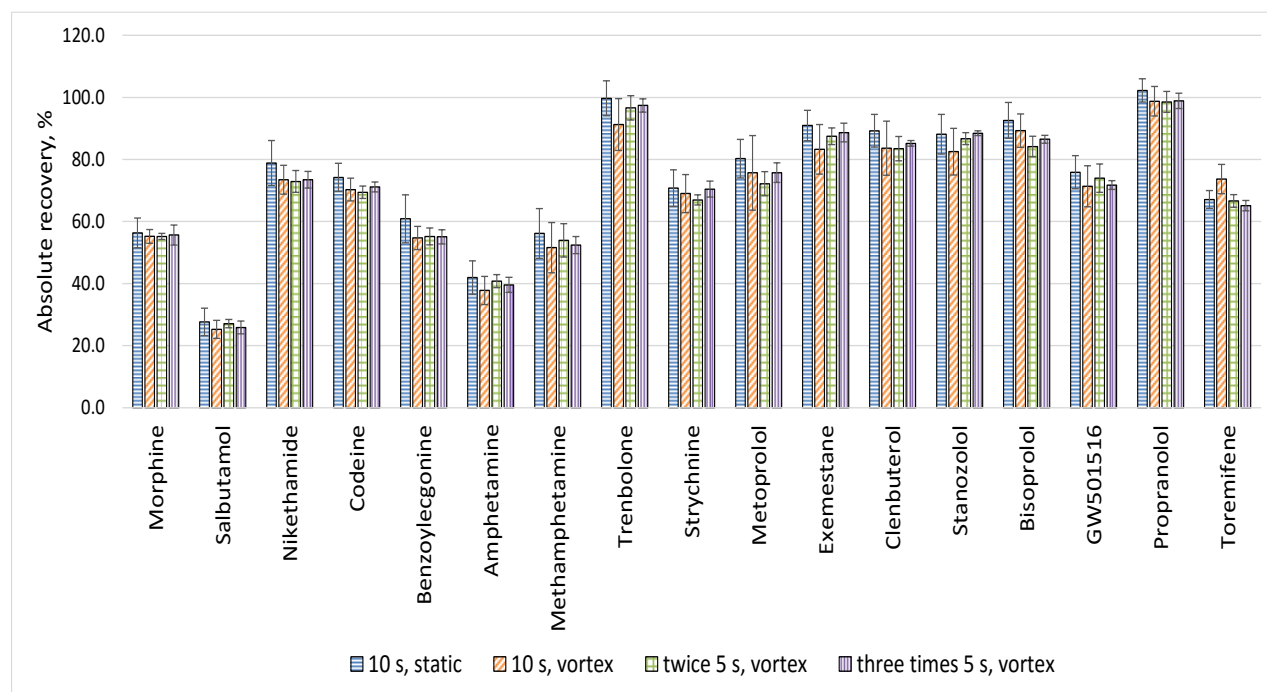
Figure 3.6. Evaluation of the effect of four different washing step approaches (10 s static, 10 s with vortex, two 5 s steps with vortex and three 5 s steps with vortex) on the final amount desorbed from rounded SPME-HLB-PBT devices (n = 4). Extractions were performed from PBS spiked at 50 ng mL^{-1} and mixed with 1 M buffer (9:1 ratio). The extraction time was set to 45 min.

Table 3.6. Figures of merit for whole blood analysis using rounded SPME-HLB-PBT devices.

Compound (log P)[a]	LOQ, ng mL^{-1}	R^2	Accuracy %, (RSD, n=3)			
			1.6 ng mL^{-1}	15 ng mL^{-1}	35 ng mL^{-1}	70 ng mL^{-1}
Morphine (0.89)	0.1	0.9984	107 (0.1)	102 (1.0)	99 (1.4)	108 (6.0)
Salbutamol (0.64)	0.1	0.9992	102 (0.1)	100 (0.3)	95 (0.7)	105 (5.0)
Nikethamide (0.33)	0.5	0.9993	110 (0.1)	101 (1.3)	91 (1.2)	106 (2.3)
Codeine (1.19)	0.1	0.9992	101 (0.1)	98 (0.3)	95 (0.5)	105 (5.5)
Benzoylecgonine (2.71)	0.5	0.9992	122 (0.2)	109 (2.0)	102 (1.7)	117 (10.6)
Amphetamine (1.76)	1	0.9994	86 (0.1)	101 (0.7)	94 (1.9)	106 (4.6)
Methamphetamine (2.07)	1	0.9987	83 (0.1)	104 (1.1)	95 (1.6)	108 (2.9)
Strychnine (1.93)	5	0.9980	-	103 (0.3)	97 (1.0)	103 (5.4)
Exemestane (3.11)	1	0.9988	87 (0.2)	94 (0.8)	95 (0.1)	104 (5.6)
Trenbolone (2.27)	1	0.9994	88 (0.1)	94 (0.5)	90 (0.9)	100 (6.8)
Metoprolol (1.88)	0.25	0.9970	97 (0.1)	99 (0.3)	94 (1.2)	100 (6.0)
Stanozolol (4.42)	5	0.9944	-	105 (2.2)	99 (3.5)	110 (5.4)
Clenbuterol (2.61)	1	0.9982	80 (0.1)	102 (0.3)	95 (0.8)	102 (5.7)
Bisoprolol (1.89)	0.25	0.9964	94 (0.1)	98 (0.5)	92 (0.5)	99 (6.4)
GW501516 (6.46)	5	0.9945	-	95 (0.5)	91 (2.6)	98 (5.2)
Propranolol (3.48)	5	0.9958	-	106 (0.9)	94 (0.4)	102 (7.5)
Toremifene (6.56)	5	0.9956	-	102 (1.8)	88 (3.1)	107 (10.0)

Regression coefficients were calculated using the LOQ value and 100 ng mL^{-1} as the lowest and highest calibration points, respectively.

[a] log P values were taken from Chemspider[150]

By following this modified SPME procedure, analytical figures of merit in whole blood were investigated. As can be seen in Table 3.6, satisfactory results in terms of linearity, LOQ, accuracy, and precision were obtained for all prohibited drugs under analysis. These findings also reflected the absence of irreversible fouling which, as already reported by several authors, can affect the kinetics of extraction with SPME.[176–178] SEM images and microscope pictures of the HLB coating after exposure to blood for 90 min (Figure 3.7) confirmed that irreversible protein attachment on the coating surface did not take place. In this regard, it is important to note that the feasibility of using the proposed devices for direct immersion in whole blood without any PAN over-coating

layer may be related to the agitation conditions, the composition of the slurry employed to prepare the devices (lower SPE particles/PAN solution ratio compared to previous reports[88]), as well as the dimensions and rounded shape of the PBT
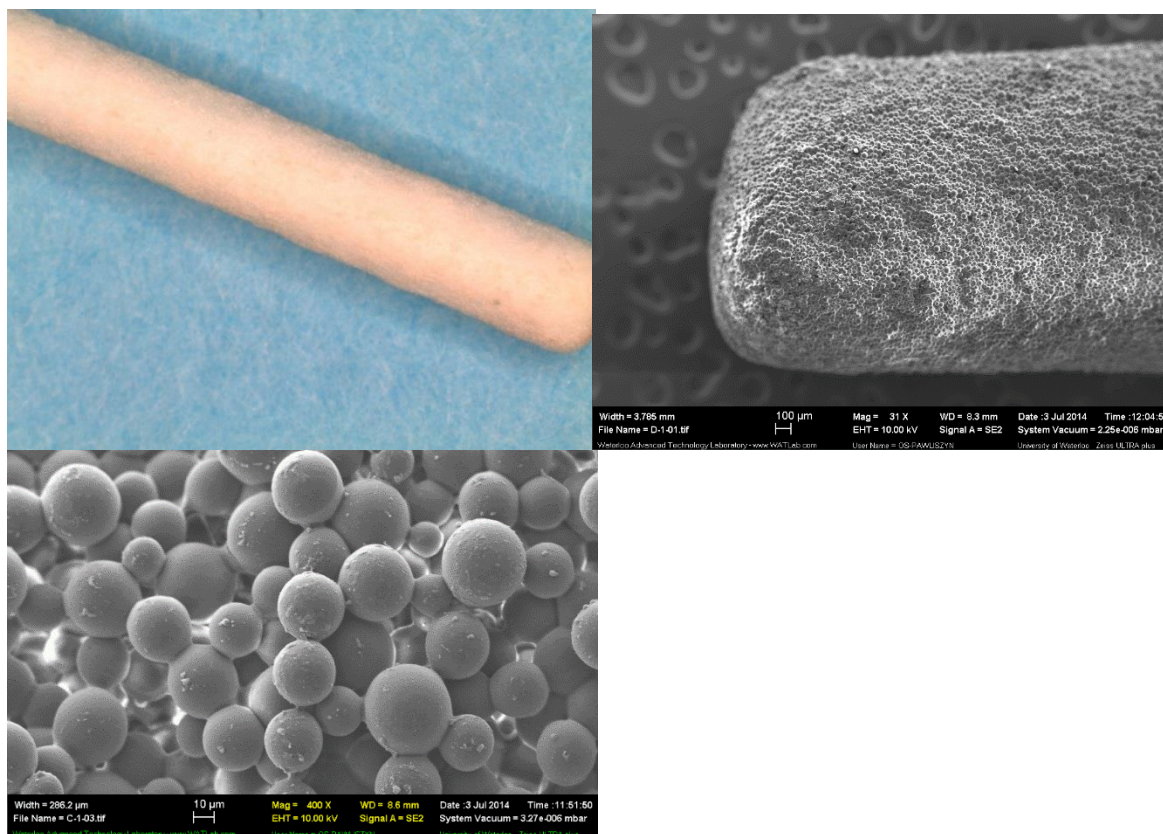
Figure 3.7. Microscope picture and SEM images (30x magnification) taken from SPME-HLB-PBT devices after being exposed for 90 min to whole blood.

support. In point of fact, shear stress imparted by blood flow conditions has been reported as a critical factor in determining whether a device is blood compatible.[179–182] The vigorous agitation provided by the multi-tube vortex system, together with the rounded shape and the specific dimensions of the coated devices (2.0 mm diameter), might have led to different shear conditions from those normally encountered when using the Concept 96 under its typical operational

configuration. Another aspect that should be also taken into account is that the evaluation of plastic devices was carried out in vials. Whole blood, when exposed to an open environment for a substantial period of time, as it occurs when using the Concept 96 system, is more prone to undergo alterations compared to blood that remains capped in a vial during the extraction process.[181] For this reason, additional considerations should be taken into account when expecting an antifouling SPME extraction phase at such conditions (*e.g.* using SPME coatings with an extra layer of PAN). Overall, the results demonstrated high blood compatibility for both the coating and support employed at the selected experimental condition for the proposed devices.

The presence of an absolute matrix effect after extracting from whole blood was assessed in the same manner reported for urine and plasma (Table 3.7). As presented in Table 3.7, no significant ion suppression/enhancement was found for any of the evaluated compounds at the selected experimental conditions. Indeed, using vortex stirring for the washing steps provided very effective cleaning/removal of possible interferences due to the strong agitation provided by the vortex. As a second approach to verify the performance of the plastic SPME devices in terms of analytical specificity at the tested conditions, transition ratios were also calculated for all the evaluated biofluids. In quantitative analysis using mass spectrometry, the ratio between qualifier and quantifier transition signals should be the same for both the standards and biological samples.[183] Results presented in Table 3.8 evidenced an overall satisfactory performance of the proposed methodology for the majority of the model compounds. Only trenbolone extracted from blood showed a significant deviation from the ratio calculated in standard; however, this may be overcome by improving the separation conditions.

Table 3.7. Absolute matrix effects assessed in whole blood

Compound	Ionization mode	Blank blood extract spiked at 50 ng mL^{-1}		Neat solvent, 50 ng mL^{-1}		Absolute matrix effects, %
		Average area counts	RSD, %	Average area counts	RSD, %	
Morphine	+	790613	6.8	746645	6.5	106
Salbutamol	+	1752803	6.4	1683275	7.4	104
Nikethamide	+	1770978	9.4	1698455	12.0	104
Codeine	+	901379	6.6	865793	6.5	104
Benzoylecgonine	+	2123832	5.5	2011989	5.7	106
Amphetamine	+	613793	7.8	597718	9.7	103
Methamphetamine	+	1472182	7.4	1403228	8.4	105
Strychnine	+	982709	4.9	892247	5.0	110
Exemestane	+	294528	3.8	284409	4.6	104
Trenbolone	+	294309	6.9	290659	7.0	101
Metoprolol	+	810327	7.8	807978	8.2	100
Stanozolol	+	2112271	4.9	2073968	5.3	102
Clenbuterol	+	2884970	6.2	2804007	7.6	103
Bisoprolol	+	4809840	6.2	4617177	6.8	104
GW501516	+	13394571	5.0	12500394	4.8	107
Propranolol	+	3172468	6.0	3189958	7.6	99
Toremifene	+	3873108	6.6	3851666	3.3	101

Table 3.8. Transition ratios calculated from standards and from the tested matrices. Values were calculated by dividing the qualifier transition signal by the quantifier transition. Concentrations of up to 3 times LOQ values were considered for this calculation.

Compound	Transition ratios Qual/Quant				Deviation from standard, %		
	Standard	Urine	Plasma	Blood	Urine	Plasma	Blood
Morphine	0.71	0.74	0.80	0.69	5	14	2
Salbutamol	0.24	0.24	0.29	0.29	2	22	21
Nikethamide	0.26	0.26	0.22	0.26	1	13	1
Codeine	0.82	0.89	0.76	0.87	8	6	7
Benzoylecgonine	0.31	0.29	0.30	0.29	7	4	8
Amphetamine	0.24	0.26	0.20	0.25	7	19	3
Methamphetamine	0.26	0.20	0.24	0.24	25	10	10
Strychnine	0.68	0.64	0.58	0.71	6	15	5
Exemestane	0.72	0.68	0.82	0.75	4	14	5
Trenbolone	0.95	0.90	0.93	1.73	5	2	83
Metoprolol	0.66	0.74	0.71	0.78	13	9	19
Stanozolol	0.45	0.35	0.46	0.49	21	3	11
Clenbuterol	0.44	0.34	0.42	0.42	22	4	4

Bisoprolol	0.16	0.14	0.16	0.17	16	1	7
GW501516	0.26	0.25	0.26	0.26	4	1	2
Propranolol	0.92	0.92	0.88	0.93	0	5	0
Toremifene	0.10	0.10	0.09	0.09	1	12	9

3.3.3. Assessment of HLB-PAN coating wettability
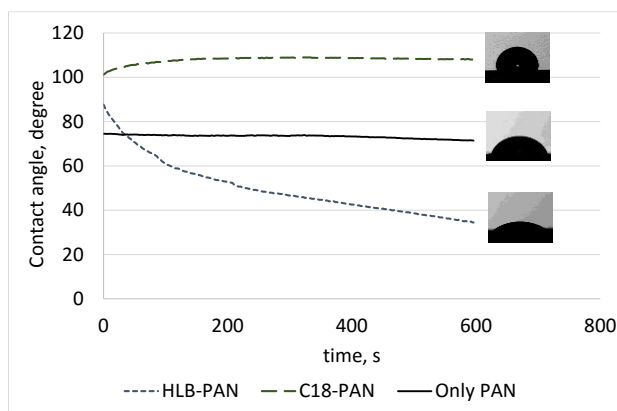
Figure 3.8. Water contact angles for HLB-PAN, C18-PAN and only-PAN coatings. Images were acquired every 2 s over a 10 min period.

Surface wettability has been traditionally conceived as an essential parameter in the design of materials with efficient resistance to protein fouling.[184,185] However, a direct relationship between low water contact angles (increasing wettability) and negligible protein adsorption or material biocompatibility has not been found in all the studied cases.[179,185–187] Despite this, determining the degree of wettability of PAN-based SPME coatings may provide important information considering the aqueous nature of biofluids. Indeed, easily wettable extraction phases are expected to facilitate the sample-coating interaction during the extraction process. Figure 3.8 shows the water contact angle variation over time found for HLB-PAN, C18-PAN and only-PAN coatings. Prior to the contact angle measurements, the HLB-PAN and C18-PAN surfaces were conditioned in a 1:1 methanol:water solution for 10 min, wiped with Kimwipes, and allowed to dry for approximately 10 min. As can be seen in Figure 3.8, although PAN was used as a binder in all the

tested surfaces, HLB particles imparted a high degree of wettability to the coating. On the other hand, C18 conferred significant hydrophobicity to the extraction phase, yielding estimated water contact angles above 100˚ over the entire measurement time. In relation to SPME extraction phases, these results suggest that using HLB combined with PAN, or even using other wettable materials, may provide improved performance compared to other sorbents, such as C18, when dealing with biological samples. As such, the development of SPME devices intended for spot sampling or even for *in vivo* sampling, where convection is certainly restricted, may need to include the determination of coating wettability as an important criterion.

3.3.4. Evaluation of the robustness and reusability of SPME thin-film devices prepared on plastic substrate using high-throughput configuration.

After verifying the suitability of PBT as a substrate for SPME devices, the robustness of the PAN-based coatings prepared on the new support was evaluated through multiple extractions from plasma and whole blood. Although there are cases where single-use samplers are certainly required, other analytical applications might be more flexible, and reusable SPME devices are a most convenient and cost-effective option. To validate the suitability of the new device for multiple use applications, SPME-HLB-PBT samplers made on flat support (with and without over-coating) were arranged in a Concept 96-compatible fashion, as shown in Figure 3.1D. Given that these devices were prepared by coating a PBT surface that was subsequently cut into smaller pieces, an initial assessment of inter-thin-film reproducibility was carried out. As can be seen in Table 3.9, RSD values below 7 and 3.5% (n=6) were found for SPME devices with and without PAN over-coating, respectively. In addition to carrying out an assessment of inter-device reproducibility, SPME-HLB-PBT samplers were physically inspected by taking microscope pictures of the coatings and of the interface between the coating and the plastic support (Figure 3.9). The obtained
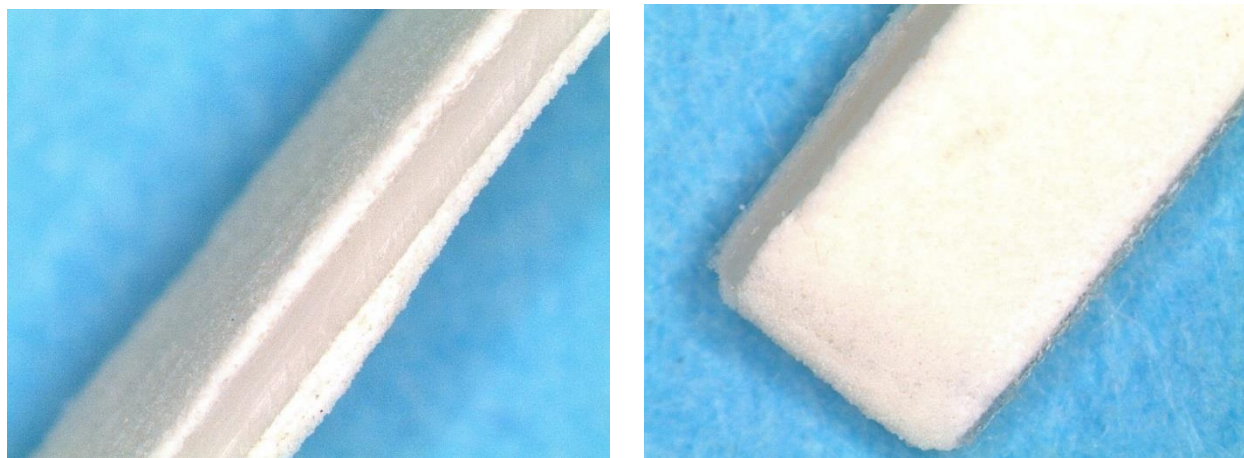
Figure 3.9. Microscope pictures of PAN-HLB thin-films obtained by cutting pieces of 2.3 mm width from a coated flat PBT rectangular piece (8 x 10 cm).

images of the lateral view of the devices confirm that good attachment was achieved between the PAN-based coatings and the PBT surface. It is worth highlighting that even after undergoing a cutting process, the SPME coating remained firmly adhered to the polymeric material. Regarding reusability, no statistical differences were observed between recovery values obtained in the first and twentieth trials performed in plasma (Figure 3.10). In the case of whole blood, propranolol and stanozolol showed a slightly lower recovery during the first extraction when compared to all subsequent experiments. This observed outcome may be due to the extra layer of PAN applied to the HLB coating which, in addition to slowing down the extraction kinetics, might require that the overcoated HLB coating receive more extensive conditioning in comparison to coatings without this over-coating; however, this effect was observed only for the two least polar drugs tested. Overall, the obtained results suggest that using PBT as a substrate may provide the same coating robustness and stability obtained with the use of etched stainless steel.

Table 3.9. Average absolute recoveries obtained when using HLB thin-films prepared on PBT support to extract from PBS spiked at 70 ng mL^{-1} (n=6 thin-films).

Compound	No overcoated		Overcoated	
	Abs. recovery, %	RSD, %	Abs. recovery, %	RSD, %
Salbutamol	38.7	5.2	5.0	7.1
Codeine	83.2	4.4	8.4	5.1
Stanozolol	75.5	1.5	45.9	6.6
Clenbuterol	91.7	2.9	12.1	2.3
Bisoprolol	93.9	1.2	10.0	2.9
Propranolol	91.4	2.4	20.5	3.7
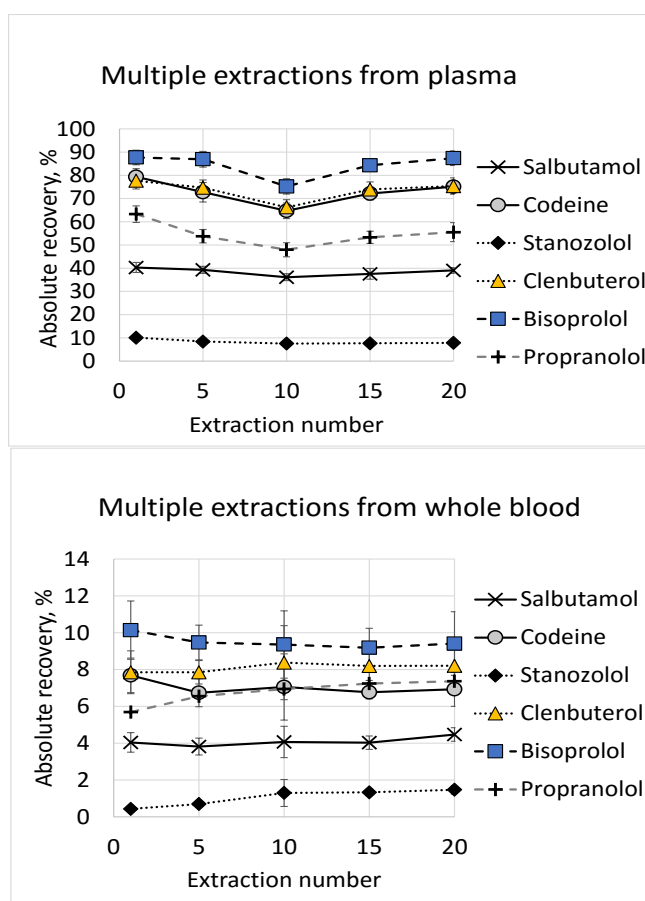
Figure 3.10. Evaluation of the stability and robustness of the HLB-PAN coating applied on PBT support. Consecutive extractions were performed from plasma (A) and whole blood (B) spiked at 70 ng mL^{-1} and mixed with 1 M phosphate buffer in a 9:1 ratio (sample:buffer) (n=6). Extractions from whole blood were carried out using HLB thin-films with PAN-over coating.

3.4. Conclusions

In this work, the suitability of PBT as a support to manufacture SPME devices that could be potentially employed as disposable samplers was demonstrated. Robust PAN-HLB coatings, free of background interferences and able to stand exposure to organic solvents for long periods of time, were attained by following a modified coating preparation procedure. Since no etching with hydrochloric acid was required, a greener manufacturing process with a reduced production of chemical waste was possible. Rewarding figures of merit were found when these SPME samplers were used for quantitative analysis of multiple doping substances in urine, plasma, and whole blood. LOQ values determined in urine met or were below the MRPL requirements set by WADA. In the case of plasma and whole blood, LOQ levels were in the low ng mL^{-1} which is within the range of expected concentrations in such matrices.[124] Absence of an absolute matrix effect in extracts obtained from the three tested biofluids proved that the SPME-HLB-PBT devices provided satisfactory sample clean-up. Indeed, whole blood analysis was facilitated by utilizing rounded SPME-HLB-PBT devices together with the implementation of multiple washing steps and vortex agitation conditions. HLB-PAN was demonstrated to be a more easily wettable coating than C18-PAN, which may be an important criterion to consider when developing disposable devices for spot sampling. The high stability of the biocompatible coating applied on PBT permitted the cutting of smaller portions from an already large coated piece, which may be convenient in cases where tailor-made sizes are needed. Although these devices were developed considering the concept of single-use, they can be re-used in applications where carryover at trace levels does not represent a serious concern. Overall, the introduction of alternative materials, such as polymeric substrates, may represent an important opportunity for new advances in the commercialization and acceptance of SPME in the bioanalytical field. Besides traditional fiber and

flat thin-film configurations, the development of other SPME geometries may be facilitated by integrating new materials as supports, and by taking advantage of technologies such as 3-D printing to create innovative samplers.

Chapter 4: The effect of hematocrit on solid phase microextraction

4.1.Preamble and introduction

4.1.1. Preamble

The results presented in this chapter have not yet been published in any journal. Nathaly Reyes-Garcés designed the experiments, conducted all the experimental work, processed the data, and wrote the corresponding discussion herein presented. Md. Nazmul Alam also participated in the data interpretation and discussion.

4.1.2. Introduction

Many bioanalytical studies and clinical tests rely on the quantitative determination of small molecules in whole blood samples. Given the complexity of this type of matrix, developing simple analytical workflows that can provide satisfactory results while remaining compliant with health regulations can be a challenging undertaking. Whole blood is comprised of two main components: plasma and blood cells. Blood plasma is an aqueous solution of solubilized proteins, low and high molecular weight components, metabolites, mineral salts, and ions. Plasma has a relatively simpler composition than whole blood, which makes it a commonly-used matrix for many routine bioanalytical determinations, the most representative case of which being the therapeutic monitoring of multiple drugs. The second main component of whole blood is the cells, which can be classified into three main types: red blood cells (erythrocytes, ~96%), white blood cells, and platelets.[188] Hematocrit (Hct) is a term that refers to the fraction of blood volume made up of red blood cells, and its typical values are within the ranges of 40 – 50% for men, and 36 – 44% for women.[189] However, Hct levels can fall outside of these ranges in particular cases, such as individuals living at high altitudes, newborns, or anemic people.[14] Although plasma and serum are

the specimens of choice for several standardized analytical procedures, the direct analysis of whole blood is required in certain instances (*e.g.* the determination of immunosuppressive drugs). Hence, understanding and evaluating Hct's effect on whole blood analysis should always be a matter of consideration.

Numerous sample preparation methodologies for analyzing small compounds (<1500 Da) in whole blood using liquid chromatography coupled to mass spectrometry have been reported in the literature.[11,73,190–195] Among such approaches, liquid-liquid extraction (LLE) and protein precipitation (PP)—which, in some cases is followed by cleaning steps involving online or offline solid-phase extraction—are perhaps the most commonly used strategies. For substances that display a high affinity for red blood cells, the use of additives that induce hemolysis and the release of compounds from erythrocyte membranes (*e.g.* zinc sulfate) have been reported as effective means of normalizing the sample matrix composition.[196–198] Nonetheless, the use of appropriate internal standards is always recommended in order to ensure satisfactory method accuracy and precision. Due to the highly-invasive nature of traditional blood collection, alternative blood micro sampling strategies have been garnering much interest. For instance, dried blood spots (DBSS), which is a well-established sampling and whole-blood-analysis methodology, has been broadly reported in several applications due to its low invasiveness.[12,123,134,193,195,199] In DBSS, a small drop of whole blood is placed on filter paper, allowed to dry, and subsequently analyzed by desorbing fixed-diameter discs punched out from the dried spots. Prior studies have found that Hct's effect on DBSS analysis is mostly associated with the variable spreading pattern that blood samples exhibit when spotted onto DBSS cards;[14,189,193] the viscosity of blood samples is directly related to their Hct values, and samples with higher Hct values produce smaller spot radii. Other critical factors in determining the degree of bias in DBSS measurements are the analyte characteristics

and the paper type. The best strategy for overcoming Hct's impact in relation to variable blood spreading is to analyze whole spots of volumetrically-applied blood.[14,16,193] The incorporation of appropriate internal standards via spraying prior to DBSS extraction has proven to be a feasible way of mitigating the variations related to matrix effects or recoveries.[200,201] Another absorptive-based approach recently introduced to overcome the Hct issues associated with DBSS is volumetric absorptive microsampling (VAMS),[194] which uses an absorptive polymeric material immobilized on a pipette tip to collect fixed volumes of blood via wicking. Several studies have demonstrated that VAMS devices are able to collect reproducible blood volumes independent of their Hct levels. [194,202,203] However, some issues with VAMS have also been reported, particularly in relation to bias in the determination of blood concentrations, low recoveries at high Hct levels, and interoperator variability. [202,203] Further evaluation of VAMS is still required as it is still a relatively new microsampling approach.

Solid phase microextraction (SPME) is a non-exhaustive extraction technique that uses a matrix-compatible coating structure, which enables the analysis of complex samples, such as plasma and even whole blood. In fact, the literature contains several prior studies that document SPME's usefulness as a sample preparation approach for such matrices prior to LC-MS or direct MS instrumental analysis.[73,162,166,204–206] Interestingly, SPME's applicability is not only limited to *ex vivo* determinations; indeed, several studies have documented its suitability for *in vivo* blood analysis in different animal models.[103,104,168,207–211] In regards to the principle of SPME, it is worth mentioning that the extraction and pre-concentration of analytes occurs by directly exposing a defined amount of a biocompatible extraction phase to the sample matrix for a given period of time. The amount of analyte collected during the extraction process is proportional to the analyte's concentration and depends on the analyte's affinity for the biocompatible coating and for the

sample matrix at the extraction conditions. Considering that the SPME matrix compatible coating is highly selective for small compounds and that a washing step is carried out after the extraction, the presence of proteins, salts, and other interferences that could affect the instrumental analysis is easily avoided. In regards to the extraction mechanism, it is worth emphasizing that, in SPME, the uptake of analytes from the sample media to the coating material happens via free analyte concentration.[212] Therefore, if we consider a complex system, such as blood, where multiple co-existing phases can display an affinity for a given target compound, the amount of analyte extracted by the SPME probe will be correlated to the free concentration of analyte at the end of the extraction. As a matter of fact, parameters such as lipophilicity, charge, molecular weight, diffusion coefficient, and structural moieties govern the distribution of any compound into different blood compartments.[213] Likewise, such parameters strongly determine the affinity that a target analyte exhibits for a particular SPME coating. In addition to the analyte's physicochemical characteristics, there are other factors that play an important role in the microextraction process; for example, extraction time, extraction phase characteristics, temperature, and convection conditions all determine the final recovery provided by an SPME device. Given that red blood cells comprise a significant portion of a whole blood sample, this work aims to investigate how varying Hct levels affect the amount of analyte extracted by SPME devices. For this purpose, ten drugs with different polarities and physicochemical properties were chosen as model compounds, and blood samples with three different Hct levels (20%, 45%, and 70%) were selected as sample matrices. The effects of the coating type, sample convection, and extraction time were also taken into consideration.

4.2. Experimental section

4.2.1. Materials and supplies

Methamphetamine, stanozolol, codeine, codeine-d$_3$, ($\pm$)11-nor-9-carboxy-Δ9-THC (THCCOOH), ($\pm$)11-nor-9-carboxy-Δ9-THC-d$_3$ (THCCOOH-d$_3$), oxycodone-d$_3$, testosterone-d$_3$, cannabidiol-d$_3$ and methadone-d$_3$ standards were obtained from Cerilliant Corporation (Round Rock, TX, USA). Nikethamide, propranolol, metoprolol, clenbuterol, exemestane, and salbutamol were purchased from Millipore Sigma (Oakville, ON, Canada), and salbutamol-d$_3$ was purchased from CDN Isotopes (Pointe Claire, Quebec, Canada). Sodium chloride, potassium chloride, potassium phosphate monobasic, sodium phosphate dibasic, and formic acid were also purchased from Millipore Sigma (Oakville, ON, Canada). LC-MS grade acetonitrile, methanol, and water were obtained from Fisher Scientific.

Biocompatible SPME fibres (MM-F) coated with a mixed-mode extraction phase (C18 and benzene sulfonic acid functionalities, 1.5 cm coating length, 45 µm coating thickness, and a total diameter of 300 µm) were generously provided by Millipore Sigma (Bellefonte, PA, USA). SPME devices prepared on a plastic support with a hydrophilic lipophilic balanced (HLB) extraction phase (HLB-D) (2 cm coating length, 150 µm coating thickness, and 2 mm total diameter) were made as described in [204].

Blood samples were purchased from Bioreclamation IVT (Westbury, New York, USA). These samples were from healthy donors (with K2-EDTA as anticoagulant), and had Hct levels that had been adjusted to 20%, 45%, and 70%.

4.2.2. Working solutions

A stock methanolic solution (20 µg mL^{-1}) containing all analytes was prepared and further dilution was done as required. A stock solution (8 µg mL^{-1}) containing different deuterated compounds as internal standards was prepared in methanol.

4.2.3. SPME procedure

Prior to the experiments, the blood with adjusted Hct content was spiked with stock methanolic solutions containing all the analytes, while ensuring that the organic solvent content was kept below 1% in all cases. For the construction of the calibration curves, the spiked blood was pre-incubated for at least 1 hour at constant agitation; for the determination of the extraction time profiles, blood incubation was allowed overnight. Before the extractions, MM-F and HLB-D were first pre-conditioned in a 1:1 (v/v) methanol:water solution for 30 min using vortex agitation at 1500 (revolutions per minute) rpm. Subsequently, all devices were rinsed in ultrapure water for 10 s to remove any remaining organic solvent from the coating surface. In order to guarantee a stable sample pH over the entire extraction process, 1080 µL of spiked blood aliquots were mixed with 120 µL of 1 M phosphate buffer adjusted at a pH of 7. Furthermore, 15 µL of internal standard solution were added to the samples used for the calibration curve experiments. The extractions were then carried out by immersing both types of SPME devices into the sample matrix for a pre-set period of time at constant agitation conditions. To construct the calibration curves, the extraction time was set at 90 min, the calibration range was set between 5 and 100 ng mL^{-1} for all target analytes, and four calibration curve replicates were constructed on two consecutive days. Time points of 15, 30, 60, 90, 120 and 180 min were selected for the extraction time profiles, and all the extractions were conducted in triplicates. The agitation parameters were set as follows: vortex agitation was set at 1500 rpm for the HLB-D, and orbital shaking agitation was set at 400 rpm for the MM-F. Once the extraction step was completed, three consecutive rinsing steps in water (5 s each) were performed following the procedure reported by Reyes-Garcés et al.[204] After the rinsing step, it was verified that no blood cells remained attached to the matrix-compatible coating. Finally, desorption of the devices was carried out for 20 min at 1500 rpm in 300 and 600

μL of desorption solution (4:1 methanol:acetonitrile) for MM-F and HLB-D, respectively. To determine the amount of analyte extracted by the SPME devices in each experiment, an instrumental calibration curve (from 0.1 to 150 ng mL^{-1}) was prepared using the same solvent composition that was used for the desorption solution.

4.2.4. LC-MS/MS conditions and data processing

All the collected extracts and the instrumental calibration curve were run using LC-MS/MS conditions already reported.[204] Briefly, the LC-MS/MS system was comprised of an Accela autosampler, an Accela pump, and a TSQ vantage triple quadrupole mass spectrometer with a heated electrospray ionization source operating in positive mode (Thermo Scientific, San Jose, USA). Chromatographic separation was attained using a Kinetex pentafluorophenyl core shell column (1.7 µm, 2.1 mm x 10 mm) that had been connected to a PFP security guard ultracartridge (Phenomenex, Torrance, CA, USA), and LC separation was achieved using a mobile phase system consisting of 0.1% formic acid (A), acetonitrile with 0.1% formic acid (B), and methanol with 0.1% formic acid (C). The gradient elution conditions were set as follows: A, B, and C were held at 90%, 5%, and 5 %, respectively, for 0.5 min; B and C were then increased linearly to 50% over the course of 6.5 min; C was then increased to 75% and B was decreased to 25% over the course of 5 min and held for 3.5 min. Finally, the column was kept at the initial gradient composition for 2 min. The column temperature was kept at 35 ˚C, the total run time was 17.5 min, and the column flow was set at 0.3 mL min^{-1}. Samples were stored in the autosampler at 5 ˚C, and the injection volume was 10 µL. MS analysis was conducted using selective reaction monitoring (SRM) mode (Table 4.1), and the conditions of each compound were optimized by directly infusing the standards. The following transitions were selected for the deuterated compounds that were employed as internal standards: salbutamol-d$_3$: 243.16 →151.12; codeine-d$_3$: 303.15 →165.10;
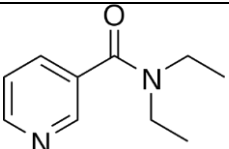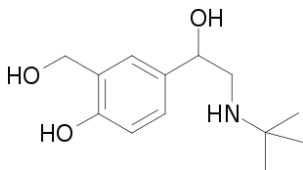
oxycodone-d$_3$: 319.12 → 259.15; methadone-d$_3$: 313.21 → 105.10; testosterone-d$_3$: 292.25 → 97.14; and THCCOOH-d$_3$: 348.16 → 302.28. Other parameters were set as follows: spray voltage = 1300 V; vaporizer temperature = 275˚C; sheath gas = 45 units; auxiliary gas = 30 units; and capillary temperature = 280˚C.
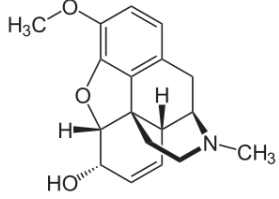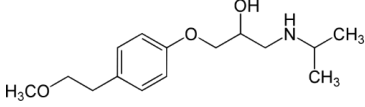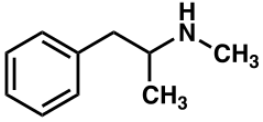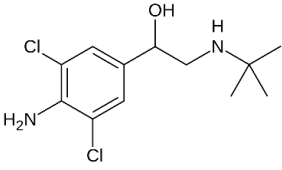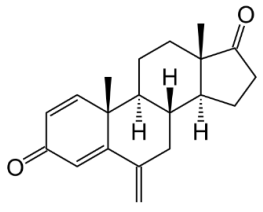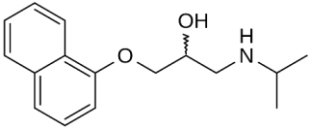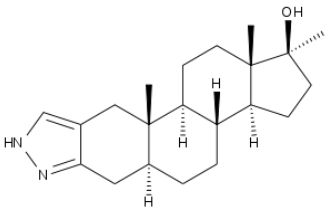
4.2.5. Data analysis
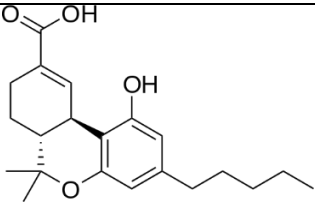
Xcalibur software (2.0.7 SP1) was employed for data acquisition and processing. For the purpose of this study, the slopes of the calibration curves constructed for each compound with different Hct levels were statistically compared. Statistical analysis was carried out using one-way ANOVA, one-tail t-test (equal and unequal variances), and relative standard deviations (RSDs).

4.3. Results and discussion

Table 4.1. Model compounds with their corresponding physicochemical properties and MS/MS detection parameters. Analytes are listed in order of hydrophobicity.

Compound SRM transition Collision energy, S-lenses	Structure (molecular weight, MW)	logP[150]	Plasma protein binding, %[151]
Nikethamide 179.10 → 108.10 18, 76	MW: 178.23	0.33	NA
Salbutamol 240.14 → 148.10 18, 59	MW: 239.31	0.64	8[214]

Codeine 300.11 → 165.10 64, 104	MW: 299.36	1.19	7 – 25
Metroprolol 268.14 →116.15 18, 94	MW: 267.36	1.88	12
Methamphetamine 150.11 →91.12 19, 45	MW: 149.24	2.07	10 – 20
Clenbuterol 277.068 → 203.049 15, 70	MW: 276.08	2.61	89 - 98[215]
Exemestane 297.173 →121.118 19, 72	MW: 296.18	3.11	90
Propranolol 260.12 →116.14 17, 89	MW: 259.16	3.48	> 90
Stanozolol 329.229 → 81.108 44, 130	MW:	4.42	NA

	MW: 328.25		
THCCOOH 345.153 →299.27 18, 90	 MW: 344.45	6.36	92.0 ± 8.7^{153}

NA= not available

In order to elucidate the effect that various Hct levels can have on SPME recovery rates, an analyte's affinity for the main blood components (aqueous phase, proteins, and red blood cells) should be taken into consideration. For this reason, analytes with distinct physicochemical properties were selected for this work because they can be expected to display variable affinities for blood constituents (Table 4.1). In addition to using various model compounds, two experimental setups were employed: MM-F at 400 rpm and HLB-D at 1500 rpm. Although both types of SPME devices have been documented as being suitable and biocompatible for the analysis of whole blood,[83,104,204] the mechanical attachment of macromolecules is usually observed in the case of MM-F under aggressive agitation conditions and long extraction times. Consequently, an orbital shaker operating at 400 rpm was chosen as the agitation setup for MM-F extractions. In the case of HLB-D, satisfactory results for whole blood analysis were already found when using vortex agitation at 1500 rpm; therefore, the same parameters were kept.[204] Although high agitation speeds such as 1500 rpm are likely to induce lysis in red blood cells—and therefore changes in the Hct content during the extraction[216]—the main purpose of the evaluation was to assess the overall effect of different red blood cell contents on SPME extractions under typical experimental conditions.

Table 4.2 presents the results corresponding to the calculated slopes for each of the model analytes in blood samples with different Hct levels as determined by the two different experimental setups. It is worth emphasizing that slope calculation was selected as parameter for investigating Hct effect because it is a well-accepted approach for assessing relative matrix effects.[154] As shown in Table 4.2, different outcomes were found depending on the analyte and the experimental conditions; therefore, in order to simplify things, we classified the observations into four different cases. In the first case (Case I), no statistically significant Hct effect was observed for any of the study conditions (MM-F at 400 rpm and HLB-D at 1500 rpm). Interestingly, salbutamol, nikethamide, codeine, and methamphetamine, which are all characterized as being relatively polar and/or for having low protein-binding affinities, were categorized in this first group. In order to explain the obtained results, parameters such as the polarity and affinity of an analyte for the matrix components and the extraction phases should be taken into account. With regards to an analyte's polarity, it is important to emphasize that highly-polar compounds typically display shorter equilibration times due to their low affinities for SPME coatings (low K values). This is confirmed by Equation 1, where the equilibration time in SPME is expressed as a function of the boundary layer thickness (δ_s), the distribution constant (K), the thickness of the SPME coating (L), the diffusion coefficient of the analyte in the sample matrix (D_s), and the coating capacity (Γ_{max}).[217]

$$t_{eq} \approx t_{95\%} = \frac{\delta_s K L}{D_s \Gamma_{max}} \qquad (1)$$

In this context, it is worth mentioning that, when extractions are performed at conditions close to equilibrium, the amount of analyte collected is mostly determined by the analyte's distribution constant. Conversely, when the extraction process is interrupted at an earlier stage, the diffusion of the analytes in the sample matrix plays a more important role. Since 90 min was chosen as the

Table 4.2. Slopes of the calibration curves constructed using blood with different Hct levels in the range between 5 and 100 ng mL^{-1} (no internal standard).

Compound (case)	Slopes (n=4)[a] (average ± standard deviation)									
	MM-F, 400 rpm					HLB-D, 1500 rpm				
	20% Hct	45% Hct	70% Hct	RSD %	F [c]	20% Hct	45% Hct	70% Hct	RSD% [b]	F [c]
Salbutamol (I)	0.018 ± 0.003	0.016 ±0.006	0.017 ± 0.004	4.0	0.090	0.25 ± 0.02	0.24 ± 0.037	0.23 ± 0.02	3.0	0.230
Nikethamide (I)	0.042 ± 0.004	0.044 ± 0.004	0.039 ± 0.004	6.6	0.017	0.71 ± 0.06	0.73 ± 0.110	0.75 ± 0.06	3.0	0.238
Methamphetamine (I)	0.058 ± 0.005	0.053 ± 0.009	0.048 ± 0.003	9.5	2.865	0.55 ±0.04	0.54 ±0.071	0.54 ±0.04	1.0	0.022
Codeine (I)	0.034 ± 0.002	0.030 ± 0.004	0.029 ± 0.002	8.0	3.090	0.69 ±0.06	0.69 ±0.051	0.69 ±0.07	0.1	3.41e^{-4}
Propranolol (II)	0.047 ± 0.002	0.036 ± 0.003	0.027 ± 0.003	26.0	61.138	0.56 ± 0.05	0.57 ± 0.057	0.58 ± 0.04	2.0	0.232
Metroprolol (II)	0.077 ± 0.008	0.064 ± 0.008	0.053 ± 0.006	19.0	11.108	0.83 ±0.08	0.85 ±0.099	0.88 ±0.08	3.0	0.243
Clenbuterol (II)	0.072 ±0.004	0.059 ±0.005	0.045 ±0.004	14.0	36.232	0.69 ±0.04	0.70 ±0.044	0.73 ±0.05	3.0	1.031
Exemestane (III)	0.034 ±0.005	0.023 ±0.001	0.013 ±0.003	45.0	37.719	0.31 ±0.05	0.28 ±0.027	0.21 ±0.03	20.0	7.597
THCCOOH (IV)[d]	0.010 ±0.002	0.011 ±0.001	0.012 ±0.001	9.6	1.370	0.026 ± 0.001	0.032 ±0.0062	0.036 ±0.002	16.2	8.851
Stanozolol (IV)	0.040 ± 0.006	0.036 ±0.003	0.034 ±0.004	7.7	1.539	0.047 ±0.004	0.053 ±0.0060	0.066 ±0.007	18.0	11.865

[a] Average slopes calculated from the equation $y=mx+b$, where y is the amount extracted in ng and x is the concentration spiked in blood.

[b] inter-slope RSD estimated from the values obtained for each Hct level.

[c] F crit = 4.256 (α=0.05), if F > F crit the null hypothesis that the three slopes are equal is rejected (one-way ANOVA).

[d] The lowest concentration level was 25 ng mL^{-1}.
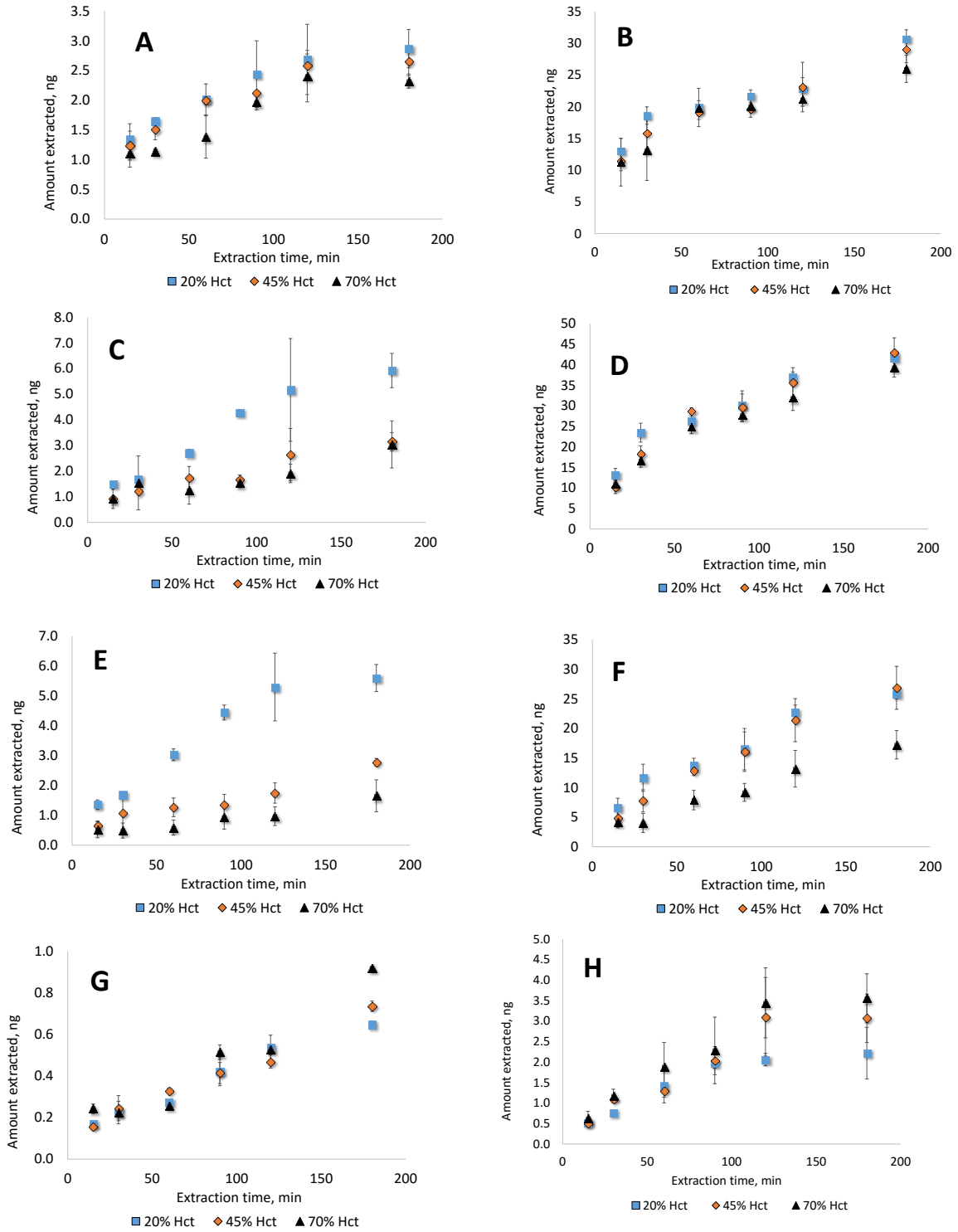
Figure 4.1. Extraction time profiles for salbutamol (a and b), propranolol (c and d), exemestane (e and f), THCCOOH (g and h). Plots on the left side summarize results for MM-F at 400 rpm, and plots on the right side summarize results for HLB-D at 1500 rpm.

extraction time for the Hct effect assessment, it was relevant for the interpretation of the results to determine at what point of the extraction process the comparison was being conducted. As shown in Figure 4.1A, a relatively polar compound like salbutamol was close to reaching equilibrium after 90 min of extraction using MM-F at 400 rpm. This means that variations in the analyte's diffusivity due to differences in the matrix viscosity will not have an important effect on the analyte's uptake. Moreover, as can be seen in the same plot, minimal differences were found in the profiles constructed at the three Hct levels. Considering salbutamol's high polarity and low protein binding, variable levels of matrix constituents are not expected to greatly affect SPME recoveries as a result of decreasing the analyte's free concentration. In the case of HLB-D, a slightly different situation was observed for the same compound. As can be seen in Figure 4.1B, although there is an overlap in the constructed time profiles for blood adjusted at different Hct levels, a plateau in the extracted amounts of salbutamol was not achieved, even after 180 min of extraction at high-speed agitation. These results can be explained based on HLB's much higher affinity for polar analytes and the thicker HLB-D coatings that permit the extraction of much larger amounts of analyte. Under such experimental conditions, the stronger affinity that HLB-D displays for the target analytes—compared to the one exhibited by the matrix constituents—will contribute to lessening the differences that can occur in SPME recoveries due to variations in the matrix composition. It is also noteworthy that the convection parameters in the HLB-D experiments were significantly higher than those in the MM-F extractions. Faster agitation conditions allow for a decrease in the thickness of the boundary layer, which in turn accelerates the mass transfer process occurring from the sample matrix to the SPME coating. Given this principle, the combination of improved convection conditions and HLB-D's strong extraction capacity will result in a reduced Hct effect in the extraction of analytes that do not show a specific affinity for erythrocytes. In the

case of compounds such as methamphetamine and codeine, which are less polar than salbutamol and nikethamide but still meet the conditions to be classified as Case I, it is noteworthy that the slopes of the calibrations curves constructed with MM-F showed higher RSD values (9.5% and 8%) than those obtained with HLB-D (1% and 0.1%). In fact, when MM-F was used, the slopes for methamphetamine and codeine were statistically higher in blood adjusted at 20 % Hct than for blood adjusted at 70% Hct (methamphetamine (20% vs 70% Hct): one-sample $t(6)=3.52$, p-value<0.01; codeine (20% vs 70% Hct): one-sample $t(6)=4.42$, p<0.01). Since these compounds are slightly hydrophobic, and considering the fact that codeine binds to the red blood cell plasma membrane, the presence of variable levels of matrix components is likely to alter the concentration of analytes available for SPME extractions.[218] Interestingly, this effect becomes more pronounced when devices with weaker affinities and lower extraction capacities, such as MM-F, are employed for extraction. In light of the discussed results, it is clear that the affinity of target analytes for the coating and the matrix components has a highly-significant effect on the final SPME recoveries when analyzing blood with different Hct levels.

In order to explain the experimental findings corresponding to Case II, the same rationale regarding various analytes' affinities for coatings and for matrix constituents should be taken into consideration. As can be seen in Table 4.2, Case II analytes had different outcomes that were dependent on the SPME experimental parameters. On the one hand, a pronounced decrease in the slopes as a function of erythrocyte levels was observed in the experiments conducted with MM-F; on the other hand, the statistical comparison of the slopes showed no Hct effect for extractions carried out with HLB-D (propranolol: $F(2,9)=0.232$, p-value=0.80; metoprolol: $F(2,9)=0.243$, p-value=0.79; clenbuterol: $F(2,9)=1.031$, p-value=0.40). The lack of observed differences when HLB was used can be attributed to the high convection conditions, as well as the fact that, as was

discussed in relation to Case I, HLB-D has a much higher affinity for the target analytes than MM-F and matrix components. Moreover, since the Case II analytes are overall less polar than those in Case I, they can be expected to have a higher degree of interaction with matrix components (lower free concentrations) and larger K values, and therefore longer equilibration times (Equation 1). Figure 4.1C presents the extraction time profile constructed for propranolol using MM-F at 400 rpm. As can be seen, the recoveries corresponding to the profile in 20% Hct blood are considerably higher than those obtained for the other two Hct levels. This outcome can be explained based on the fact that higher concentrations of matrix components—in this case, red blood cells—lead to lower concentrations of propranolol available for SPME extraction; thus, lower amounts of propranolol are collected at 70% Hct. Given that MM-F lacks sufficient extraction capability for inducing the release of bound analytes in order to further enhance the extraction recoveries, such experimental conditions tend to exhibit a significant Hct effect. Moreover, taking into account that the extraction process is still close to the linear regime at 90 min, it is possible that differences in the analyte's diffusivity as a function of matrix viscosity could be partly responsible for variations in the uptake rate.[219] Although equilibrium is far from being reached at 90 min in HLB-D (Figure 4.1D), its high affinity for propranolol and the high convection conditions largely mitigate any effect that variable Hct levels can have on the final recoveries. Indeed, HLB's high capacity for adsorption is able to deplete the analyte's free concentration and induce the release of bound analytes back to their free forms, thereby increasing the total recovery. While possible changes in the matrix composition due to vigorous agitation[216] should be considered when explaining the different recoveries obtained using the two experimental setups, the results that will be presented in the next case clearly indicate that red blood cells remain a significant compartment after 90 min of vortex agitation.

In the third case noted in this study (Case III), a similar Hct effect for both MM-F and HLB-D was found; that is, the amount of analyte extracted decreased in proportion to the blood erythrocyte levels. This particular behavior was observed for exemestane, a relatively non-polar steroidal compound (Figures 4.1E and 4.1F). As shown in Table 4.2, extractions conducted with both MM-F and HLB-D produced smaller calibration curve slopes for 70% Hct blood than for the ones calculated at 20% (MM-F (20% vs 70% Hct): one-sample $t(5)=7.25$, $p<0.01$; HLB-D (20% vs 70% Hct): one-sample $t(4)=3.37$, $p<0.05$). In the case of MM-F, a more pronounced variation was observed in the slopes of the calibration curves constructed at the different Hct levels due to the previously described effects of lower coating affinity and slower agitation. To the best of our knowledge, there is no information in the literature regarding the partitioning of exemestane into red blood cells. In fact, stanozolol, another steroidal compound that was used as a model analyte in this study, did not exhibit the same Hct effect. In order to confirm that exemestane was being partitioned into the erythrocytes, the recoveries of extractions from 70% Hct blood and fully-hemolyzed 70% Hct blood were compared using HLB-D. Complete blood hemolysis was achieved by storing pre-spiked 70% Hct blood for two hours at -80 °C (*i.e.* freeze and thaw). As shown in Figure 4.2, the recovery of exemestane increased by approximately 60% when extracted from hemolyzed blood; this confirms that this drug is being partitioned into the red blood cells. Based on these results, it is evident that exemestane's affinity for the matrix is much higher than that of other model analytes categorized in the previous cases such that even pronounced differences are observed when HLB-D are used. Therefore, the use of an internal standard that displays the same affinity for red blood cells is crucial to ensuring the successful analysis of exemestane in blood samples obtained from different patients.
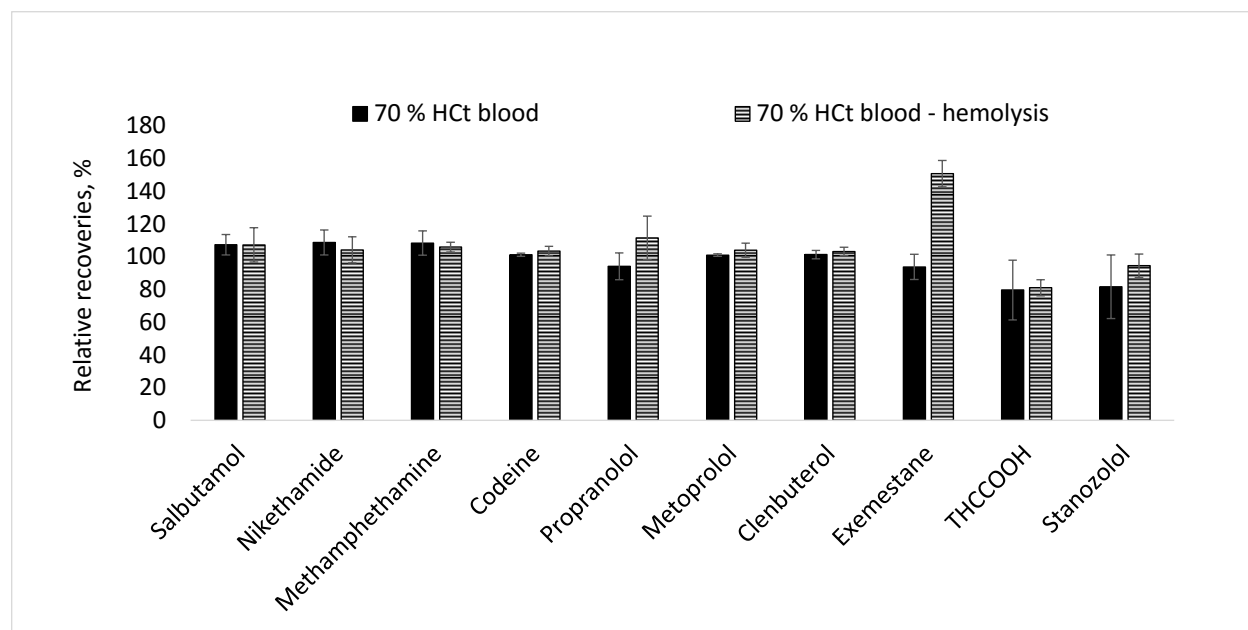
Figure 4.2. Relative recoveries obtained after extracting from 70% Hct blood (hemolyzed vs. non-hemolyzed). These experiments were conducted using HLB-D at 1500 rpm and an extraction time of 90 min.

Similar to Case II, two different trends that were dependent on the SPME experimental conditions were observed in Case IV. Interestingly, the model compounds that were categorized within this last case are highly lipophilic and capable of significant protein binding. The slopes for these analytes were significantly higher at 70% Hct content when the extractions were carried out using HLB-D at 1500 rpm (THCCOOH (20% vs 70% Hct): one-sample $t(5)=-8.58$, $p<0.01$; stanozolol (20% vs 70% Hct): one-sample $t(6)=-4.89$, $p<0.01$) (Table 4.2). On the contrary, no statistical differences in the slopes were observed for the calibration curves constructed with MM-F (THCCOOH: $F(2,8)=1.371$, p-value=0.31; stanozolol: $F(2,9)=1.539$, p-value=0.27). One of the model compounds that exhibited this behavior was THCCOOH, the main secondary metabolite of THC. THCCOOH is a considerably non-polar analyte (logP 6.38) with $92.0 \pm 8.7\%$ protein binding.[153] In addition, according to previous studies, THCCOOH's distribution into red blood cells is restricted.[153,220] Based on this behavior, the concentration of THCCOOH in plasma will be

significantly higher than its concentration in whole blood (blood-to-plasma ratio = 0.65).[153] Therefore, if we take into account that the volume of plasma is substantially less at 70% Hct than at 20% and 45% Hct, we can anticipate that a higher free analyte concentration will be available for SPME extractions at 70% Hct than at the other two Hct levels. This trend is reflected in the slopes for THCCOOH that were obtained with HLB-D (Table 4.2), and in its extraction time profile (Figure 4.1H). A similar behavior was also observed in the slopes for stanozolol that were constructed under the same conditions. Stanozolol is also known for being highly lipophilic (logP 4.43), but, to the best of our knowledge, there have been no prior studies that have analyzed its distribution in different blood components. With respect to the results obtained using MM-F, we hypothesize that the concentration available for SPME extractions, the convection conditions, and the diffusion of analytes all played an important role in the final outcome. As can be seen in Figure 4.1G, the THCCOOH uptake in MM-F is still in its linear regime at 90 min due to the slow convection and the compound's high affinity for the coating. Hence, the analytes' diffusion has a more significant effect on the extraction process than it does in cases where extractions are closer to equilibrium. In addition, it is important to consider that the flux of analyte from the sample matrix towards the coating (or analyte uptake) is proportional to the concentration gradient between the coating surface and the sample. Since a higher concentration of analyte is available for SPME extractions at 70% Hct, a higher uptake rate can be expected due to the concentration gradient. Based on this information, the estimated slopes for MM-F represent a combination of both the variation in analyte diffusion at different sample viscosities, and the changes in analyte uptake rates due to the concentrations available for SPME extractions at different Hct levels.

As has been discussed so far, the Hct effect in SPME is completely dependent on the analytes of interest, and different outcomes can be obtained by changing the experimental conditions.

Parameters such as an analyte's physicochemical properties (lipophilicity, molecular weight, diffusivity, etc), distribution constants, convection conditions, and, to some extent, sample viscosity are all important in determining how Hct differences affect SPME recoveries. Nevertheless, as in any other sample preparation approach, the use of internal standards represents the best way to account for any matrix variability. Table 4.3 presents the slopes after internal standard correction for those cases where F>Fcrit. Unfortunately, none of the available deuterated standards exhibited the same affinity for red blood cells shown by exemestane; as such, we could not provide the corrected data for that compound. As can be seen in Table 4.3, the RSD values corresponding to the corrected slopes of those analytes that were significantly affected by variable red blood cell content were rewarding. Interestingly, compounds that were not necessarily deuterated analogues of the target analytes were able to provide adequate correction. Several studies in which SPME was used to analyze multiple substances in biofluids have described the use of a small set of internal standards as a practical and cost-effective strategy for correcting all of the target analytes.[80,162,204] However, as has been noted above, the behavior of a given analyte in a specific matrix depends on several factors, and a proper assessment of an internal standard's suitability at various Hct levels is required when dealing with real blood samples. Indeed, although a given internal standard can effectively correct for extraction variations in a single blood lot, this does not necessarily mean that the same internal standard will properly account for varying Hct content.

Further investigation should be conducted into alternative strategies for overcoming the Hct effect observed in SPME. These strategies may focus on full red blood cell lysis via a combination of using additives (*e.g.* zinc sulfate or organic solvents) or freezing and the addition of appropriate internal standards, preferably deuterated analogues. In the case of *in vivo* blood sampling, special

attention should be given to the Hct effect when external calibration curves are used for quantitation, as no internal standard can be introduced into the samples.

Table 4.3. Corrected calibration curve slopes for those cases where F>Fcrit.

Compound (internal standard)	Slopes (n=4)[a] (average ± standard deviation)				
	20 % Hct	45 % Hct	70 % Hct	RSD %	F[b]
Propranolol, MM-F (Methadone-d_3)	0.018 ±0.002	0.019 ±0.001	0.017 ±0.001	5.4	2.538
Metroprolol, MM-F (Methadone-d_3)	0.0053 ±0.0002	0.0054 ±0.0002	0.0055 ± 0.0003	1.2	0.331
Clenbuterol, MM-F (Methadone-d_3)	0.024 ±0.001	0.024 ±0.001	0.023 ±0.001	3.1	3.058
THCCOOH[b], HLB-D (THCCOOH-d_3)	0.011 ±0.001	0.011 ±0.001	0.012 ±0.001	5.8	3.872
Stanozolol, HLB-D (THCCOOH-d_3)	0.41 ±0.05	0.42 ±0.02	0.46 ±0.03	5.9	1.653

[a] Average slopes calculated from the equation $y=mx+b$, where y is the ratio area analyte/area internal standard and x is the concentration spiked in blood.

[b] F crit = 4.256 (α=0.05), if F > F crit the null hypothesis that the three slopes are equal is rejected (one-way ANOVA).

[c] The lowest concentration level was 25 ng mL^{-1}.

4.4.Conclusions

In this study, the effect of varying levels of Hct on SPME recoveries was investigated by using distinct model compounds and two different experimental setups. As expected, the observed effect was dependent on the analyte's characteristics and the extraction parameters. For instance, variable Hct levels did not show any effect on the recovery of polar compounds with low protein affinities (*e.g.* salbutamol) under any of the study conditions. However, the extraction of more hydrophobic analytes, such propranolol, was strongly affected by the red blood cell content only when MM-F

was used at 400 rpm. Similarly, for compounds such as methamphetamine, codeine, propranolol, metoprolol and clenbuterol, the use of HLB-D with high convection conditions produced negligible differences in the SPME recoveries from blood adjusted at various Hct levels. This demonstrated that an analyte's relative affinity for the matrix and the extraction phase is critical when matrices with varying compositions are analyzed. Other model analytes, such as exemestane and THCCOOH, exhibited a negative and positive correlation, respectively, between the SPME recoveries and the Hct content due to their opposite affinity for red blood cells. Lastly, despite variations in analyte recovery due to different erythrocyte contents, it was possible to correct for relative matrix effects by using appropriate internal standards. Overall, since each analyte can display different Hct effects, variable red blood cell levels within the final experimental conditions should be always properly assessed when analyzing whole blood samples with SPME.

Chapter 5: Evaluation of solid phase microextraction as a sample preparation tool for untargeted analysis of brain tissue

5.1. Preamble and introduction

5.1.1. Preamble

The results presented in this chapter have yet to be published in any journal. Nathaly Reyes-Garcés and Dr. Ezel Boyacı equally contributed to the experimental work, the data processing, and the discussion herein presented. The chromatographic conditions employed for the analysis of lipids were provided by the research group led by Prof. Dajana Vuckovic from Concordia University as part of a collaborative project funded by Brain Canada. The results presented in this chapter are part of an ongoing research project which commenced in August 2015. Nathaly Reyes-Garcés was the sole writer of the text presented here.

5.1.2. Introduction

Metabolomics platforms, particularly those based on mass spectrometry (MS), have been garnering a wealth of interest in the biomedical field in recent years.[221–224] Both targeted and untargeted metabolomics approaches have opened up a range of possibilities towards the elucidation of biochemical pathways affected under particular conditions (e.g. disease and treatment). Indeed, the last decade has evidenced a growing number of published studies documenting the use of MS-based metabolomics to investigate a wide variety of medical conditions, such as different types of cancer, diabetes, neurological diseases, coronary heart disease, and cystic fibrosis, among others.[225–230] As for the experimental workflows developed for such investigations, diverse analytical strategies applicable to different study cases have been

described and reviewed in detail.[34–36,191,231,232] In this regard, parameters such as matrix specimen (type and availability), required metabolite coverage (targeted or untargeted approach), cohort size, and instrument availability play a critical role when choosing a set of experimental conditions for a particular metabolomics study. While biofluids (e.g. plasma, serum, blood, urine, saliva, exhale breath condensate, cerebrospinal fluid) are most commonly selected as matrices of choice due to the meaningful information they can impart as well as their relative ease of collection,[33,40,45,191] in specific cases, the utilization of tissue specimens as matrix cannot be avoided despite the invasiveness of tissue sampling procedures, as certain information, such as site-specific information, can only be gathered through such means.[2,33,34] In metabolomics investigations, the successful isolation of metabolites of interest from such complex biological matrices constitutes a critical step in determining the quality of the gathered data. To this extent, it is imperative that factors such as the representativeness of the extracted metabolome for the biological state of the system under investigation (metabolism quenching), and the reproducibility of the recoveries over large numbers of samples be carefully considered during method development. The advantages and challenges associated with the sample preparation strategies most frequently used in the processing of biological specimens in metabolomics investigations have been reviewed by several authors.[2,34,37,50,191] For studies involving biofluids, most commonly employed methodologies include the use of dilute-and-shoot and solvent precipitation for global metabolomics, whereas liquid-liquid extraction with different organic solvents (methanol, chloroform, and methyl tert-butyl ether mixtures) is the approach of choice when targeting lipids.[2,36,191] With respect to tissue, although solvent-based extraction applications comprise the most utilized sample preparation methods for investigations involving this matrix, additional steps are required prior to the extraction process due to the high complexity of tissue samples. In typical

workflows, collected tissue samples are first rinsed with either water or buffer so as to avoid contamination or inclusion of artefacts stemming from blood and/or from anesthetics used during the sample collection process.[34,46] Subsequently, samples are subjected to shock freezing with liquid nitrogen to ensure metabolism quenching, followed by homogenization of the frozen tissue to induce cell disruption.[34,50] Finally, according to the metabolite coverage that is desired, the extraction step is carried out by employing one or various solvents (single phase, two-phase, or multi-step extractions). Single extraction steps combined with appropriate instrumental platforms are preferred in most cases; in addition to being less timing consuming, such methodologies are less prone to errors in comparison to two-phase or multi-step extractions. Naz et al. have comprehensively reviewed traditional analytical protocols for untargeted analysis of biological tissues.[34] Undoubtedly, a common denominator among all sample preparation approaches for tissue handling is that they are time consuming and labor intensive. Considering the abovementioned limitations surrounding currently available analytical workflows for metabolomics studies that involve tissue analysis, new efforts must be sustained towards the development and implementation of alternative strategies capable of streamlining the analytical workflow, while ensuring the integrity of the metabolome.

Solid phase microextraction (SPME) is a non-exhaustive extraction technique that integrates sampling and sample preparation in a single step.[212] In the last decade, SPME has been successfully applied towards various metabolomics studies, including applications in the clinical field that have yielded promising results.[113,115,158,208,233] In SPME, a small amount of extraction phase immobilized on the outer part of a solid support is used to extract either volatile (headspace) or non-volatile (direct immersion) compounds from a given sample matrix.[212] Although several authors have reported application of headspace (HS) SPME-gas chromatography (GC)-MS for

metabolic profiling of volatile compounds,[108,158,233,234] direct immersion (DI) SPME combined with liquid chromatography (LC)-MS analysis is generally preferred for untargeted studies, as it allows for analysis of a more comprehensive range of metabolites.[235,236] Indeed, use of DI-SPME coupled with LC-MS has enabled determinations of multiple classes of metabolites encompassing a wide range of polarities.[57,114,117] Furthermore, a comparative study between SPME, ultrafiltration, and solvent precipitation demonstrated that SPME was able to provide complementary information by reducing ionization suppression (SPME vs solvent precipitation) and through improved coverage of hydrophobic compounds (SPME vs ultrafiltration).[114] However, while these findings endorse the applicability of this technology for untargeted studies in the clinical field, further evaluations of SPME conditions in different matrices are still needed to further validate its implementation in such investigations. In addition to the abovementioned advantages, another positive characteristic of SPME is the advantage afforded by the biocompatibility of its sampling devices. LC-amenable SPME coatings, which are comprised of sorbent particles immobilized with a biocompatible binder, allow for high selectivity towards small molecules, avoid the co-extraction of proteins and other macromolecules, and do not induce adverse reactions when immersed in biological matrices (anti-fouling surface).[83] Moreover, SPME biocompatible extraction phases are also suitable for *in vivo* analysis. Undoubtedly, one of the most attractive features of *in vivo* SPME as a tool in metabolomics is that it integrates sampling, extraction, and metabolism quenching in a single step, thus minimizing the likelihood of samples incurring the type of metabolome alterations associated with traditional procedures.[57,208] On this note, it is worth emphasizing that the general DI-SPME workflow used for both *in vivo* and *ex vivo* analyses is significantly straightforward, only involving the following steps: i) conditioning and rinsing of the SPME coating (also sterilization if required); ii) exposure of the coating to the sample

121

matrix for a defined period of time; iii) quick rinsing of the SPME probe to remove any macromolecules loosely attached to the coating surface; iv) and desorption of the extracted metabolites into an appropriate solvent. This methodology is largely suitable for studies that require analysis of tissue specimens, as it simplifies the time-consuming steps of typical sample preparation workflows. Other advantages of SPME in tissue analysis include the viability of tuning the geometry of the device to target specific sampling sites, its low invasiveness in comparison to standard tissue sampling approaches, the non-destructive nature of the extraction procedure, and in particular for *in vivo* studies, the feasibility of monitoring the same subjects at multiple time points. Until now, only a few studies have reported application of DI-SPME for monitoring of metabolic changes in animal tissue, including muscle, lung, liver, and also brain specimens.[115,116,237] In SPME brain analysis studies, the use of DI-SPME and LC-MS/MS enabled *in vivo* measurement of changes in neurotransmitters after fluoxetine administration. Remarkably, the results obtained by DI-SPME in this study were comparable to those obtained with microdialysis (MD), the technique of choice for *in vivo* monitoring of neurotransmiters.[237] Among the many insights obtained through this study, its findings certainly support the applicability of SPME as a complementary tool to MD; as observed in that work, while SPME facilitates the extraction of non-polar metabolites such as lipids, MD favors the detection of more polar metabolites. Thus, the concomitant use of these techniques enables monitoring of a wider range of compounds, allowing for a more complete snapshot of a given system under study. Yet, despite the promising results reported in the few reports where tissue analysis was carried out by DI-SPME, a complete assessment regarding the effect of different experimental conditions on the metabolic coverage of this technique has yet to be published. The currently presented work seeks to fill this gap by presenting an evaluation of SPME as a sample preparation tool in untargeted

brain studies. The work included an evaluation of the metabolite coverage provided by C18, MM, and HLB coatings after extraction from cow brain homogenate at static conditions, with parameters such as desorption solvent, features detected in different chromatographic modes, washing steps, and extraction time all taken into consideration. The findings of this work support the applicability of SPME in brain metabolomics studies, providing insightful information regarding the performance of DI-SPME in untargeted tissue analysis.

5.2. Experimental

5.2.1. Materials and supplies

7 mm long C18 and mixed mode (C18 and benzene sulfonic acid functionalities, MM) fibers (45 µm thickness) were kindly provided by Millipore Sigma (Bellefonte, PA, USA). 7 mm hydrophilic-lipophilic balanced (HLB) fibers were manufactured in-house by dipping nitinol wires multiple times in a slurry containing polyacrylonitrile (PAN) dissolved in dimethylformamide (DMF), and 5 µm HLB particles (40 µm coating thickness). Cow brain homogenate was selected as a model matrix for all experiments due to its ready commercial availability. All fibers were pre-conditioned in 1:1 (v/v) methanol:water for at least 30 min prior to extraction. Following their conditioning, SPME fibers were rinsed with ultra-pure water to remove any excess organic solvent remaining on the coating surface.

5.2.2. Investigation of SPME coating coverage and desorption conditions

Cow brain homogenate was placed in 300 µL vials with the help of a disposable Luer lock syringe. All vials were carefully filled from the bottom to the top, ensuring no air pockets remained in the vial, as their presence could disturb the extraction process and potentially introduce errors to the data gathered. C18, HLB, and MM fibers (n=16 per coating type) were exposed to brain

123

homegenate for 30 min at room temperature and at static conditions. Each fiber was thoroughly wiped with a Kimwipe, then quickly dipped in ultra-pure water following extraction so as to remove adhering macromolecules and tissue debris from the coating surface. Desorption evaluations were carried out for four different desorption solvents: methanol, acetonitrile (ACN), 1:1 (v/v) ACN:water, and 1:1 (v/v) isopropanol:methanol. The first three solvents were evaluated in terms of their desorption strength for metabolomics analysis, while 1:1 (v/v) isopropanol:methanol was selected to test the lipid coverage capacity of the selected coatings. In total, four fibers of each coating chemistry were used to test each desorption solvent. For methanol and ACN desorptions, solvent volume was set to 100 µL, with further dilution with 100 µL of water carried out after desorption of fibers so as to ensure good chromatographic retention. For 1:1 (v/v) ACN:water and 1:1 (v/v) isopropanol:methanol, 200 µL of solvent was selected as desorption volume. All fibers were desorbed under constant vortex agitation (1500 rpm) for 1 hour.

5.2.3. Evaluation of the washing step in SPME lipid analysis

The effect of the washing step was assessed as a factor of analytical variability in SPME lipid extraction from brain tissue. Four different washing strategies were evaluated at 10 s vortex each: pure water, 10 % (v/v) acetone, 10 % (v/v) methanol, and 10 % (v/v) isopropanol. The rinsing step was carried out by employing a manual vortex agitator at 3200 rpm. For this experiment, C18 fibers (n=5 for each washing strategy) were deployed in 30 min extractions carried out in both plasma and brain homogenate. The findings of this evaluation indicated the parameters 10 s vortex in 10 % (v/v) acetone to be the best rinsing strategy for lipid analysis; as such, this approach was later implemented for the construction of extraction time profiles using C18 fibers.

5.2.4. Extraction time investigation

Following investigations of coating coverage, desorption conditions, and washing step, extraction time profiles for all coating chemistries were constructed. C18, HLB, and MM fibers were used to extract from brain homogenate for 5, 10, 20, 30, and 40 min under static conditions. All extractions were carried out in a randomized order. Four fibers of each coating type were used per extraction point. Following desorption of HLB and MM fibers in 100 µL of methanol, all resulting extracts were submitted to instrumental analysis, using the chromatographic method for metabolomics analysis described in section 5.2.5. Conversely, following desorption of C18 fibers in 1:1 (v/v) isopropanol:methanol, obtained extracts were submitted to LC-MS analysis in accordance to the chromatographic method described in Section 5.2.5 for analysis of lipids.

5.2.5. LC-MS analysis

All extracts were run on a LC-MS system consisting of an Accela pump, an Accela autosampler, and an Orbitrap mass spectrometer Exactive equipped with a heated electrospray (H-ESI) source (Thermo Scientific, San Jose, USA). Chromatographic separation was carried out using one of two methods, targeting either small metabolites, or lipids. In accordance with previous work carried out in our group, separation and detection of small metabolites was conducted on a pentafluorophenyl (PFP) column, chosen due to its selectivity and satisfactory performance in retaining certain small polar compounds and non-polar metabolites with different moieties.[114,238] Summaries of settings selected for both LC-MS methods are provided in Tables 5.1 and 5.2. Xcalibur software (2.0.7 SP1) was employed for data acquisition. To ensure appropriate mass accuracy over the course of the sequence, the MS instrument was calibrated every two days using the Pierce™ LTQ Velos ESI Positive Ion Calibration Solution and the Pierce™ Negative Ion Calibration Solution (Thermo Scientific, San Jose, USA). Moreover, 391.2843, and 255.2329 m/z

were used as lock masses for positive and negative acquisition modes, respectively, corresponding to diisooctyl phthalate (a common plasticizer) and palmitic acid, common background contaminants present in electrospray analysis. A pooled quality control (QC) sample (prepared by mixing equal aliquots of each extract) was run multiple times across the instrumental sequence (about every ten injections) so as to ensure instrumental stability for all extracted features. Samples were run in a randomized manner as a means of avoiding sequence bias related to instrumental drift. Fibers and solvent blanks were also analyzed as controls of possible artefacts.

Table 5.1. Chromatographic conditions employed for this study.

Metabolites analysis[114]	Lipids analysis
Column: Supelco Discovery HS F5, 2.1 x 100 mm, 3 µm	**Column:** Waters, XSelect CSH C18 Column, 130Å, 3.5 µm, 2.1 mm X 75 mm
Mobile phases **A (positive):** Water with 0.1 % (v/v) formic acid **B (positive):** ACN with 0.1 % (v/v) formic acid **A (negative):** 1 mM acetic acid **B (negative):** 1 mM acetic acid in ACN	**Mobile phases** **A:** 40:60 methanol/water with 10 mM ammonium acetate and 1 mM acetic acid **B:** 90:10 isopropanol:methanol with 10 mM ammonium acetate and 1 mM acetic acid
Gradient | Time, min	%B
0	0
3	0
25	90
34	90
35	0
40	0		**Gradient** | Time, min	%B
0	20
2	20
3	80
16	95
24	95
24.1	20
32	20	
Column temperature 25 ºC	**Column temperature** 55 ºC
Autosampler temperature: 5 °C	**Autosampler temperature:** 5 °C
Flow 300 µL/min	**Flow** 200 µL/min

Table 5.2. MS conditions for untargeted analysis of brain extracts.

	MS conditions
Electrospray voltage, kV	4000 (-2900 negative mode)
Sheath gas, AU	30
Auxiliary gas, AU	10
Sweep gas, AU	5
Capillary temperature, °C	300
Vaporizer temperature, °C	300
MS resolution	High 50,000 at 2 Hz (FWHM* 200 m/z)
Acquisition range, m/z	100 – 1000
Automatic gain control	Balanced 1e6
Injection time	100 ms

*Full-width at half maximum (FWHM)

5.2.6. Data analysis

Raw files were converted to mzXML files using the peak picking function (centroid data) from ProteoWizard MS Convert version 3.0. 10095 64 bits. Converted files were then processed using the platform XCMS online, which is available for free (https://xcmsonline.scripps.edu/landing_page.php?pgcontent=mainPage). Parameters employed in XCMS online were set as follows: feature detection was conducted using the centWave with 5 ppm as the maximal tolerated m/z deviation; 7 s as the minimum peak width; and 120 s as the maximum peak width (other parameters were S/N=6, mzdiff=0.01, integration method through

descent on the Mexican hat filtered data, prefilter data=3, and prefilter intensity=100); retention time correction was carried out using the orbiwarp method (profStep=1); for feature alignment, bw=10 s, mzwid=0.015 m/z, minfrac=0.5; feature annotation (isotopes and adducts) was conducted using CAMERA (a package integrated in the XCMS online platform) at 5 ppm and 0.015 as m/z absolute error. The software SIMCA P+ 14.0.0 (Umetrics, Umeå, Sweden) was employed for multivariate analysis of data. Principal component analysis (PCA) and orthogonal partial least squared – discriminant analysis (OPLS-DA) were carried out by employing the aligned data obtained from XCMS online. For PCA and OPLS-DA, the data was scaled using Pareto scaling. Metabolites corresponding to important metabolite features were putatively identified based on accurate mass (within 5 ppm) searches on different databases (METLIN and Human Metabolome Data Base). The identification process accounted for information regarding annotated adducts and isotopes detected at the same retention time. Provided their availability, standards were then run to verify the identity of the metabolites.

5.3.Results and discussion

Several publications have reported the applicability of SPME for metabolomics studies of different biological matrices, including tissue.[158] Although positive results in terms of sample clustering and metabolite coverage have been documented in the literature, an evaluation and subsequent optimization of experimental conditions aimed at maximizing the information obtained by SPME in applications involving tissue samples had yet to be presented.

One of challenges in tissue analysis of brain is derived from the intrinsic complexity of this organ, as its intricate structure is mirrored in its rich chemical composition. Indeed, the brain is a heterogeneous organ divided into different regions with diverse biochemical functions that, in turn, are composed of various cell types, proteins, lipids, and small molecules. As metabolomics

applications have as their main goal the comprehensive capture of low molecular weight metabolites (<1000 Da) that represent the biological state of a given system, the development of any analytical workflow chosen for such a purpose should, ideally, be able to fulfill that requirement. In most comparisons of exhaustive extraction technologies versus microextraction techniques (such as SPME) it is anticipated that the former would likely outperform the latter in terms of metabolite recoveries and coverage. However, for *in vivo* metabolomics analysis, the simplicity and low invasiveness of this microextraction technique afford SPME a key advantage over traditional approaches. Moreover, the non-lethal and non-exhaustive nature of SPME enables multiple samplings of the same animal or biological system, thus allowing for paired tests or matched pair comparisons (same animal before and after a treatment), and facilitating metabolomics studies of a longitudinal nature. While cow brain homogenate was selected as model matrix for initial assessments and optimization of parameters, the final optimized conditions provided by this study are intended to be used for *in vivo* rat brain investigations.

5.3.1. Assessment of SPME coverage for the analysis of brain tissue metabolome

In the first part of this study, different SPME coating chemistries available for bioanalytical applications were evaluated in terms of metabolite coverage. In this context, HLB fibers (home-made), commercial C18 fibers, and MM fibers (currently provided by Millipore Sigma Aldrich) were selected for this evaluation owing to their previously documented performances in bioanalytical studies. To date, most of the SPME-based metabolomics studies reported in the literature have employed MM fibers due to the wide coverage provided by their C18 and strong cationic exchanger (benzene sulfonic acid) functionalities.[56,57,115,116] However, recent work carried out by our group has also demonstrated the advantages of using HLB for the analysis of a broad

range of compounds.[117,118,162,204] Based on this, HLB was also included as one of the coating chemistries to be tested for untargeted brain studies.

In addition to evaluating different coating types, several desorption solvents were compared. In SPME method development, the establishment of optimum desorption conditions for SPME constitutes a critical step in ensuring maximum sensitivity and satisfactory precision. Considering that the number of metabolites extracted from cow brain tissue via SPME is unknown, a comparison was conducted based on the relative intensities of detected metabolite features, the information provided by different desorption solvents, and the analytical precision of each set of conditions. Based on the fact that a metabolite feature corresponds to a detected ion that has a unique m/z and retention time, several metabolite features corresponding to isotopes, different adducts, and also in-source fragments are detected when a single metabolite or compound is analyzed via MS.

Figures 5.1 and 5.2 depict results corresponding to the relative intensities of features detected after 30 min extractions from cow brain homogenate, using the three aforementioned coating chemistries. For this initial comparison, following desorption of the probes in three different solvents (methanol, 1:1 (v/v) ACN:water, and ACN), obtained extracts were submitted to LC-MS instrumental analysis in both positive and negative modes in accordance with the described LC-MS method for metabolomics analysis using a PFP column. Only those features having both pooled QC/fiber blank area intensity ratios above 5 and average intensities above 1000 were considered for the plots (2405 features in positive mode; 1294 features in negative mode). The obtained data was then further filtered based on information gathered from fiber blanks so as to avoid erroneous inclusions of artefacts originating from either the coatings or solvents as features extracted from the homogenate. The average intensities of individual features were estimated by

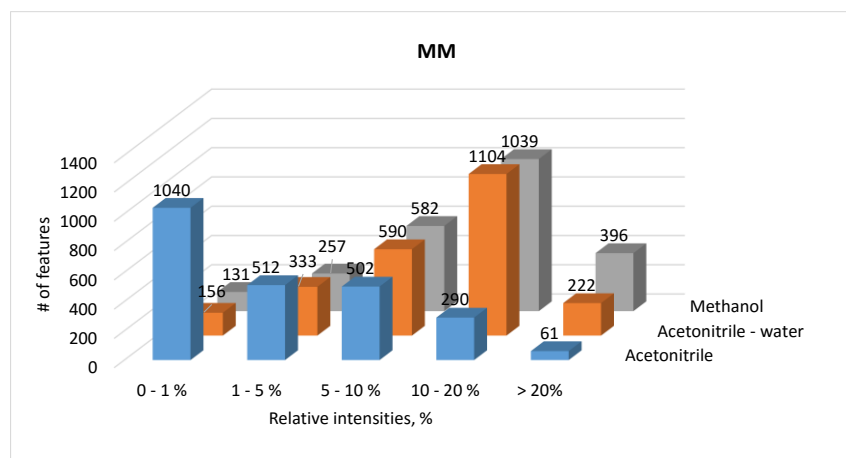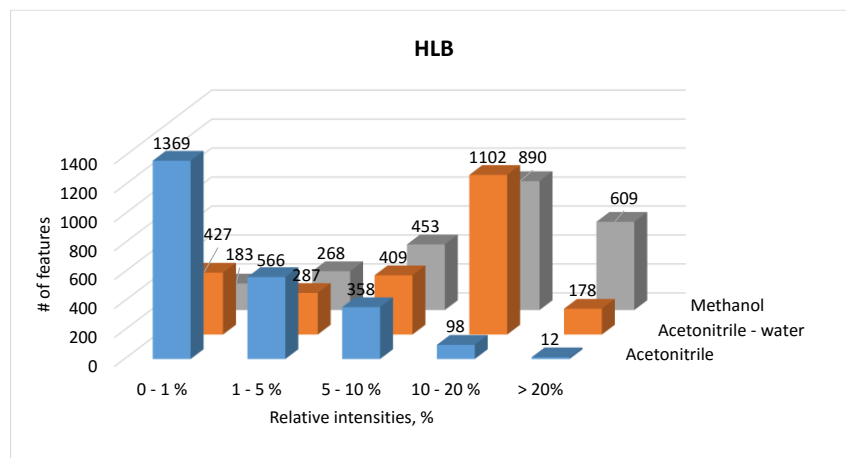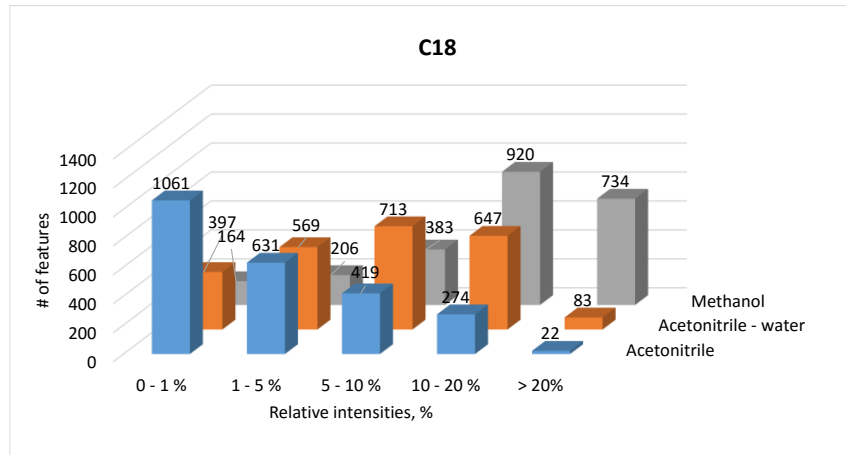**Figure 5.1.** Features detected per coating type at different desorption conditions (positive mode). Features were classified according to their average relative intensities (n=4 fibers per coating).
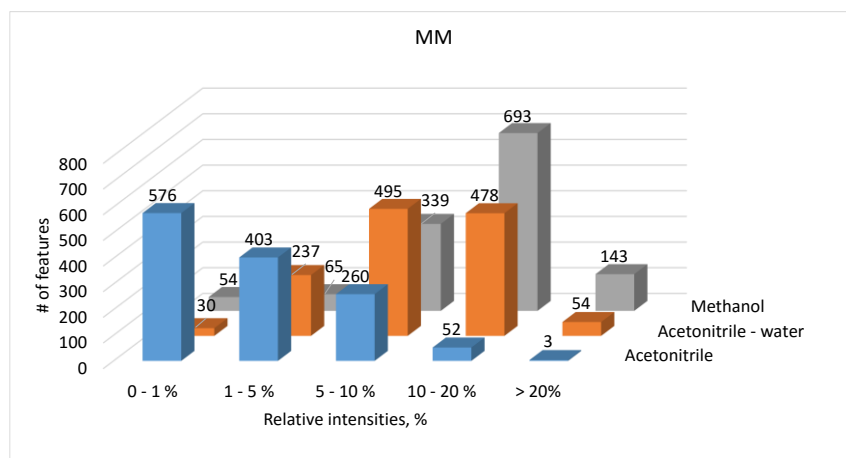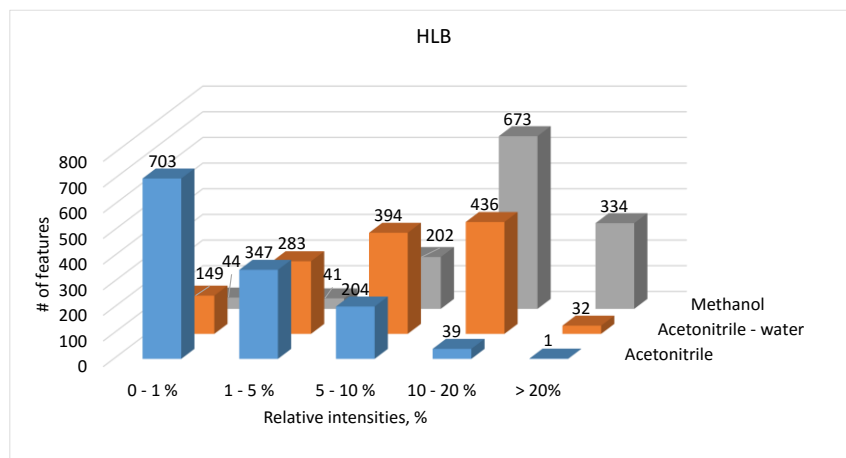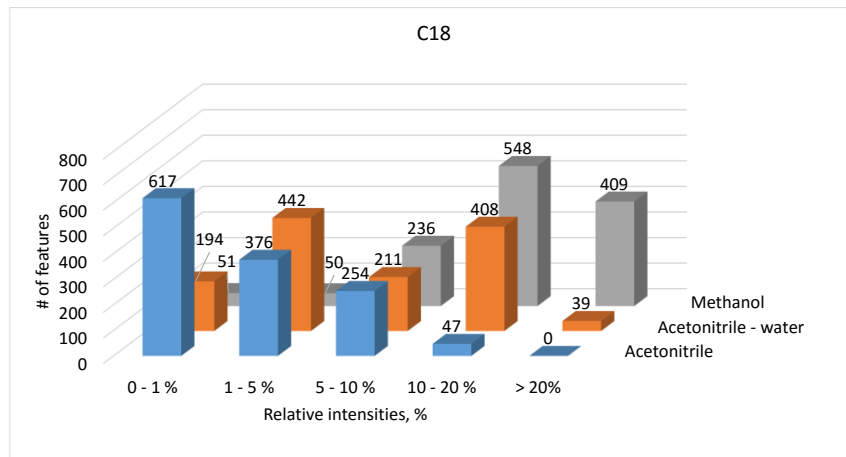
Figure 5.2. Features detected per coating type at different desorption conditions (negative mode). Features were classified according to their average relative intensities (n=4 fibers per coating).

calculating the total sum of areas for each metabolite feature (including all coatings and desorption solvents) and dividing it by 36 (4 fibers * 3 solvents * 3 coating types). The relative intensities for each feature, in turn, were calculated as a percentage of the total sum of areas of the same feature detected in all the extracts obtained per coating type. For example, the relative intensity for a feature X detected in methanol via C18 fiber #1 (F1) was calculated as follows: relative intensity of feature X $_{(C18, F1, methanol)}$= (area feature X$_{(C18, F1, methanol)}$/($\sum$areas feature X $_{C18, methanol (F1,2,3 and 4)}$ + $\sum$areas feature X$_{C18, 1:1(v/v)ACN:water (F1,2,3 and 4)}$ + $\sum$areas feature X$_{C18, ACN (F1,2,3 and 4)}$))*100. Considering that four replicates were carried out per coating-solvent pair, the data plotted in Figures 5.1 and 5.2 correspond to the averages of the relative intensities. As shown, ACN presented the poorest desorption strength for all tested coatings, with most of the features detected showing relative intensities below 5%. The observed findings thus support that as an SPME solvent, ACN was unable to significantly decrease the coating/elution media distribution constant for most of the extracted metabolites; therefore, ACN was discarded as an option among the desorption solvent possibilities. Methanol, on the other hand, showed the highest desorption efficiency for all tested extraction phases. In both positive and negative modes, all three evaluated coatings exhibited an overall increase in the number of features with relative intensities above 20% when methanol was used as desorption solvent. This trend was, however, more pronounced in the results obtained in negative mode. Lastly, the desorption efficiencies of the 1:1 (v/v) ACN:water solvent were shown to be superior to those obtained by ACN; however, based on the relative intensities obtained for all three solvents, methanol was concluded to yield the best elution performance among the tested solvents.

Subsequent to this initial assessment, an evaluation was carried out to assess the performance of each coating in relation to its coverage as well as quality of data provided. For this purpose,

obtained data for each coating was filtered so as to only retain features with pooled QC/blank (solvent and fiber blanks) ratios above 5, pooled QC RSD values below 30 %, and intensities above 3000. As shown in Figures 5.3 and 5.4, similar feature numbers matching the specified filtering conditions were found for all extracts in both positive and negative modes. This certainly confirms that carrying out evaluations of the coverage of a given extraction phase as well as of the performance of a desorption solvent based solely on the number of features attained through their application is insufficient for optimization of these parameters. Indeed, a cursory examination of these results (Figures 5.3 and 5.4) would certainly seem to indicate that any of the three coatings desorbed in any of the tested solvents would provide virtually the same information. With aims of gaining further clarification on the effect of each solvent on the extraction recoveries, ratios between the average intensities detected in methanol and in 1:1 (v/v) ACN:water were estimated. As presented in Table 5.3, the number of features with intensities 1.5 times higher in methanol

Table 5.3. Comparison of feature intensities as a function of their desorption solvent (methanol vs. 1:1 (v/v) ACN:water). Only features with pooled QC/blank (solvent and fiber blanks) ratios above 5, RSD values below 30 %, and intensities above 3000 were taken into consideration for this comparison.

	Features with intensities 1.5 times higher in methanol	**Features with intensities 1.5 times higher in 1:1 (v/v) ACN:water**
C18, pos	161	72
C18, neg	246	74
HLB, pos	115	131
HLB, neg	164	47
MM, pos	81	142
MM, neg	215	89
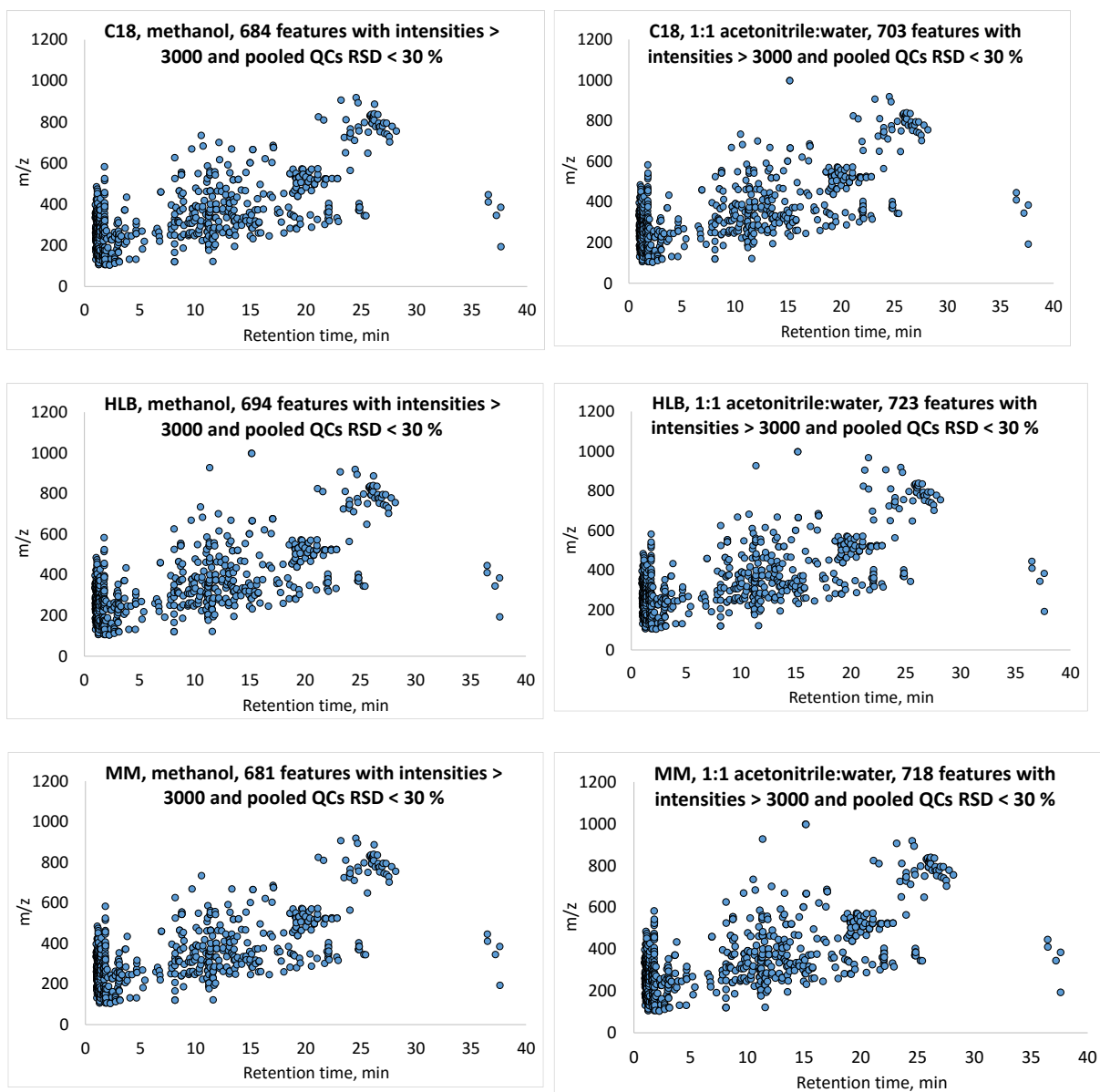
Figure 5.3. Ion maps corresponding to features detected in positive mode after extraction from brain homogenate with C18, MM, and HLB 7 mm fibers. Desorptions were carried out in methanol (left) and 1:1 (v/v) ACN:water (right). Only features having pooled QC/blanks (solvent and fiber blanks) ratios above 5, RSD values below 30 % in the pooled QC, and intensities above 3000 were plotted.
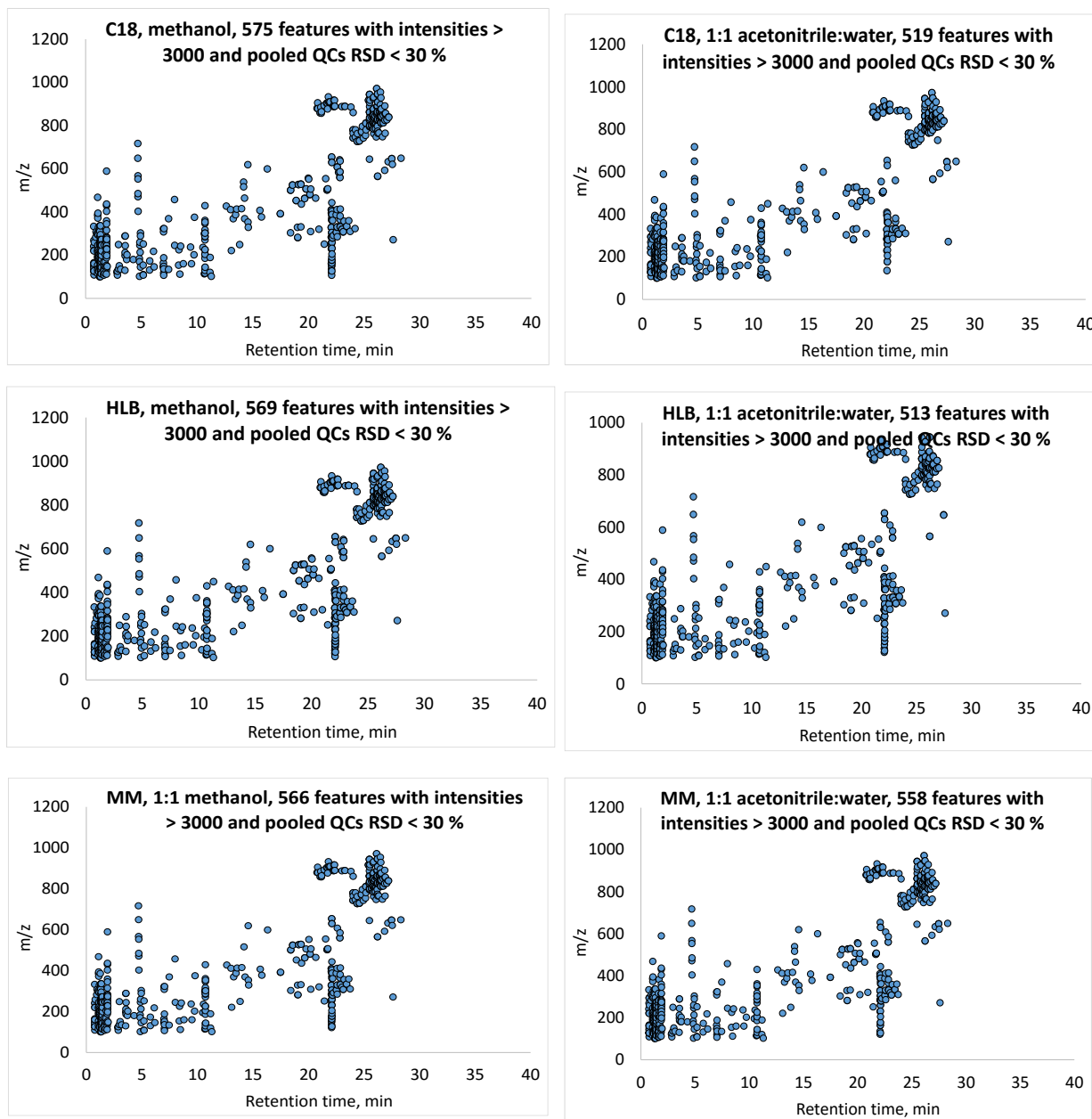
Figure 5.4. Ion maps corresponding to features detected in negative mode after extraction from brain homogenate with C18, MM, and HLB 7 mm fibers. Desorptions were carried out in methanol (left) and 1:1 (v/v) ACN:water (right). Only features having pooled QC/blanks (solvent and fiber blanks) ratios above 5, RSD values below 30 % in the pooled QC, and intensities above 3000 were plotted.

than in 1:1 (v/v) ACN:water was significantly larger for extracts of C18 (both positive and negative modes), HLB in negative mode, and MM in negative mode. On the other hand, the number of

features with 1.5 times higher intensities in 1:1 (v/v) ACN:water as compared with methanol was larger in HLB and MM extracts run in positive mode. While no marked differences were observed between methanol and 1:1 (v/v)ACN:water for HLB extracts, the obtained results seem to indicate that use of 1:1 (v/v) ACN:water as solvent would yield better results for untargeted analysis in positive mode in cases where the MM coating is used.

In addition to carrying out an assessment of solvent and coating performance with aims of identifying the combinations capable of yielding the highest number of features with the highest intensities, an investigation into the type of information attained by solvent type was carried out with aims of assessing whether the use of different solvents would introduce significant differences to the obtained information. To this end, principal components analysis (PCA) and orthogonal partial least squares discriminant analysis (OPLS-DA) were employed to analyze the data. As shown in Figure 5.5, clear clusterings of observations obtained according to type of desorption solvent used were found for both positive and negative modes. This evidently indicates that in SPME, significant differences in the composition of final extracts may occur due to selective desorption of extracted metabolites. To determine which features contributed to the observed differentiation, multivariate supervised analysis, more specifically OPLS-DA, was carried out (Figure 5.6) on the obtained data. Interestingly, the main discriminating features in the S-plots ($|p_1|$ > 0.05 and $|p(corr)_1|$ > 0.8) depicted in Figure 5.6 corresponded to polar metabolites eluting at retention times below 2 min and to non-polar compounds eluting at retention times close to 25 min. The p_1 axis provides information regarding the influence of each feature towards the observed separation between the two groups, while the $p(corr)_1$ axis describes the reliability of each variable in the discrimination of the two groups.[239] As shown in Figure 5.7, our results revealed that the use of methanol facilitated the desorption of less polar compounds, while 1:1 (v/v) ACN:water
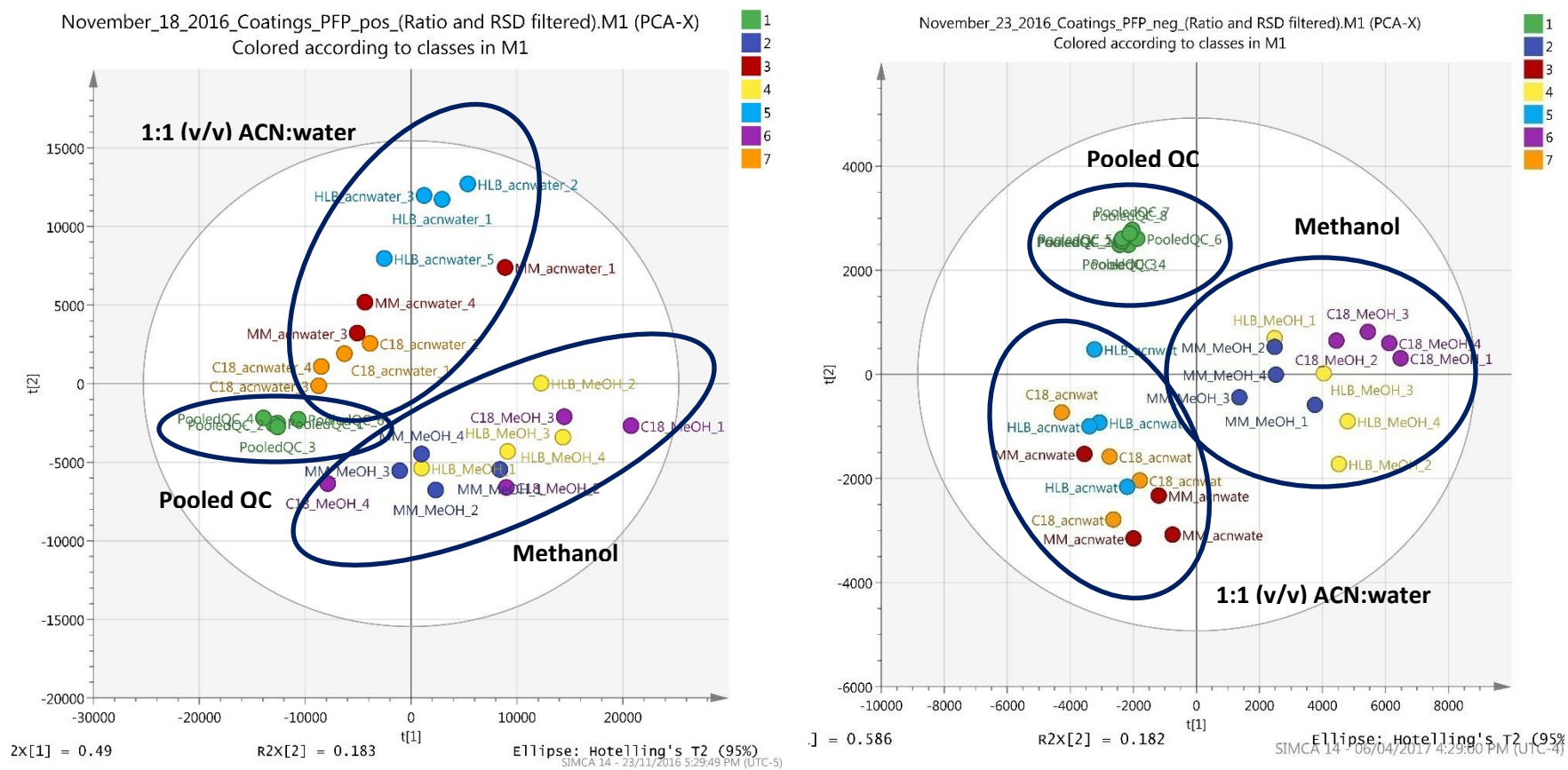
Figure 5.5. Principal component analysis (PCA) plots corresponding to C18, MM and HLB desorption extracts obtained in methanol and ACN:water in positive mode (left) and negative mode (right). Only features exhibiting pooled QC/blank (solvent blanks and fiber blanks) ratios above 5 and having pooled QC RSD values below 30 % were considered for these plots.
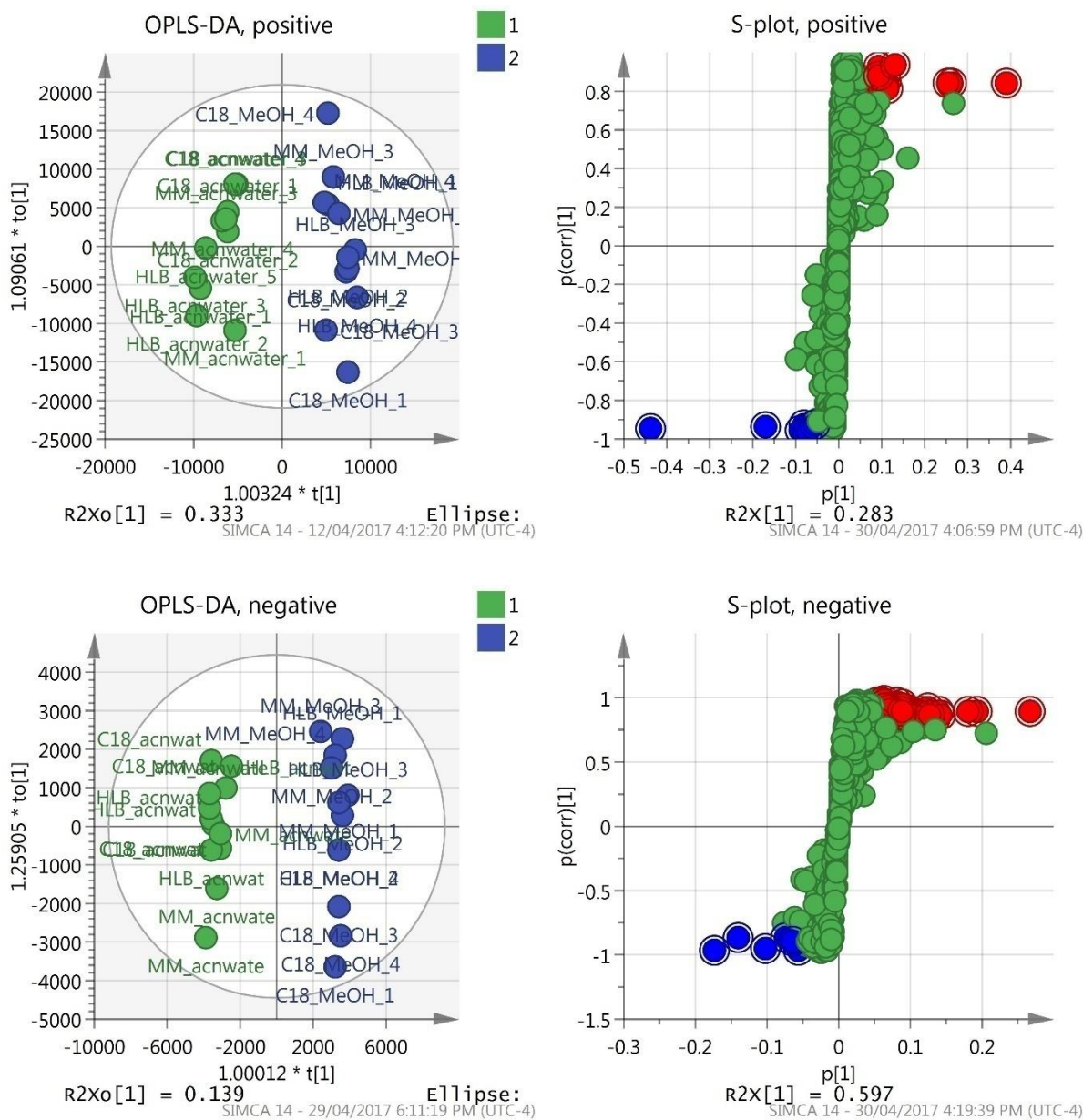
Figure 5.6. OPLS-DA plots (left) and S-plots (right) corresponding to the comparison of 1:1(v/v) ACN:water (1) and methanol (2) extracts from all the coating types in positive (above) and negative (below) modes. Features highlighted have $|p_1| > 0.05$ and $|p(corr)_1| > 0.8$.
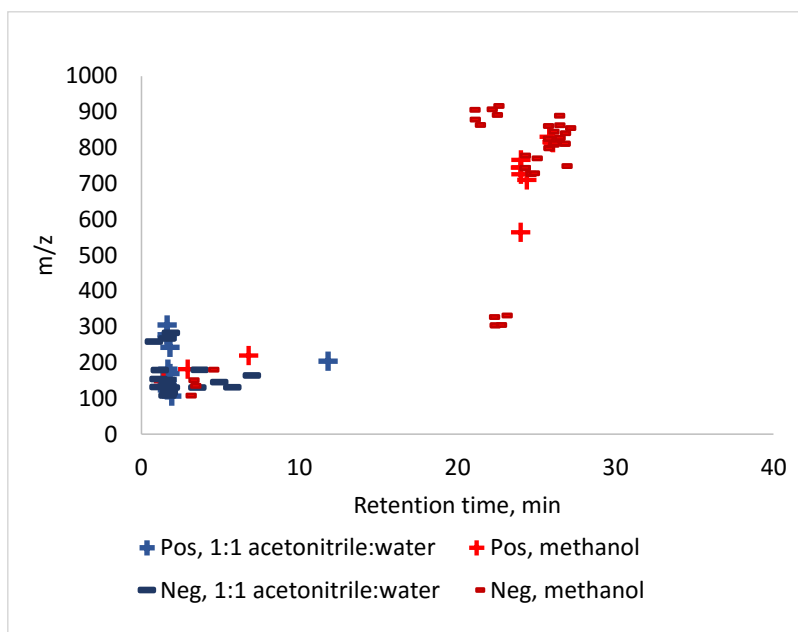
Figure 5.7. Summary of the main features discriminating 1:1 (v/v)ACN:water and methanol extracts (from the S-plots). The markers represent the features with the highest intensities at each of the specified conditions.

provided better recovery for certain polar metabolites. Among the non-polar discriminating features determined to contribute to the observed differentiation are lipids belonging to phosphatidylcholine (PC), phosphatidylethanolamine (PE), and glucosyl/galactosylceramide (Glc/galCer). In regards to polar metabolites, compounds having in their structure a purine base such as xanthine, inosine, guanosine, and deoxyguanosine were found to be present at much higher levels in 1:1 (v/v) ACN:water extracts (Figures 5.8 and 5.9). While the number of features exhibiting higher intensities was in general larger for extracts desorbed in methanol than for those in 1:1 (v/v) ACN:water, the findings of this investigation certainly evidence that certain metabolome information can be omitted from the final extract based on the solvent selected for desorption. As untargeted metabolomics studies aim to provide a thorough snapshot of the system under study, better metabolite coverage can then be attained by combining extracts from both desorption solvents, which can be achieved by employing fiber duplicates in experiments.

Following the conclusion of desorption evaluations for 1:1 (v/v) ACN:water and methanol, a comparison of detected features by coating type was carried out. Indeed, the behaviour and affinity of each coating type for the broad range of metabolites found in brain tissue can be predicted based on the extraction phase chemistry of the coating. C18, for instance, is expected to show high affinity towards non-polar components, as its extraction mechanism occurs mostly through hydrophobic interactions. On the other hand, HLB and MM are expected to provide better recoveries for polar compounds and analytes with aromatic moieties (via pi-pi interactions) given the types of functionalities these coatings possess. HLB contains divinyl benzene and vinylpyrrolidone moieties that enable the extraction of both non-polar and polar compounds, whereas MM contains C18, and also a strong cation exchanger functionality (benzene sulfonic acid), which increases the affinity of the coating for polar charged metabolites. With this in mind, an initial comparison of experimental data obtained from brain extracts collected via C18 fibers versus data obtained via HLB and MM coatings was carried out, and the intensities of representative discriminating metabolite features were plotted, as seen in Figures 5.8 and 5.9. In regards to 1:1 (v/v) ACN:water extracts, our results showed that higher intensities were obtained for polar compounds such as niacinamide, phenylalanine, tryptophan, xanthine, arginine, and choline from extracts originating from MM and HLB fibers (Figure 5.8). Some of these compounds are not only polar, but also contain an aromatic functionality or a positive charge, which function to increase their affinity for HLB and MM coatings. Interestingly, several fatty acids also exhibited higher intensities in MM and HLB extracts obtained with 1:1 (v/v) ACN:water. As shown next, these findings relate to the poor efficiency of 1:1 (v/v) ACN:water in
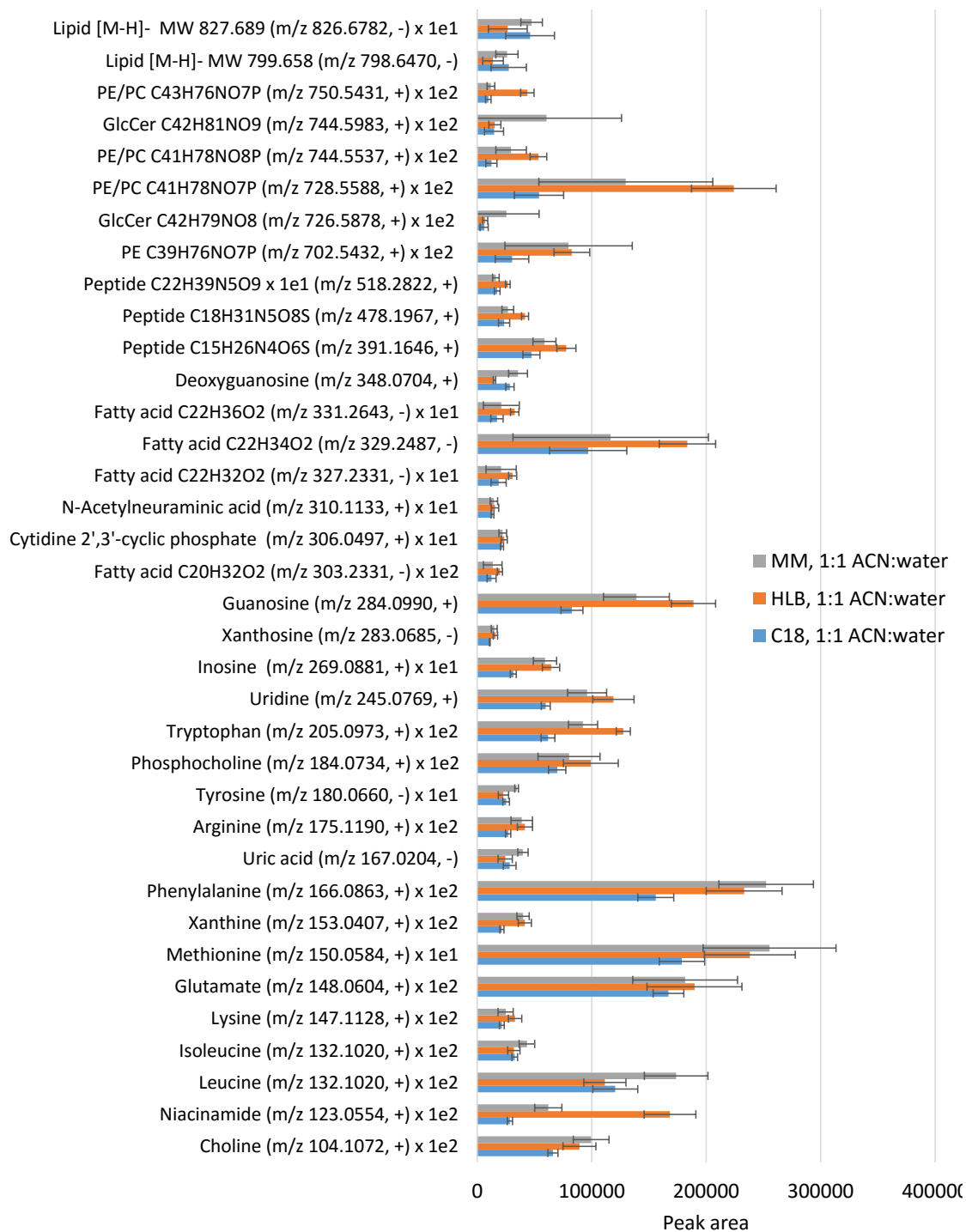
Figure 5.8. Representative metabolites identified in brain extracts obtained with the three different coating types using 1:1 (v/v)ACN:water as desorption solvent (n=4 fibers).
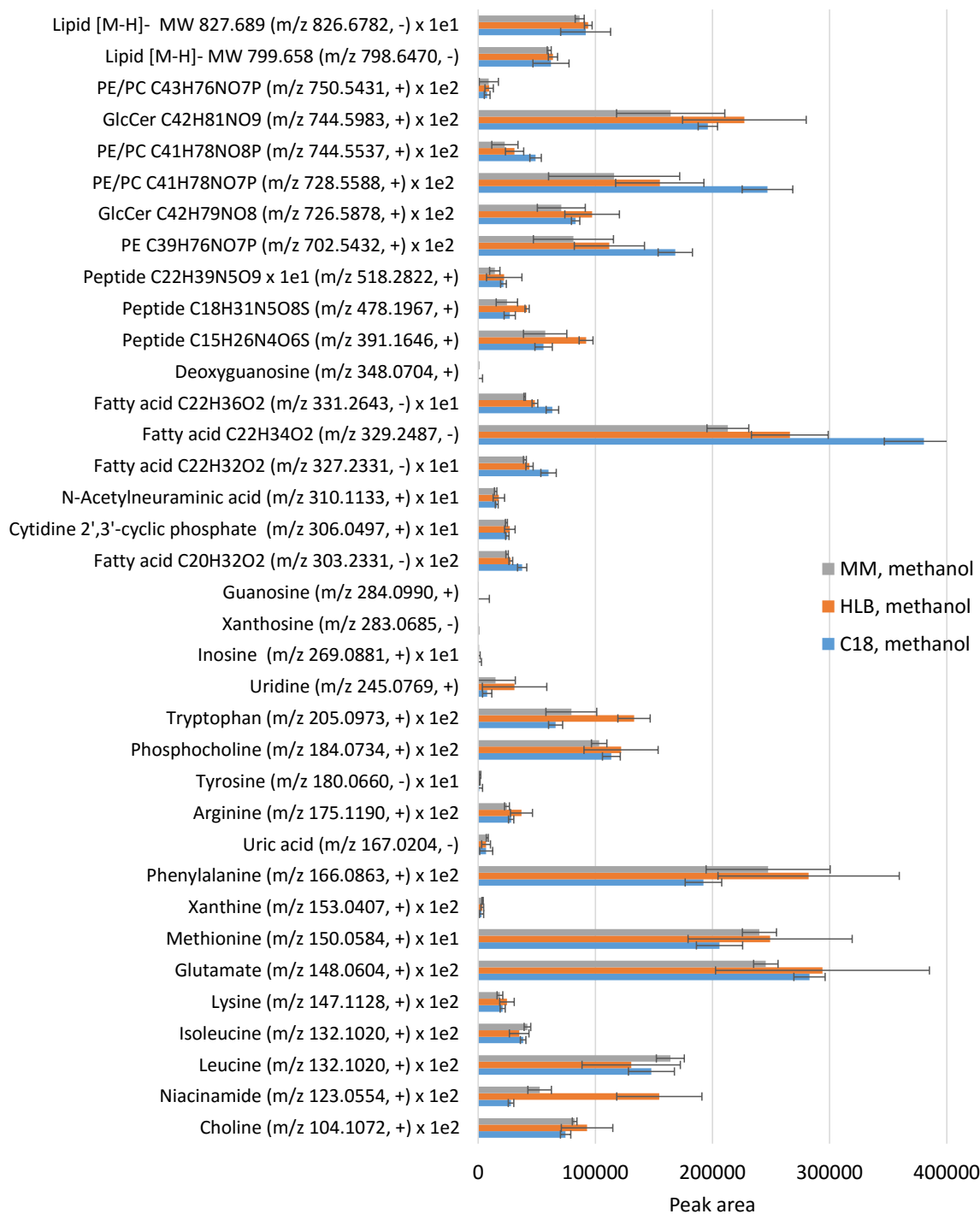
Figure 5.9. Representative metabolites identified in brain extracts obtained with the three different coating types using methanol as desorption solvent (n=4 fibers).

eluting non-polar metabolites from C18, and not to actual differences in coating affinities. A similar trend was observed for several polar metabolites with respect to SPME extracts obtained in methanol. Again, compounds such as niacinamide, phenylalanine, and tryptophan showed higher intensities in HLB and MM brain extracts in comparison with those extracted via C18 fibers (Figure 5.9). Although these findings confirm that HLB and MM display high affinities for these types of polar compounds, decent peak areas for the same metabolites were nonetheless found for all extracts corresponding to the C18 fibers. Such a phenomenon can be explained by considering the presence of active silanol groups in the sorbent material, which enable secondary polar interactions. With respect to non-polar metabolites such as lipids and fatty acids, desorption in methanol was evidenced to provide an overall increase in their peak intensities. As can be seen in Figure 5.9, C18 extracts yielded the highest peak areas for several non-polar compounds in instances where methanol was used as the desorption solvent. This data supports the previous assertion that selective metabolite desorption occurs based on solvent composition, further validating the approach previously proposed in this chapter, which would see the use of more than one desorption solvent per coating type. To conclude the evaluation of coating coverage for metabolomics studies, an assessment of possible differences between HLB and MM in terms of information provided was conducted. To this end, features detected in HLB and MM extracts following their submission to PFP chromatography were compared via OPLS-DA loading S-plots (Figure 5.10). The results of this comparison demonstrated that although there are some differences in the intensities of several metabolite features such as those corresponding to niacinamide and tryptophan (Figures 5.8 and 5.9), in most cases, all filtered features can be easily detected with either coating types. In fact, only 12 features exhibited $|p1| > 0.05$ and $|p(corr)1| > 0.8$ in both

positive and negative modes. Further discussion regarding metabolite extraction kinetics will be

provided in Section 5.3.3.
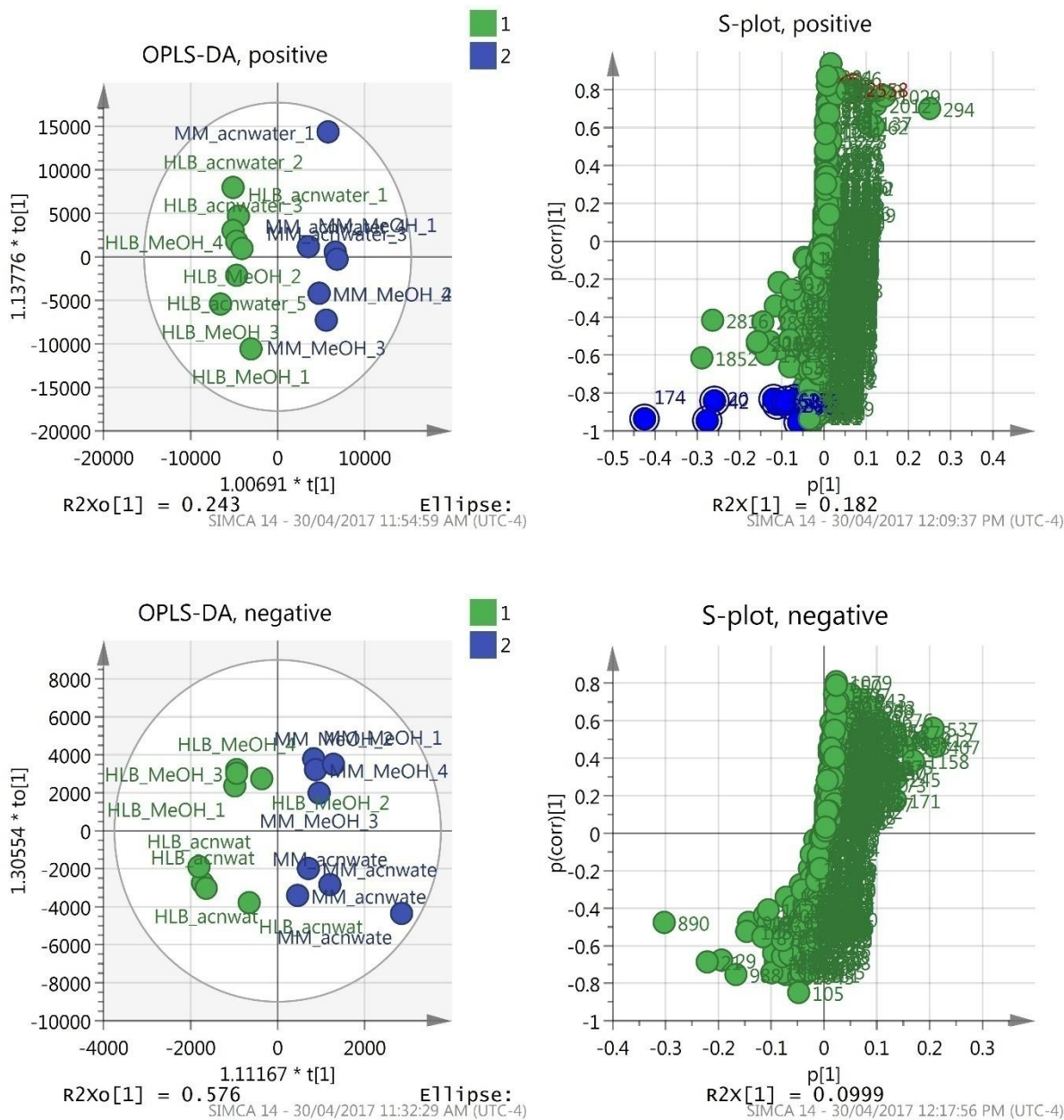
Figure 5.10. OPLS-DA plots and S-plots corresponding to a comparison of HLB(1) and MM (2) extracts in positive (above) and negative (below) modes. Features highlighted have |p1| > 0.05 and |p(corr)1| > 0.8.

Part of the initial assessment of different SPME coatings for brain metabolomics studies also involved inter-fiber variability determinations. This is a critical aspect of both targeted and untargeted metabolomics, as the analytical methodology of choice should guarantee that the differences observed between any two sample groups are due to biological changes, and not to experimental errors introduced in any of the steps of the workflow. Table 5.4 presents a summary of inter-fiber RSDs for features that had pooled QC/blank (solvent and fiber blanks) ratios above 5, pooled QC RSDs below 30 %, and intensities above 3000. As can be seen, the use of methanol in the desorption of C18 extractions considerably improved the precision of the method for features detected in both positive and negative mode. This improvement is due to the strength of this solvent in regards to quantitative desorption of non-polar metabolites such as fatty acids, which are highly abundant in brain tissue. Similarly for HLB and MM, results showed that for negative mode, the use of methanol as a desorption solvent significantly increased the percentage of features with RSD values below 30%. Conversely, in positive mode, HLB showed better inter-fiber RSDs when 1:1 (v/v) ACN:water was employed as desorption solution, whereas for MM fibers, no significant differences were observed between the two desorption solvents. Considering the complexity of the matrix, the fact that no internal standards were used, and that the extraction was conducted using 7 mm-length fibers at static conditions, the encouraging results obtained in this study certainly support the applicability of SPME for untargeted *in vivo* brain studies.

5.3.2. Assessment of SPME coverage for the analysis of lipids in brain tissue

As a next step, the capability of SPME towards extraction of lipids from brain homogenate was investigated. For that purpose, 30 min extractions were carried out from brain homogenate via the three coating chemistries, followed by desorptions in 1:1 (v/v) methanol: isopropanol. 1:1 (v/v) methanol: isopropanol was selected for this evaluation due to its already tested efficiency in the

desorption of lipids from SPME fibers, as well as its demonstrated compatibility with the chromatographic conditions selected for lipid analysis.[240] Figures 5.11 and 5.12 show data

Table 5.4. Summary of RSD values estimated for features detected in positive and negative mode using the PFP method (n=4). Only features with pooled QC/blank (solvent and fiber blanks) ratios above 5, pooled QC RSDs below 30 %, and intensities above 3000 were considered.

Positive mode, # of metabolite features						
RSD, %	**C18, 1:1 ACN:water**	**C18, methanol**	**HLB, 1:1 ACN:water**	**HLB, methanol**	**MM, 1:1 ACN:water**	**MM, methanol**
0 - 10 %	187	220	103	38	59	158
10 - 20 %	197	232	289	136	225	145
20 - 30 %	104	79	146	181	175	136
30 - 40 %	57	25	90	94	102	105
> 40%	160	129	98	247	158	139
Total # of features	705	685	726	696	719	683
% of features with RSDs below 30 %	**69**	**78**	**74**	**51**	**64**	**64**
Negative mode, # of metabolite features						
RSD, %	**C18, 1:1 ACN:water**	**C18, methanol**	**HLB, 1:1 ACN:water**	**HLB, methanol**	**MM, 1:1 ACN:water**	**MM, methanol**
0 - 10 %	105	268	68	122	114	184
10 - 20 %	119	193	145	175	117	162
20 - 30 %	43	51	119	119	67	110
30 - 40 %	51	36	74	69	37	51
> 40%	200	26	106	83	222	58
Total	518	574	512	568	557	565
% of features with RSDs below 30 %	**52**	**89**	**65**	**73**	**54**	**81**

corresponding to features detected in positive and negative modes using the chromatographic conditions for lipids analysis. Similarly to what was already reported in Section 3.1, the relative intensities plotted in Figures 5.11 and 5.12 correspond to the percentage represented by a given feature intensity over the total sum of peak areas of the same feature detected in all extracts. Thus, the relative intensity for feature X detected in the extract attained from the C18 fiber #1 (F1) was calculated as follows: relative intensity of feature X (C18, F1)= (area feature $X_{C18, F1}$/($\sum$areas feature X in C18 extracts$_{F1, 2, 3 and 4}$ + $\sum$areas feature X in HLB extracts$_{F1, 2, 3 and 4}$+ $\sum$areas feature

Figure 5.11. Lipid-related features detected in positive mode for each coating type after extraction from brain tissue. Features were classified according to their average relative intensities (n=4 fibers per coating type).
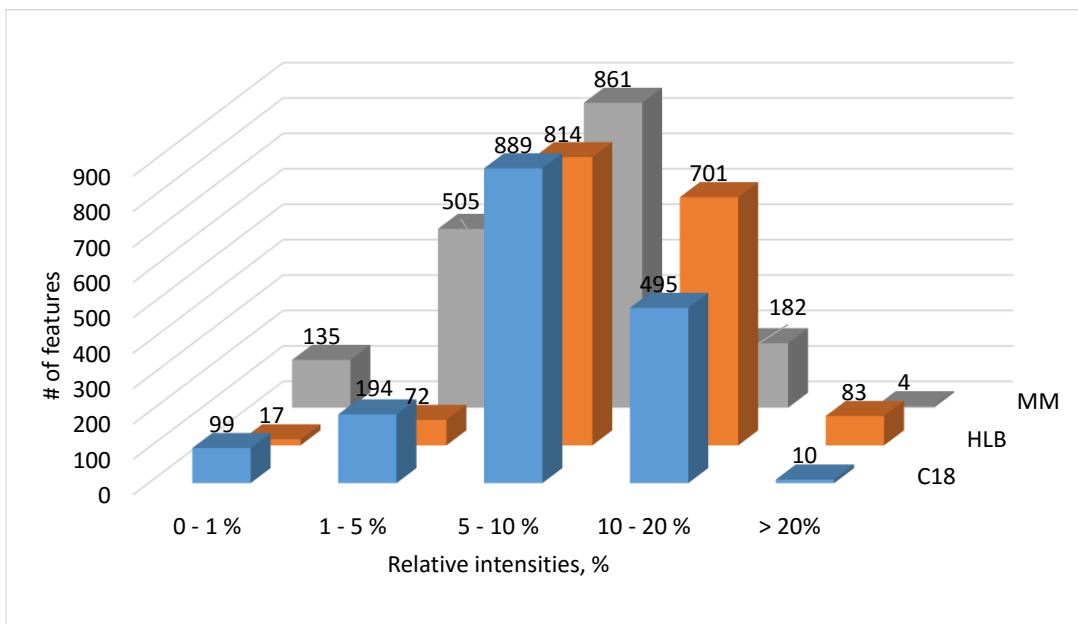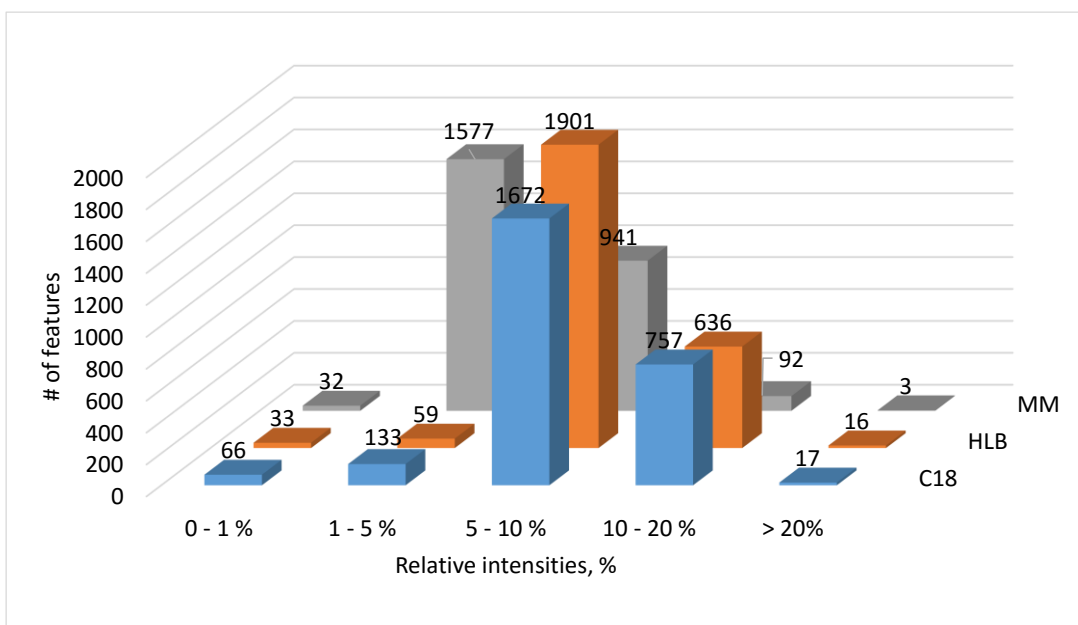

Figure 5.12. Lipid-related features detected in negative mode for each coating type after extraction from brain tissue. Features were classified according to their average relative intensities (n=4 fibers per coating type).

X in MM extracts$_{F1, 2, 3 \text{ and } 4}$))*100. Since four replicates were carried out per coating type, the data plotted in Figures 5.11 and 5.12 correspond to the averages of the relative intensities of the features obtained by coating type. As shown, among the three coatings evaluated, HLB exhibited the largest number of features in the highest ranges of relative intensities. C18 certainly yielded a comparable but slightly lower performance than HLB, while MM provided the largest number of features in the low range of relative intensities. As in the initial assessment of SPME for metabolomics analysis, only features having pooled QC/fiber blank ratios higher than 5 and average intensities above 1000 were considered. Interestingly, after applying the specified filtering criteria, 1688 features still remained in positive mode, whereas 2646 features were kept in negative mode. With aims of further discerning the coverage capabilities and content of information provided by each coating, ion maps were plotted by utilizing only features having pooled QC/blank (solvent and fiber blanks) ratios above 5, pooled QC RSD values below 30 %, and intensities above 3000, as presented in Figures 5.13 and 5.14. As easily gathered through a comparison of Figures 5.13 and 5.14 versus Figures 5.3 and 5.4, which represent mostly small metabolite features, SPME clearly displays significant capabilities towards extraction of lipids from brain tissue. As inferred by the experimental findings shown in Figures 5.11 and 5.12, HLB yielded the best performance in terms of relative intensities of features detected using the lipids analysis conditions. In view of this, comparisons between HLB and MM and between HLB and C18 were carried out. As shown in Table 5.5, in all cases, HLB exhibited the largest number of features with the highest intensities. These results suggest that HLB is able to provide balanced metabolite coverage as it facilitates the analysis of polar and small metabolites, while also yielding satisfactory results for extraction of lipids. Although C18 extracts provided slightly lower recoveries for lipid-related features in

Figure 5.13. Ion maps corresponding to lipid-related features detected in positive mode after extraction from brain homogenate for 30 min with C18, MM, and HLB 7 mm fibers, followed by desorption in 1:1 (v/v) methanol:isopropanol. Only features having pooled QC/blank (solvent and fiber blanks) ratios above 5, RSD values below 30 % in the pooled QC, and intensities above 3000 were considered.
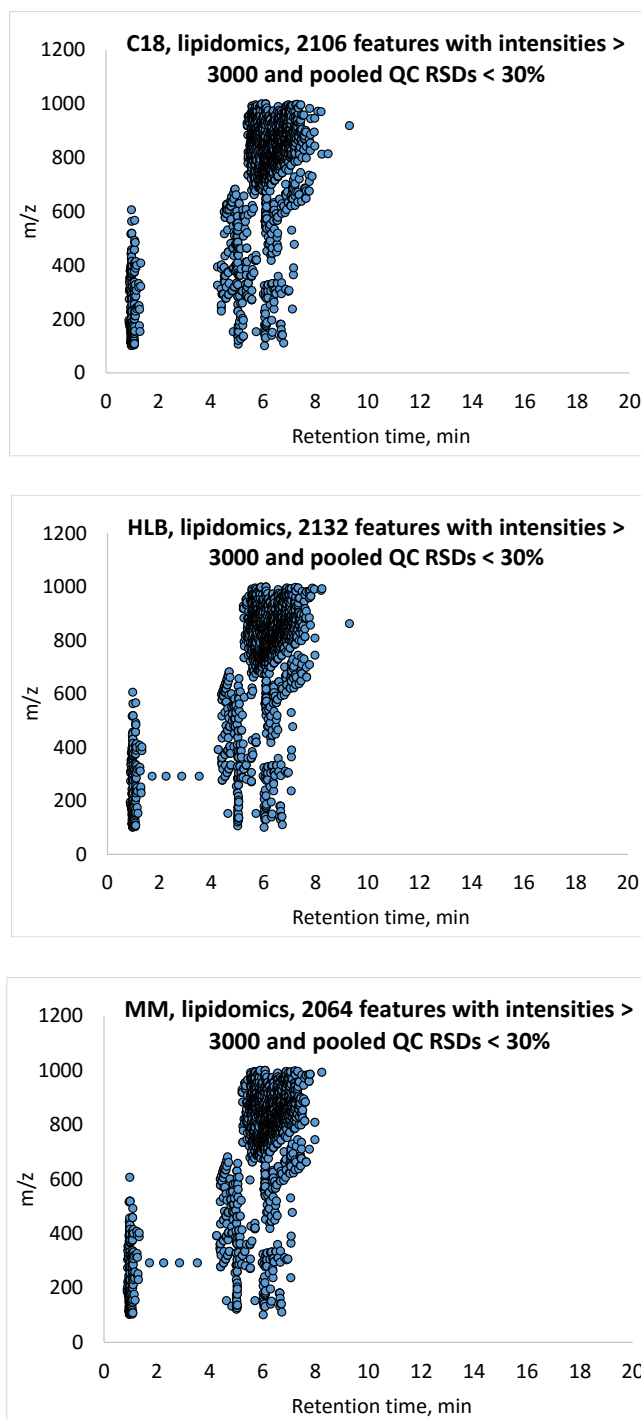
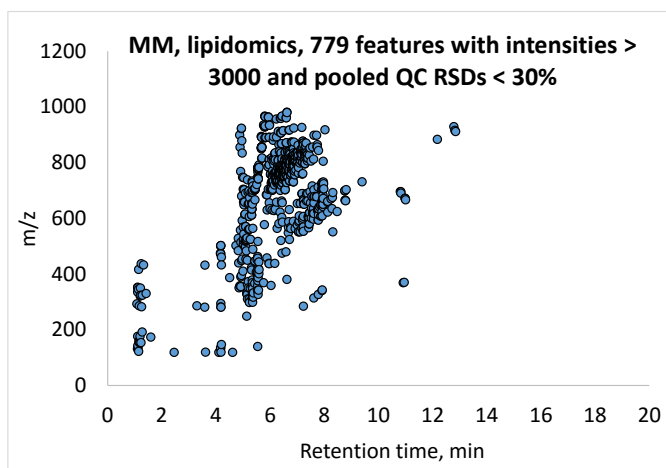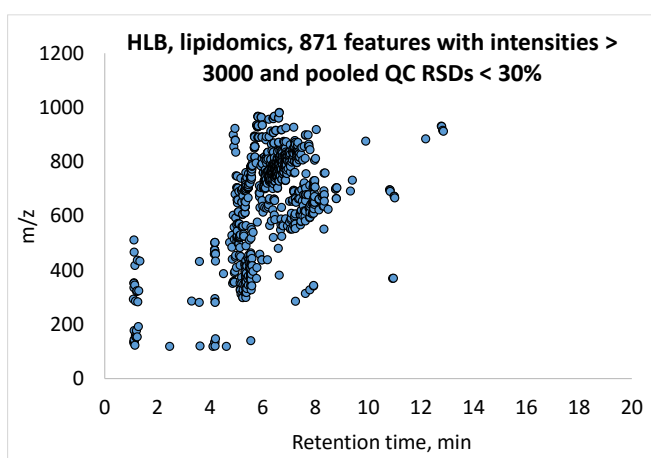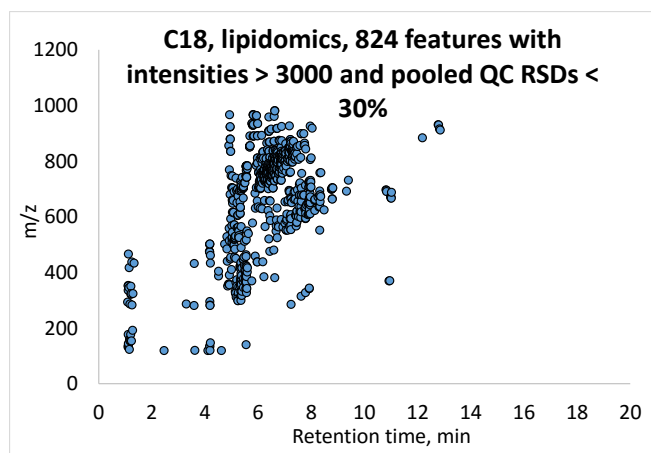**Figure 5.14.** Ion maps corresponding to lipid-related features detected in negative mode after extraction from brain homogenate for 30 min with C18, MM, and HLB 7 mm fibers, followed by desorption in 1:1 (v/v) methanol:isopropanol. Only features having pooled QC/blank (solvent and fiber blanks) ratios above 5, RSD values below 30 % in the pooled QC, and intensities above 3000 were considered.

Table 5.5. Comparison of detected lipid-related features by coating type. Only features with pooled QC/blank (solvent and fiber blanks) ratios above 5, RSD values below 30 %, and intensities above 3000 were taken into consideration. All ratios were calculated using peak areas.

	Features with A/B ratios > 1.5	Features with B/A ratios > 1.5	Total number of compared features
HLB (A) vs MM (B), pos	<u>423</u>	48	729
HLB (A) vs MM (B), neg	<u>1507</u>	51	2019
HLB (A) vs C18 (B), pos	<u>160</u>	66	729
HLB (A) vs C18 (B), neg	<u>125</u>	92	2019
C18 (A) vs MM (B), pos	<u>414</u>	126	729
C18 (A) vs MM (B), neg	<u>1506</u>	93	2019

comparison to extracts obtained via HLB, this coating should be still considered as a suitable coating for lipids studies, especially since it is commercially available. Interestingly, a comparison between the C18 and MM fibers provided by Millipore Sigma demonstrated that C18 offers better sensitivity for lipids as 57% and 75 % of the features detected with the chromatographic method for lipid analysis in positive and negative mode, respectively, exhibited higher intensities than those obtained via MM (Table 5.5).

Following the above-discussed evaluation, which sought to assess the capability of the studied coatings to extract lipids based on the relative intensities of the detected lipid-related features obtained for each coating, an assessment of inter-fiber reproducibility was carried out for all three fibers. Table 5.6 presents results corresponding to RSD values calculated for lipid-related features, filtered using the same parameters defined in Figures 5.13 and 5.14. Conversely to what was observed for features detected using the PFP chromatographic method, in this part of the study, HLB showed the poorest performance in terms of inter-fiber precision for features obtained in both

positive and negative mode. While the goal of the evaluation discussed in this section pertains to lipid-related features, whereas the investigation discussed in Section 5.3.1 had as focus mostly metabolites of low molecular weight, the use of a different batch of HLB fibers could have certainly contributed to the high inter-fiber variability that is shown in Table 5.6. In regards to the inter-fiber reproducibility of C18 and MM coating types, the percentages of features detected in positive mode that presented RSD values below 30% were comparable. However, results obtained in negative mode showed that MM was superior to the two other coatings in this regard, as 76 % of the detected features by MM were in the lowest range of inter-fiber RSDs.

Table 5.6. Summary of RSD values estimated for lipid-related features detected in positive and negative mode (n=4). Only features with pooled QC/blank (solvent and fiber blanks) ratios above 5, pooled QC RSDs below 30 %, and intensities above 3000 were considered for the calculations.

Positive mode, # of metabolite features			
RSD, %	C18	HLB	MM
0 - 10 %	67	53	39
10 - 20 %	130	91	113
20 - 30 %	220	103	189
30 - 40 %	92	219	85
> 40%	314	404	352
Total # of features	823	870	778
% of features with RSDs below 30 %	**51**	**28**	**44**
Negative mode, # of metabolite features			
RSD, %	C18	HLB	MM
0 - 10 %	70	36	188
10 - 20 %	251	173	735
20 - 30 %	397	276	638
30 - 40 %	580	591	202
> 40%	807	1025	294
Total	2105	2101	2057
% of features with RSDs below 30 %	**34**	**23**	**76**

Several factors should be considered when aiming to investigate the sources of variability that could affect the precision of the developed method for extraction of lipids from brain tissue via

SPME. First of all, the high binding that lipids display for several matrix components will be reflected in considerably low free concentrations of lipids available for SPME extraction. The smaller extraction amounts expected for lipids in comparison to other small metabolites, in turn, could lead to high inter-fiber variations. Moreover, the risk of incurring non-specific binding due to the physical attachment of matrix components to the probe should be carefully considered. In such cases, any tissue debris remaining on the coating surface would be further extracted in the desorption step, introducing variations to the metabolite composition of the final extracts. With this in mind, the effect of an added post-extraction rinsing/cleaning step was evaluated for its impact on inter-fiber reproducibility. For this purpose, the feasibility of incorporating organic solvent into the washing step was explored based on recent work conducted in our group, wherein rewarding SPME method precision was attained by introducing acetone in a rinsing solution, which was utilized to rinse fibers following extraction of pesticides from avocado.[241] To this end, acetone, isopropanol, and methanol were evaluated as additives in the washing step at a set proportion of 10 % (v/v). C18 fibers were used for this experiment in view of their satisfactory performance towards lipid extraction, their current availability in the market, and their high inter-fiber variability in terms of lipid-related features, as was shown in Table 5.6. In order to further study the impact of convection and matrix type on inter-fiber RSD, in addition to carrying out a washing step evaluation using brain homogenate as matrix, plasma aliquots were also sampled under agitation conditions. Figure 5.15 depicts results corresponding to the washing step evaluation after extraction from both matrices. As can be seen, for extractions conducted in plasma, addition of acetone and methanol to the washing solution contributed to a decrease in the percentage of features with RSD values higher than 40 %. Indeed, the percentages of lipid-related features with RSD values below 30 % were 63%, 75%, and 54 % for acetone (10 %), methanol

(10 %), and water, respectively. In tissue extractions, it is evident that acetone (10 %) yielded the best results among the tested strategies, with 62 % of the detected features yielding RSDs below
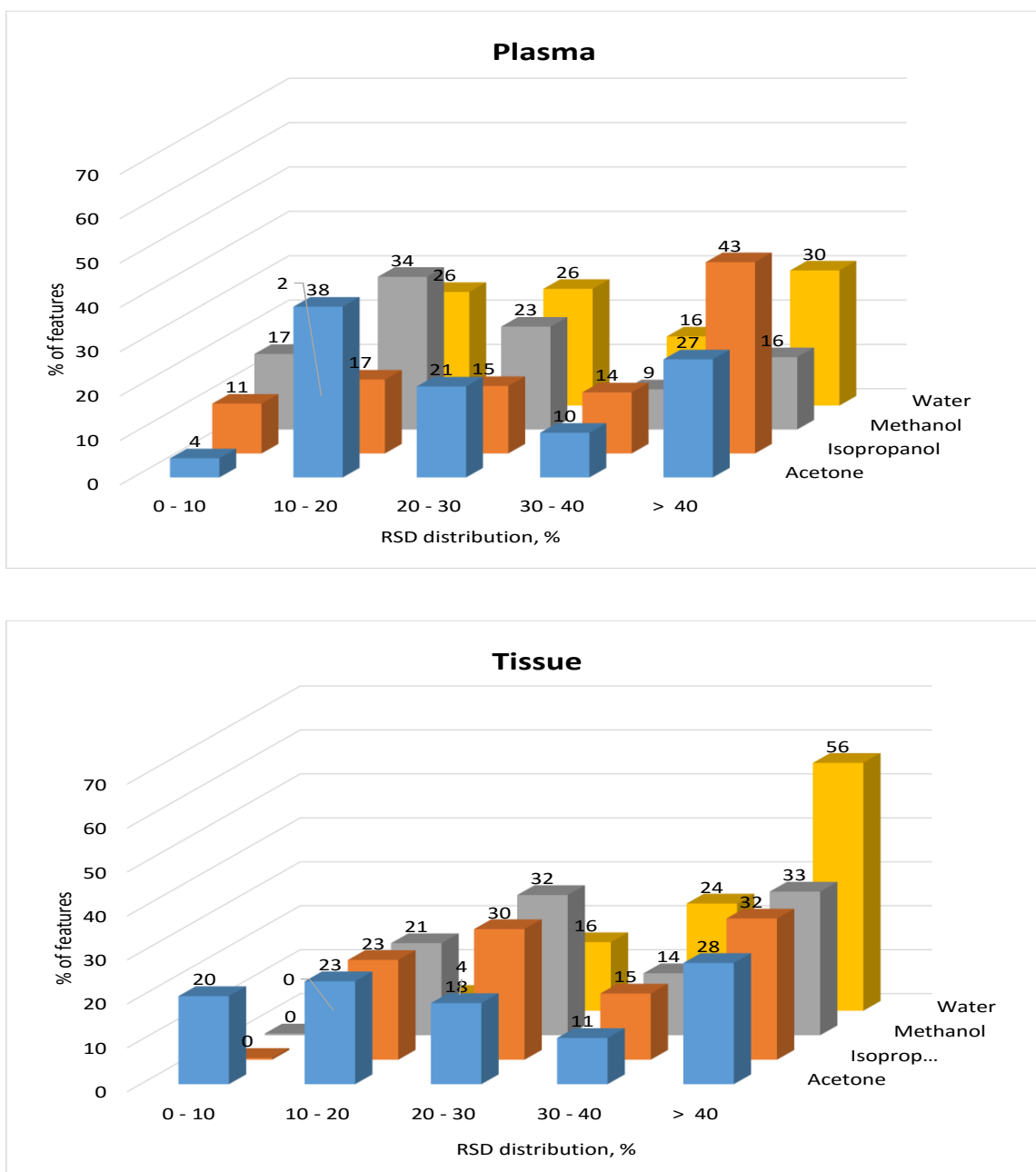
Figure 5.15. Evaluation of different washing solutions after 30 min extractions from plasma (above) and brain homogenate (below). RSD values were calculated based on peak areas detected in five SPME fibers (n=5).

30 %. Isopropanol and methanol displayed similar outcomes, as 53 % of the detected features yielded RSD values below 30 % in both cases. While higher variation was observed in the washing step assessment for water in comparison to the results presented in Table 5.6, the use of a different batch of C18 fibers was suspected to contribute towards some of the observed variability. With the purpose of confirming our findings, the use of 10 % acetone as rinsing solution was evaluated once again by extracting from brain homogenate with a third batch of C18 fibers. As can be seen in Table 5.7, satisfactory results were obtained, with almost 80% of features detected in both positive and negative modes yielding RSD values below 30 %. Based on these and our previous findings, the use of acetone in the rinsing step was adopted as a strategy for analysis of lipids from brain tissue.

Table 5.7. Second assessment of RSD values estimated for lipid-related features detected in positive and negative mode via C18 fibers (n=4). Only features with pooled QC/blank (solvent and fiber blanks) ratios above 5, pooled QC RSDs below 30 %, and intensities above 3000 were considered for the calculations.

RSD ranges	C18, lipids, positive mode	C18, lipids, negative mode
0 - 10 %	71	115
10 - 20 %	199	552
20 - 30 %	174	380
30 - 40 %	52	155
> 40%	64	135
Total	560	1337
% of features with RSDs below 30 %	79	78

As previously emphasized at the beginning of this chapter, final metabolite concentrations obtained via SPME are expected to be lower in comparison with those obtained through exhaustive sample preparation techniques. Based on the results presented so far, an average of 500 (HLB, MM) and 436 (HLB, MM) metabolite features with RSD values below 30 % can be measured via

independent SPME extractions, following the general metabolomics method in positive and negative mode, respectively. As for lipid-related features, 444 (C18) and 1047 (C18) features in positive and negative mode, respectively, meet the same criteria. Although a fair comparison with other methodologies reported in the literature for tissue analysis cannot be easily made, as the employed chromatographic conditions and instrumentation in such studies differ from those employed in this work, our results are nonetheless very encouraging, particularly in view of the simplicity of the SPME workflow and its applicability for *in vivo* studies. For instance, in a protocol using in-vial dual extraction for metabolite analysis from rat brain cerebellum, Ebshiana *et al.* reported a total of 1040, 1783, 1733, and 2603 metabolite features with RSD values below 30 %, detected with reversed phase (RP) positive, RP negative, HILIC positive and HILIC negative LC-MS conditions, respectively (features present in 85 % of the samples).[53] Although the removal of background ions was not reported for this study, the number of acceptable features detected using RP chromatography, which correspond mostly to lipid-related features, was only approximately two times higher than the number of filtered features obtained in the present work via SPME and the described lipidomics LC-MS method. In another work involving the analysis of lung tissue via solvent extraction followed by instrumental analysis by LC-MS, a total number of 1350 and 352 features remained in positive and negative mode, respectively, after aligning samples and QC samples prepared to assess the method's reproducibility.[20] While this methodology provided more than twice the number of features in positive mode in comparison with the average number of features obtained in the present work through employment of the PFP chromatographic method at the same ionization conditions, the currently presented SPME method yielded a slightly higher number of metabolite features in negative mode in comparison with the abovementioned work. While other studies involving untargeted tissue analysis have reported a much larger number

of significant features with acceptable RSD values, [242,243] these studies are all comprised of labor intensive methodologies, wherein the amounts of tissue needed per sample vary from 100 to 400 mg. Despite the fact that the recoveries offered by SPME are considerably lower in comparison with such approaches, in many cases, the application of this microextraction technology can provide complementary information to traditional methodologies since the system under study is accessed *in vivo*, thus minimizing the risks of metabolome alterations that are typically incurred in traditional workflows.

5.3.3. Extraction time profiles

The construction of extraction time profiles in SPME can provide valuable information regarding the affinity of a given compound for the employed SPME coating at a defined set of conditions. In SPME, equilibration time is defined as the time necessary for 95% of the equilibrium amount of a given analyte to be extracted onto the fiber. Parameters such as convection, matrix composition, temperature, analyte physicochemical properties, coating chemistry, and coating thickness all influence the equilibration time. With this in mind, extraction time profiles for metabolite features detected in each of the SPME coating types tested (C18, HLB, and MM) were investigated in homogenized cow brain tissue. Extracts obtained from HLB and MM fibers were run using the PFP method, whereas desorption solutions from C18 fibers were run using the chromatographic method for the analysis of lipids. On this note, methanol was used as desorption solution for HLB and MM fibers, whereas 1:1 (v/v) isopropanol:methanol and 10 % acetone (v/v) were employed as desorption and washing solutions for the C18 fibers, respectively. As already described in the experimental section, 5, 10, 20, 30, and 40 min were chosen as extraction points. Longer extraction times were not considered due to their unsuitability for *in vivo* tissue sampling applications.

5.3.3.1.Extraction time profiles corresponding to metabolite features detected using the PFP chromatographic method

Aiming to estimate the types of metabolites that fail to reach an extraction plateau after 40 min of extraction, pairwise comparisons were carried out between 5 and 40 min extracts, and between 30 and 40 min extracts, employing the pairwise comparison tool provided by XCMS online. Statistical analyses were carried out using the unpaired parametric Welch t-test, while data visualization was enabled through the cloud plot option offered by the aforementioned platform, as shown in Figures 5.15 and 5.16. Circles in green represent features exhibiting higher intensities at 40 min, whereas circles in red correspond to those features having higher intensities at 5 and 30 min. Here, the circle radius is proportional to the fold changes observed, while p-value significance is proportional to the shade of the colour. Data was filtered by only retaining features with p-values lower than 0.05, fold changes higher than 1.5, and intensities above 3000. As the cloud plot tool employed for this determination does not enable the removal of background artefacts, all detected features were taken into account for these comparisons. Although extracts were run in both positive and negative modes, for practical purposes, only plots obtained in positive mode were included. As can be seen in Figures 5.15 and 5.16, for both HLB and MM coatings, a considerably lower number of features showing statistical differences was found in a pairwise comparison of 30 vs. 40 min extracts as opposed to 5 vs. 40 min, indicating that various metabolites were able to reach equilibrium after 30 min of extraction, despite the lack of agitation and the slower diffusion that is expected to occur in brain tissue. To better understand the extraction kinetics behaviour observed at the described conditions, extraction time profiles were plotted for selected representative metabolites.
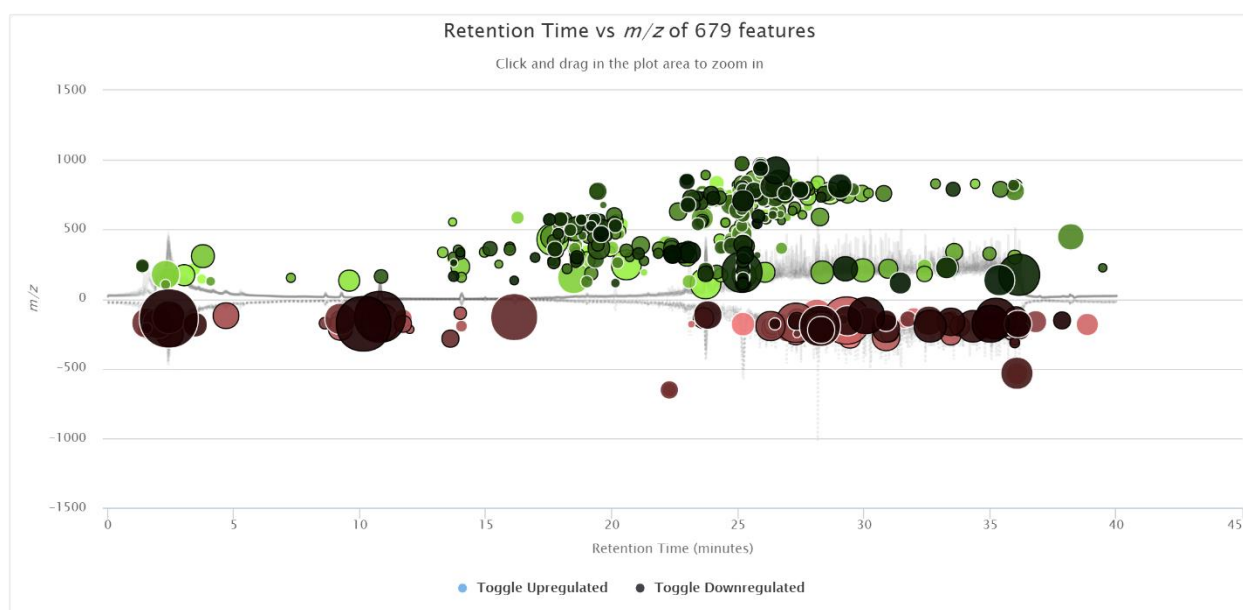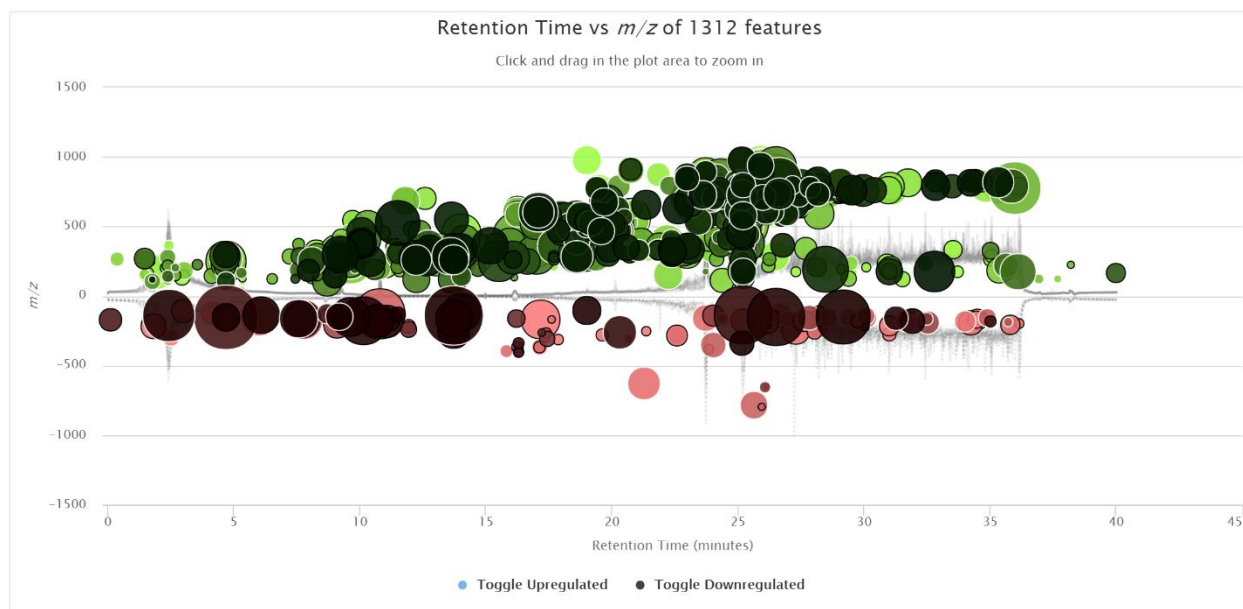
Figure 5.16. Cloud plots corresponding to a pairwise comparison of HLB extracts obtained in positive mode. Features showing significant differences (p-value<0.05 and fold changes > 1.5) in a comparison between two pairwise groupings, 5 versus 40 min extractions (above) and 30 versus 40 min extractions (below), are represented in green (higher intensities in 40 min extracts) and red circles (higher intensities in 5 and 30 min extracts).

Figure 5.17. Cloud plots corresponding to a pairwise comparison of MM extracts obtained in positive mode. Features showing significant differences (p-value<0.05 and fold changes > 1.5) in a comparison between 2 pairwise groupings, 5 versus 40 min extractions (above) and 30 versus 40 min extractions (below), are represented in green (higher intensities in 40 min extracts) and red circles (higher intensities in 5 and 30 min extracts).
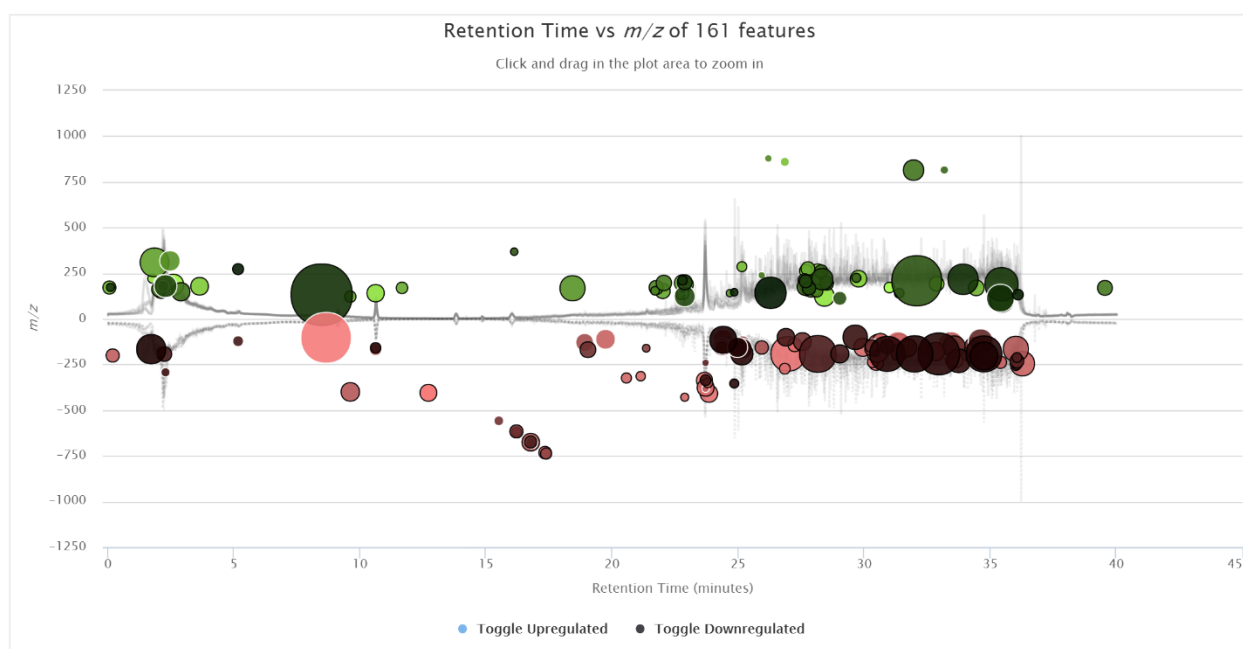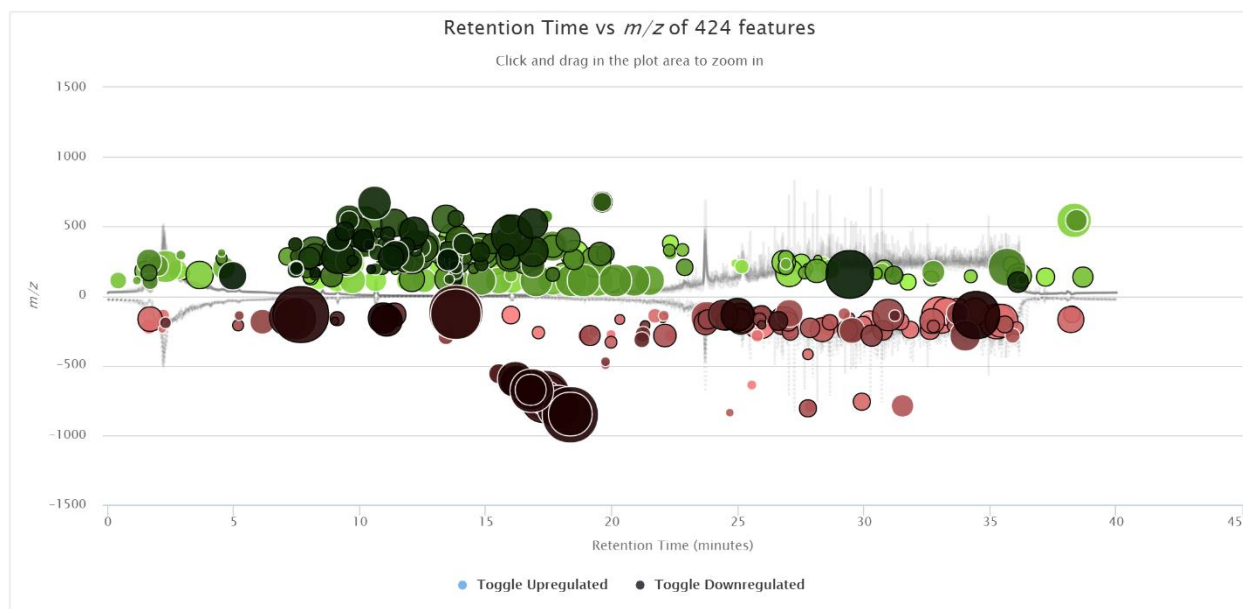
161

As can be seen in Figure 5.18, highly polar compounds such as choline, citrulline, tyrosine, arginine, isoleucine, and carnitine were able to achieve equilibrium in less than 10 min of extraction. Other compounds such as tryptophan and niacinamide, which are slightly less polar and bear aromatic functionalities in their structure, exhibited longer equilibration times, owing to their higher affinities for both HLB and MM extraction phases. Conversely, the extraction of riboflavin was observed to still be within its linear regime past the 40 minute extraction period. Considering that the extraction process is mediated by the diffusion of the analyte towards the coating under the tested conditions, as expected, no significant differences were observed between the two coating types. Despite the high polarity of this metabolite, the aromatic moieties that riboflavin possesses in its structure enhance its affinity for both HLB and MM functionalities, leading to longer equilibration times that are even more pronounced at static extraction conditions. Although, as previously emphasized, all features that remained after data filtering were detectable using both HLB and MM coatings, our results suggest that the vinyl pyrrolidone functionality of HLB provides slightly improved recoveries for some polar metabolites. Nevertheless, as the employed HLB fibers were made in house, high standard deviations due to inter-fiber variability were also noticed for this particular experiment. Irrespective of the fiber being employed, however, considering the observed differences among various metabolites in terms of equilibration times and extraction kinetics, precise control of the time that the SPME probe is exposed to the sample matrix is imperative when performing untargeted studies. Longer extraction times will ensure better method precision, but will come with a compromise in temporal resolution, as the final amount of analyte extracted is proportional to its average concentration over the extraction period. Other parameters to be taken into consideration when selecting an extraction time in SPME,
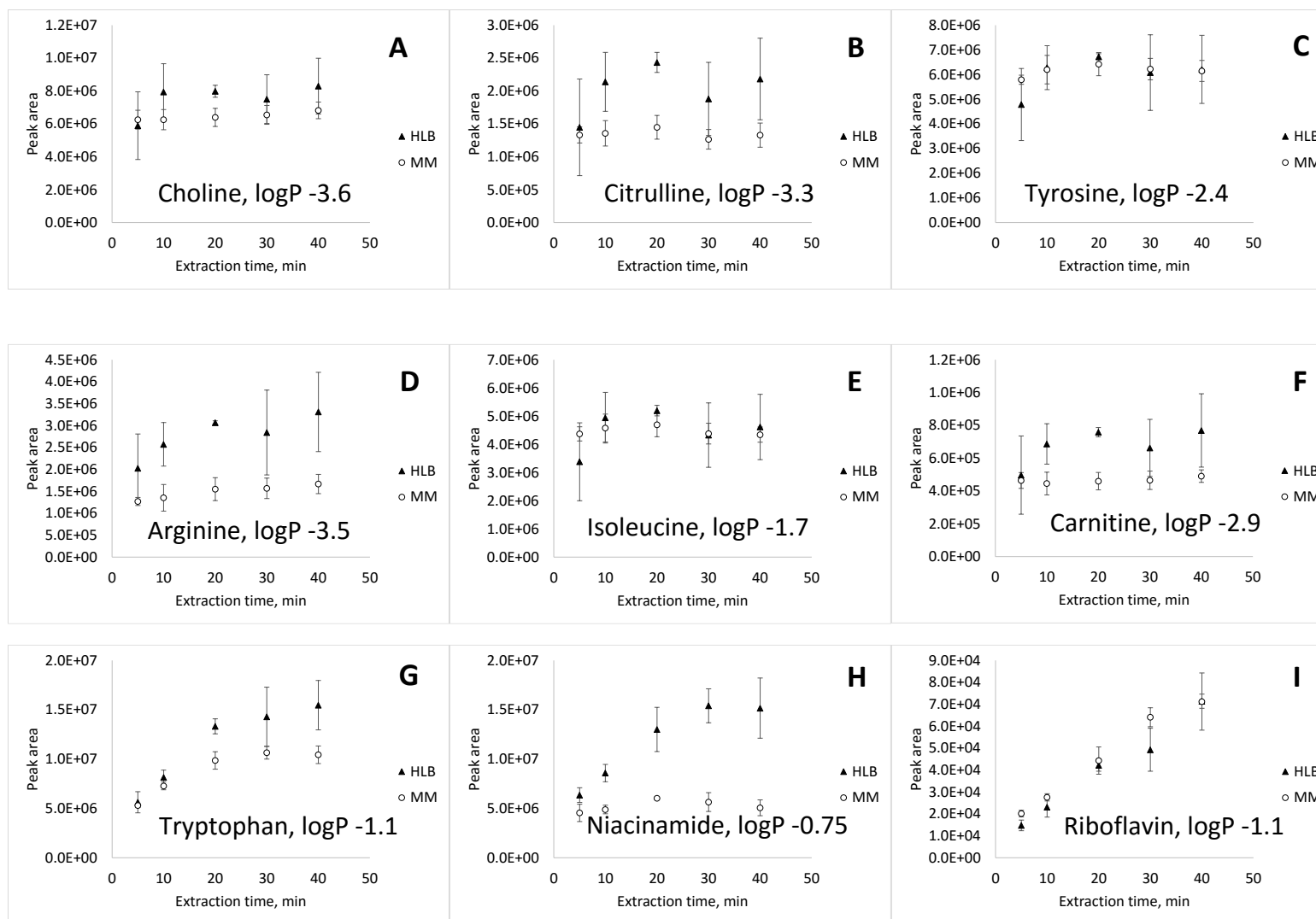
Figure 5.18. Extraction time profiles constructed with HLB and MM coatings corresponding to representative metabolites occurring in brain tissue (n=4).

particularly for *in vivo* studies, relate to the technical aspects of the experiment being undertaken. In studies in which multiple animals are employed as subject, the time lapse required to place/remove the SPME probes in/from each animal is also important. If the extraction time selected is too short (few minutes), SPME fibers set to extract first may need to be removed before all probes have been placed in all subjects. This presents an inconvenience, especially in cases where the availability of personnel qualified to handle animals is limited. As an alternative, animals can be studied in smaller groups; however, this could lead to a reduction in analysis throughput, particularly when conducting studies that involve pre and post analysis of long treatments. For these reasons, extraction times ranging between 20 and 40 min would offer a good compromise for such applications.

5.3.3.2.Extraction time profile corresponding to lipid related features

An initial screening was also carried out with respect to lipids and fatty acids able to achieve equilibrium within 30 min of extraction. Using the same strategy and parameters described in section 3.3.1, comparisons between 5 and 40 min and between 30 and 40 min extractions were carried out. As can be seen in Figure 5.19, 193 and 289 metabolite features detected in positive and negative mode, respectively, exhibited statistically significant differences in a comparison between features obtained for 5 and 40 min extracts. Conversely, only close to half of those features showed statistical variations in a comparison between 30 and 40 min extracts (Figure 5.20). Considering that the total number of detected unfiltered features used for this comparison amounted to 3651 and 5885 in positive and negative mode, respectively, these findings demonstrate that at the experimental conditions selected for this study, relatively fast equilibration times can be reached for large non-polar metabolites such as lipids. Based on the high hydrophobicity of lipids and fatty acids, these compounds are expected to exhibit high
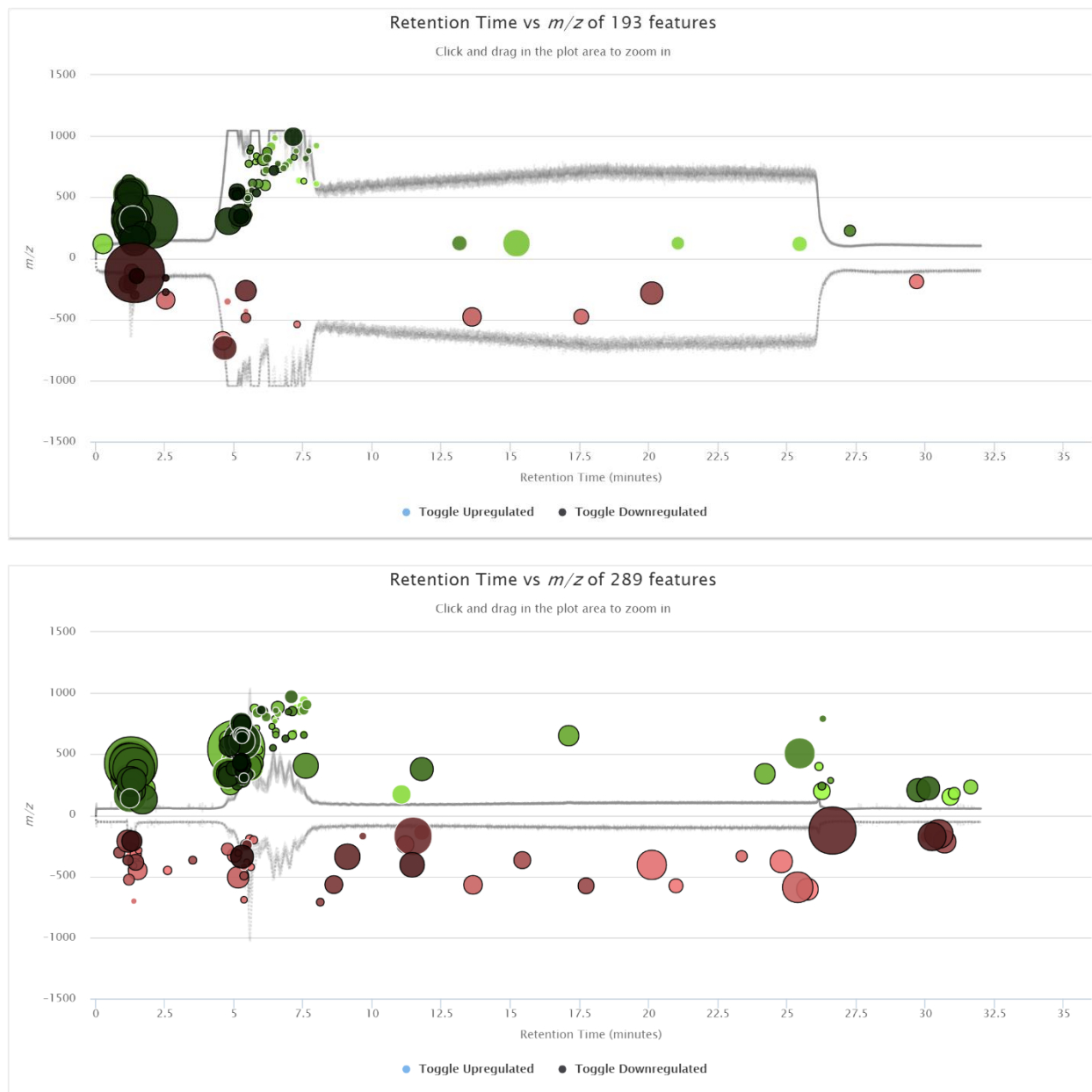
Figure 5.19. Cloud plots corresponding to the pairwise comparison of 5 versus 40 min extractions conducted with C18 fibers and run using the LC-MS method for lipids analysis. Features showing significant differences (p-value<0.05 and fold changes > 1.5) in positive (above) and negative (below) modes are represented in green (higher intensities in 40 min extracts) and in red circles (higher intensities in 5 min extracts).
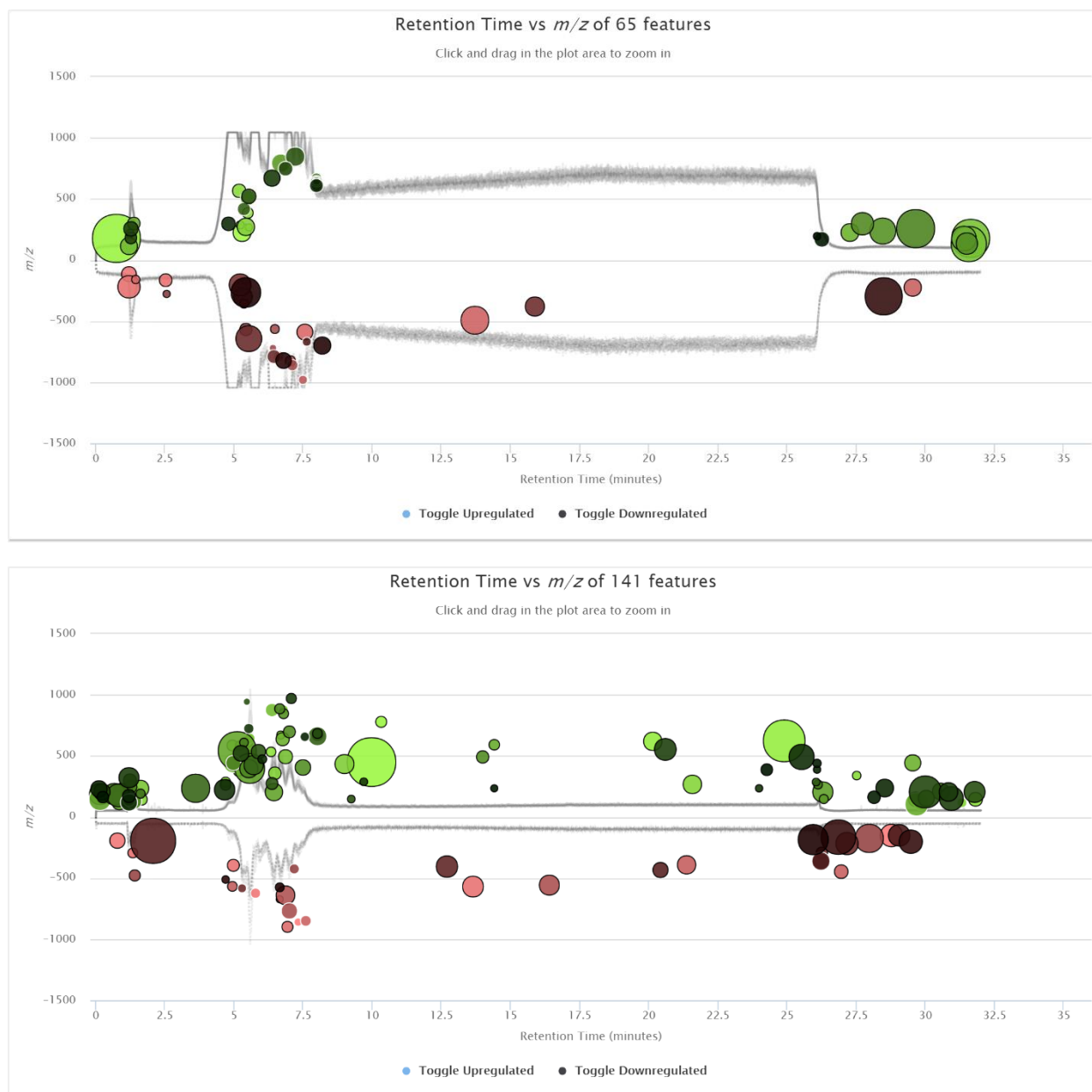
Figure 5.20. Cloud plots corresponding to a pairwise comparison of 30 versus 40 min extractions conducted with C18 fibers, and run using the LC-MS method for lipids analysis. Features showing significant differences (p-value<0.05 and fold changes > 1.5) in positive (above) and negative (below) modes are represented in green (higher intensities in 40 min extracts) and red circles (higher intensities in 30 min extracts).
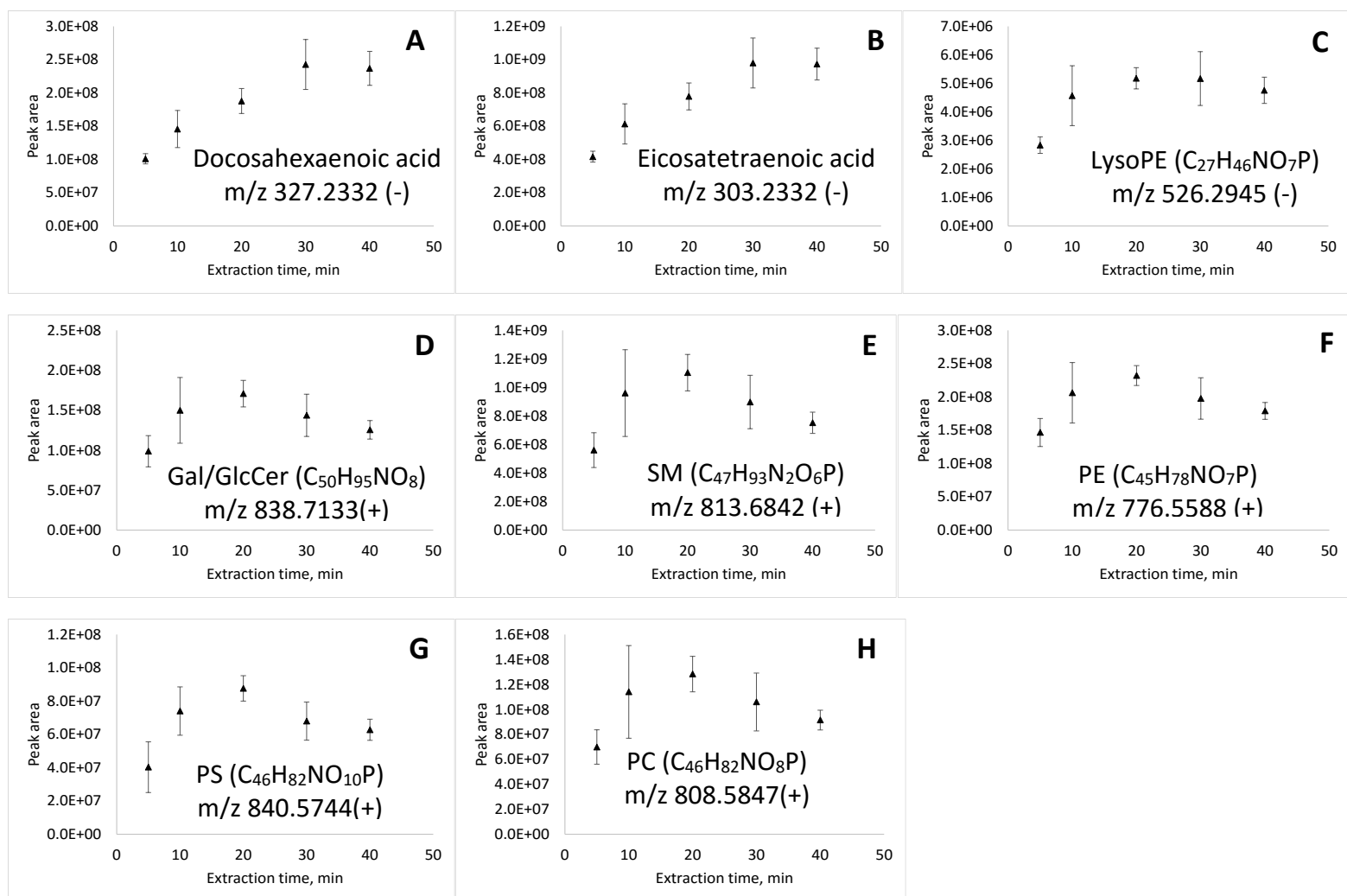
Figure 5.21. Extraction time profiles corresponding to representative fatty acids and lipids occurring in brain tissue (n=4). Extractions were conducted using C18 fibers, and the post-extraction rinsing step was carried out in 10 % acetone (v/v). Lysophosphatidyletha-nolamine (LysoPE), galactosyl or glucosyl ceramide (Gal/GlcCer), sphingomyelin (SM), phosphatidylethanolamine (PE), phosphatidylserine (PS), and phosphatidylcholine (PC).

affinities for SPME coatings, as well as long equilibration times when present in aqueous matrices. However, considering that the matrix is brain tissue, which is substantially hydrophobic, metabolites such as lipids will display low coating distribution constants along with short equilibration times due to the high affinity of these compounds for the sample matrix. In order to obtain a clearer picture in respect to the extraction kinetics of lipids and fatty acids, extraction time profiles corresponding to representative metabolites were plotted. As can be seen in Figure 5.21, equilibration times for lipids of different classes ranged around 10 min, whereas fatty acids required an average of 30 min to reach an extraction plateau. Although further investigation of the mass transfer processes occurring in complex matrices such as brain tissue are needed, our results indicate that employment of extraction times ranging between 20 to 30 min will allow for optimum SPME recoveries and precision. As a means to verify the effect of extraction time on method precision for lipid-related features, an evaluation of the inter-fibre RSD values corresponding to the different time points selected for this study was conducted. As shown in Table 5.8, longer extraction times enabled improved RSD values, a finding that is in agreement with the above discussion.

Table 5.8. Assessment of RSD values estimated for lipid-related features detected in positive and negative mode at different extraction times using C18 fibers (n=4).

Lipid related features, positive mode	Extraction time, min				
	5	**10**	**20**	**30**	**40**
Number of features with RSD less than 30%	309	291	468	421	464
% of features with RSDs below 30 %	57	54	86	78	85
Total number of features 543					
Lipid related features, negative mode	**5**	**10**	**20**	**30**	**40**
Number of features with RSD less than 30%	907	739	1075	1009	1106
% of features with RSDs below 30 %	69	57	82	77	85
Total number of features 1307					

5.4. Conclusions

In this study, a comprehensive evaluation of SPME as a sample preparation tool for untargeted studies in brain tissue was presented for the first time. In terms of coating chemistries, HLB yielded the best results among the three tested coatings based on its broad metabolite coverage and on the intensities attained for significant detected features. Nonetheless, high HLB inter-fiber RSD values were also found in some of the experiments, as the devices were prepared using an in-house protocol. In regards to the performance of the commercially available coatings, the performance of MM was comparable to HLB with respect to the extraction of polar compounds, whereas C18 was able to offer satisfactory results in the extraction of non-polar metabolites such as lipids and fatty acids. In addition to a coating chemistry evaluation, this work demonstrated that the use of different desorption solvents greatly influences the final composition of brain extracts obtained with SPME. The use of methanol, for instance, facilitated the desorption of non-polar metabolites such as lipids and fatty acids, which are highly abundant in brain, while the use of 1:1 (v/v) ACN:water allowed for improved recoveries of some polar compounds such as those that contain a purine base in their structure (*e.g.* xanthine, inosine, guanosine, or deoxyguanosine). Therefore, employment of more than one solvent per coating type, and of at least two fibers in the same sampling point are recommended. The results of this study also revealed that despite the non-exhaustive nature of SPME, rewarding results in terms of method precision can be achieved through optimization of this method. For all evaluated coating types, 60 to 80 % of the detected brain-related features showed RSD values below 30 % at optimized desorption conditions. In respect to highly hydrophobic metabolites such as lipids, the introduction of a washing step with 10 % acetone (v/v) enabled their reproducible analysis from brain tissue. As for equilibration times attained in brain homogenate, highly polar metabolites were observed to be able to reach an extraction plateau in 5 min or less. Surprisingly, for highly hydrophobic metabolites such as lipids,

relatively short times (close to 10 min) were needed for equilibrium to be reached due to the high affinity that these compounds display for the matrix under study. Considering the simplicity of SPME, the practicability of performing sampling and sample preparation in a single step, the biocompatibility of the SPME probes, which enables their use *in vivo*, and the broad coverage offered by SPME coatings, further implementation of SPME in multiple applications involving tissue analysis is foreseen. Although the results of this study provide a reliable basis for the future application of SPME in untargeted brain studies, current work is being conducted in our lab to fully characterize the metabolites that can be extracted via SPME from brain tissue through employment of high resolution MS/MS and other chromatographic methods such as hydrophilic interaction chromatography (HILIC).

Chapter 6: Application of solid phase microextraction (SPME) for *in vivo* monitoring of metabolic changes after deep brain stimulation (DBS)

6.1. Preamble and introduction

6.1.1. Preamble

The research project related to this section started in August 2015, and is still ongoing. The results presented in this chapter have not yet been published in any journal. *In vivo* sampling was carried out in the facilities of the Center for Addiction and Mental Health (CAMH) in Toronto. Clement Hamani, Barbara Bojko, and Janusz Pawliszyn participated in the design of the experiment. Clement Hamani surgically implanted the sampling cannulas and DBS electrodes into the brains of the animals. All animals used in this study were solely handled by Mustansir Diwan. Barbara Bojko, Ezel Boyaci, German A. Gómez-Ríos, Nathaly Reyes-Garcés, and Tijana Vasilejvic participated in *in vivo* sampling procedures. German A. Gómez-Ríos designed the fibre holder used for *in vivo* sampling, while its construction was undertaken by the Machine Shop of the University of Waterloo. Ezel Boyaci and Nathaly Reyes-Garcés desorbed all probes and ran the corresponding extracts in the LC-MS system. Nathaly Reyes-Garcés conducted all the data processing and wrote the corresponding discussion herein presented.

6.1.2. Introduction

Deep brain stimulation (DBS) is a medical therapy successfully used to treat several disorders, including Parkinson's disease, essential tremor, epilepsy, chronic pain, and depression, among others.[244] In DBS, electrical pulses are delivered in specific brain regions by surgically implanting electrodes in the target area. The effectiveness of this treatment in alleviating symptoms of neurological and psychiatric conditions presenting in patients resistant to available medical

treatments is reflected in the growing number of new patients receiving DBS devices per year (8,000 – 10,000 new patients per year worldwide).[245] Despite the fact that DBS has been used for decades, a clear understanding regarding the neurophysiological mechanisms behind this technique has yet to be presented.[246–248] One of the main questions that remains to be answered is whether DBS inhibits or excites neuronal elements.[244,246] Considering that the effects of DBS are comparable to those of stereotactic lesions (a technique involving the infliction of precise, irreversible lesions to the brain), both treatments were originally believed to function by inhibiting the activity of local neurons.[247] However, while scientific evidence supports that DBS inhibits neuronal activity in some cases,[249,250] DBS has also been demonstrated to elicit an excitatory effect in neuronal elements at certain conditions.[251,252] Indeed, the effect of DBS has been shown to be largely dependent on the stimulation parameters under use, on the region of the brain stimulated, as well as on the disease under treatment.[244,246,247] In view of this, a general conclusion regarding the mechanisms of action of DBS cannot be easily obtained solely based on experimental findings garnered at different conditions.

Various studies, involving application of electrophysiological, imaging, biochemical, and molecular methods, have been previously undertaken by researchers with aims of gathering further insights into the mechanisms of action of DBS.[244] However, the currently presented study focuses solely on the elucidation of DBS mechanisms from a biochemical and molecular perspective. The majority of studies related to metabolic changes in the brain due to DBS have targeted neurotransmitter systems. Dopamine, for instance, is an important signaling compound involved in the modulation of body movements and of neuronal firing within the globus pallidus internus (GPi) and in the subthalmic nucleus (STN).[253] Several studies carried out in animals have demonstrated that STN DBS induces an increase in extracellular dopamine in the striatum of

normal rats, partially 6-hydroxydopamine (6-OHDA) lesioned rats (rat model of Parkinsonism), and in Parkinsonian rhesus monkeys.[254–257] However, other reports establish that no statistical changes were observed in the striatal dopamine of rats after stimulation. Similarly, studies employing positron emission tomography (PET) in human Parkinson's disease (PD) patients did not show evidence of increases in dopamine levels after DBS.[258,259] Although most results obtained by employment of PET are limited by this technique's poor sensitivity towards measurements of small concentration changes, the controversial results obtained in the abovementioned study support the importance of further validating findings obtained in animal models through human studies. Other neurotransmitters that have been previous subjects of study with aims of unravelling DBS mechanisms include gamma-aminobutyric acid (GABA), glutamate, and serotonin. For instance, levels of GABA, a key neurotransmitter in different control mechanisms due to its inhibitory role in neuronal excitability, have been shown to increase in the basal ganglia (BG) region after application of STN and GPi DBS.[260,261] Likewise, increases in GABA concentrations were detected in cerebrospinal fluid of PD patients after 6 months of DBS treatment.[262] For glutamate, increases in the levels of this neurotransmitter after DBS have been observed in several animal experiments. Windel et al., for instance, reported a rise in extracellular glutamate in the STN, GPi, and substantia nigra pars reticulate (SNpr) of normal rodents after STN DBS.[263] Furthermore, enhancements in glutamate levels, detected using *in vivo* microdialysis, were observed to occur in the nucleus accumbens and in the dorsal raphe after electrical stimulation of the ventromedial prefrontal cortex (vmPFC) of normal rats.[264,265] Interestingly, no significant changes in glutamate levels were observed in human PD patients following STN DBS treatment; however, for the same group of patients, an increase in cyclic guanosine monophosphate (cGMP), a secondary messenger of glutamate, was noted to occur, indicating DBS had an effect in the

modulation of the glutamatergic pathway.[266] Changes in serotonin levels may also vary according to the stimulation conditions selected for DBS. For instance, a decrease in extracellular serotonin has been found to occur after application of STN DBS in animal studies. Considering that STN DBS is used for the treatment of PD, this finding may correlate to depression and suicidal tendencies in PD patients undergoing DBS.[267,268] On the other hand, stimulation of the vmPFC and lateral habenula (LHb) regions has been shown to exert a modulatory effect in the serotonergic system, resulting in increases in hippocampal and striatal serotonin levels, respectively.[269,270] In fact, an increase in serotonin levels has been found in the blood and hippocampus of chronic unpredictable mild stress model (CUMS) animals following chronic LHb DBS treatment.[271] Based on these and other findings, the antidepressant effect of DBS has been suggested to be linked to serotonin projections to areas such as the hippocampus and the prefrontal cortex, both areas known to be affected by depression disorders. [272] Save for reported measurements of metabolic changes in adenosine and noradrenaline, few other metabolites have been targeted in studies involving DBS.[265,273] This certainly opens up a range of possibilities for the investigation of DBS mechanisms using untargeted metabolomics platforms.

In terms of methodologies available to measure the aforementioned metabolites, microdialysis (MD) and electrochemical techniques are perhaps the mostly used approaches, owing to their suitability for *in vivo* analysis. As was already emphasized in Section 1.1.2., MD is a sampling approach widely accepted in the neuroscientific community, as it allows for analysis of free small molecules (*e.g.* neurotransmitters) present in extracellular brain fluid. Selective determination of a number of target metabolites is made possible through analysis of the collected "extract" or dialysate in appropriate instrumentation. Some limitations of MD include the high content of inorganic salts present in the dialysate, which can hinder the use of mass spectrometry; the low

concentration of metabolites collected in the dialysates; and the difficulties associated with the analysis of less polar and larger compounds, which are known to sometimes adhere to the MD membrane. Electrochemical methods, in turn, rely on the measurement of currents or potentials, which are generated as a result of charge-transfer processes that occur at the surface of an electrode. Considering the high ionic strength of biological media, and the fact that several brain metabolites such as neurotransmitters are electrochemically detectable, electrochemical methods are well suited for analytical measurements of different metabolites present in the central nervous system. The main advantages of electrochemical methods lie in their ability to provide high temporal and spatial resolution, as such approaches allow for the monitoring of rapid changes in metabolite concentrations, while the size of their electrodes can be up to twenty times smaller than typical microdialysis probes. However, electrochemical-based techniques are limited by their low selectivity, as well as their inherent inaptitude towards determination of non-electroactive species.[274] For that reason, analytical methods that involve application of MD coupled to liquid chromatography used in combination with various detector types have gained broad acceptability within the scientific community.

Application of solid phase microextraction (SPME) offers a valuable opportunity toward further elucidation of metabolic changes resulting from DBS treatments. As previously discussed, SPME is a useful sample preparation tool with demonstrated suitability for investigations of different biological systems, including *in vivo* measurement of metabolic changes in rat brains.[56] The small size of the sampling probes and the availability of biocompatible SPME coatings make of this technology an attractive approach for *in vivo* determinations. Taking advantage of such features, in this section, we present results corresponding to the application of SPME for monitoring of *in vivo* metabolic changes occurring in the hippocampus of rat brains after application of DBS in

their prefrontal cortex. As already emphasized, the hippocampus and the prefrontal cortex are critical brain regions known to be affected by depression.[275] The results of this work aim to shed light on the mechanisms behind DBS, particularly in cases where the vmPFC region is stimulated to produce anti-depression-like effects.

6.2. Experimental procedure

6.2.1. Materials

4 mm C18 and MM fibers (45 µm thickness) were provided by Supelco (Bellefonte, PA, USA). All fibers were pre-conditioned in 1:1 methanol:water for at least 30 min prior to extraction. After conditioning, SPME fibers were rinsed with nanopure water so as to remove any organic solvent excess remaining on the coating surface. For *in vivo* extractions, each SPME probe was assembled in the sampling holder, as shown in Figure 6.1. These holders facilitated the introduction and precise positioning of the SPME fibres into the brain of freely moving rats.
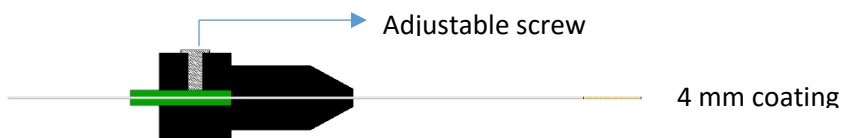
Figure 6.1. Sampling holder designed for *in vivo* brain sampling of rats.

6.2.2. SPME sampling procedure and analysis
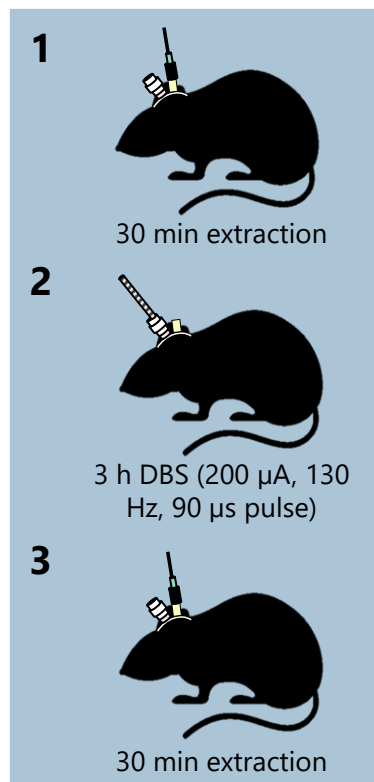
Figure 6.2. General schematic of the sampling procedure.

Four-month-old male Fischer rats were used as subjects to investigate metabolic changes resulting from DBS. Prior to the experiment, electrodes used to deliver electrical pulses in the pre-frontal cortex region of the brain and cannulas used to guide the sampling devices directly to the hippocampus were surgically implanted in each animal. All animal experiments were conducted in the Centre for Addiction and Mental Health (Toronto, ON) under ethical approval. Two groups of animals were considered for the study: a treatment group, sampled before treatment (baseline (BL)) and after DBS (n=17); and a control group (n= 13), which did not undergo DBS therapy, but nonetheless received the surgical implantation of the electrodes. The sampling procedure was carried out as shown in Figure 6.2. First, SPME probes mounted on the previously described sampling holders were exposed to rat brain for 30 min (C18 fibres were deployed first, with subsequent deployment of MM fibres). Following sampling, which included sampling periods of

30 minutes for each extraction phase, all animals in the treatment group were then submitted to 3 hours of DBS (200 µA, 130 Hz, 90 µs pulses). Once the DBS treatment was completed, new SPME probes were exposed to each animal's brain for the same period of time (30 minutes per fiber). As SPME allows for non-lethal extraction, the sampling procedure was repeated in the same animals two weeks after the first sampling. During the two-week period in between the two samplings, animals were subjected to DBS therapy every day for 8 hours (chronic DBS). However, for the purpose of this thesis, only the metabolic changes occurring as a result of acute DBS exposure (3 hours) are presented and discussed. Subsequent to the completion of the extraction process, all probes were cleaned with Kimwipes, quickly rinsed with LC-MS grade water, and stored at -80 °C for further analysis. Employed mixed mode fibres were desorbed in 300 µL of 1:1 water:acetonitrile, whereas C18 probes were first desorbed in 100 µL of methanol, with the obtained solution then further diluted with 100 µL of water to ensure good chromatographic retention.

6.2.3. LC- mass spectrometry (MS) analysis

All brain extracts were run using a pentafluorophenyl (PFP) column at the same instrumental conditions described in Section 5.2.5. For metabolite identity confirmation, MS/MS analysis was conducted using an Q-Exactive Quadrupole-Orbitrap Mass Spectrometer (ThermoFisher Scientific, Waltham, MA) coupled to a Dionex UltiMate 3000 UPLC System (Dionex Corporation, Bannockburn, IL), and equipped with a heated electrospray (H-ESI) source. The MS system was operated under parallel reaction monitoring (PRM) conditions using an inclusion list. Other MS conditions were set as follows: MS resolution = 35000, automatic gain control (AGC) target = 2e5, and normalized collision energies (NCE) = 20 and 40. MS/MS spectra were compared against

standard fragmentation patterns obtained at the same conditions (when available) and against the METLIN MS/MS database.

6.2.4. Data analysis

The same data processing parameters described in Section 5.2.6 were applied to analyse the data obtained from experiments discussed in this current section. Statistical analysis was carried out by employing the non-parametric Mann-Witney test (univariate analysis), with false discovery rate (FDR) correction applied (q-values) to the obtained data. Features with p-value ≤ 0.01, q-value ≤ 0.05, and a fold change ≥ 1.5 were considered significant. Identification of statistically significant features was undertaken by comparing their accurate masses with METLIN and HMDB databases, and by running available standards and comparing their MS/MS spectra.

6.3. Results and discussion

Aiming to gather a better understanding of the chemistry behind the effect of DBS on the hippocampus in response to vmPFC stimulation, an *in vivo* MS-metabolomics study in rodents (Fischer rats) was conducted, with SPME employed as a sampling tool. Scientific evidence has been presented by several researchers regarding the clinical benefits associated with application of electrical stimulation in specific brain areas of patients diagnosed with major depressive disorder.[276–279] Brain regions targeted to treat depression disorders via electrical stimulation include the subcallosal cingulate, the nucleus accumbens, the ventral capsule/ventral striatum, the medial forebrain bundle, the inferior thalamic penducle, and the lateral habenula.[280–284] Given the limitations associated with human studies, animal models represent a viable alternative to investigate the mechanisms underlying therapies such as DBS. In this work, DBS electrodes were surgically implanted in the ventromedial prefrontal cortex (vmPFC) of rodents, as this area has been found to be homologous with the Broadman area 25 of the cingulate region in humans.[275]

179

Monitoring of metabolic changes induced by vmPFC DBS in the hippocampus of animals was enabled through surgical implantation of microdialysis cannulas that allowed for precise sampling positioning. It is worth highlighting that the hippocampus is a complex brain structure strongly correlated to mood disorders and depressive episodes.[272] Previous rodents studies have demonstrated that vmPFC DBS can produce a positive behavioral effect, as observed in forced swim tests, as well as through an increase in serotonin levels in the hippocampus.[269,275] In view of this, further investigations of metabolic changes occurring in the hippocampal region in response to electrical stimulation of the vmPFC were seen as a valuable line of inquiry that may lead to a better understanding of the biochemical effect of DBS on patients diagnosed with major depressive disorders. The sampling probes employed in this study were composed of nitinol wires with a 4 mm coating on their tips. The length of the coating enabled the monitoring of changes in a defined brain region, providing a certain degree of spatial resolution. As described in Section 6.2.2, two coating chemistries were used for these experiments (immobilized C18 particles with a benzene sulfonic functionality (mixed mode), and C18 particles), with two types of solvents selected for desorption of probes. As presented in Chapter 5, employment of different SPME extraction sorbents and different desorption solutions can facilitate broad metabolite coverage, a highly desired outcome in this particular case.

As one of the main advantages of using SPME is that it allows for non-lethal sampling, all animals employed in investigations were submitted to sampling at different time points: rats submitted to treatment were monitored before and after each vmPFC DBS treatment (2 sampling sessions in total), for a total of 4 distinct samplings per specimen. Similarly, control groups were sampled once in each sampling session for comparison of profiles and elucidation into metabolic changes resulting from DBS. Brain metabolic profiles collected from all animals, before vmPFC DBS and

after 3 hours of treatment, were compared for statistically significant differences between data sets. The list of metabolic features retrieved by XCMS online was filtered so that only features exhibiting less than 20% relative standard deviation in the pooled QC were retained. Considering that approximately 70% of those filtered features (for each coating type and for each ionization mode) did not meet the assumption of normality once the Shapiro-Wilk test (data not shown) was employed on the data, a non-parametric test (Mann-Witney) was used for univariate analysis. For brain extracts obtained with mixed mode coatings, 105 and 93 features in positive and negative modes, respectively, were found, using a threshold value of p-value < 0.01 and fold changes >1.5. In the case of C18, 255 features in positive mode and 295 features in negative mode were found to meet the same threshold. Although the number of dysregulated features seems to be small, it is worth noting that SPME is a non-exhaustive extraction technique, and the advantages of its easy applicability for *in vivo* studies comes along with a compromise in terms of sensitivity. Following feature detection, some of the dysregulated features associated with metabolic changes occurring after DBS were then characterized. Table 6.1 presents a list of these characterized features and their corresponding identities.

The first finding worth of discussion is the upregulation of citrulline. As shown in Table 6.1 and in Figure 6.3, a substantial increase in the hippocampal citrulline level (↑5 fold change, p-value<0.0001, q-value<0.0001) was observed after DBS. Citrulline is a known co-product of the enzymatic generation of nitric oxide (NO), a reaction that is catalyzed by nitric oxide synthase (NOS), where arginine is the only substrate of all NOS isoforms. NO is a key signaling molecule involved in multiple cellular functions, including neurotransmission, blood pressure regulation, and immune response.[285] In the central nervous system (CNS), this gaseous compound has been

Table 6.1. Dysregulated metabolites tentatively characterized by MS/MS and employment of authentic standards (when available).

Compound	Time (min)	m/z	Δ ppm	BL vs DBS			Control vs DBS			Other adducts	Isotopes	Standard
				Fold	p-value	q-value	Fold	p-value	q-value			
Aldohexose carbohydrate C6H12O6	1.2	179.0555 [M-H]-	3	↑3.1	1.1E-05	9.2E-04	↑3.4	2.0E-05	1.4E-03			Yes
Taurine	1.3	126.0220 [M+H]+	1	↑9.0	3.0E-13	5.0E-10	↑7.6	1.9E-10	4.8E-07	[M+Na]+ [M-H]-		Yes
Citrulline	1.4	176.1029 [M+H]+	0	↑4.6	3.3E-09	3.0E-05	↑6.2	2.3E-11	2.1E-07	[M-H]-		Yes
Histidine	1.8	156.0768 [M+H]+	0	↑2.1	3.9E-06	5.8E-03	↑2.0	3.5E-6	2.5E-03			Yes
Proline	1.5	116.0708 [M+H]+	1	↑1.9	6.2E-06	7.0E-03	↑2.1	6.4E-7	9.2E-04	[M-H]-		Yes
Phenylalanine	8.6	166.0863 [M+H]+	0	↑1.7	1.2E-05	9.2E-03	↑1.9	3.0E-05	1.4E-02	[M-H]-		Yes
Lysine	1.9	147.1128 [M+H]+	0	↑1.5	1.7E-05	1.0E-02	↑1.5	5.4E-04	<u>1.4E-01</u>			Yes
Asparagine	1.3	133.0609 [M+H]+	0	↑1.7	3.0E-05	1.3E-02	↑2.0	3.5E-06	2.5E-03			Yes
Leucine	4.8	132.1020 [M+H]+	0	↑1.9	3.0E-05	1.5E-02	↑2.4	6.4E-07	1.0E-03			Yes
Isoleucine	5.5	132.1020 [M+H]+	0	↑1.9	9.0E-05	3.0E-02	↑2.1	5.7E-06	3.0E-03	[M-H]-		Yes
Uric acid	1.6	169.0357 [M+H]+	0	↑2.6	4.0E-05	1.5E-02	↑3.1	3.0E-05	1.4E-02	[M-H]-		Yes
Methionine	2.7	150.0583 [M+H]+	0	↑1.7	4.9E-05	1.7E-02	↑1.9	6.0E-05	2.2E-02			Yes
Methionine sulfoxide	1.4	166.0532 [M+H]+	0	↑1.8	1.0E-04	3.1E-02	↑2.0	5.7E-06	3.4E-03			No
Choline	4.4	104.1072 [M+H]+	2	↑1.7	1.2E-04	7.2E-03	↑1.9	3.1E-04	2.7E-02			Yes
Serine	1.3	106.0501 [M+H]+	2	↑1.8	1.4E-04	4.0E-02	↑1.8	8.4E-06	4.8E-03			Yes
Threonine	1.4	120.0656 [M+H]+	1	↑1.8	1.4E-04	4.0E-02	↑2.2	3.9E-06	2.7E-03	[M-H]-		Yes
Glutamate	1.4	148.0604 [M+H]+	0	↑1.7	2.2E-04	5.5E-02	↑1.9	4.0E-05	1.7E-02			Yes

Carnitine	4.8	162.1125 [M+H]+	0	↑1.8	3.1E-04	1.6E-02	↑1.6	4.4E-03	<u>1.8E-01</u>			Yes
Cyclopentone prostanglandin or Cyclopentone isoprostane C20H30O4	15.1	333.2075 [M-H]-	1	↑2.9	8.4E-05	2.0E-03	↑2.6	5.2E-04	1.5E-02	[M-H-H20]-		No
Very likely an oxidation product of docosahexaenoic acid C22H32O3	16.2	343.2283 [M-H]-	1	↑10.6	8.3E-08	8.3E-06	↑10.7	1.3E-06	1.3E-04			No
LysoPE(18:2)	18.6	478.2928 [M+H]+	0	↑1.8	1.5E-04	8.8E-03	↑2.1	8.0E-05	8.5E-03	[M-H]-	[M]+ [M+1]+ [M]- [M+1]-	No
SM C39H81N2O7P	23.2	721.5852 [M+H]+	No hits	↑7.4	3.0E-09	1.7E-06	↑8.4	1.2E-08	1.4E-05		[M]+ [M+1]+	No
GluCer or GalCer (d18:1/16:0)	23.8	700.5726 [M+H]+	0	↑4.5	1.4E-04	8.2E-03	↑5.1	3.5E-05	4.3E-03	[M-H]- [M+H-H20]	[M]+ [M+1]+ [M]- [M+1]-	No
GluCer or GalCer (d18:0/16:0)	24.0	702.5878 [M+H]+	0	↑8.7	2.3E-06	2.5E-04	↑8.8	1.6E-06	3.1E-04			No (only hit)
SM(d18:0/16:0)	24.4	705.5910 [M+H]+	0	↑5.8	4.7E-08	1.4E-05	↑5.9	8.6E-08	4.3E-05		[M]+ [M+1]+ [M+2]+	No (only hit)
SM C41H81N2O6P	24.4	729.5902 [M+H]+	0	↓2.0	7.1E-05	4.5E-03	↓2.4	2.5E-04	2.3E-02		[M]+ [M+1]+	No
PE (22:6/16:0)	25.3	764.5223 [M+H]+	0	↓3.0	2.1E-05	1.6E-03	↓3.0	1.3E-04	1.3E-02	[M-H]-	[M]+ [M+1]+ [M+2]+ [M]- [M+1]- [M+2]-	No
PE (22:6/18:1)	25.5	790.5381 [M+H]+	0	↓6.0	1.3E-07	2.6E-05	↓6.2	2.2E-08	1.9E-05	[M-H]-	[M]+ [M+1]+ [M]- [M+1]-	No

PE (20:4/16:0)	25.5	740.5223 [M+H]+	0	↓2.2	3.2E-07	4.5E-05	↓2.2	2.6E-06	4.7E-04	[M-H]-	[M]+ [M+1]+ [M]- [M+1]-	No
PE (P-16:0/22:6)	25.7	748.5275 [M+H]+	0	↓2.4	2.7E-05	2.0E-03	↓2.2	9.7E-04	5.8E-02	[M-H]-	[M]+ [M+1]+ [M+2]+ [M+3]+ [M]- [M+1]- [M+2]- [M+3]-	No
PE(O-16:0/18:2)	25.9	700.5276 [M+H]+	0	↑4.8	2.8E-06	2.8E-04	↑4.7	1.1E-05	1.6E-03	[M-H]-	[M]+ [M+1]+ [M]- [M+1]-	No
PE (22:6/18:0)	26.2	792.5536 [M+H]+	0	↓2.6	1.8E-04	1.0E-02	↓2.5	4.9E-04	3.8E-02	[M-H]-	[M]+ [M+1]+ [M+2]+ [M+3]+ [M]- [M+1]-	No
PC (38:6)	26.5	806.5694 [M+H]+	0	↓2.1	1.2E-07	2.4E-05	↓2.0	1.5E-05	2.2E-03		[M]+ [M+1]+ [M+2]+	No
PC (32:1)	26.7	732.5535 [M+H]+	0	↓1.8	6.8E-06	6.2E-04	↓1.8	2.9E-03	1.3E-01		[M]+ [M+1]+	No
PC (40:7)	26.8	832.5848 [M+H]+	0	↓2.6	1.5E-06	1.7E-04	↓2.4	2.9E-04	2.5E-02		[M]+ [M+1]+	No
PC (38:5)	27.2	808.5850 [M+H]+	0	↓2.5	2.2E-07	3.5E-05	↓2.2	1.4E-03	7.7E-02		[M]+ [M+1]+	No
PC C42H82NO7P	29.5	744.5901 [M+H]+	0	↑9.2	2.0E-08	7.3E-06	↑9.3	5.4E-08	3.3E-05			No

Lysophosphatidylethanolamine (LysoPE), cerebroside (glucosylceramide (GluCer) or galactosylceramide (GalCer)), sphingomyelin (SM), phosphatidylethanolamine (PE) and phosphocholine (PC).
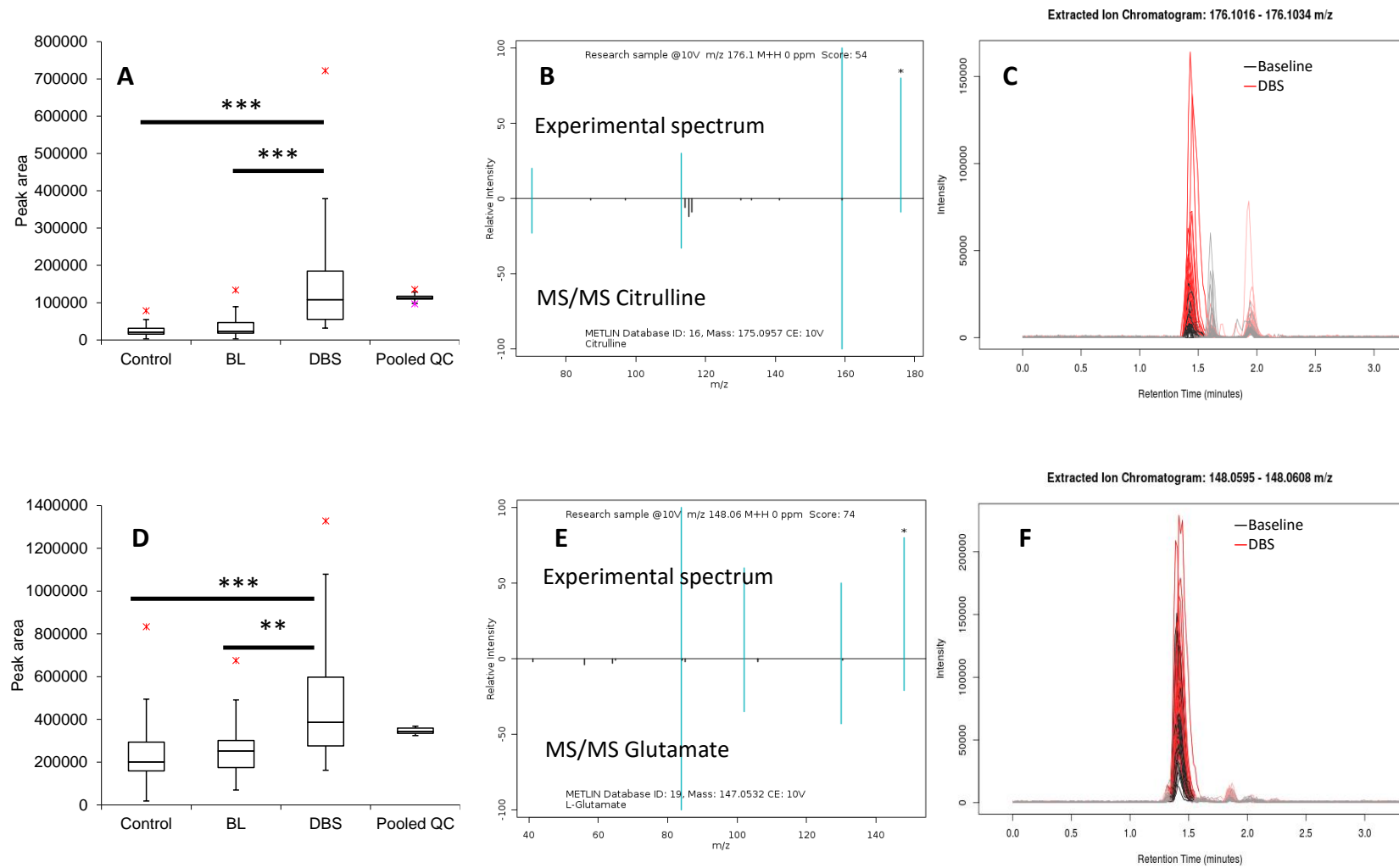
Figure 6.3. Box plots, MS/MS spectra obtained at 20 NCE, and overlaid extracted ion chromatograms corresponding to citrulline (A, B and C) and glutamate (D, E and F). *** p-value<0.0001, ** p-value<0.001, * p-value<0.01.

associated with cognitive and physiological functions such as memory, sleep, feeding behaviour, pain reception, thermoregulation, and microcirculation, among others.[286] The synthesis of NO in specific brain regions is definitely dependent on several factors, including the availability of arginine and NOS. In addition, the activation of N-methyl-D-aspartate (NMDA) receptors by glutamate has been shown to function as a signal for the synthesis of NO.[287] Taking into account that increases in glutamate levels in response to vmPFC DBS have already been reported ,[264,265] and that in this study, a rise in glutamate was also observed (↑1.7 fold change, p-value<0.001, q-value<0.05) (Figure 6.3), NO upregulation can be then be presumed to be one of the effects exerted by vmPFC DBS when the technique is applied at the specified conditions. Interestingly, in recent work published by Chakravarty et al., statistical increases of the hippocampal and thalamic volumes, as well as in the diameter of blood vessels in the hippocampus were observed after vmPFC DBS.[288] This finding also supports our hypothesis, considering that NO has an important role in the neuronal control of brain blood flow, where it induces a vasodilating effect by either activating the production of cGMP, or by inhibiting the synthesis of 20-hydroxyeicosatetraenoic acid (20-HETE), a known vasoconstrictor.[289] However, further studies are required to confirm this correlation. Another compound that has been found to be upregulated by activation of glutamate receptors is taurine.[290] In this work, taurine levels were found to be remarkably higher in post-DBS extracts in comparison to BL measurements (↑9 fold change, p-value < 0.0001, q-value<0.0001) (Figure 6.4). This ubiquitous sulphur-containing amino acid has been found to exert a neuroprotective role in cases of excessive release of excitatory amino acids such as glutamate, known as the major excitatory neurotransmitter.[291,292] Indeed, overstimulation of excitatory amino acid receptors can contribute to neuronal death, as is known to occur in cases of ischemia and in
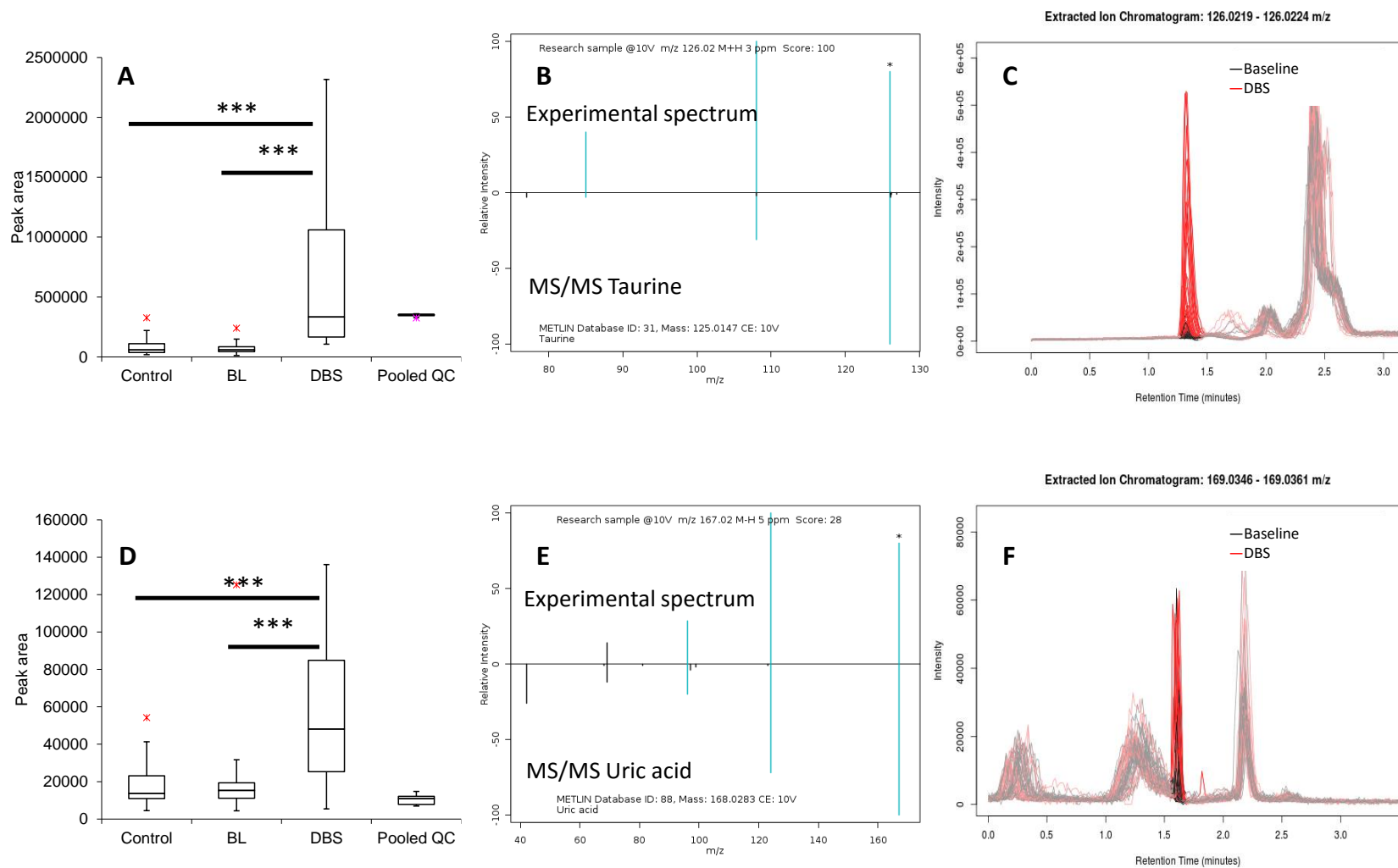
Figure 6.4. Box plots, MS/MS spectra obtained at 20 NCE, and overlaid extracted ion chromatograms corresponding to taurine (A, B and C) and uric acid (D, E and F). *** p-value<0.0001, ** p-value<0.001, * p-value<0.01.

some neurological diseases.[290] Considering that a rise in glutamate was observed after DBS, one could expect that such an increase could have contributed to an enhancement in hippocampal taurine levels. In addition, taurine release is also modulated by the NO cascade.[293] *In vitro* studies using slices from mouse hippocampus have demonstrated that an increase in taurine levels takes place after addition of NO donors to the medium.[294] Similarly, *in vivo* upregulation of extracellular taurine in rat striatum has been observed after administration of NO release-inducing substances.[295] Likewise, results supporting the NO modulatory role in taurine release were reported after taurine inhibition was observed in relation to the administration of the NO synthase inhibitor NG-nitro-L-arginine methyl ester.[293] Based on the currently presented findings, the upregulation of NO is postulated to also induce taurine release in the rat hippocampus as an excitotoxicity avoidance mechanism. To this end, it is worth noting that depending on its concentration, NO can be either neuroprotective or neurotoxic.[285] High concentrations of NO can lead to nitrosative stress, a condition caused by the inability of a given system to eliminate reactive nitrogen species.[285] At excitotoxic conditions, and at a low arginine concentration, enzymatic production of superoxide radicals can occur via NOS.[296,297] Superoxide radicals are oxidative species that can react with NO to produce peroxynitrite $ONOO^-$, a highly toxic oxidative anion that can induce DNA damage and lipid oxidation.[298] Although our results indicate that at the specified experimental conditions, vmPFC DBS can induce NO upregulation, the reached concentration levels of NO resulting from DBS could not be established at this time. However, it is worth mentioning that uric acid, a potent antioxidant and free radical scavenger, is among the compounds found to undergo significant increases after DBS treatment (↑2.6 fold change, p-value<0.0001, q-value<0.05) in this study (Figure 6.4). Uric acid is generated from an enzymatic reaction undertaken by xanthine in the presence of xanthine oxidoreductase (XOR).[299] *In vitro* experiments with rat hippocampal neurons

have shown that this product of purine catabolism is able to suppress the accumulation of reactive oxygen species, preserve the mitochondrial function at conditions of cerebral ischemia, and attenuate free cellular calcium levels induced by glutamate exposure. In addition, administration of uric acid to adult rats prior to middle cerebral artery occlusion was shown to cause a remarkable reduction in ischemic damage to the cerebral cortex and striatum.[300] Based on this information, vmPFC DBS could be postulated to induce an oxidative environment in the brain that in turn elicits metabolic changes such as the release of uric acid, which at the specified conditions, plays a neuroprotective role against oxidative species. It should be noted that an increase in carnitine levels after DBS was also observed (↑1.8 fold change, p-value<0.001, q-value<0.05). Considering that carnitine has shown antioxidant properties as a scavenger of reactive oxygen species,[301] this finding may also support the hypothesis of DBS inducing an oxidative response in the brain.

Several amino acids are also present among the group of small metabolites that displayed statistical changes after electrical stimulation (Table 6.1). Among these amino acids is proline (↑1.9 fold change, p-value<0.0001, q-value<0.01), an amino acid that is synthesized from glutamate and ornithine, a compound resulting from the enzymatic cleavage of arginine to urea. Proline has been suggested to be capable of potentiating glutamate transmission, as at certain levels, this amino acid is known to activate NMDA and α-amino-3-hydroxy-5-methyl-4-isoxazole propionic acid (AMPA) receptors.[302] Additionally, proline can display excitotoxic properties at high concentrations; for instance, it is known to inhibit the uptake of glutamate by astrocytes, a neuroprotective mechanism activated by glutamatergic excitotoxicity.[303] Other amino acids upregulated after DBS include threonine (↑1.8 fold change, p-value < 0.001, q-value <0.05), an essential amino acid; serine (↑1.8 fold change, p-value < 0.001, q-value <0.05), involved in several metabolic pathways, including the synthesis of phospholipids and sphingolipids;[304] and histidine

(↑2.1 fold change, p-value < 0.0001, q-value <0.01), an amino acid essential in protein synthesis that is metabolized through three different pathways, including the synthesis of histamine. Methionine and methionine sulfoxide also exhibited an increase in their levels after DBS (methionine: ↑1.7 fold change, p-value < 0.0001, q-value <0.05; methionine sulfoxide: ↑1.8 fold change, p-value < 0.001, q-value <0.05). Interestingly, the presence of methionine residues in proteins has been reported to represent an important scavenging system against oxidative conditions. Under the presence of different oxidants, methionine is readily oxidized into methionine sulfoxide, which in turn is converted back into methionine by methionine sulfoxide reductase.[305] Although SPME is only able to extract from the free fractions of compounds present in a given system, an increase in methionine sulfoxide may also support our findings in regards to DBS favoring oxidative conditions in the brain environment.

Another finding of this work worthy of discussion corresponds to the upregulation of feature m/z 333.2075, which was detected in negative mode (↑2.9 fold change, p-value < 0.0001, q-value <0.01) (Table 6.1). Based on the MS/MS fragmentation pattern, this ion was tentatively identified to represent either a cyclopentone prostaglandin (prostaglandin (PG)A$_2$ or PGJ$_2$) or a cyclopentone isoprostane (IsoPs), more specifically 8-isoPGA$_2$ (Figure 6.5). In regards to PGA$_2$ and PGJ$_2$, very little evidence can be found in the literature regarding their endogenous production. Conversely, past research has evidenced the substantial presence of cyclopentone IsoPs in *in vivo*.[306,307] As the formation of cyclopentone IsoPs takes place due to the peroxidation of arachidonic acid in the presence of free radicals, the upregulation of such compound is in agreement with the already discussed results. However, further confirmation of the identity of this compound through certified standard identification is required for further clarifications regarding its possible role in metabolic changes associated with DBS.

In addition to enabling measurements of changes in concentrations of several small and/or polar compounds, SPME enabled the detection of variations in hydrophobic metabolites with m/z values
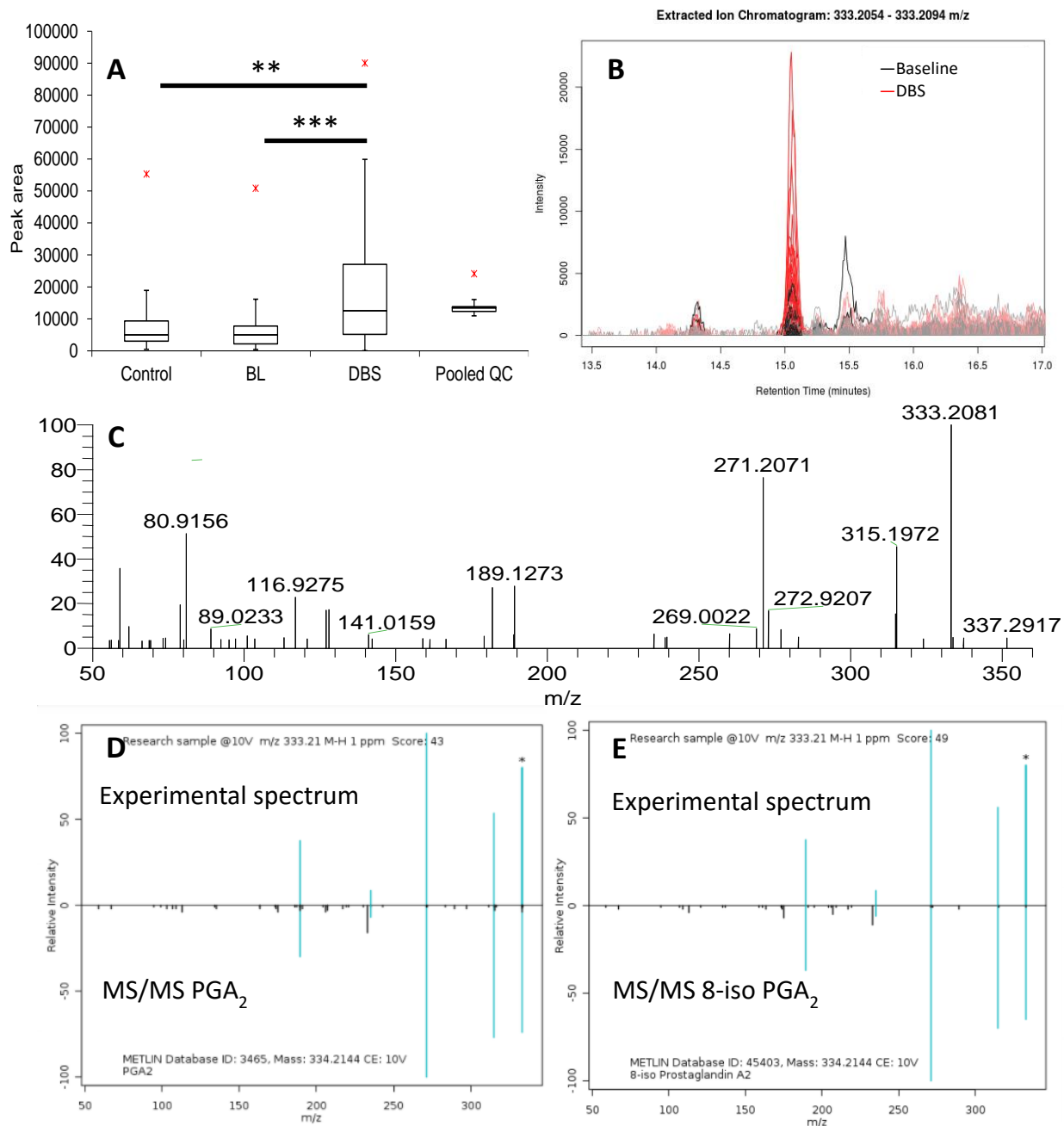

Figure 6.5. Box plots (A), overlaid extracted ion chromatograms (B), and MS/MS spectrum obtained at 20 NCE (C) for the feature m/z 333.2075. Comparison of experimental MS/MS spectrum with PGA$_2$ (D), and 8-iso PGA$_2$ (E) MS/MS spectra. *** p-value<0.0001, ** p-value<0.001, * p-value<0.01.

above 700. Figures 6.6 and 6.7 present cloud plots depicting features captured with C18 probes that exhibited statistically significant changes between baseline and post-DBS, and control versus treated groups (p-value<0.01 and fold changes>1.5). As can be seen, the several circles found in the 20 to 35 min region indicate significant variations occurred for non-polar compounds. MS/MS analysis of several of these features revealed them to correspond to different lipid classes (Table 6.1 and Figure 6.8). Among the lipids characterized are lysophosphatidylethanolamine (LysoPE), cerebroside (glucosylceramide (GluCer) or galactosylceramide (GalCer)), sphingomyelin (SM), phosphatidylethanolamine (PE), and phosphocholine (PC) species. Considering that MD is not well-suited to monitor large non-polar metabolites, our results confirm that one of the most remarkable advantages of the proposed SPME platform relies on its capacity for extraction of lipids *in vivo*. However, due to the small size of the probes and the non-exhaustive extraction capabilities of SPME, some of the statistically changing metabolites could not be easily analyzed via MS/MS due to low signal intensities (data not shown).

Regarding the correlation of the findings herein presented and the antidepressant-like effects associated with application of DBS in animals and also in humans, additional studies under more specific experimental conditions are required for further insights into DBS mechanisms in the treatment of depression. For instance, the upregulation of NO after DBS that is suggested by our work is contradictory to results reported by other studies, where different NOS inhibitors have been demonstrated to exert antidepressant-like effects in various animal models.[308] Interestingly, evidence showing correlations between increased NO levels and antidepressant-like effects has been reported as well in other works.[309,310] Regarding the role of glutamate, the modulation of the hippocampal glutamatergic system by administration of NMDA antagonists or by otherwise
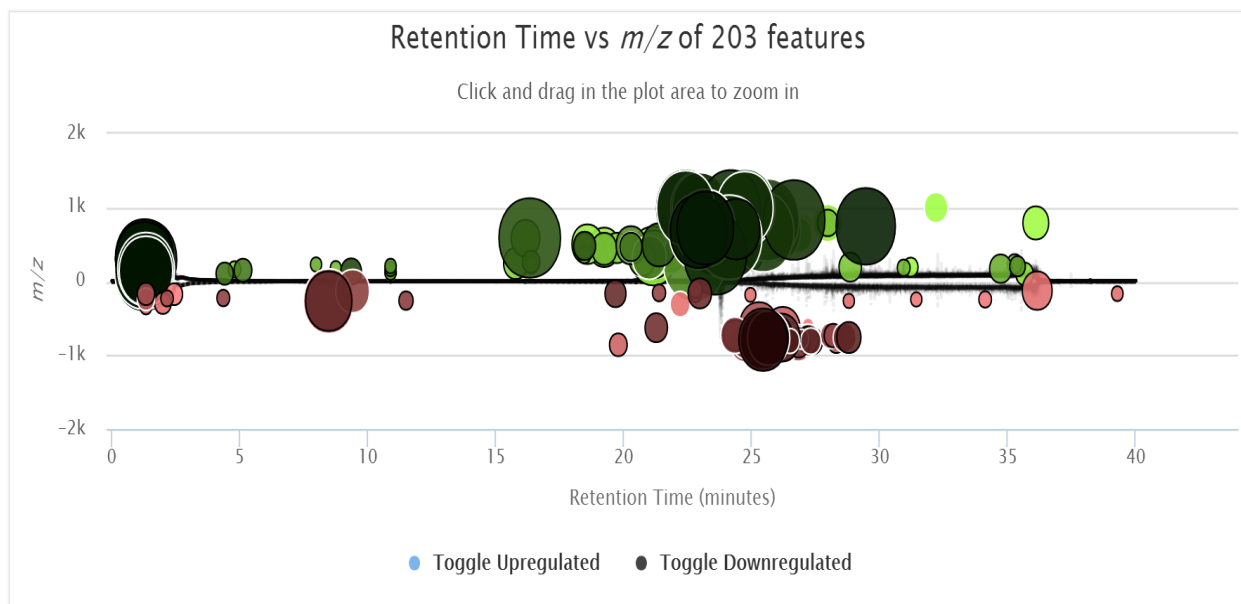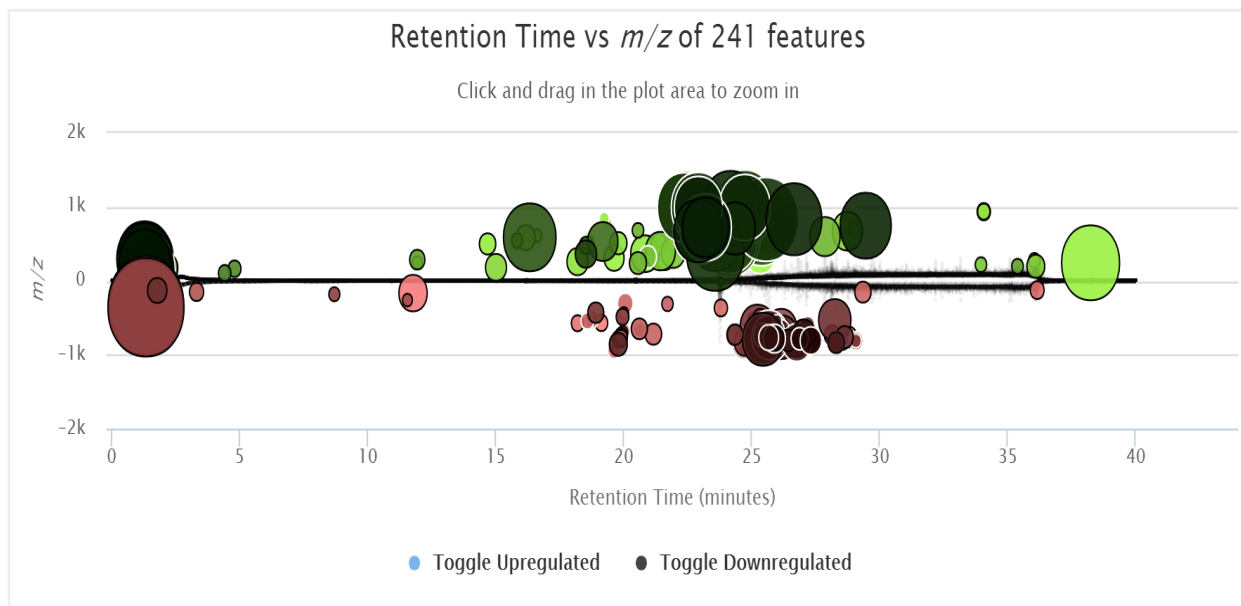
Figure 6.6. Metabolomic cloud plots representing upregulated (green) and downregulated (red) features (p-value<0.01, fold change>1.5) detected in positive mode using C18 fibres. Comparisons of baseline versus post-DBS extracts, and controls versus treated animals are shown above and below, respectively.

Figure 6.7. Metabolomic cloud plots representing upregulated (green) and downregulated (red) features (p-value<0.01, fold change>1.5) detected in negative mode using C18 fibres. Comparisons of baseline versus post-DBS extracts, and controls versus treated animals are shown above and below, respectively.
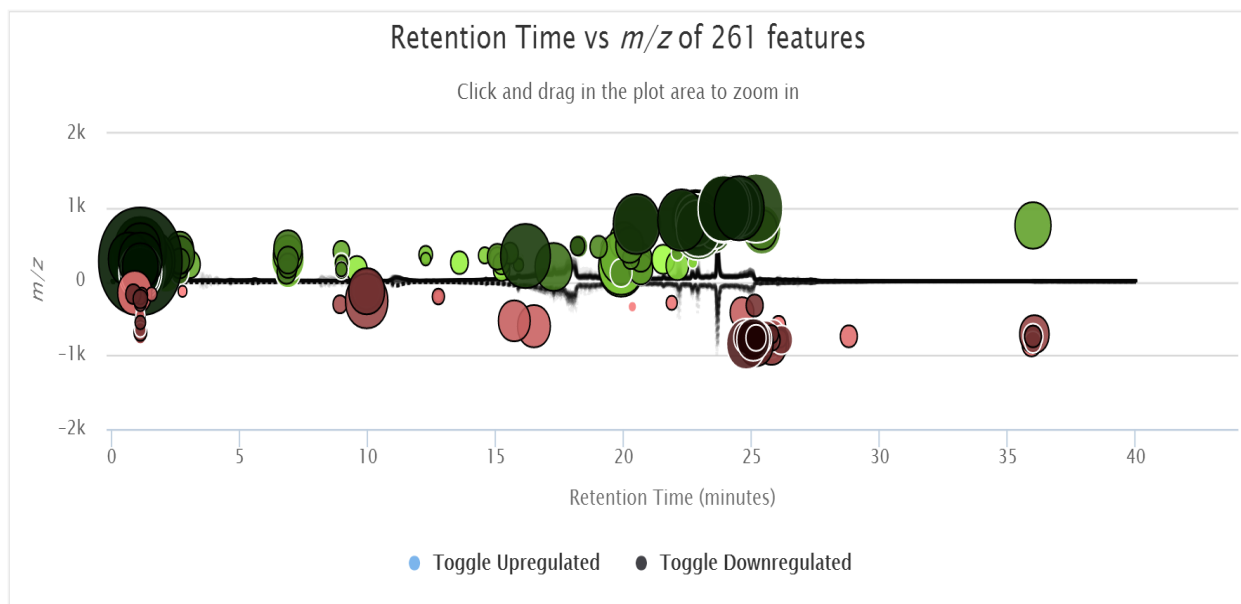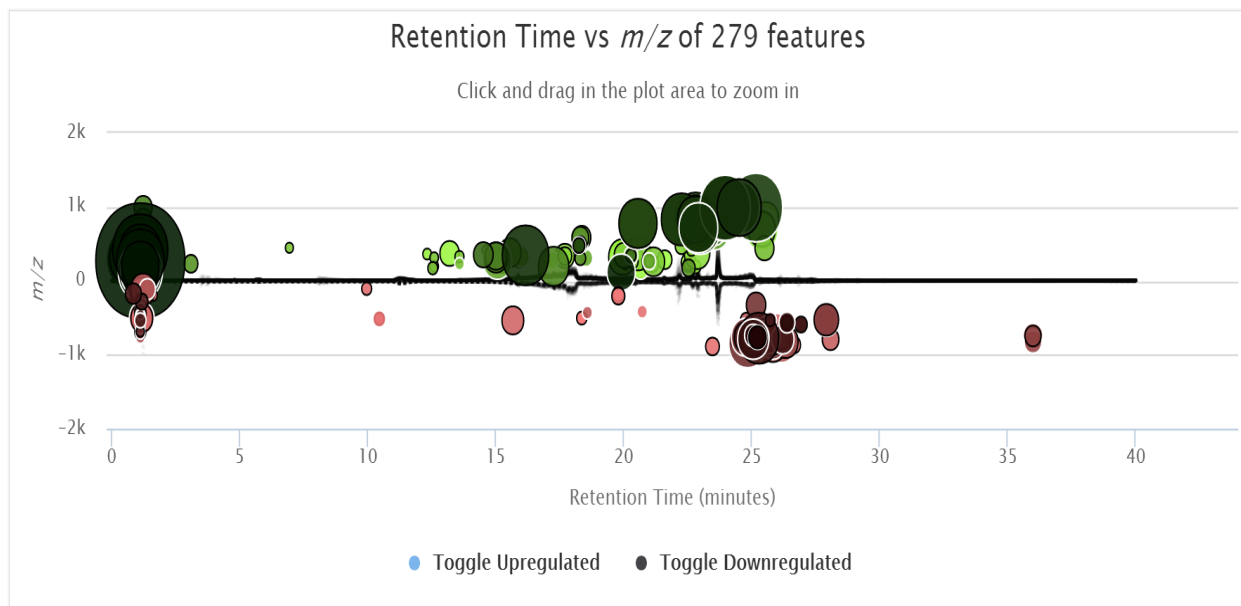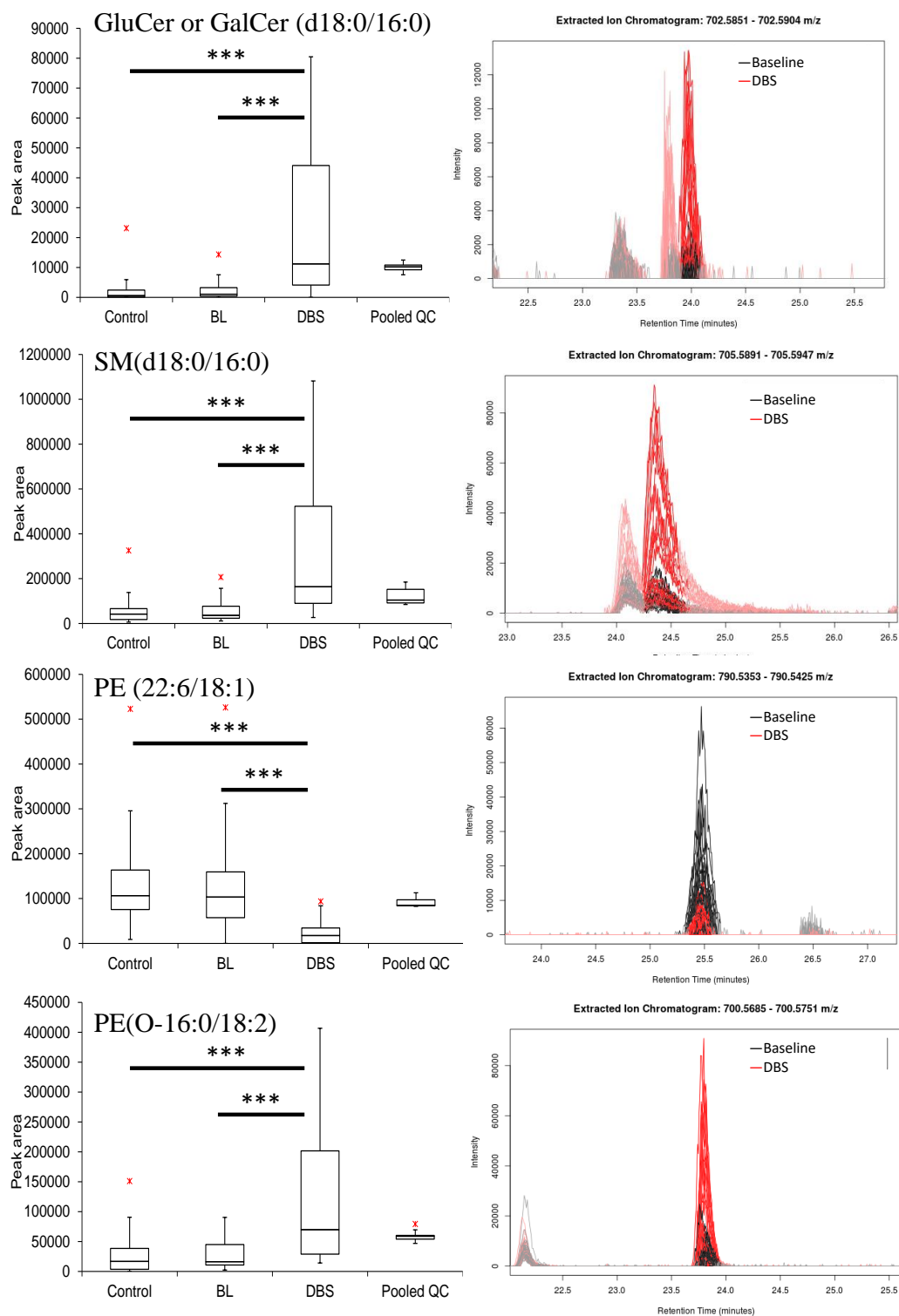
Figure 6.8. Boxplots and overlaid extracted ion chromatograms of representative lipids showing statistically significant differences when comparing before (BL) versus after DBS and control versus after DBS extracts *** p-value<0.0001, ** p-value<0.001, * p-value<0.01.

inducing a decrease in the local release of glutamate has been shown to induce positive antidepressant-like effects.[311] On the other hand, works conducted to assess DBS mechanisms to treat depression have reported increased glutamate levels in the nucleus accumbens and dorsal raphe after electrical stimulation of the VmPFC.[264,265] Based on the high complexity of the brain, multiple biochemical changes are expected to occur in response to DBS; however, future studies oriented towards the elucidation of the DBS antidepressant mechanism should be focused on targeting specific metabolic pathways, such as the urea cycle. In relation to taurine, supplementation of this amino acid to rats has been shown to elicit an antidepressant-like effect; for instance, its administration was shown to reduce immobility in forced swim tests, as well as play a role in the modification of various signaling cascades in the hippocampus.[312,313] Furthermore, past work has reported a remarkable reduction in hippocampal taurine levels of male rats displaying anxiety-like behaviours caused by maternal deprivation at 11 days of age.[314] To the best of our knowledge, no reports concerning DBS studies to treat depression provide information regarding changes in taurine levels before and after stimulation. However, a rise in extracellular levels of taurine was observed in Parkinsonian rats after stimulation of the STN.[315] Uric acid, another metabolite that exhibited significant changes after DBS in this study, has also been linked to mechanisms of mood regulation.[316] Interestingly, lower levels of uric acid have been found in serum samples of patients with major depression in comparison to healthy controls[317,318] As the currently reported work established that levels of uric acid were increased after electrical stimulation, further investigation of involved pathways may shed light onto the mechanisms activated by DBS in relation to its positive effect on depression symptoms. Finally, changes in the brain lipidome in relation to mood disorders have also been documented.[319,320] Indeed, recent research has demonstrated that the mechanism of action of antidepressant drugs such as

amitriptyline and fluoxetine is mediated by the acid sphingomyelinase-ceramide system.[321] In fact, high levels of ceramide in the hippocampus have been found to be correlated with low rates of neuronal proliferation, and with depression-like behaviours. On the other hand, a reduction of acid sphingomyelinase activity, associated with the intake of antidepressant drugs, has been shown to lead to a decrease in ceramide levels, allowing for behavioral improvements in depressed rodents. In addition to sphingolipids, polyunsaturated fatty acids, glycerolipids, and glycerophospholipids have also been found to play crucial roles in anxiety and depression behaviours.[320,322] In regards to the results obtained in this work, no well-defined trends could be established in relation to the specific classes corresponding to the dysregulated lipids uncovered in this study. However, among the characterized compounds that showed a remarkable increase after electrical stimulation, two different sphingomyelins were characterized; in light of the facts just discussed, further exploration of the role of this class of lipids in DBS mechanisms of action should be considered. Although additional experiments are required to validate the lipid variations observed with the use of *in vivo* SPME, efforts to explain DBS mechanisms should be also focused on monitoring lipidome alterations.

6.4. Conclusions

The featured work presented an *in vivo* untargeted metabolomics study oriented at an elucidation of the metabolic changes occurring in rat hippocampus after DBS of the vmPFC. Use of *in vivo* SPME allowed for the monitoring of significant variations, not only in small polar metabolites such as amino acids, but also in lipids belonging to different classes. The changes observed in citrulline and glutamate levels are possible indicators of alterations to the citrulline-NO cycle caused by electrical stimulation. Moreover, metabolites previously found to be involved in mechanisms trigged to counteract the presence of oxidative species in the brain such as taurine,

uric acid, and carnitine were shown to undergo significant increases after DBS. These findings, together with the demonstrated upregulation of some compounds previously associated with oxidative stress conditions, may provide new insights into metabolic modifications induced in the hippocampal region by vmPFC DBS. Lastly, statistical variations in several lipids belonging to sphingolipid and glycerophospholipid classes demonstrate that DBS also induces alterations in the brain lipidome. Despite the need for further studies to confirm the contribution of these biochemical changes to the overall DBS effect in the treatment of depression, our work provides new directions towards a better understanding of the mechanisms involved in electrical stimulation of the vmPFC.

Chapter 7: Summary and future directions

7.1. Summary

The analysis of complex biological matrices via liquid chromatography-mass spectrometry (LC-MS) is more often than not subjected to sample preparation workflows that are either time consuming, or prone to undesired ionization effects, often resulting in low throughput and/or poor analytical performance. In this regard, alternative sample preparation approaches such as solid-phase microextraction (SPME) offer new opportunities for expansion in the selection of tools currently available for bioanalytical determinations. Indeed, the large number of studies available in the literature to date evidence the usefulness of SPME for the quantitation of different target compounds in various matrices of bioanalytical interest. A summary of the main advantages of this technique in regards to its application for the analysis of diverse biological systems is presented in Figure 7.1. However, from a practical perspective, SPME is still far from being a broadly adopted tool in the clinical laboratory; in this sense, further acceptance and successful adaptation of unconventional methodologies such as microextraction-based techniques in clinical applications can be said to be directly related to the degree to which their principles and capabilities are understood. This thesis contributes to the progress and further implementation of SPME in the analysis of biological samples by presenting new insights into the performance of this microextraction technology towards the analysis of complex matrices, and by introducing novel SPME applications and developments. In chapters 2 and 3, the suitability of SPME coupled with LC-MS/MS is demonstrated for the concomitant quantitation of a broad range of substances in plasma, urine, and blood samples with the use of various doping compounds as model analytes.

Following relatively simple analytical workflows, satisfactory clean-up with minimum sample pre-treatment and rewarding figures of merit were obtained by employing biocompatible SPME
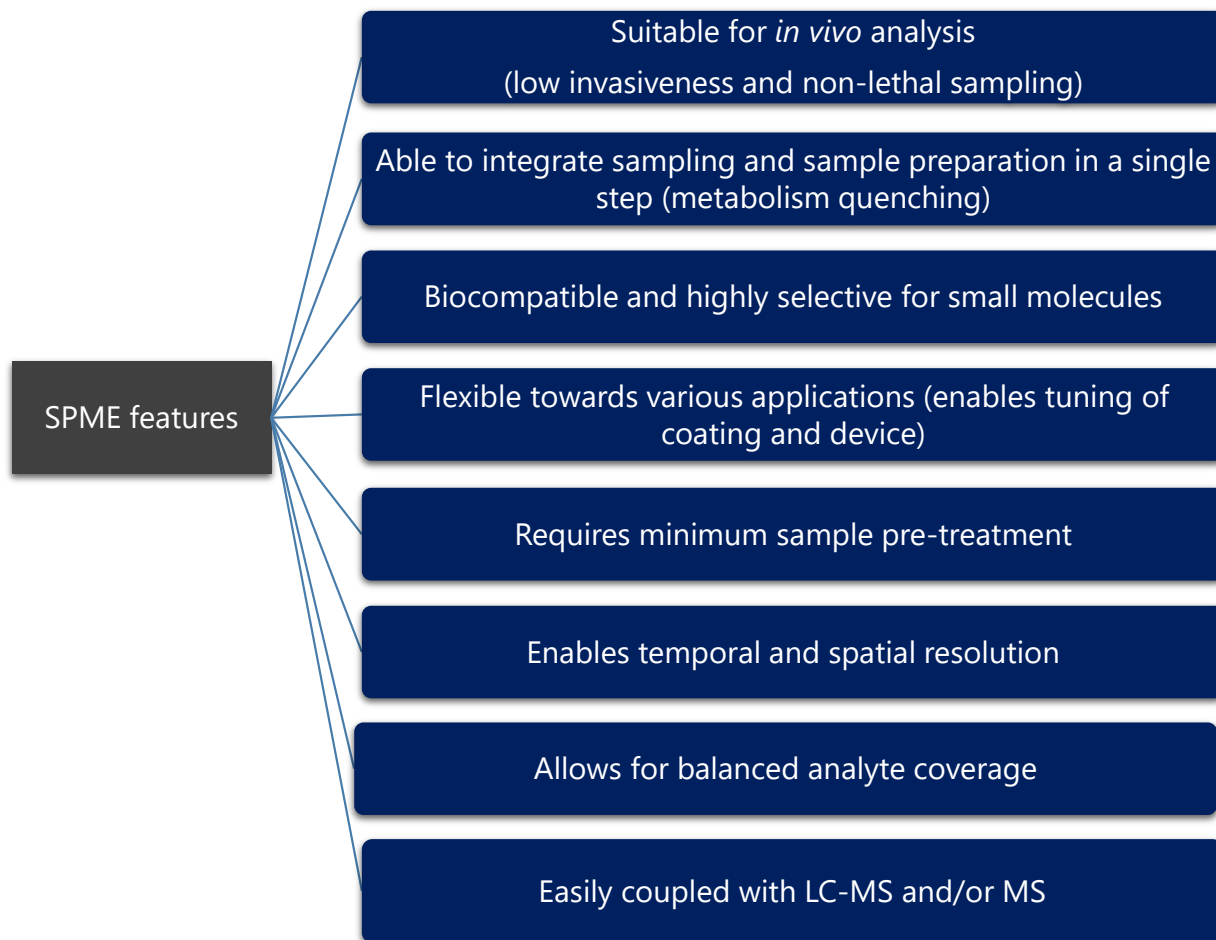

SPME features
Suitable for *in vivo* analysis (low invasiveness and non-lethal sampling)
Able to integrate sampling and sample preparation in a single step (metabolism quenching)
Biocompatible and highly selective for small molecules
Flexible towards various applications (enables tuning of coating and device)
Requires minimum sample pre-treatment
Enables temporal and spatial resolution
Allows for balanced analyte coverage
Easily coupled with LC-MS and/or MS

Figure 7.1. Summary of the advantages of SPME as a sample preparation technique in the investigation of biological samples and systems.

devices made of hydrophilic-lipophilic balanced (HLB) particles embedded in polyacrylonitrile (PAN). In Chapter 2, SPME was presented in a high throughput and fully automated configuration that enabled the easy determination of multiple doping substances in human plasma samples. In

addition, the developed approach was also shown to facilitate the multi-residue analysis of matrices with high protein content. Unlike SPE, the open-bed configuration of SPME is not vulnerable to clogging, and limitations related to breakthrough volumes are not a matter of concern due to the non-exhaustive extraction nature of SPME. Chapter 3, in turn, introduced an alternative material, polybutylene terephthalate (PBT), as a flexible, chemically stable, and cost-effective support for preparation of single-use and multi-purpose SPME devices compatible with complex matrices. Definitely, the adoption of new materials in the manufacturing of SPME devices opens up new opportunities for the introduction of this technique in novel applications. Considering that SPME is a non-exhaustive extraction technique where the uptake of analytes occurs via the free portion of analytes present in the matrix, the presence of variable matrix components able to display certain affinity for compounds of interest introduces a potential source of error that should be carefully evaluated. For this reason, Chapter 4 discussed the effect of variable red blood cell content, known as the hematocrit (Hct) of a blood sample, on SPME recovery of various analytes. The main findings of this investigation showed that while the effect of the Hct varies according to the characteristics of a given analyte, that effect is also dependent on the experimental conditions selected for extraction. Interestingly, the relative affinity of a given compound for the matrix components versus its affinity for the coating material proved to be one of the main factors governing the effect of different erythrocyte levels on SPME recoveries. Despite the demonstrated effect of Hct on the uptake of certain analytes, and the dependency of this phenomena on the selected parameters for sampling, correction of matrix variability was made feasible with the use of appropriate internal standards, thereby enabling correct quantification of analytes.

In addition to the applicability of SPME for targeted studies, the potential of this sample preparation technique for untargeted analysis has been demonstrated in several applications.

Indeed, the suitability of SPME for *in vivo* determinations is undoubtedly one of its most attractive features, particularly for metabolomics studies. Although typical analytical workflows followed in untargeted studies have shown outstanding robustness and satisfactory results in the identification of metabolites that are significantly altered due to a particular condition or disease, the complexity of biological sample matrices (*e.g.* tissue), and indeed, of the metabolome itself, both pose a remarkable challenge to the isolation of a truly representative snapshot of the metabolic status of a given system under investigation. In this regard, implementation of *in vivo* SPME can offer a complementary perspective to that offered by traditional approaches. As further acceptance of SPME towards metabolomics applications relies on a thorough assessment of its performance in different matrices, Chapter 5 presented remarkable results corresponding to the evaluation of three SPME extraction phases for untargeted analysis of brain tissue, taking into consideration a variety of parameters, such as extraction phase chemistry, desorption solvent, and extraction time. Among the coatings tested throughout this assessment, HLB was revealed to offer the best compromise in terms of metabolite coverage. Solvent optimization, in turn, revealed that selection of desorption solvent plays a major role in the composition of the final extract. Further, use of 10 % acetone in the washing step was shown to facilitate reproducible analysis of hydrophobic metabolites such as lipids in brain tissue. Aiming to demonstrate the potential of SPME for untargeted *in vivo* studies, the optimized procedure was then applied towards the monitoring of metabolic changes occurring in rat brain following deep brain stimulation (DBS) of the ventromedial prefrontal cortex (vmPFC). In these experiments, employment of 4 mm SPME probes mounted in a custom-made holder enabled direct measurements of metabolic variations occurring in the hippocampus of freely moving rats. As shown in Chapter 6, application of SPME coupled with LC-high resolution MS allowed for the capture of several classes of metabolites (*e.g.* amino acids and lipids) exhibiting

statistically significant changes after DBS treatment. To the best of our knowledge, this work represents the first untargeted study aimed at the elucidation of DBS mechanisms. Although further studies are needed to establish a correlation between the biochemical changes observed in this study and the anti-depressant mechanisms of DBS, this work provided new insights into the effect of vmPFC DBS on the brain hippocampus.

7.2. Future directions

Considering the satisfactory performance of different biocompatible SPME devices for analysis of complex biological systems, further application of these techniques in novel studies of clinical and bioanalytical interest is certainly anticipated. Undoubtedly, a key determinant factor in the implementation of SPME is the availability of cost-effective coating chemistries suitable for different analytical purposes. For instance, the rewarding results exhibited by HLB-PAN coated devices in the determination of a broad range of compounds demand the commercial availability of such SPME extraction phases. The availability of materials capable of offering selectivity for targeted analysis, improved affinity for polar compounds, and high reproducibility, all while ensuring biocompatibility, will also aid in the further implementation of SPME in the analysis of biological systems. In addition to the availability of a variety of coating types, the high throughput feature offered by SPME plays a crucial role in the future development of this microextraction technology. In this regard, the results of this work contribute to the further validation of thin film in high throughput format as a well-suited approach for the simultaneous analysis of a broad range of analytes in complex matrices. However, future studies should be oriented towards achieving shorter analysis times and higher enrichment factors with minimum sample volumes. In addition,

the feasibility of incorporating matrix modification techniques (*e.g.* addition of organic solvent, use of high extraction temperatures, etc.) in analytical workflows as a means of enhancing free analyte concentrations, increasing extraction recoveries, and normalizing relative matrix effects should be further evaluated for the analysis of biological matrices via SPME and LC-MS.

The introduction of alternative materials for the manufacture of novel devices also plays an important role in the adoption of SPME for innovative applications. For instance, the use of polymers as coating support materials may expand the suitability of SPME for various new biological applications through the creation of biocompatible SPME samplers optimized for easy sample collection and analysis. The coupling of such alternative devices with analytical approaches such as desorption electrospray ionization (DESI), either for imaging or sample profiling, presents itself as an attractive line of research for the near future.

In terms of untargeted analysis, SPME opens new paths for investigations of biochemical processes. By enabling *in vivo* (or close to *in vivo*) sampling of complex biological systems, SPME streamlines the metabolism quenching step, thus facilitating the capture of unstable metabolites. Unquestionably, a large number of studies could benefit from the complementary information that this microextraction technology can provide in relation to data obtained via traditional sample preparation methodologies. In addition, as *in vivo* SPME enables non-lethal and/or non-destructive sampling, thus allowing for multiple samplings to be carried out from the same animal or sample, time course-based metabolomics studies are also facilitated through employment of this technology. However, further work is necessary in order to demonstrate and validate the performance of SPME in untargeted metabolomics investigations. To this end, future outlooks should involve a thorough comparison of SPME versus traditional sample preparation approaches through applications of both workflows to already studied animal models (*e.g.* control vs.

diabetes). Such studies will help elucidate the type of information that SPME is able to provide compared to typical extraction approaches, and will support further application of this microextraction tool in the metabolomics field. The suitability of SPME for the extraction of a broad range of metabolites also opens new pathways for SPME-based fast-profiling applications. Indeed, new developments in SPME technology, including the coupling of SPME directly to MS, point towards the use of such analytical platforms for fast sample discrimination. From a bioanalytical and clinical perspective, the application of SPME-MS approaches towards fast diagnosis and monitoring of different drugs and biomarkers offers promising new directions, possibly allowing for the development of alternative protocols that enable faster, greener, and more cost-effective analyses. Moreover, based on the capabilities of SPME for lipid extraction, combinations of this microextraction technique with shotgun lipidomics strategies present an opportunity for the development of new platforms aimed at facilitating tissue analysis. Other future directions targeted at the integration of SPME in the study of biological systems involve the use of smaller probes for improved spatial resolution, the coupling of SPME with more sensitive and advanced instrumentation, and the development of novel SPME samplers aimed at facilitating SPME operation by personnel from different fields. Owing to its versatility and simplicity, SPME is a promising technology, with a myriad of possible future applications directed at providing new insights into the processes that define biological systems.

Letter of copyright permission

Copyright permission for the materials in Chapter 1

Reprinted from TrAC Trends in Analytical Chemistry, 71, Erica A. Souza-Silva, Nathaly Reyes-Garcés, German A. Gómez-Ríos, Ezel Boyaci, Barbara Bojko, Janusz Pawliszyn, A critical review of the state of art of solid-phase microextraction of complex matrices III. Bioanalytical and clinical applications, 249-264, Copyright (2015), with permission from Elsevier.

Copyright permission for the materials in Chapter 2

Reprinted from Journal of Chromatography A, 1374, Nathaly Reyes-Garcés, Barbara Bojko, Janusz Pawliszyn, High throughput quantification of prohibited substances in plasma using thin film solid phase microextraction, 40-49, Copyright (2014), with permission from Elsevier.

Copyright Clearance Center **RightsLink®**

Home | Account Info | Help

Title:	High throughput quantification of prohibited substances in plasma using thin film solid phase microextraction
Author:	Nathaly Reyes-Garcés,Barbara Bojko,Janusz Pawliszyn
Publication:	Journal of Chromatography A
Publisher:	Elsevier
Date:	29 December 2014

Copyright © 2014 Elsevier B.V. All rights reserved.

Logged in as:
Nathaly Reyes Garces
Account #:
3001100928

LOGOUT

Order Completed

Thank you for your order.

This Agreement between Nathaly Reyes Garces ("You") and Elsevier ("Elsevier") consists of your license details and the terms and conditions provided by Elsevier and Copyright Clearance Center.

Your confirmation email will contain your order number for future reference.

Printable details.

License Number	4146131079978
License date	Jul 11, 2017
Licensed Content Publisher	Elsevier
Licensed Content Publication	Journal of Chromatography A
Licensed Content Title	High throughput quantification of prohibited substances in plasma using thin film solid phase microextraction
Licensed Content Author	Nathaly Reyes-Garcés,Barbara Bojko,Janusz Pawliszyn
Licensed Content Date	Dec 29, 2014
Licensed Content Volume	1374
Licensed Content Issue	n/a
Licensed Content Pages	10
Type of Use	reuse in a thesis/dissertation
Portion	full article
Format	both print and electronic
Are you the author of this Elsevier article?	Yes
Will you be translating?	No
Order reference number	
Title of your thesis/dissertation	Solid Phase Microextraction as a Sample Preparation Tool for Targeted and Untargeted Analysis of Biological Matrices
Expected completion date	Jul 2017
Estimated size (number of pages)	230
Elsevier VAT number	GB 494 6272 12
Requestor Location	Nathaly Reyes Garces 200 University Avenue West

Waterloo, ON N2L3G1 Canada Attn: Nathaly Reyes Garces |

Copyright permission for the materials in Chapter 3

Reprinted from Analytical Chemistry, 87, Nathaly Reyes-Garcés, Barbara Bojko, Dietmar Hein, Janusz Pawliszyn, Solid phase microextraction devices prepared on plastic support as potential single-use samplers for bioanalytical applications, 9722–9730, Copyright (2015), with permission from American Chemical Society.

References

(1)   Nováková, L. *J. Chromatogr. A* **2013**, *1292*, 25–37.

(2)   Vuckovic, D. *Anal. Bioanal. Chem.* **2012**, *403* (6), 1523–1548.

(3)   Rentsch, K. M. *Trends Anal. Chem.* **2016**, *84*, 88–93.

(4)   Ashri, N. Y.; Abdel-Rehim, M. *Bioanalysis* **2011**, *3* (17), 2003–2018.

(5)   Polson, C.; Sarkar, P.; Incledon, B.; Raguvaran, V.; Grant, R. *J. Chromatogr. B* **2003**, *785*, 263–275.

(6)   Yadav, M.; Contractor, P.; Upadhyay, V.; Gupta, A.; Guttikar, S.; Singhal, P.; Goswami, S.; Shrivastav, P. S. *J. Chromatogr. B* **2008**, *872*, 167–171.

(7)   Ma, J.; Shi, J.; Le, H.; Cho, R.; Chi-jou Huang, J.; Miao, S.; Wong, B. K. *J. Chromatogr. B* **2008**, *862*, 219–226.

(8)   Kole, P. L.; Venkatesh, G.; Kotecha, J.; Sheshala, R. *Biomed. Chromatogr.* **2011**, *25* (1), 199–217.

(9)   Namera, A.; Saito, T. *Bioanalysis* **2013**, *5* (8), 915–932.

(10)   Miller, V. P. *Bioanalysis* **2012**, *4* (9), 1111–1121.

(11)   Abdel-Rehim, M. *J. Chromatogr. A* **2010**, *1217*, 2569–2580.

(12)   Déglon, J.; Thomas, A.; Mangin, P.; Staub, C. *Anal. Bioanal. Chem.* **2012**, *402* (8), 2485–2498.

(13)   Demirev, P. A. *Anal. Chem.* **2013**, *85* (2), 779–789.

(14)   De Kesel, P. M.; Sadones, N.; Capiau, S.; Lambert, W. E.; Stove, C. P. *Bioanalysis* **2013**, *5* (16), 2023–2041.

(15)   Déglon, J.; Thomas, A.; Daali, Y.; Lauer, E.; Samer, C.; Desmeules, J.; Dayer, P.; Mangin, P.; Staub, C. *J. Pharm. Biomed. Anal.* **2011**, *54* (2), 359–367.

(16)   Verplaetse, R.; Henion, J. *Anal. Chem.* **2016**, *88* (13), 6789–6796.

(17)   Oliveira, R. V; Henion, J.; Wickremsinhe, E. *Anal. Chem.* **2014**, *86* (2), 1246–1253.

(18)   Smith, K. M.; Xu, Y. *Bioanalysis* **2012**, *4* (6), 741–749.

(19)   Wilson, I. D. *Sampling and Sample Preparation for LC-MS-Based Metabonomics / Metabolomics of Samples of Mammalian Origin*; Elsevier, 2012; Vol. 3.

(20)   Naz, S.; García, A.; Barbas, C. *Anal. Chem.* **2013**, *85* (22), 10941–10948.

(21)   Musteata, F. M. *TrAC Trends Anal. Chem.* **2013**, *45*, 154–168.

(22)   Lanckmans, K.; Sarre, S.; Smolders, I.; Michotte, Y. *Talanta* **2008**, *74*, 458–469.

(23)   Van Wanseele, Y.; De Prins, A.; De Bundel, D.; Smolders, I.; Van Eeckhaut, A.

Bioanalysis **2016**, *8* (18), 1965–1985.

(24) Caille, S.; Alvarez-Jaimes, L.; Polis, I.; Stouffer, D. G.; Parsons, L. H. *J. Neurosci.* **2007**, *27* (14), 3695–3702.

(25) Ma, R. H.; Yang, J.; Qi, L. W.; Xin, G. Z.; Wang, C. Z.; Yuan, C. S.; Wen, X. D.; Li, P. *J. Pharm. Biomed. Anal.* **2012**, *61*, 22–29.

(26) Kim, M.; Lee, J.; Ha Yang, C.; Lee, S. *Anal. Chim. Acta* **2016**, *923*, 55–65.

(27) Carrozzo, M. M.; Troisi, L.; Cannazza, G.; Cazzato, A. S.; Braghiroli, D.; Parenti, C.; Guiducci, S.; Zoli, M. *J. Pharm. Biomed. Anal.* **2012**, *70*, 563–566.

(28) Kottegoda, S.; Shaik, I.; Shippy, S. A. *J. Neurosci. Methods* **2002**, *121* (1), 93–101.

(29) Kennedy, R. T. *Curr. Opin. Chem. Biol.* **2013**, *17*, 860–867.

(30) Cepeda, D. E.; Hains, L.; Li, D.; Bull, J.; Lentz, S. I.; Kennedy, R. T. *J. Neurosci. Methods* **2015**, *242*, 97–105.

(31) Slaney, T. R.; Nie, J.; Hershey, N. D.; Thwar, P. K.; Linderman, J.; Burns, M. A.; Kennedy, R. T. *Anal. Chem.* **2011**, *83* (13), 5207–5213.

(32) Dettmer, K.; Aronov, P. A.; Hammock, D. *Mass Spectrom. Rev.* **2007**, *26*, 51–78.

(33) Zhang, A.; Sun, H.; Wang, P.; Han, Y.; Wang, X. *J. Proteomics* **2012**, *75*, 1079–1088.

(34) Naz, S.; Moreira dos Santos, D. C.; García, A.; Barbas, C. *Bioanalysis* **2014**, *6* (12), 1657–1677.

(35) Ivanisevic, J.; Zhu, Z.-J.; Plate, L.; Tautenhahn, R.; Chen, S.; O'Brien, P. J.; Johnson, C. H.; Marletta, M. a; Patti, G. J.; Siuzdak, G. *Anal. Chem.* **2013**, *85* (14), 6876–6884.

(36) Cajka, T.; Fiehn, O. *Anal. Chem.* **2016**, *88* (1), 524–545.

(37) León, Z.; García-Cañaveras, J. C.; Donato, M. T.; Lahoz, A. *Electrophoresis* **2013**, *34* (19), 1–29.

(38) Hou, Y.; Braun, D. R.; Michel, C. R.; Klassen, J. L.; Adnani, N.; Wyche, T. P.; Bugni, T. S. *Anal. Chem.* **2012**, *84* (10), 4277–4283.

(39) Wolfender, J.-L.; Marti, G.; Thomas, A.; Bertrand, S. *J. Chromatogr. A* **2015**, *1382*, 136–164.

(40) Psychogios, N.; Hau, D. D.; Peng, J.; Guo, A. C.; Mandal, R.; Bouatra, S.; Sinelnikov, I.; Krishnamurthy, R.; Eisner, R.; Gautam, B.; Young, N.; Xia, J.; Knox, C.; Dong, E.; Huang, P.; Hollander, Z.; Pedersen, T. L.; Smith, S. R.; Bamforth, F.; Greiner, R.; McManus, B.; Newman, J. W.; Goodfriend, T.; Wishart, D. S. *PLoS One* **2011**, *6* (2).

(41) Khamis, M. M.; Adamko, D. J.; El-Aneed, A. *Mass Spectrom. Rev.* **2017**, *36* (2), 115–134.

(42) Saude, E. J.; Sykes, B. D. *Metabolomics* **2007**, *3* (1), 19–27.

(43) Wedge, D. C.; Allwood, J. W.; Dunn, W.; Vaughan, A. A.; Simpson, K.; Brown, M.;

Priest, L.; Blackhall, F. H.; Whetton, A. D.; Dive, C.; Goodacre, R. *Anal. Chem.* **2011**, *83* (17), 6689–6697.

(44) Denery, J. R.; Nunes, A. A. K.; Dickerson, T. J. *Anal. Chem.* **2011**, *83* (3), 1040–1047.

(45) Álvarez-Sánchez, B.; Priego-Capote, F.; Luque de Castro, M. D. *TrAC Trends Anal. Chem.* **2010**, *29* (2), 111–119.

(46) Nikolskiy, I.; Mahieu, N. G.; Chen, Y. J.; Tautenhahn, R.; Patti, G. J. *Anal. Chem.* **2013**, *85* (16), 7713–7719.

(47) Gika, H. G.; Macpherson, E.; Theodoridis, G. A.; Wilson, I. D. *J. Chromatogr. B* **2008**, *871*, 299–305.

(48) Want, E. J.; O 'maille, G.; Smith, C. A.; Brandon, T. R.; Uritboonthai, W.; Qin, C.; Trauger, S. A.; Siuzdak, G. *Curr. Opin. Mol. Ther* **2002**, *4* (1), 224–228.

(49) Bruce, S. J.; Tavazzi, I.; Parisod, V.; Rezzi, S.; Kochhar, S.; Guy, P. A. *Anal. Chem.* **2009**, *81* (9), 3285–3296.

(50) Álvarez-Sánchez, B.; Priego-Capote, F.; Castro, M. D. L. De. *TrAC Trends Anal. Chem.* **2010**, *29* (2), 120–127.

(51) Cajka, T.; Fiehn, O. *TrAC - Trends Anal. Chem.* **2014**, *61*, 192–206.

(52) Whiley, L.; Godzien, J.; Ruperez, F. J.; Legido-Quigley, C.; Barbas, C. *Anal. Chem.* **2012**, *84* (14), 5992–5999.

(53) Ebshiana, A. A.; Snowden, S. G.; Thambisetty, M.; Parsons, R.; Hye, A.; Legido-Quigley, C. *PLoS One* **2015**, *10* (4), 1–20.

(54) Michopoulos, F.; Lai, L.; Gika, H.; Theodoridis, G.; Wilson, I. *J. Proteome Res.* **2009**, *8* (4), 2114–2121.

(55) Sitnikov, D. G.; Monnin, C. S.; Vuckovic, D. *Sci. Rep.* **2016**, *6*, 38885.

(56) Cudjoe, E.; Bojko, B.; de Lannoy, I.; Saldivia, V.; Pawliszyn, J. *Angew. Chemie Int. Ed.* **2013**, *52* (46), 12124–12126.

(57) Vuckovic, D.; De Lannoy, I.; Gien, B.; Shirey, R. E.; Sidisky, L. M.; Dutta, S.; Pawliszyn, J. *Angew. Chemie Int. Ed.* **2011**, *50*, 5344–5348.

(58) Jiang, S.; Liang, Z.; Hao, L.; Li, L. *Electrophoresis* **2016**, *37*, 1031–1038.

(59) Förster, Y.; Schmidt, J. R.; Wissenbach, D. K.; Pfeiffer, S. E. M.; Baumann, S.; Hofbauer, L. C.; von Bergen, M.; Kalkhof, S.; Rammelt, S. *PLoS One* **2016**, *11* (7), e0159580.

(60) Forcisi, S.; Moritz, F.; Kanawati, B.; Tziotis, D.; Lehmann, R.; Schmitt-Kopplin, P. *J. Chromatogr. A* **2013**, *1292*, 51–65.

(61) Gika, H. G.; Theodoridis, G. A.; Plumb, R. S.; Wilson, I. D. *J. Pharm. Biomed. Anal.* 2014, pp 12–25.

(62) Rojo, D.; Barbas, C.; Rupérez, F. J. *Bioanalysis* **2012**, *4* (10), 1235–1243.

(63)   Mastrangelo, A.; Ferrarini, A.; Rey-Stolle, F.; García, A.; Barbas, C. *Anal. Chim. Acta* **2015**, *900*, 21–35.

(64)   Vinaixa, M.; Samino, S.; Saez, I.; Duran, J.; Guinovart, J. J.; Yanes, O. *Metabolites* **2012**, *2* (4), 775–795.

(65)   Tautenhahn, R.; Patti, G. J.; Rinehart, D.; Siuzdak, G. *Anal. Chem.* **2012**, *84* (11), 5035–5039.

(66)   Kind, T.; Fiehn, O. *Bioanal. Rev.* **2010**, *2* (1), 23–60.

(67)   Yin, P.; Xu, G. *J. Chromatogr. A* **2014**, *1374*, 1–13.

(68)   Kuhl, C.; Tautenhahn, R.; Böttcher, C.; Larson, T. R.; Neumann, S. *Anal. Chem.* **2012**, *84* (1), 283–289.

(69)   Ai, J. *Anal. Chem.* **1997**, *69* (6), 1230–1236.

(70)   Ouyang, G.; Pawliszyn, J. *Anal. Chim. Acta* **2008**, *627* (2), 184–197.

(71)   Souza-Silva, E. A.; Jiang, R.; Rodríguez-Lafuente, A.; Gionfriddo, E.; Pawliszyn, J. *TrAC Trends Anal. Chem.* 2015, pp 224–235.

(72)   Souza-Silva, E. A.; Gionfriddo, E.; Pawliszyn, J. *TrAC - Trends Anal. Chem.* **2015**, *71*, 236–248.

(73)   Souza-Silva, É. a.; Reyes-Garcés, N.; Gómez-Ríos, G. a.; Boyacı, E.; Bojko, B.; Pawliszyn, J.; Boyaci, E.; Bojko, B.; Pawliszyn, J. *TrAC Trends Anal. Chem.* **2015**, *71*, 249–264.

(74)   Vuckovic, D.; Zhang, X.; Cudjoe, E.; Pawliszyn, J. *J. Chromatogr. A* **2010**, *1217* (25), 4041–4060.

(75)   Bruheim, I.; Liu, X.; Pawliszyn, J. *Anal. Chem.* **2003**, *75* (4), 1002–1010.

(76)   Jiang, R.; Pawliszyn, J. *Trends Anal. Chem.* **2012**, *39*, 245–253.

(77)   Jiang, R.; Pawliszyn, J. *Anal. Chem.* **2014**, *86* (1), 403–410.

(78)   Grandy, J. J.; Boyaci, E.; Pawliszyn, J. *Anal. Chem.* **2016**, *88* (3), 1760–1767.

(79)   Cudjoe, E.; Vuckovic, D.; Hein, D.; Pawliszyn, J. *Anal. Chem.* **2009**, *81* (11), 4226–4232.

(80)   Boyacı, E.; Gorynski, K.; Rodriguez-Lafuente, A.; Bojko, B.; Pawliszyn, J. *Anal. Chim. Acta* **2014**, *809*, 69–81.

(81)   Vuckovic, D.; Cudjoe, E.; Musteata, F. M.; Pawliszyn, J. *Nat. Protoc.* **2010**, *5* (1), 140–161.

(82)   Pawliszyn, J. *Handbook of Solid Phase Microextraction*; Pawliszyn, J., Ed.; Chemical Industry Press: Beijing, 2009.

(83)   Musteata, M. L.; Musteata, F. M.; Pawliszyn, J. *Anal. Chem.* **2007**, *79* (18), 6903–6911.

(84)   Simões A., R.; Bonato, P. S.; Mirnaghi, F. S.; Bojko, B.; Pawliszyn, J. *Bioanalysis* **2015**, *7*

(1), 65–77.

(85) Bojko, B.; Vuckovic, D.; Cudjoe, E.; Hoque, M. E.; Mirnaghi, F.; Wąsowicz, M.; Jerath, A.; Pawliszyn, J. *J. Chromatogr. B* **2011**, *879* (32), 3781–3787.

(86) Togunde, O. P.; Oakes, K. D.; Servos, M. R.; Pawliszyn, J. *Environ. Sci. Technol.* **2012**, *46* (10), 5302–5309.

(87) Vuckovic, D.; Shirey, R.; Chen, Y.; Sidisky, L.; Aurand, C.; Stenerson, K.; Pawliszyn, J. *Anal. Chim. Acta* **2009**, *638* (2), 175–185.

(88) Mirnaghi, F. S.; Chen, Y.; Sidisky, L. M.; Pawliszyn, J. *Anal. Chem.* **2011**, *83* (15), 6018–6025.

(89) Bojko, B.; Vuckovic, D.; Mirnaghi, F.; Cudjoe, E.; Wasowicz, M.; Jerath, A.; Pawliszyn, J. *Ther. Drug Monit.* **2012**, *34* (1), 31–37.

(90) Gorynski, K.; Bojko, B.; Kluger, M.; Jerath, A.; Wąsowicz, M.; Pawliszyn, J. *J. Pharm. Biomed. Anal.* **2014**, *92*, 183–192.

(91) Birjandi, A. P.; Mirnaghi, F. S.; Bojko, B.; Wąsowicz, M.; Pawliszyn, J. *Anal. Chem.* **2014**, *86* (24), 12022–12029.

(92) Du, F.; Alam, M. N.; Pawliszyn, J. *Anal. Chim. Acta* **2014**, *845*, 45–52.

(93) Lan, H.; Gan, N.; Pan, D.; Hu, F.; Li, T.; Long, N.; Shen, H.; Feng, Y. *J. Chromatogr. A* **2014**, *1365*, 35–44.

(94) Olszowy, P.; Szultka, M.; Ligor, T.; Nowaczyk, J.; Buszewski, B. *J. Chromatogr. B* **2010**, *878*, 2226–2234.

(95) Gionfriddo, E.; Boyacl, E.; Pawliszyn, J. *Anal. Chem.* **2017**, *89* (7), 4046–4054.

(96) Kataoka, H.; Ishizaki, A.; Saito, K. *Anal. Methods* **2016**, *8*, 5773–5788.

(97) Fernández-Amado, M.; Prieto-Blanco, M. C.; López-Mahía, P.; Muniategui-Lorenzo, S.; Prada-Rodríguez, D. *Anal. Chim. Acta* **2016**, *906*, 41–57.

(98) Xie, W.; Mullett, W. M.; Miller-Stein, C. M.; Pawliszyn, J. *J. Chromatogr. B* **2009**, *877* (4), 415–420.

(99) Xie, W.; Mullett, W.; Pawliszyn, J. *Bioanalysis* **2011**, *3* (23), 2613–2625.

(100) Peng, F. M.; Xie, P. H.; Shi, Y. G.; Wang, J. D.; Liu, W. Q.; Li, H. Y. *Chromatographia* **2007**, *65* (5–6), 331–336.

(101) Ouyang, G.; Vuckovic, D.; Pawliszyn, J. *Chem. Rev.* **2011**, *111* (4), 2784–2814.

(102) Cudjoe, E.; Bojko, B.; Togunde, P.; Pawliszyn, J. *Bioanalysis* **2012**, *4* (21), 2605–2619.

(103) Musteata, F. M.; Musteata, M. L.; Pawliszyn, J. *Clin. Chem.* **2006**, *52* (4), 708–715.

(104) Vuckovic, D.; De Lannoy, I.; Gien, B.; Yang, Y.; Musteata, F. M.; Shirey, R.; Sidisky, L.; Pawliszyn, J. *J. Chromatogr. A* **2011**, *1218* (21), 3367–3375.

(105) Lord, H. L.; Zhang, X.; Musteata, F. M.; Vuckovic, D.; Pawliszyn, J. *Nat. Protoc.* **2011**, *6* (6), 896–924.

(106) Togunde, O. P.; Oakes, K. D.; Servos, M. R.; Pawliszyn, J. *J. Chromatogr. A* **2012**, *1261*, 99–106.

(107) Xu, J.; Huang, S.; Wu, R.; Jiang, R.; Zhu, F.; Wang, J.; Ouyang, G. *Anal. Chem.* **2015**, *87* (6), 3453–3459.

(108) Ali, S. E.; Farag, M. A.; Holvoet, P.; Hanafi, R. S.; Gad, M. Z. *Sci. Rep.* **2016**, *6* (1), 36359.

(109) Loureiro, C. C.; Oliveira, A. S.; Santos, M.; Rudnitskaya, A.; Todo-Bom, A.; Bousquet, J.; Rocha, S. M. *Allergy Eur. J. Allergy Clin. Immunol.* **2016**, *71* (9), 1362–1365.

(110) Rocha, S. M.; Caldeira, M.; Carrola, J.; Santos, M.; Cruz, N.; Duarte, I. F. *J. Chromatogr. A* **2012**, *1252*, 155–163.

(111) Nizio, K. D.; Perrault, K. A.; Troobnikoff, A. N.; Ueland, M.; Shoma, S.; Iredell, J. R.; Middleton, P. G.; Forbes, S. L. *J. Breath Res.* **2016**, *10* (2), 26008.

(112) Bajtarevic, A.; Ager, C.; Pienz, M.; Klieber, M.; Schwarz, K.; Ligor, M.; Ligor, T.; Filipiak, W.; Denz, H.; Fiegl, M.; Hilbe, W.; Weiss, W.; Lukas, P.; Jamnig, H.; Hackl, M.; Haidenberger, A.; Buszewski, B.; Miekisch, W.; Schubert, J.; Amann, A. *BMC Cancer* **2009**, *9*, 348.

(113) Ahmed, I.; Greenwood, R.; De, B.; Costello, L.; Ratcliffe, N. M.; Probert, C. S. *PLoS One* **2013**, *8* (3).

(114) Vuckovic, D.; Pawliszyn, J. *Anal. Chem.* **2011**, *83* (6), 1944–1954.

(115) Bojko, B.; Gorynski, K.; Gomez-Rios, G. A.; Knaak, J. M.; Machuca, T.; Spetzler, V. N.; Cudjoe, E.; Hsin, M.; Cypel, M.; Selzner, M.; Liu, M.; Keshavjee, S.; Pawliszyn, J. *Anal. Chim. Acta* **2013**, *803*, 75–81.

(116) Bojko, B.; Gorynski, K.; Gomez-Rios, G. A.; Knaak, J. M.; Machuca, T.; Cudjoe, E.; Spetzler, V. N.; Hsin, M.; Cypel, M.; Selzner, M.; Liu, M.; Keshjavee, S.; Pawliszyn, J. *Lab. Investig.* **2014**, *94*, 586–594.

(117) Mousavi, F.; Bojko, B.; Pawliszyn, J. *Anal. Chim. Acta* **2015**, *892*, 95–104.

(118) Mousavi, F.; Bojko, B.; Bessonneau, V.; Pawliszyn, J. *J. Proteome Res.* **2016**, *15*, 963–975.

(119) Mousavi, F.; Gionfriddo, E.; Carasek, E.; Souza-Silva, E. A.; Pawliszyn, J. *Metabolomics* **2016**, *12* (169).

(120) World Antidoping Agency (WADA), Prohibited List, 2014 http://www.wada-ama.org/Documents/World_Anti-Doping_Program/WADP-Prohibited-list/2014/WADA-prohibited-list-2014-EN.pdf (accessed Jul 19, 2014).

(121) World Antidoping Agency (WADA) - Minimum Required Performance Levels http://www.wada-ama.org/Documents/World_Anti-Doping_Program/WADP-IS-

Laboratories/Technical_Documents/WADA-TD2014MRPL-v1-Minimum-Required-Performance-Levels-EN.pdf (accessed Jul 19, 2014).

(122) Thevis, M.; Thomas, A.; Schänzer, W. *Anal. Bioanal. Chem.* **2013**, *405* (30), 9655–9667.

(123) Thomas, A.; Geyer, H.; Schänzer, W.; Crone, C.; Kellmann, M.; Moehring, T.; Thevis, M. *Anal. Bioanal. Chem.* **2012**, *403* (5), 1279–1289.

(124) Thomas, A.; Guddat, S.; Hohler, M.; Krug, O.; Schanzer, W.; Petrou, M.; Thevis, M. *Rapid Commun. Mass Spectrom.* **2010**, *24* (24), 1124–1132.

(125) Schamasch, P.; Rabin, O. *Bioanalysis* **2012**, *4* (13), 1691–1701.

(126) Thevis, M.; Thomas, A.; Pop, V.; Schänzer, W. *J. Chromatogr. A* **2013**, *1292*, 38–50.

(127) Schwope, D. M.; Scheidweiler, K. B.; Huestis, M. a. *Anal. Bioanal. Chem.* **2011**, *401* (4), 1273–1283.

(128) Pedersen, A. J.; Dalsgaard, P. W.; Rode, A. J.; Rasmussen, B. S.; Müller, I. B.; Johansen, S. S.; Linnet, K. *J. Sep. Sci.* **2013**, *36* (13), 2081–2089.

(129) Jones, a W.; Holmgren, a; Kugelberg, F. C. *Forensic Sci. Int.* **2008**, *177* (2–3), 133–139.

(130) Rook, E. J.; Hillebrand, M. J. X.; Rosing, H.; van Ree, J. M.; Beijnen, J. H. *J. Chromatogr. B* **2005**, *824* (1–2), 213–221.

(131) Forsdahl, G.; Vatne, H. K.; Geisendorfer, T.; Gmeiner, G. *Drug Test. Anal.* **2013**, *5*, 826–833.

(132) Ho, E. N. M.; Kwok, W. H.; Wong, A. S. Y.; Wan, T. S. M. *Drug Test. Anal.* **2013**, *5*, 509–528.

(133) Kaabia, Z.; Dervilly-Pinel, G.; Hanganu, F.; Cesbron, N.; Bichon, E.; Popot, M. a; Bonnaire, Y.; Le Bizec, B. *J. Chromatogr. A* **2013**, *1284*, 126–140.

(134) Thomas, A.; Geyer, H.; Guddat, S.; Schänzer, W.; Thevis, M. *Drug Test. Anal.* **2011**, *3*, 806–813.

(135) Liu, Y.; Uboh, C. E.; Soma, L. R.; Li, X.; Guan, F.; You, Y.; Rudy, J. A.; Chen, J.-W. *Drug Test. Anal.* **2011**, *3* (1), 54–67.

(136) Liu, Y.; Uboh, C. E.; Soma, L. R.; Li, X.; Guan, F.; You, Y.; Chen, J.-W. *Anal. Chem.* **2011**, *83* (17), 6834–6841.

(137) Kwok, W. H.; Leung, D. K. K.; Leung, G. N. W.; Wan, T. S. M.; Wong, C. H. F.; Wong, J. K. Y. *J. Chromatogr. A* **2010**, *1217* (19), 3289–3296.

(138) Gosetti, F.; Mazzucco, E.; Gennaro, M. C.; Marengo, E. *J. Chromatogr. B* **2013**, *927*, 22–36.

(139) French, D. *Bioanalysis* **2013**, *5* (22), 2803–2820.

(140) Thevis, M. *Mass Spectrometry in Sports Drug Testing: Characterization of Prohibited Substances and Doping Control Analytical Assays*; John Wiley & Sons, I., Ed.; Hoboken,

New Jersey, 2010.

(141) Vuckovic, D.; Cudjoe, E.; Hein, D.; Pawliszyn, J. *Anal. Chem.* **2010**, *80* (18), 6870–6880.

(142) Risticevic, S.; Lord, H.; Górecki, T.; Arthur, C. L.; Pawliszyn, J. *Nat. Protoc.* **2010**, *5* (1), 122–139.

(143) Nilsson, L. B. *Bioanalysis* **2013**, *5* (24), 3033–3050.

(144) Abdel-Rehim, M.; Carlsson, G.; Bielenstein, M.; Arvidsson, T.; Blomberg, L. G. *J. Chromatogr. Sci.* **2000**, *38* (10), 458–464.

(145) Fura, A.; Harper, T. W.; Zhang, H.; Fung, L.; Shyu, W. C. *J. Pharm. Biomed. Anal.* **2003**, *32* (3), 513–522.

(146) Kodama, H.; Kodama, Y.; Itokazu, N.; Shinozawa, S.; Kanemaru, R.; Sugimoto, T. *J. Clin. Pharm. Ther.* **2001**, *26* (3), 175–179.

(147) Vogeser, M.; Briegel, J. *Clin. Biochem.* **2007**, *40* (9–10), 724–727.

(148) Xu, J.; Winkler, J.; Derendorf, H. *J. Pharmacokinet. Pharmacodyn.* **2007**, *34* (3), 355–372.

(149) Rocci, M. L.; D'Ambrosio, R.; Johnson, N. F.; Jusko, W. J. *Biochem. Pharmacol.* **1982**, *31* (3), 289–292.

(150) ChemSpider | Search and share chemistry http://www.chemspider.com/?gclid=Cj0KEQjw0tCuBRDIjJ_Mlb6zzpQBEiQAyjCoBuRu clLsjhkbZ_HWuKBN5uhjex7TiSjf_30nthgViMwaAh1M8P8HAQ (accessed Aug 19, 2015).

(151) DrugBank http://www.drugbank.ca/ (accessed Jul 6, 2014).

(152) Skopp, G.; Pötsch, L.; Ganssmann, B.; Aderjan, R.; Mattern, R. *J. Anal. Toxicol.* **1998**, *22* (4), 261–264.

(153) Skopp, G.; Pötsch, L.; Mauden, M.; Richter, B. *Forensic Sci. Int.* **2002**, *126* (1), 17–23.

(154) Matuszewski, B. K.; Constanzer, M. L.; Chavez-Eng, C. M. *Anal. Chem.* **2003**, *75* (13), 3019–3030.

(155) U.S. Department of Health and Human Services. *Food and Drug Administration. Guidance for Industry: Bioanalytical Method Validation.*; 2001.

(156) Mirnaghi, F. S.; Goryński, K.; Rodriguez-Lafuente, A.; Boyacı, E.; Bojko, B.; Pawliszyn, J. *J. Chromatogr. A* **2013**, *1316*, 37–43.

(157) Bojko, B.; Cudjoe, E.; Pawliszyn, J.; Wasowicz, M. *TrAC Trends Anal. Chem.* **2011**, *30* (9), 1505–1512.

(158) Bojko, B.; Reyes-Garcés, N.; Bessonneau, V.; Goryński, K.; Mousavi, F.; Souza Silva, E. a.; Pawliszyn, J. *TrAC Trends Anal. Chem.* **2014**, *61*, 168–180.

(159) Musteata, M. L.; Musteata, F. M. *Bioanalysis* **2009**, *1* (6), 1081–1102.

(160) Vuckovic, D. *TrAC Trends Anal. Chem.* **2013**, *45*, 136–153.

(161) Boyacı, E.; Sparham, C.; Pawliszyn, J. *Anal. Bioanal. Chem.* **2014**, *406* (2), 409–420.

(162) Reyes-Garcés, N.; Bojko, B.; Pawliszyn, J. *J. Chromatogr. A* **2014**, *1374*, 40–49.

(163) Souza Silva, E. a.; Risticevic, S.; Pawliszyn, J. *TrAC Trends Anal. Chem.* **2013**, *43*, 24–36.

(164) Xu, J.; Zheng, J.; Tian, J.; Zhu, F.; Zeng, F.; Su, C.; Ouyang, G. *TrAC - Trends Anal. Chem.* **2013**, *47*, 68–83.

(165) Jiang, R.; Pawliszyn, J. *J. Chromatogr. A* **2014**, *1338*, 17–23.

(166) Gómez-Ríos, G. A.; Pawliszyn, J. *Angew. Chem. Int. Ed. Engl.* **2014**, *53* (52), 14503–14507.

(167) Gómez-Ríos, G. A.; Pawliszyn, J. *Chem. Commun. (Camb).* **2014**, *50* (85), 12937–12940.

(168) Vuckovic, D.; de Lannoy, I.; Gien, B.; Shirey, R. E.; Sidisky, L. M.; Dutta, S.; Pawliszyn, J. *Angew. Chem. Int. Ed. Engl.* **2011**, *50* (23), 5344–5348.

(169) Blass, C. R. *Polymers in disposable medical devices: A European perspective*; Rapra Technology Ltd., 1999.

(170) *Polymeric Biomaterials, Revised and Expanded*, Second edi.; Dumitriu, S., Ed.; Marcel Dekker, Inc, 2002.

(171) Mirnaghi, F. S.; Pawliszyn, J. *Anal. Chem.* **2012**, *84* (19), 8301–8309.

(172) Dias, N. C.; Poole, C. F. *Chromatographia* **2002**, *56* (5–6), 269–275.

(173) Fontanals, N.; Marcé, R. M.; Borrull, F. *TrAC - Trends Anal. Chem.* **2005**, *24* (5), 394–406.

(174) Weigel, S.; Kallenborn, R.; Hühnerfuss, H. *J. Chromatogr. A* **2004**, *1023* (2), 183–195.

(175) Liu, R.; Zhou, J. L.; Wilding, A. *J. Chromatogr. A* **2004**, *1022* (1–2), 179–189.

(176) Heringa, M. B.; Hermens, J. L. M. *TrAC Trends Anal. Chem.* **2003**, *22* (9), 575–587.

(177) Heringa, M. B.; Hogevonder, C.; Busser, F.; Hermens, J. L. M. *J. Chromatogr. B. Analyt. Technol. Biomed. Life Sci.* **2006**, *834* (1–2), 35–41.

(178) Kramer, N. I.; van Eijkeren, J. C. H.; Hermens, J. L. M. *Anal. Chem.* **2007**, *79* (18), 6941–6948.

(179) Spijker, H. *Biomaterials* **2003**, *24* (26), 4717–4727.

(180) Chang, X.; Gorbet, M. *J. Biomater. Appl.* **2013**, *28* (3), 407–415.

(181) Streller, U.; Sperling, C.; Hübner, J.; Hanke, R.; Werner, C. *J. Biomed. Mater. Res. - Part B Appl. Biomater.* **2003**, *66* (1), 379–390.

(182) Basmadjian, D.; Sefton, M. V.; Baldwin, S. A. *Biomaterials* **1997**, *18* (23), 1511–1522.

(183) Kushnir, M. M.; Rockwood, A. L.; Nelson, G. J.; Yue, B.; Urry, F. M. *Clin. Biochem.* **2005**, *38* (4), 319–327.

(184) Chen, S.; Li, L.; Zhao, C.; Zheng, J. *Polymer (Guildf).* **2010**, *51* (23), 5283–5293.

(185) Rodriguez-Emmenegger, C.; Brynda, E.; Riedel, T.; Houska, M.; Šubr, V.; Alles, A. B.; Hasan, E.; Gautrot, J. E.; Huck, W. T. S. *Macromol. Rapid Commun.* **2011**, *32* (13), 952–957.

(186) Rodriguez Emmenegger, C.; Brynda, E.; Riedel, T.; Sedlakova, Z.; Houska, M.; Alles, a B. *Langmuir* **2009**, *25* (11), 6328–6333.

(187) Menzies, K. L.; Jones, L. *Optom. Vis. Sci.* **2010**, *87* (6), 1.

(188) Schaller, J.; Gerber, S. A.; Kampfer, U.; Lejon, S.; Trachsel, C. *Human Blood Plasma Proteins: Structure and Function*; John Wiley & Sons, 2008.

(189) Denniff, P.; Spooner, N. *Bioanalysis* **2010**, *2* (8), 1385–1395.

(190) Nováková, L.; Vlcková, H. *Anal. Chim. Acta* **2009**, *656* (1–2), 8–35.

(191) Gika, H.; Theodoridis, G. *Bioanalysis* **2011**, *3* (14), 1647–1661.

(192) Grote-Koska, D.; Czajkowski, S.; Brand, K. *Ther. Drug Monit.* **2015**, *37* (3), 400–404.

(193) Li, W.; Tse, F. L. S. *Biomed. Chromatogr* **2010**, *24*, 49–65.

(194) Denniff, P.; Spooner, N. *Anal. Chem.* **2014**, *86* (16), 8489–8495.

(195) Wagner, M.; Tonoli, D.; Varesio, E.; Hopfgartner, G. *Mass Spectrom. Rev.* **2016**, *35* (3), 361–368.

(196) Jain, D. S.; Subbaiah, G.; Sanyal, M.; Pande, U. C.; Shrivastav, P. *J. Chromatogr. B* **2006**, *834*, 149–154.

(197) Seger, C.; Tentschert, K.; Stöggl, W.; Griesmacher, A.; Ramsay, S. L. *Nat. Protoc.* **2009**, *4* (4), 526–534.

(198) Koster, R. A.; Dijkers, E. C. F.; Uges, D. R. A. *Ther. Drug Monit.* **2009**, *31* (1), 116–125.

(199) Ji, Q. C.; Liu, G.; D'Arienzo, C. J.; Olah, T. V; Arnold, M. E. *Bioanalysis* **2012**, *4* (16), 2059–2065.

(200) Abu-Rabie, P.; Denniff, P.; Spooner, N.; Chowdhry, B. Z.; Pullen, F. S. *Anal. Chem.* **2015**, *87* (9), 4996–5003.

(201) Abu-Rabie, P.; Spooner, N.; Chowdhry, B. Z.; Pullen, F. S. *Bioanalysis* **2015**, *7* (21), 2763–2775.

(202) De Kesel, P. M. M.; Lambert, W. E.; Stove, C. P. *Anal. Chim. Acta* **2015**, *881*, 65–73.

(203) Spooner, N.; Denniff, P.; Michielsen, L.; De Vries, R.; Ji, Q. C.; Arnold, M. E.; Woods, K.; Woolf, E. J.; Xu, Y.; Boutet, V.; Zane, P.; Kushon, S.; Rudge, J. B. *Bioanalysis* **2015**, *7* (6), 653–659.

(204) Reyes-Garcés, N.; Bojko, B.; Hein, D.; Pawliszyn, J. *Anal. Chem.* **2015**, *87* (19), 9722–9730.

(205) Gómez-Ríos, G. A.; Reyes-Garcés, N.; Bojko, B.; Pawliszyn, J. *Anal. Chem.* **2016**, *88* (2), 1259–1265.

(206) Piri-Moghadam, H.; Ahmadi, F.; Gómez-Ríos, G. A.; Boyaci, E.; Reyes-Garcés, N.; Aghakhani, A.; Bojko, B.; Pawliszyn, J. *Angew. Chemie - Int. Ed.* **2016**, *55* (26), 7510–7514.

(207) Chung, J.; De Lannoy, I.; Gien, B.; Vuckovic, D.; Yang, Y.; Bojko, B.; Pawliszyn, J. *Anal. Chim. Acta* **2012**, *742*, 37–44.

(208) Vuckovic, D.; Risticevic, S.; Pawliszyn, J. *Angew. Chem. Int. Ed. Engl.* **2011**, *50* (25), 5618–5628.

(209) Zhang, X.; Es-Haghi, A.; Cai, J.; Pawliszyn, J. *J. Chromatogr. A* **2009**, *1216* (45), 7664–7669.

(210) Musteata, F. M.; de Lannoy, I.; Gien, B.; Pawliszyn, J. *J. Pharm. Biomed. Anal.* **2008**, *47* (4–5), 907–912.

(211) Zhang, X.; Es-haghi, A.; Musteata, F. M.; Ouyang, G.; Pawliszyn, J. *Anal. Chem.* **2007**, *79* (12), 4507–4513.

(212) Bojko, B.; Cudjoe, E.; Gómez-Ríos, G. a; Gorynski, K.; Jiang, R.; Reyes-Garcés, N.; Risticevic, S.; Silva, É. a S.; Togunde, O.; Vuckovic, D.; Pawliszyn, J. *Anal. Chim. Acta* **2012**, *750*, 132–151.

(213) Hinderling, P. H. *Pharmacol. Rev.* **1997**, *49* (3), 279–295.

(214) Obach, R. S.; Lombardo, F.; Waters, N. J. *Drug Metab. Dispos.* **2008**, *36* (7), 1385–1405.

(215) Yamamoto, I.; Iwata, K.; Nakashima, M. *J. Pharmacobiodyn.* **1985**, *8* (5), 385–391.

(216) Tan, A.; Gagné, S.; Lévesque, I. A.; Lachance, S.; Boudreau, N.; Lévesque, A. *J. Chromatogr. B* **2012**, *901*, 79–84.

(217) Alam, M. N.; Ricardez-Sandoval, L.; Pawliszyn, J. *Ind. Eng. Chem. Res.* **2017**, *56* (13), 3679–3686.

(218) Mohammed, S. S.; Christopher, M. M.; Mehta, P.; Kedar, A.; Gross, S.; Derendorf, H. *J. Pharm. Sci.* **1993**, *82* (11), 1112–1117.

(219) Pries, A. R.; Neuhaus, D.; Gaehtgens, P. *Am. J. Physiol.* **1992**, *263* (6 Pt 2), H1770-8.

(220) Huestis, M. A. *Clin. Chem.* **2005**, *51* (12), 2289–2295.

(221) Zhao, Y. Y.; Cheng, X. L.; Vaziri, N. D.; Liu, S.; Lin, R. C. *Clinical Biochemistry*. 2015, pp 16–26.

(222) Ramautar, R.; Berger, R.; van der Greef, J.; Hankemeier, T. *Curr. Opin. Chem. Biol.* **2013**, *17* (5), 841–846.

(223) Vinayavekhin, N.; Homan, E. A.; Saghatelian, A. *ACS Chem. Biol.* **2009**, *5* (1), 91–103.

(224) Becker, S.; Kortz, L.; Helmschrodt, C.; Thiery, J.; Ceglarek, U. *J. Chromatogr. B* **2012**, *883–884*, 68–75.

(225) Armitage, E. G.; Barbas, C. *J. Pharm. Biomed. Anal.* **2014**, *87*, 1–11.

(226) Liesenfeld, D. B.; Habermann, N.; Owen, R. W.; Scalbert, A.; Ulrich, C. M. *Cancer Epidemiol. Biomarkers Prev.* **2013**, *22* (12), 2182–2201.

(227) Wang, T. J.; Larson, M. G.; Vasan, R. S.; Cheng, S.; Rhee, E. P.; McCabe, E.; Lewis, G. D.; Fox, C. S.; Jacques, P. F.; Fernandez, C.; O'Donnell, C. J.; Carr, S. A.; Mootha, V. K.; Florez, J. C.; Souza, A.; Melander, O.; Clish, C. B.; Gerszten, R. E. *Nat. Med.* **2011**, *17* (4), 448–453.

(228) Wood, P. L. *Neuropsychopharmacol. Rev.* **2014**, *39* (1), 24–33.

(229) Sabatine, M. S.; Liu, E.; Morrow, D. A.; Heller, E.; McCarroll, R.; Wiegand, R.; Berriz, G. F.; Roth, F. P.; Gerszten, R. E. *Circulation* **2005**, *112* (25), 3868–3875.

(230) Robroeks, C. M. H. H. T.; van Berkel, J. J. B. N.; Dallinga, J. W.; Jobsis, Q.; Zimmermann, L. J. I. U. C. J. I.; Hendriks, H. J. E. A. N. J. E.; Wouters, M. F. M.; van der Grinten, C. P. M.; van de Kant, K. D. G.; van Schooten, F.-J. J.; Dompeling, E.; Joebsis, Q.; Zimmermann, L. J. I. U. C. J. I.; Hendriks, H. J. E. A. N. J. E.; Wouters, M. F. M.; van der Grinten, C. P. M.; van de Kant, K. D. G.; van Schooten, F.-J. J.; Dompeling, E.; Grinten, C. P. M. V. A. N. D. E. R.; Pulmonology, P.; Pediatrics, L. J. I. Z.; Medicine, R. *Pediatr. Res.* **2010**, *68* (1), 75–80.

(231) Dunn, W. B.; Broadhurst, D.; Begley, P.; Zelena, E.; Francis-McIntyre, S.; Anderson, N.; Brown, M.; Knowles, J. D.; Halsall, A.; Haselden, J. N.; Nicholls, A. W.; Wilson, I. D.; Kell, D. B.; Goodacre, R. *Nat. Protoc.* **2011**, *6* (7), 1060–1083.

(232) Sellick, C. A.; Hansen, R.; Stephens, G. M.; Goodacre, R.; Dickson, A. J. *Nat. Protoc.* **2011**, *6* (8), 1241–1249.

(233) Silva, C.; Passos, M.; Câmara, J. *Br. J. Cancer* **2011**, *105*, 1894–1904.

(234) Dixon, E.; Clubb, C.; Pittman, S.; Ammann, L.; Rasheed, Z.; Kazmi, N.; Keshavarzian, A.; Gillevet, P.; Rangwala, H.; Couch, R. D. *PLoS One* **2011**, *6* (4), e18471.

(235) Risticevic, S.; DeEll, J. R.; Pawliszyn, J. *J. Chromatogr. A* **2012**, *1251*, 208–218.

(236) Gionfriddo, E.; Souza-Silva, R. A.; Pawliszyn, J. *Anal. Chem.* **2015**, *87* (16), 8448–8456.

(237) Cudjoe, E.; Bojko, B.; de Lannoy, I.; Saldivia, V.; Pawliszyn, J. *Angew. Chem. Int. Ed. Engl.* **2013**, *52* (46), 12124–12126.

(238) Gertsman, I.; Gangoiti, J. A.; Barshop, B. A. *Metabolomics* **2014**, *10* (2), 312–323.

(239) Tugizimana, F.; Steenkamp, P. A.; Piater, L. A.; Dubery, I. A. *Metabolites* **2016**, *6* (4), 1–18.

(240) Birjandi, A. P.; Bojko, B.; Ning, Z.; Figeys, D.; Pawliszyn, J. *J. Chromatogr. B* **2017**,

1043, 12–19.

(241) De Grazia, S.; Gionfriddo, E.; Pawliszyn, J. *Talanta* **2017**, *167*, 754–760.

(242) Vorkas, P. A.; Isaac, G.; Anwar, M. A.; Davies, A. H.; Want, E. J.; Nicholson, J. K.; Holmes, E. *Anal. Chem.* **2015**, *87* (8), 4184–4193.

(243) Leuthold, P.; Schaeffeler, E.; Winter, S.; Büttner, F.; Hofmann, U.; Mürdter, T. E.; Rausch, S.; Sonntag, D.; Wahrheit, J.; Fend, F.; Hennenlotter, J.; Bedke, J.; Schwab, M.; Haag, M. *J. Proteome Res.* **2017**, *16* (2), 933–944.

(244) Udupa, K.; Chen, R. *Prog. Neurobiol.* **2015**, *133*, 27–49.

(245) Shah, R. S.; Chang, S.; Min, H.; Cho, Z.-H.; Blaha, C. D.; Lee, K. H. *J. Clin. Neurol.* **2010**, *6* (4), 167.

(246) Kringelbach, M. L.; Jenkinson, N.; Owen, S. L. F.; Aziz, T. Z. *Nat. Rev. Neurosci.* **2007**, *8* (8), 623–635.

(247) Chiken, S.; Nambu, A. *Front. Syst. Neurosci.* **2014**, *8*, 33.

(248) Torres-Sanchez, S.; Perez-Caballero, L.; Berrocoso, E. *Progress in Neuro-Psychopharmacology and Biological Psychiatry*. Elsevier Inc. 2017, pp 1–10.

(249) Filali William Hutchison Vanessa N Palter Andres M Lozano Jonathan O Dostrovsky, M. D. *Exp Brain Res* **2004**, *156*, 274–281.

(250) Lafreniere-Roula, M.; Kim, E.; Hutchison, W. D.; Lozano, A. M.; Hodaie, M.; Dostrovsky, J. O. *Exp Brain Res* **2010**, *205*, 251–261.

(251) Galati, S.; Mazzone, P.; Fedele, E.; Pisani, A.; Peppe, A.; Pierantozzi, M.; Brusa, L.; Tropepi, D.; Moschella, V.; Raiteri, M.; Stanzione, P.; Bernardi, G.; Stefani, A. *Eur. J. Neurosci.* **2006**, *23* (11), 2923–2928.

(252) Reese, R.; Leblois, A.; Steigerwald, F.; Pötter-Nerger, M.; Herzog, J.; Mehdorn, H. M.; Deuschl, G.; Meissner, W. G.; Volkmann, J. *Exp. Neurol.* **2011**, *229*, 517–521.

(253) Rommelfanger, K. S.; Wichmann, T. *Front. Neuroanat.* **2010**, *4*, 139.

(254) He, Z.; Jiang, Y.; Xu, H.; Jiang, H.; Jia, W.; Sun, P.; Xie, J. *Behav. Brain Res.* **2014**, *263*, 108–114.

(255) Bruet, N.; Windels, F.; Bertrand, A.; Feuerstein, C.; Poupard, A.; Savasta, M. *J. Neuropathol. Exp. Neurol.* **2001**, *60* (1), 15–24.

(256) Meissner, W.; Harnack, D.; Reese, R.; Paul, G.; Reum, T.; Ansorge, M.; Kusserow, H.; Winter, C.; Morgenstern, R.; Kupsch, A. *J. Neurochem* **2003**, *85*, 601–609.

(257) Zhao, X.-D.; Cao, Y.-Q.; Liu, H.-H.; Li, F.-Q.; You, B.-M.; Zhou, X.-P. *Brain Res.* **2009**, *1286*, 230–238.

(258) Abosch, A.; Kapur, S.; Lang, A. E.; Hussey, D.; Sime, E.; Miyasaki, J.; Houle, S.; Lozano, A. M.; Starr, P.; Broggi, G.; Bakay, R. A. E.; Boulis, N.; Rezai, A. R. *Neurosurgery* **2003**, *53* (5), 1095–1105.

(259) Strafella, A. P.; Sadikot, A. F.; Dagher, A. *Neuroreport* **2003**, *14* (9), 1287–1289.

(260) Li, T.; Thümen, A.; Moser, A. *Neurochem. Int.* **2006**, *48* (2), 83–86.

(261) Feuerstein, T. J.; Kammerer, M.; Lücking, C. H.; Moser, A. *Naunyn. Schmiedebergs. Arch. Pharmacol.* **2011**, *384* (1), 1–20.

(262) Ogura, M.; Nakao, N.; Nakai, E.; Uematsu, Y.; Itakura, T. *J. Neurosurg.* **2004**, *100* (6), 997–1001.

(263) Windels, F.; Bruet, N.; Poupard, A.; Feuerstein, C.; Bertrand, A.; Savasta, M. *J. Neurosci. Res.* **2003**, *72* (2), 259–267.

(264) You, Z. B.; Tzschentke, T. M.; Brodin, E.; Wise, R. A. *J Neurosci* **1998**, *18* (16), 6492–6500.

(265) Jiménez-Sánchez, L.; Castañé, A.; Pérez-Caballero, L.; Grifoll-Escoda, M.; López-Gil, X.; Campa, L.; Galofré, M.; Berrocoso, E.; Adell, A. *Cereb. Cortex* **2016**, *26* (6), 2778–2789.

(266) Stefani, A.; Fedele, E.; Galati, S.; Pepicelli, O.; Frasca, S.; Pierantozzi, M.; Peppe, A.; Brusa, L.; Orlacchio, A.; Hainsworth, A. H.; Gattoni, G.; Stanzione, P.; Bernardi, G.; Raiteri, M.; Mazzone, P. *Ann. Neurol.* **2005**, *57* (3), 448–452.

(267) Creed, M. C.; Hamani, C.; Nobrega, J. N. *Brain Stimul.* **2013**, *6*, 506–514.

(268) Voon, V.; Krack, P.; Lang, A. E.; Lozano, A. M.; Dujardin, K.; Schu«, M.; D'ambrosia, J.; Thobois, S.; Tamma, F.; Herzog, J.; Speelman, J. D.; Samanta, J.; Kubu, C.; Rossignol, H.; Poon, Y.-Y.; Saint-Cyr, J. A.; Ardouin, C.; Moro, E. *Brain* **2008**, *131*, 2720–2728.

(269) Hamani, C.; Diwan, M.; Isabella, S.; Lozano, A. M.; Nobrega, J. N. *J. Psychiatr. Res.* **2010**, *44*, 683–687.

(270) Kalén, P.; Strecker, R. E.; Rosengren, E.; Björklund, A. *Brain Res.* **1989**, *492* (1–2), 187–202.

(271) Meng, H.; Wang, Y.; Huang, M.; Lin, W.; Wang, S.; Zhang, B. *Brain Res.* **2011**, *1422*, 32–38.

(272) Drevets, W. C.; Price, J. L.; Furey, M. L. *Brain Struct Funct* **2008**, *213* (1–2), 93–118.

(273) Herrington, T. M.; Cheng, J. J.; Eskandar, E. N. *J. Neurophysiol.* **2016**, *115* (1), 19–38.

(274) Borland, L. M.; Michael, A. C. In *Electrochemical Methods for Neuroscience*; CRC Press/Taylor & Francis, 2007; pp 1–16.

(275) Hamani, C.; Diwan, M.; Macedo, C. E.; Brandão, M. L.; Shumake, J.; Gonzalez-Lima, F.; Raymond, R.; Lozano, A. M.; Fletcher, P. J.; Nobrega, J. N. *Biol. Psychiatry* **2010**, *67* (2), 117–124.

(276) Mayberg, H. S.; Lozano, A. M.; Voon, V.; McNeely, H. E.; Seminowicz, D.; Hamani, C.; Schwalb, J. M.; Kennedy, S. H. *Neuron* **2005**, *45* (5), 651–660.

(277) Holtzheimer, P. E. *Arch. Gen. Psychiatry* **2012**, *69* (2), 150.

(278) Kennedy, S. H.; Giacobbe, P.; Rizvi, S. J.; Placenza, F. M.; Nishikawa, Y.; Mayberg, H. S.; Lozano, A. M. *Am. J. Psychiatry* **2011**, *168* (5), 502–510.

(279) Lozano, A. M.; Mayberg, H. S.; Giacobbe, P.; Hamani, C.; Craddock, R. C.; Kennedy, S. H. *Biol. Psychiatry* **2008**, *64* (6), 461–467.

(280) Malone, D. A.; Dougherty, D. D.; Rezai, A. R.; Carpenter, L. L.; Friehs, G. M.; Eskandar, E. N.; Rauch, S. L.; Rasmussen, S. A.; Machado, A. G.; Kubu, C. S.; Tyrka, A. R.; Price, L. H.; Stypulkowski, P. H.; Giftakis, J. E.; Rise, M. T.; Malloy, P. F.; Salloway, S. P.; Greenberg, B. D. *Biol. Psychiatry* **2009**, *65* (4), 267–275.

(281) Bewernick, B. H.; Hurlemann, R.; Matusch, A.; Kayser, S.; Grubert, C.; Hadrysiewicz, B.; Axmacher, N.; Lemke, M.; Cooper-Mahkorn, D.; Cohen, M. X.; Brockmann, H.; Lenartz, D.; Sturm, V.; Schlaepfer, T. E. *Biol. Psychiatry* **2010**, *67* (2), 110–116.

(282) Schlaepfer, T. E.; Bewernick, B. H.; Kayser, S.; Mädler, B.; Coenen, V. A. *Biol. Psychiatry* **2013**, *73* (12), 1204–1212.

(283) Jiménez, F.; Nicolini, H.; Lozano, A. M.; Piedimonte, F.; Salín, R.; Velasco, F. *World Neurosurg.* **2013**, *80* (3–4), S30.e17-S30.e25.

(284) Schneider, T. M.; Beynon, C.; Sartorius, A.; Unterberg, A. W.; Kiening, K. L. *Neurosurgery* **2013**, *72* (2 Suppl Operative), ons184-ons193.

(285) Calabrese, V.; Mancuso, C.; Calvani, M.; Rizzarelli, E.; Butterfield, D. A.; Stella, A. M. G. *Nat. Rev. Neurosci.* **2007**, *8* (10), 766–775.

(286) Szabo, C. *Brain Research Bulletin*. 1996, pp 131–141.

(287) Grima, G.; Benz, B.; Do, K. Q. *Eur. J. Neurosci.* **1997**, *9*, 2248–2258.

(288) Chakravarty, M. M.; Hamani, C.; Martinez-canabal, A.; Ellegood, J.; Laliberté, C.; Nobrega, J. N.; Sankar, T.; Lozano, A. M.; Frankland, P. W.; Lerch, J. P. *Neuroimage* **2016**, *125*, 422–427.

(289) Attwell, D.; Buchan, A. M.; Charpak, S.; Lauritzen, M.; MacVicar, B. A.; Newman, E. A. *Nature* **2010**, *468* (7321), 232–243.

(290) Saransaari, P.; Oja, S. S. *Prog. Neurobiol.* **2000**, *62*, 407–425.

(291) French, E. D.; Vezzani, A.; Whetsell, W. O.; Schwarcz, R. *Adv. Exp. Med. Biol.* **1986**, *203*, 349–362.

(292) Trenkner, E. In *Excitatory Amino Acids and Neuronal Plasticity Edited*; Y. Ben-Ari, Ed.; Springer US, 1990; pp 239–244.

(293) Scheller, D.; Korte, M.; Szathmary, S.; Tegtmeier, F. *Neurochem. Res.* **2000**, *25* (6), 801–807.

(294) Saransaari, P.; Oja, S. S. *Neuroscience* **1999**, *89* (4), 1103–1111.

(295) Guevara-Guzman, R.; Emson, P. C.; Kendrick, K. M. *J. Neurochem.* **1994**, *62* (2), 807–810.

(296) Pou, S.; Pou, W. S.; Bredt, D. S.; Snyder, S. H.; Rosen, G. M. *J. Biol. Chem.* **1992**, *267* (34), 24173–24176.

(297) Xia, Y.; Tsai, A. L.; Berka, V.; Zweier, J. L. *J. Biol. Chem.* **1998**, *273* (40), 25804–25808.

(298) Carr, A. C.; McCall, M. R.; Frei, B. *Arterioscler. Thromb. Vasc. Biol.* **2000**, *20* (7).

(299) Valko, M.; Leibfritz, D.; Moncol, J.; Cronin, M. T. D.; Mazur, M.; Telser, J. *Int. J. Biochem. Cell Biol.* **2007**, *39* (39), 44–84.

(300) Yu, Z. F.; Bruce-Keller, a J.; Goodman, Y.; Mattson, M. P. *J. Neurosci. Res.* **1998**, *53* (5), 613–625.

(301) Jones, L. L.; McDonald, D. A.; Borum, P. R. *Prog. Lipid Res.* **2010**, *49* (1), 61–75.

(302) Wyse, A. T. S.; Netto, C. A. *Metab. Brain Dis.* **2011**, *26* (3), 159–172.

(303) Cohen, S. M.; Nadler, J. V. *Brain Res.* **1997**, *761* (2), 271–282.

(304) De Koning, T. J.; Fuchs, S. A.; Klomp, L. W. J. In *Handbook of Neurochemistry and Molecular Neurobiology: Amino Acids and Peptides in the Nervous System*; 2007; pp 23–45.

(305) Levine, R. L.; Mosoni, L.; Berlett, B. S.; Stadtman, E. R. *Proc. Natl. Acad. Sci. U. S. A.* **1996**, *93* (26), 15036–15040.

(306) Chen, Y.; Zackert, W. E.; Roberts, L. J.; Morrow, J. D. *Biochim. Biophys. Acta - Mol. Cell Biol. Lipids* **1999**, *1436* (3), 550–556.

(307) Milne, G. L.; Musiek, E. S.; Morrow, J. D. *Antioxid. Redox Signal.* **2005**, *7* (1–2), 210–220.

(308) Joca, S. R. L.; Ferreira, F. R.; Guimarães, F. S. *Stress* **2007**, *10* (3), 227–249.

(309) da Silva, G. D.; Matteussi, A. S.; dos Santos, A. R.; Calixto, J. B.; Rodrigues, A. L. *Neuroreport* **2000**, *11* (17), 3699–3702.

(310) Kordjazy, N.; Haj-Mirzaian, A.; Amiri, S.; Ostadhadi, S.; Kordjazy, M.; Sharifzadeh, M.; Dehpour, A. R. *Eur. J. Pharmacol.* **2015**, *762*, 411–418.

(311) Sanacora, G.; Treccani, G.; Popoli, M. *Neuropharmacology* **2012**, *62*, 63–77.

(312) Toyoda, A.; Iio, W. In *Advances in experimental medicine and biology*; 2013; Vol. 775, pp 29–43.

(313) Caletti, G.; Olguins, D. B.; Pedrollo, E. F.; Barros, H. M. T.; Gomez, R. *Amino Acids* **2012**, *43* (4), 1525–1533.

(314) Barbosa Neto, J. B.; Tiba, P. A.; Faturi, C. B.; De Castro-Neto, E. F.; Da Graa Naffah-Mazacoratti, M.; De Jesus Mari, J.; De Mello, M. F.; Suchecki, D. *Neuropharmacology* **2012**, *62* (1), 518–526.

(315) Melon, C.; Chassain, C.; Bielicki, G.; Renou, J.-P.; Kerkerian-Le Goff, L.; Salin, P.; Durif, F. *J. Neurochem.* **2015**, *132* (6), 703–712.

(316) Ortiz, R.; Ulrich, H.; Zarate, C. A.; Machado-Vieira, R. *Prog. Neuro-Psychopharmacology Biol. Psychiatry* **2015**, *57*, 117–131.

(317) Kesebir, S.; Tatlıdil Yaylacı, E.; Süner, O.; Gültekin, B. K. *J. Affect. Disord.* **2014**, *165*, 131–134.

(318) Chaudhari, K.; Khanzode, S.; Khanzode, S.; Dakhale, G.; Saoji, A.; Sarode, S. *Indian J. Clin. Biochem.* **2010**, *25* (1), 77–81.

(319) Jernigan, P. L.; Hoehn, R. S.; Grassmé, H.; Edwards, M. J.; Müller, C. P.; Kornhuber, J.; Gulbins, E. *NeuroSignals* **2015**, *23* (1), 49–58.

(320) Oliveira, T. G.; Chan, R. B.; Bravo, F. V; Miranda, A.; Silva, R. R.; Zhou, B.; Marques, F.; Pinto, V.; Cerqueira, J. J.; Di Paolo, G.; Sousa, N. *Mol. Psychiatry* **2016**, *21* (1), 80–88.

(321) Gulbins, E.; Palmada, M.; Reichel, M.; Lüth, A.; Böhmer, C.; Amato, D.; Müller, C. P.; Tischbirek, C. H.; Groemer, T. W.; Tabatabai, G.; Becker, K. A.; Tripal, P.; Staedtler, S.; Ackermann, T. F.; van Brederode, J.; Alzheimer, C.; Weller, M.; Lang, U. E.; Kleuser, B.; Grassmé, H.; Kornhuber, J. *Nat. Med.* **2013**, *19* (7), 934–938.

(322) Müller, C. P.; Reichel, M.; Muehle, C.; Rhein, C.; Gulbins, E.; Komhuber, J.; Mueller, C. P.; Reichel, M.; Muehle, C.; Rhein, C.; Gulbins, E.; Komhuber, J.; Müller, C. P.; Reichel, M.; Muehle, C.; Rhein, C.; Gulbins, E.; Komhuber, J. *Biochim. Biophys. Acta-Molecular Cell Biol. Lipids* **2015**, *1851* (8), 1052–1065.